Small molecule biomarker discovery in Alzheimer's disease a Lipidomic approach

Whiley, Luke

Awarding institution:
King's College London

SMALL MOLECULE BIOMARKER DISCOVERY IN ALZHEIMER'S DISEASE: A LIPIDOMIC APPROACH

LUKE WHILEY

JUNE 2013

A THESIS SUBMITTED IN PARTIAL FULFILMENT OF THE REQUIREMENTS FOR THE DEGREE OF DOCTOR OF PHILOSOPHY

INSTITUTE OF PHARMACEUTICAL SCIENCE
KING'S COLLEGE LONDON
FRANKLIN WILKINS BUILDING
150 STAMFORD STREET
LONDON
SE1 9NH

SUPERVISION BY:
DR. CRISTINA LEGIDO-QUIGLEY
PROF. SIMON LOVESTONE

ABSTRACT

The worldwide incidence of Alzheimer's disease (AD) is rapidly increasing. Current diagnosis requires the observation of symptoms before a verdict can be reached; however, recent thinking indicates disease pathology potentially begins up to 20 years earlier. In addition, a shift is beginning to occur in pharmaceutical research, shifting towards a disease modification approach, aiming to prevent and alter disease progression from an early pre-symptomatic stage. Therefore, there is a requirement for biomarkers capable of the accurate diagnosis of the disease, before the development of symptoms.

The discovery of biomarker molecules can also provide markers to monitor response to treatment, and disease progression. This ability is of use in a clinical environment as surrogate endpoints in trials.

Current lead candidates consist of imaging, genetics and proteins, each of which has drawbacks preventing its routine use in the clinic. An alternative is the employment of circulating small molecules (<1500 Daltons) such as lipids, carbohydrates and amino acids.

Small molecule markers were investigated using experiments which employed Liquid Chromatography-Mass Spectrometry (LC-MS). Initially a hypothesis driven experiment was designed to investigate total fatty acids (FA_{TOTAL}) in human plasma (n=30). Results revealed significant decreases in eicosapentaenoic acid (EPA) (p=0.023) and a significant increase in the ratio of arachidonic acid (AA) to EPA (p=0.05).

As the project evolved, a non-targeted discovery investigation employed LC-MS in the analysis of plasma (n=35). . Following multivariate data analysis a number of lipid groups were uncovered, and were progressed for further investigation. In order to achieve this, a comprehensive lipid specific LC-MS method was designed. Key developments in the method enabled the reduction in analytical variation, whilst enabling the increase in molecular coverage.

The developed method was applied to an increased sample cohort (n=141). Results revealed three phosphatidylcholine (PC) species as significantly reduced in AD: PC16:0/20:5 (p=<0.001), PC; PC16:0/22:6 (p=<0.05); PC18:0/22:6 (p=<0.005). The data underwent a receiver operated characteristic analysis (ROC) resulting in an area under the curve of 0.827 when comparing control plasma with that of AD patients.

ACKNOWLEDGEMENTS

I would like to thank Cristina Legido-Quigley, initially for providing the opportunity to work within her research group at King's College London, and for her guidance throughout the project. Her ideas and expert insight has been greatly appreciated, and it has been fantastic experience working alongside Cristina and her team.

I would also like to thank Simon Lovestone, without whom the project would not have been possible. I am grateful for the funding and opportunity to complete a PhD under his supervision. In addition I am thankful to him for access to biological samples, as well as his expertise regarding Alzheimer's disease. It was a privilege to work within such a respected research division.

I feel fortunate to have had the highest calibre of supervision throughout the project.

In addition, I would like to thank Norman Smith for sharing his expertise in liquid chromatography, and for allowing me to use much of his laboratory equipment. His input was invaluable and I am highly thankful.

I would also like to thank Coral Barbas and her group (Vanesa Alonso, Joanna Godzien, Michal Ciborowski, Javier Rupérez, and Ángeles Lopez to name a few of many) based in Universidad San Pablo, Madrid, for the opportunity to work as part of her laboratory. The experience was one of the highlights of my PhD, and a time when I learned countless things and made many friends.

I would like to thank collaborators Petra Proitsi, Rufina Leung, Arun Sen and Po-Wah So, whose help and expertise on the project was greatly appreciated. I would also like to thank all those who are involved in the sample collection for both the AddNeuroMed and KCL DCR sample sets, without whom, the project could not have been possible

Thanks must also be extended to the laboratory and office team, whom I shared many ideas, and discussions, often over vital tea breaks! Particular thanks should go to Nicola Gray and James Heaton, for their help, advice and friendship throughout the PhD.

Finally, I would like to thank all of my friends and family, who supported me throughout the PhD project. Especial thanks goes to my parents who have supported me at every stage throughout my education. I will be forever grateful.

CONTENTS

FIGURES

TABLES

ABBREVIATIONS

$_{\alpha 2}$M	α2-Macroglobin
µg	Microgram
µL	Microlitre
Aβ	β-Amyloid Peptide
AA	Arachidonic Acid
ACM	Amyloid Cascade Model
AD	Alzheimer's Disease
ADAS-Cog	Alzheimer's Disease Assessment Scale-Cognitive Subscale
ApoE	Apolipoprotein E
APP	Amyloid Precursor Protein
ASM	Acid Sphingomyelinase
AUC	Area Under the Curve
BBB	Blood Brain Barrier
CB	Cerebellum
CDR	Clinical Dementia Rating
CER	Ceramide
CERAD	Consortium to Establish a Registry for Alzheimer's Disease
CFH	Complement Factor H
CNS	Central Nervous System
CSF	Cerebrospinal Fluid
CX	Cortex
d_8-AA	Deuterated Arachidonic Acid
DAG	Diacylglycerol
DAG-Lip	Diacylglycerol Lipase
DCR	Sample Cohort – King's College London Dementia Case Register
DHA	Docosahexaenoic Acid
DHEA	Dehydroepiandrosterone
DI-MS	Direct Ionisation Mass Spectrometry
EC	Electrochemical
ECC	Extracted Compound Chromatogram
EDTA	Ethylenediaminetetraacetic Acid
EGFR	Epidermal Growth Factor Receptor
EIC	Extracted Ion Chromatogram
ELISA	Enzyme Linked Immunosorbent Assay
EOAD	Early Onset Alzheimer's Disease
EPA	Eicosapentaenoic Acid
FA	Fatty Acid
FA_{FREE}	Free Fatty Acid
FA_{TOTAL}	Total Fatty Acid
FAD	Familial Alzheimer's Disease
GC	Gas Chromatography
FDG	Fluorodeoxyglucose
GCA	Glycholic Acid
GCDCA	Glycochenodeoxycholic Acid
GDA	Glycodeoxycholic Acid
HbA_{1c}	Glycosylated Haemoglobin

HDL	High Density Lipoprotein
HMDB	Human Metabolome Database
HP	Hippocampus
HP30	Study Human Plasma 30 (Chapter 2)
ICAM-1	Intercellular Adhesion Molecule-1
IL-I_α	Interleukin-I_α
IL-II	Interleukin-II
IL-3	Interleukin-3
IPA	Isopropanol
IUPAC	International Union of Pure and Applied Chemistry
IVDE	In Vial Dual Extraction
LC	Liquid Chromatography
LGA	Lignoceric Acid
LOAD	Late Onset Alzheimer's Disease
LysoPC	Lyso-Phosphatidylcholine
MAG	Monoacylglycerol
MAG-Lip	Monoacylglycerol Lipase
MB2	Study Mouse Brain 2 (Chapter 2)
MCI	Mild Cognitive Impairment
METLIN	METabolite LINk Database
MFG	Mid Frontal Gyrus
mL	Millilitre
MMSE	Mini Mental State Examination
MRI	Magnetic Resonance Imaging
MRS	Magnetic Resonance Spectroscopy
MS	Mass Spectrometry
MTBE	Methyl-*tert*-Butyl Ether
MTEST	Test Method in Chapter 2
MYO-IN	Myo-Inositol
M/Z	Mass to Charge Ratio
*N*AA	*N*-Acetyl Aspartate
NIA-AA	National Institute of Aging-Alzheimer's Association
NINCDS-ADRDA	National Institute of Neurological and Communicative Disorders and Stroke-Alzheimer's Disease and Related Disorders
NMR	Nuclear Magnetic Resonance
NSC	No Significant Change
OA	Oleic Acid
OF	Olfactory
OPLS-DA	Orthogonal Partial Least Squares Discriminate Analysis
PBS	Phosphate Buffered Saline
PC	Phosphatidylcholine
PCA	Principle Component Analysis
PDGF-BB	Platelet Derived Growth Factor BB
PA	Palmitic Acid
PAF	Platelet Activating Factor
PAP	Phosphatidic Acid Phosphatase
PE	Phosphatidylethanolamine
PE-*N*-MT	Phosphatidylethanolamine-*N*-Methyltransferase

PE-P	Phosphatidylethanolamine-Plasmalogen
PET	Positron Emission Tomography
PI	Phosphatidylinositol
PiB	Pittsburgh Compound B
PLA_2	Phospholipase A_2
PLD	Phospholipase D
PS	Phosphatidylserine
PSEN-1	Presenilin-1
PSEN-2	Presenilin-2
P-tau	Phosphorylated Tau
QC	Quality Control
QQQ	Triple Quadrupole
ROC	Receiver Operating Characteristic
RSD	Relative Standard Deviation
RT	Retention Time
SA	Steric Acid
SAD	Sporadic Alzheimer's Disease
SMB	Small Molecule Biomarker
SP	Sphingolipid
SPH	Sphingomyelin
ST	Striatum
STZ	Streptozotocin
TAG	Triacylglycerol
TIC	Total Ion Count
TH	Thalamus
TLC	Thin Layer Chromatography
TOF	Time of Flight
TPL	Total Phospholipid
TRAP	Ion Trap
TS	Total Signal
TUS	Total Useful Signal
UPLC	Ultra-Performance Liquid Chromatography
UV	Ultra Violet

PUBLICATIONS AND AWARDS

Publications

2013

- Evidence of altered phosphatidylcholine metabolism in Alzheimer's disease
  L Whiley, A Sen, J Heaton, P Proitsi, D García-Gómez, R Leung, NW Smith, M Thambisetty, I Kloszewska, P Mecocci, H Soininen, M Tsolaki, B Vellas, S Lovestone and C Legido-Quigley
  Under Peer Review

2012

- In-vial dual extraction for direct LC-MS analysis of plasma for comprehensive and highly reproducible metabolic fingerprinting
  L Whiley, J Godzien, FJ Ruperez, C Legido-Quigley and C Barbas
  Analytical Chemistry (84(14):5992-9)

2011

- Current strategies in the discovery of small-molecule biomarkers for Alzheimer's disease
  L Whiley and C Legido-Quigley
  Bioanalysis (3(10): 1121-42)

2010

- Evaluation of Chinese medicinal herbs fingerprinting by HPLC-DAD for the detection of toxic aristolochic acids
  J Heaton, L Whiley, Y Hong, CM Sebastian, NW Smith, C Legido-Quigley
  Journal of Separation Science (34(10):1111-5)

Awards

2012

- Fiat Group Bursary Award
  Fiat Group Bursary Award in recognition of academic achievement (http://www.fiatgroupbursary.co.uk)

2011

- Japan Society for Analytical Chemistry - Analytical Sciences Poster Presentation Award at the International Congress for Analytical Sciences 2011 for the poster entitled "Plasma Biomarkers in Alzheimer's Disease: A Metabonomic Approach" (www.ICAS2011.com)

- John Dolphin Award from the Chromatographic Society

2010

- Fiat Group Bursary Award
  Fiat Group Bursary Award in recognition of academic achievement (http://www.fiatgroupbursary.co.uk)

- European Union Erasmus Award
  European Union Erasmus grant awarded to enable collaborative study at the Universidad San Pablo CEU in Madrid

Chapter 1:
Introduction

1.1 – Introduction to Alzheimer's disease

Alzheimer's disease (AD) was first described in academic print in 1907 by Alois Alzheimer [1] (an English translation can be found at [2]). The paper describes the initial observations made regarding a 51 year old woman based at a psychiatric facility in Frankfurt, Germany. Reports describe disorientation, confusion and memory loss, with symptoms described as "sometimes stronger, sometimes weaker", with the eventual patient death occurring four and a half years later. What followed was the first reported brain autopsy of the disease, with observations of abnormal deposits of neurofibrils that form tangle structures in the cells. In addition there was a further deposit of a substance that can be observed in the cortex region of the brain. These observations laid the foundation to studies into dementia and in particular AD.

Knowledge of the disease has progressed from this first report, and it is now considered a major global health burden. Current estimates suggest that the worldwide incidence of Alzheimer's disease is 25 to 30 million people, with future predictions suggesting the number of cases will triple by the year 2040 [3] (Figure 1.1). A 2013 study has suggested cases in the United States will dramatically increase from 4.7million to 13.8million cases[4]. It is also predicted that particular expansion will occur in developing countries, including India and China as medical research becomes more proficient at treating infectious and acute disease, increasing average lifespan and expanding an already aging population. It is currently accepted that one of the major risk factors for the disease is age, with the prevalence of the disease doubling every five years in those >65 [3].

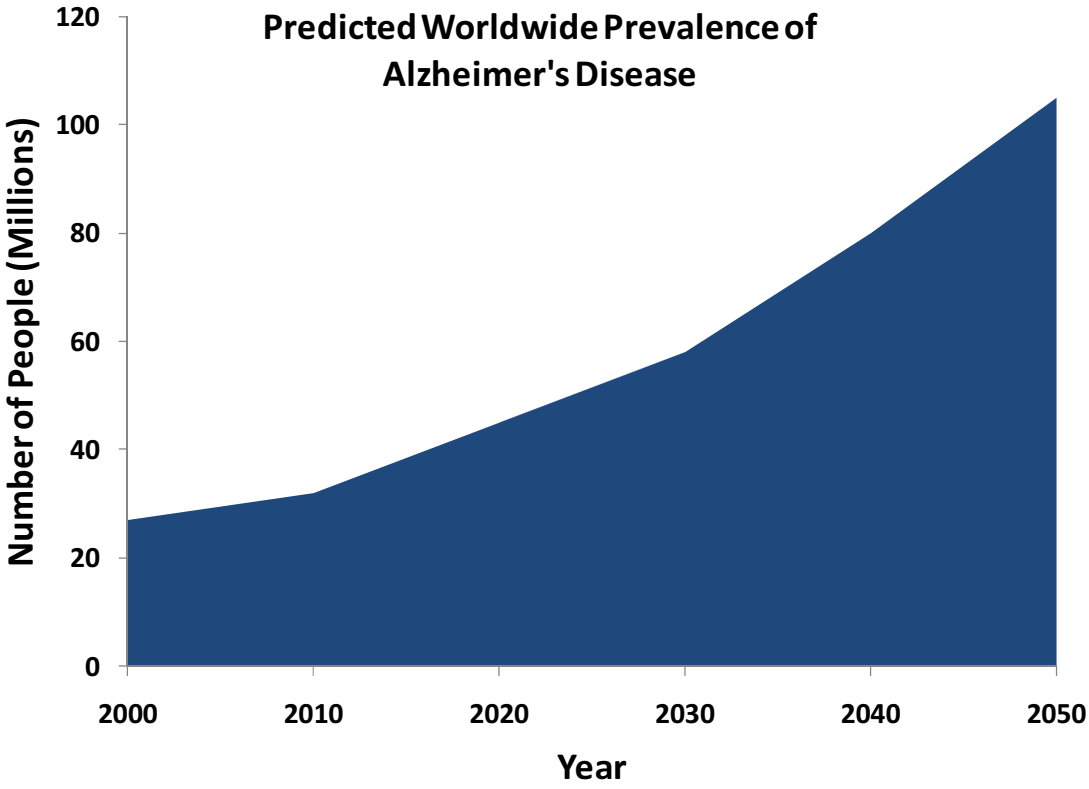

Figure 1.1: Predicted future worldwide incidence of Alzheimer's disease

The above plot signifies the predicted increase of AD over the next few decades. Incidence is expected to increase 100% in developed counties, but the major impact is predicted to occur in nations such as India and China, where an increase of up to 300% is forecast.

Figure is adapted from [5] using data reported in [3].

1.1.1 – Familial and Sporadic Alzheimer's Disease

It is now widely accepted that there are two main forms of AD:

- Familial AD (FAD)
- Sporadic AD (SAD)

1.1.2 – Familial Alzheimer's Disease

Familial AD is a genetic condition and is caused by a mutation in single genes which are inherited in an autosomal-dominant fashion. It is thought that this form of AD accounts for approximately 5% of all cases. It can often be referred to as early onset AD (EOAD) due to the reduced age of pathological progression, compared with sporadic AD. There are three major genes which are currently regarded as being responsible for the onset of familial AD, with over 150 polymorphisms reported.:

- Amyloid Precursor Protein (*APP*)
- Presenilin-1 (*PSEN-1*)
- Presenilin-2 (*PSEN-2*)

These genes are important when considering the current consensus on the mechanism of AD pathology. Termed the Amyloid Cascade Model (ACM), the theory hypothesises that the build-up of Aβ is an early mechanistic stage in the disease, and leads to neuro-degeneration [6]. To summarise, APP is a trans-membrane protein. The two main enzymes thought to degrade the protein are α-secretase and β-secretase. When APP is cleaved along the β-secretase pathway (often termed the amyloidogenic pathway), it leaves an Aβ fragment still bound to the cell membrane. Alternatively, breakdown via the α-secretase pathway (non-amyloidogenic pathway) cleaves inside the Aβ section, therefore only leaving a p3

peptide remaining bound to the membrane. The final extracellular fragment is then spliced via the protease complex γ-secretase, resulting in the release of the Aβ protein. This process is summarised in Figure 1.2.

Both the amyloidogenic and the non-amyloidogenic pathways exist in normal physiology, however, evidence suggests that it is an increase in activity of the β-secretase enzyme complex which leads to the increase in Aβ in AD [7, 8].

Additionally, genetic polymorphisms associated with familial AD are closely linked to this pathway. To date, the γ-secretase complex, has been shown to contain at least four individual proteins: presenilin, nicastrin, anterior pharynx-defective 1, and presenilin enhancer 2 [9]. Presenilin, is the catalytic subunit; and it is here where polymorphisms in the presenilin gene have been reported in familial AD.

γ-secretase demonstrates some unusual characteristics for a protease complex, and there is a certain amount of variation in the cleavage site at the C-terminal in amyloid beta proteolysis. For example, γ-secretase is known to be able to cleave APP at multiple different sites to generate a peptide fragment isoforms that range from 39 to 42 amino acids in length. The most common of these isoforms is $A\beta_{40}$, whilst $A\beta_{42}$ is the most susceptible to the aggregation process which eventually leads to amyloid fibrillogenesis and plaque formation in AD. The previously discussed polymorphisms in the genes coding for APP and both types of presenilin have been reported in association with increased $A\beta_{42}$ production in familial Alzheimer's disease [10].

The mechanism of this link to $A\beta_{42}$ in familial AD is not fully known however there is evidence to suggest that different forms of the γ-secretase complex are

differentially responsible for generating the different Aβ isoforms, suggesting specificity of the enzyme complex may play a role in Aβ aggregation [11].

Polymorphisms in the gene coding for APP have been shown to greatly increase the production of Aβ isoforms [12]. Further to this, the proteins PSEN1 and PSEN2 are known to be involved in the γ-secretase enzyme complex and again have been shown to influence the ratio of Aβ isomers, with $A\beta_{42}$ known to be the most prone to precipitation and plaque formation [13].

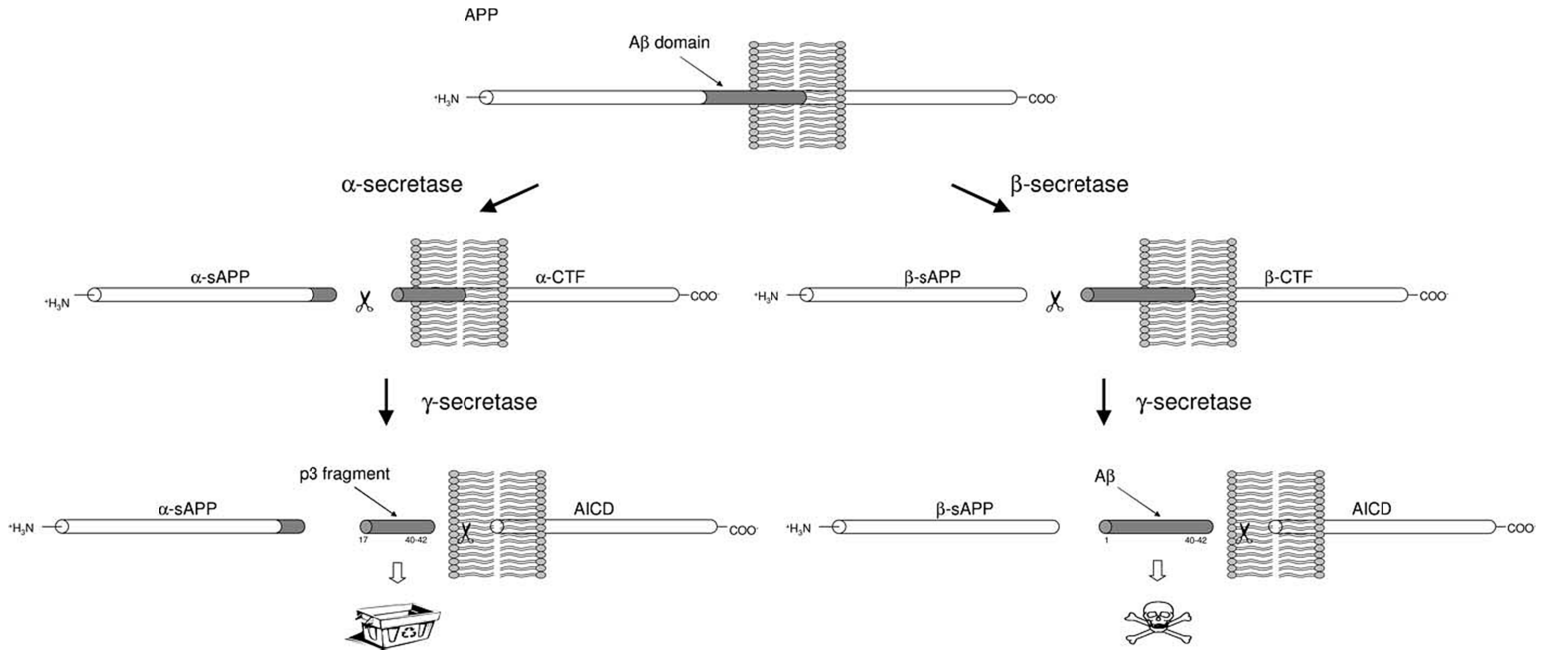

Figure 1.2: Amyloid Cascade Model of Amyloid Precursor Protein Metabolism

Two key enzyme pathways are utilised in the metabolism of amyloid precursor protein (APP). The first uses α-secretase and involves the cleaving of APP within the amyloid-β (Aβ) domain region. Following further metabolism via γ-secretase results in the release of a p3 fragment, thought to have no toxic effects. Conversely, metabolism by the β-secretase pathway is outside of the Aβ domain region. Cleavage via the γ-secretase enzyme complex then results in the release of various isoforms of the Aβ protein.

The model highlights the metabolic importance for balance in the pathways, as over activity of the β-secretase pathway leads to excess Aβ, leading to formation of plaques associated with AD pathology.

Figure obtained from reference [5].

1.1.2.1 – Sporadic Alzheimer's Disease

Sporadic Alzheimer's disease (SAD)(also termed late onset Alzheimer's disease (LOAD)) is the most common form of the disease. The diagnosis of SAD is far more challenging that FAD, as there can often be no obvious family history, or apparent cause, hence it can also be frequently referred to as sporadic AD.

Currently, the largest risk factor associated with SAD is age, with the incidence of the disease doubling every 5 years after 65 [14]. As with FAD, the disease is characterised with the formation of Aβ plaques as well as the formation of deposits of the protein tau in the brain. Although a number of genetic polymorphisms have been identified as risk factors, the full mechanism is still not fully understood.

For example, patients who are carriers of the *apolipoprotein ε4* allele coding for the E4 isoform of apolipoprotein E (ApoE), have been shown to be at increased risk of developing AD [15]. In comparison, research suggests that carriers of the *apolipoprotein ε2* allele coding for the E2 ApoE isoform have a reduced risk of developing AD. It is thought that ApoE modulates the previously discussed γ-secretase activity, and therefore affects the ratio of Aβ isomers [16]. It has also been reported that an increase in the β-secretase activity is associated with ApoE *ε4* genotype increasing the production of Aβ [17].

Further evidence exists in the literature linking sporadic AD to genetic risk factors which may predispose individuals to the disease. Recent large scale genome wide association studies have reported *APOE, CLU, PICALM, CR1, BIN1, ABCA7, MS4A6A, CD33, CD2AP, and EPHA1* as significant risk factors to AD [18, 19].

Outside of genetic mutations, some environmental risk factors have been mooted in the literature, including previous traumatic brain injury [20], previous diagnosis

of depression [21, 22], history of gum disease [23], and those patients with a low level of education or with a low level of mental capability [24]. Additionally, family history has been shown to be a risk factor of AD, without an obvious genetic link. Currently the link to family history and sporadic AD is poorly understood, however evidence suggests that family history may modulate the effect of APOE4 [25].

Again, there is no definitive risk factor which is currently employed for the diagnosis of SAD. It is in part for these reasons why the recent discussion group from the National Institute of Aging in collaboration with the Alzheimer's Association (NIA-AA) (discussed in more detail in Section 1.1.3) have targeted the development of an improvement in biomarker research, to enable the earlier detection of the disease, ideally before typical symptoms emerge. Again, because of the difficulties and the many unknowns associated with SAD, the majority of biomarker research in the literature is focused upon SAD. This is also true of the contents of the thesis presented herein and from this point forward references to AD refer to SAD, unless stated otherwise.

1.1.3 – National Institute of Aging and Alzheimer's Association Discussion Group

As technological advances have been made over time, the original description made in 1907 has been constantly refined, with the latest diagnostic guidelines being released in 2011 by the National Institute of Aging in collaboration with the Alzheimer's Association (NIA-AA) [26]. The guidelines were released as part of an international collaborative project which began in 2009 with the aim of updating the definition of the diagnosed disease from criteria previously in use since 1984 [27].

Diagnosis and classification using the 1984 guidelines is based solely around traditional approaches relying on the clinical assessment by a doctor, taking into account patient history, cognitive testing, for example by use of the 30 question mini-mental state examination (MMSE) [28] and general neurological assessment.

However, the new recommendations and targets set out to improve this in two main ways:

- Identify three stages of AD
- To incorporate biomarker research in AD diagnosis

These aims are now discussed in more detail below:

The guidelines presented by the NIA-AA aim to implement three main stages of the disease into clinical research. Previously, when using the 1984 criteria, in order for AD to be diagnosed, memory loss and reduction in cognition was required. However focus is shifting to an earlier diagnosis, with recent publications suggesting that the first pathological instances of AD might occur up to 20 years prior to the presentation of symptoms [29, 30]. This finding may lead to the earlier detection and therefore earlier treatment of the disease, ideally improving the long term quality of life of the patient.

Stage one of the new guidelines is classed as preclinical AD, and is defined as patients who have measurable changes in markers in the brain (including imaging), cerebrospinal fluid (CSF) or blood plasma or serum, however exhibit none of the traditional symptoms such as memory loss. The guidelines as yet have no definitive biomarker approved for this role, therefore implying a significant need for progression in AD biomarker research.

Stage two is defined as mild cognitive impairment (MCI) as a result of AD. MCI is a condition of reduced mental and cognitive impairment; however the individual is still able to live a relatively normal life and is able to complete day to day tasks. Current estimates suggest up to 20% of >65 year olds suffer from a form of MCI [31]. MCI is viewed as a significant risk factor for AD; however, conversion rates are unclear depending on the study. Mitchell and Shiri-Feshki recently published a systematic review of the literature and found progression to AD to be approximately 29% in population studies [32]. Currently it is unclear as to why some patients progress to more severe forms of dementia and why some remain stable. It is a frequent debate, with some research teams believing MCI is simply a pre-stage of a particular dementia, with others believing MCI is a separate condition altogether and simply acts as a risk factor for further cognitive decline. As part of the recent recommendations, it is advised that further research goes into biomarker discovery, with the aim of identifying more underlying mechanisms of the progression from MCI to AD.

The final stage of the clinical categories recommended in the NIA-AA guidelines is described as dementia due to AD. In this instance symptoms such as disorientation and memory loss are clearly apparent and are caused by AD related pathology. For this stage to be reached the symptoms are suggested to be severe to the extent that an individual's daily life is detrimentally affected.

1.2 – Biomarker Research and the Clinical Diagnosis of Alzheimer's Disease

As well as recommending the implementation of three major clinical stages of AD, the recent report by the NIA-AA also reported that reliable biomarkers for the disease are required, and therefore research in this area should expand.

This requirement for diagnostic markers is perhaps not surprising, with current diagnostic procedures being relatively subjective, relying on a clinical specialist, to observe a combination of mental cognition, patient history, family history and general physical health.

1.2.1 – Definition of a Biomarker

A biomarker of AD is defined as a parameter (physiological, biochemical, anatomic) that can be measured *in vivo* and that reflects specific features of disease related pathophysiological processes. Previous use of the term has often been used to describe fluid analytes, however in the case of AD, it can also be used to term any observations via imaging techniques [26].

A biomarker is required to be able to accurately classify those patients with the disease, this is termed sensitivity. Additionally, a biomarker should be able to classify controls and other disease variations as non-disease category, and this is termed specificity. To be suitable for clinical use a biomarker is required to have both a high sensitivity and specificity.

Many biomarker molecules are routinely used in other diseases, a classic example is the monitoring of circulating plasma glucose, and more recently the circulating level of glycosylated haemoglobin (HbA_{1c}) levels to diagnose and monitor patients suffering from diabetes mellitus [33].

1.2.2 – Current Methods of the Diagnosis of Alzheimer's Disease

Current diagnostic approaches are structured around both a clinical examination and a neuropsychological assessment of the patient. Whilst work on the implementation strategy of the NIA-AA recommendations continues [26, 34], much of immediate diagnosis still relates to the classic set of criteria presented by the National Institute of Neurological and Communicative Disorders and Stroke-Alzheimer's Disease and Related Disorders Association (NINCDS-ADRDA).[27]. However, it should also be noted that other sets of criteria are also in circulation, for example those published by the World Health Organisation (International Classification of Disease) [35] and American Psychiatric Association [36]. In each case the main clinical symptom is the presence of cognitive impairment, with a gradual progression, whilst no secondary cause of the dementia exists, for example signs of vascular dementia, intracranial mass such as a tumour, normal pressure hydrocephalus (the abnormal accumulation of CSF within brain regions) and further neuropsychiatric disorders.

Following the elimination of secondary causes the clinician can assess the patient's history and recent symptoms. Such history and details can be determined from family members, or friends, and their accounts are often used in the diagnosis. The cognitive status of patients is also a vital consideration and there are a number of ways in which this is examined.

Cognitive impairment is typically assessed using a battery of cognitive tests. A widely used example of this is the MMSE [28]. The MMSE is made up of 30 questions divided up into six sections. A typical MMSE obtained from the Guy's and St Thomas' trust can be observed in Figure 1.3. It tests the individual on a range of questions resulting in a maximum score of 30. In general, a score which is

MINI MENTAL STATE EXAMINATION (MMSE)

Patient's name:

Hospital number:

ONE POINT FOR EACH ANSWER	DATE			
ORIENTATION				
Year Month Day Date Time	____/5	____/5	____/5	____/5
Country Town District Hospital Ward	____/5	____/5	____/5	____/5
REGISTRATION Examiner names 3 objects (eg apple, table, penny) Patient asked to repeat (1 point for each correct). THEN patient to learn the 3 names repeating until correct.	____/3	____/3	____/3	____/3
ATTENTION AND CALCULATION Subtract 7 from 100, then repeat from result. Continue 5 times: 100 93 86 79 65 Alternative: spell "WORLD" backwards - dlrow.	____/5	____/5	____/5	____/5
RECALL Ask for names of 3 objects learned earlier.	____/3	____/3	____/3	____/3
LANGUAGE				
Name a pencil and watch.	____/2	____/2	____/2	____/2
Repeat "No ifs, ands, or buts".	____/1	____/1	____/1	____/1
Give a 3 stage command. Score 1 for each stage. Eg. "Place index finger of right hand on your nose and then on your left ear".	____/3	____/3	____/3	____/3
Ask patient to read and obey a written command on a piece of paper stating "Close your eyes".	____/1	____/1	____/1	____/1
Ask the patient to write a sentence. Score if it is sensible and has a subject and a verb.	____/1	____/1	____/1	____/1
COPYING Ask the patient to copy a pair of intersecting pentagons: 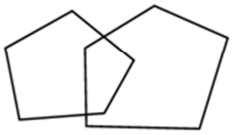	____/1	____/1	____/1	____/1
TOTAL	____/30	____/30	____/30	____/30

Figure 1.3: Example Mini-Mental State Examination

A typical Mini-Mental State Examination (MMSE), routinely used in the assessment of the cognitive condition of both patients and suspect patients of Alzheimer's disease (AD). Healthy controls with non cognitive impairment are expected to score 30, with the greater the impairment the lower the expected outcome score from the examination.

MMSE obtained online from the Guy's and St. Thomas' Trust [37].

greater than or equal to 25 indicates normal cognition. A score of 21-24 indicates mild cognitive impairment, 10-20 moderate impairment and a score of less than or equal to 9 indicated severe impairment. The score, however, only acts as an indication of cognition as an aid for diagnosis, and it is possible for a patient suffering from dementia to score 30. Other examples of cognition scales are also employed, for example the Alzheimer's Disease Assessment Scale-Cognitive subscale (ADAS-Cog) [38] and the Neuropsychological Battery for the Consortium to Establish a Registry for Alzheimer's Disease (CERAD) [39]. Further scales can also be employed such as the Global Deterioration Scale [40] and the Clinical Dementia Rating [41] which attempt to combine mental cognition, functional symptoms and neuropsychiatric elements in a single approach.

In addition, a number of various other scales and tests are completed to examine for signs of patient depression [42, 43], memory impairments such as delayed recall and poor recognition [44-46], spatial memory [47] and patient levels of apraxia [48].

There are many other scales discussed in the literature, with debates in constant evolution in attempts to define a clear methodology for AD diagnosis. However using the common techniques described here, for example, those stipulated by the NINCDS-ADRDA, the relative diagnostic accuracy varies depending on the study with values of 65-96% reported [49-54].

More problematic is the diagnosis specificity between patients with AD and those with other types of dementia, with reports suggesting diagnosis accuracy varies between as low as 23-88% [51-53].

From these figures there is clearly a pressing need to improve diagnosis accuracy, and it is here where recent proposals have suggested improved laboratory tests,

combined with structural imaging data to provide a greater reliability in the diagnosis procedure.

1.2.3 – The Advantages of Biomarkers in the Diagnosis of Alzheimer's Disease

The use of a standardised, recognised biomarker which is easily monitored in a laboratory test would be of great value. Firstly, if any biomarker candidate is successfully implemented in a clinical environment it would improve the diagnosis rates of AD. However, perhaps the most value would be obtained in any ability to diagnose the disease at an earlier time point, preferably prior to the surfacing of the major symptoms associated with the disease.

As research into the treatment of AD progresses, many novel avenues are investigating what are termed "disease modifying" treatments. These approaches are focused upon the changing of pathological processes, for example preventing the accumulation of the two major proteins β-amyloid (Aβ) and tau. The hypothesis is that this prevention would lead to a slowing of the progression of the disease, and is more likely to be more effective than attempting to manage the condition once the full pathological mechanisms have set in [55]. Therefore there is a pressing requirement to diagnose AD as early as possible, in order to give disease modifying treatments the best possible chance of success.

In addition, if a biomarker screen is able to diagnose AD, it might also be used to track both the progression and the response to treatment of the disease. This could lead to the development of personalised treatments, designed for individuals at different time points of the pathology [56].

Finally, the identification of a novel biomarker, be it a protein, gene or small molecule, has the potential for identifying novel mechanistic pathways of the disease. These can act as new targets for therapeutic research, and may lead to new approaches to pharmaceutical design. This is of particular importance as there is an on-going discussion as to whether current pharmaceutical treatments targeting the amyloid cascade pathways (Figure 1.2) are providing successful results [57]. Therefore the identification of novel biomarkers may open new avenues of therapeutic research.

1.3 – Current Lead Biomarkers in Alzheimer's Disease

There are a number of biomarker candidates that have been frequently reported and tested in the literature, those which have shown the most promise to date are discussed below.

1.3.1 – Brain Imaging

As discussed above in Section 1.2, as part of the NIA-AA recommendation on the discovery of a biomarker, the term can be applied to describe any observations obtained via the use of imaging techniques [26].

Imaging approaches have been investigated in the literature, particularly with regard to observations of brain volume and specific brain region volume. Studies have employed magnetic resonance imaging (MRI) to estimate the volumes of individual brain regions. Estimation of size is achieved following a patient MRI scan either manually [58], or more recently, via semi-automated computerised brain mapping techniques [59]. These work by using a marked reference image, and using this as a template to trace the test brain region. Algorithms for this procedure are commercially available and are widely accepted and routinely used in imaging studies [59].

Results have demonstrated that the hippocampus region of the brain is prone to reduce in size compared with controls, by as much as 12% in mild AD [60], increasing to findings of up to 37% in moderate AD [61]. Further studies have also demonstrated a significant difference in the rate of hippocampal volume reduction, with an average change of 2-6% per year in patients with AD compared with <2% in controls [62]. Hippocampal volume has been used to diagnose AD with a sensitivity and specificity of 85% and 82% respectively [61]. This was shown to

perform even better using an approach which also takes into account general aging with sensitivity and specificity figures of 90% and 91% after the age adjustment [61].

The sensitivity and specificity has also been improved by combining information on hippocampal volumes with data from magnetic resonance spectroscopy (MRS) which allows the quantification of metabolites. The diagnostic performance is particularly observed when combined with MRS data used to quantify level of the metabolite *N*-acetyl-aspartate (*N*AA) (with a reduction identified in AD patients) [63].

Despite this, challenges exist with the use of MRI in a clinical environment, mainly due to the high cost of imaging technologies. In addition, data currently has to be processed by a specialist trained at interpreting the data, adding further cost and time. Further complications are added as the undertaking of a brain scan can be an uncomfortable experience, especially for those disorientated by the symptoms of dementia. In addition, diagnostic challenges also present themselves as both a decrease in hippocampal volume and levels of *N*AA have been shown to decrease in MCI [64, 65], impacting the requirements of the NIA-AA guidelines.

An alternative imaging approach is termed positron emission tomography (PET). The technique works by detecting a labelled radionuclide molecule termed a tracer. The tracer is introduced into the body bound to a biological molecule of interest. Three-dimensional images of tracer concentration within the body are then constructed by computer analysis. With regard to Alzheimer's disease PET is useful for the quantification of metabolites *in vivo* in the brain. A particular advantage of the technique is that is allows imaging of Aβ load in living patients using the tracer Pittsburgh compound B (PiB), that binds to Aβ.

Studies have reported a marked retention in PiB in AD patients, compared with controls. PiB retention has been reported at increased levels most prominently in frontal cortex ($p = 0.0001$), whilst increases also were observed in parietal ($p = 0.0002$), temporal ($p = 0.002$), and occipital ($p= 0.002$) as well as the cortex and striatum ($p = 0.0001$). In the brain regions known to be relatively unaffected by amyloid deposition in AD (such as subcortical white matter, pons, and cerebellum), PiB retention has been shown to be at similar levels in both AD and control cases [66].

PET imaging has also been applied to monitoring glucose metabolism in AD using a fluoro-2-deoxy-D-glucose (FDG) tracer. Results have revealed reductions in glucose metabolism in the parieto-temporal, frontal and posterior regions of AD brain. The results have been used for prediction of future AD cases as well as in distinguishing AD from other neurodegenerative diseases. FDG-PET has demonstrated a 90% sensitivity in identifying AD cases, however, specificity in differentiating AD from other dementias is reported as low as 53% [67]. Further disadvantages include the relatively high cost of PET scan, as well as considerations with regard to radiolabelled tracers, with limits on the number of repeat scans achievable with individual patients, so as not to over expose them to the radioactive isotopes.

Example PET scans of both PiB (Aβ) and FDG (glucose) can be seen in Figure 1.4.

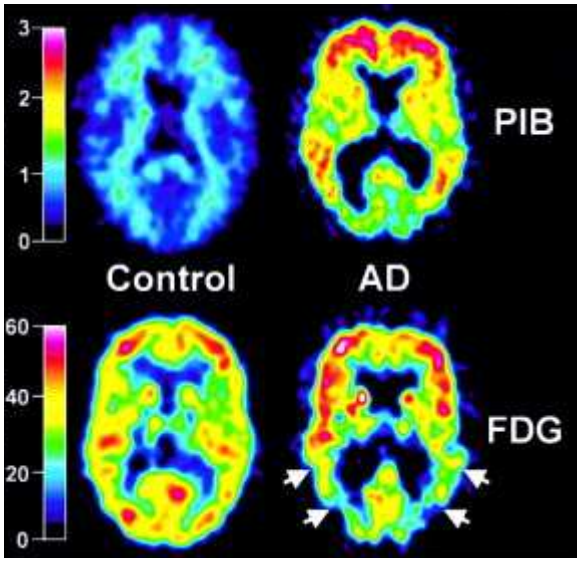

Figure 1.4: Example Positron Emission Tomography

The upper section demonstrates Pittsburgh Compound B (PiB) PET imaging of Aβ in control and AD brain. Increased Aβ retention can clearly be seen in AD.

The lower image is an example of fluoro-2-deoxy-D-glucose (FDG) PET imaging of glucose metabolism. Control demonstrates normal FDG uptake, whilst the AD image shows a typical pattern of FDG hypometabolism (arrows - bottom right) along with preserved metabolic rate in the frontal cortex. Figure obtained from reference [66].

1.3.2– Genotyping in Alzheimer's Disease

1.3.2.1 – Apolipoprotein E4

A current biomarker benchmark of the disease is the genotyping for at least one ε4 allele which codes for the E4 isoform of the protein apolipoprotein E (ApoE). The ApoE protein is coded by an allele pair, which can be made up of any combination of ε2, ε3 or ε4. Results have shown that individuals who carry at least one ε4 allele in the pair are at increased risk of developing AD.

In one study investigating the diagnosis of AD in a patient cohort of 2188, consisting of both AD patients and those suffering from other forms of dementia, it was found that 65% of those who were pathologically diagnosed with AD at autopsy held one of the alleles. Results concluded that the genotyping the alleles on their own currently does not hold the required diagnostic power (sensitivity and specificity against controls of 65% and 68% respectively), however when used in combination with traditional clinical diagnosis such as the NINCDS-ADRDA criteria, it can improve diagnosis specificity, particularly against other dementias from 55% to 85% [68].

Further research presented and discussed in a review by Ashford [15], shows the increased relative risk of the diagnosis of AD in those carrying the ε4 allele. The review presented data from two population studies and reported a large relative risk of AD when one or two ε4 alleles are inherited. Data that was presented in the review, taken from a publication by Saunders et al [69] described a relative risk of 2.07 for an allele pair combination of ε3+ε4 and 7.50 for presence of allele pair ε4+ε4. This compares with a relative risk of ε3+ε3 (0.58), ε3+ε2 (0.31) and ε2+ε2 (0.00). Similarly data presented by Farrer et al. [70] suggested a relative risk of ε3+ε4 of 1.92 and for ε4+ε4 of 8.22. Again the comparative risk of other allele

combinations ε3+ε3 (0.6), ε3+ε2 (0.38) and ε2+ε2 (0.25) was reduced. Interestingly, results show that when an individual carries the ε2 and ε4 in combination (ε2ε4), the overall effect is a reduced risk of AD incidence. For example, the relative risk for ε2+ε4 was 1.00 and 0.52 in the two data sets discussed above [69, 70]. It is currently thought that the presence of ε2 has a protective effect on AD development, although the exact mechanism is not clear.

A full understanding of ApoE with regard to the increased risk of AD has not yet been fully elucidated, however current research has shown that the ApoE protein is linked to the regulation of Aβ, with research showing that ApoE protein promotes its degradation [71]. Further results in the study suggested that the ApoE protein from the ε4 allele is less efficient at catalysing the reaction than other variations of the lipoprotein and, therefore, presence of the allele may be in part responsible for the build-up of Aβ [71]. Further evidence in the literature suggests that ApoE is involved in the regulation of the γ-secretase cascade and, therefore, it may influence the ratio of Aβ isomer ratios [16].

However, despite the research on ApoE genotyping it is still not common place in AD diagnosis and instead is more utilised in the research environment. This is mainly because of its limitations when it comes to disease prediction, but also because of psychological effects that results have on patients, particularly those who are asymptomatic, and the resulting effect on their treatment management [72].

1.3.3 – Lead Protein Markers in Alzheimer's Disease

The proteins Aβ and tau, which are considered to be a cause of much of the AD pathology, have also been mooted in the literature as potential biomarker candidates. Although it is well documented that accumulation of the proteins in

the brain is a common result of the disease pathology, it is clearly currently unfeasible to take a biopsy of brain for diagnostic testing purposes. It is for this reason that definitive diagnosis can currently only be achieved post mortem. Therefore, for a protein biomarker such as tau and Aβ to be useful in a clinical environment it must be shown to be present and detectable in a periphery biofluids which can be obtained via a relatively non-invasive procedure such as urine or plasma (although CSF has also been the source of research).

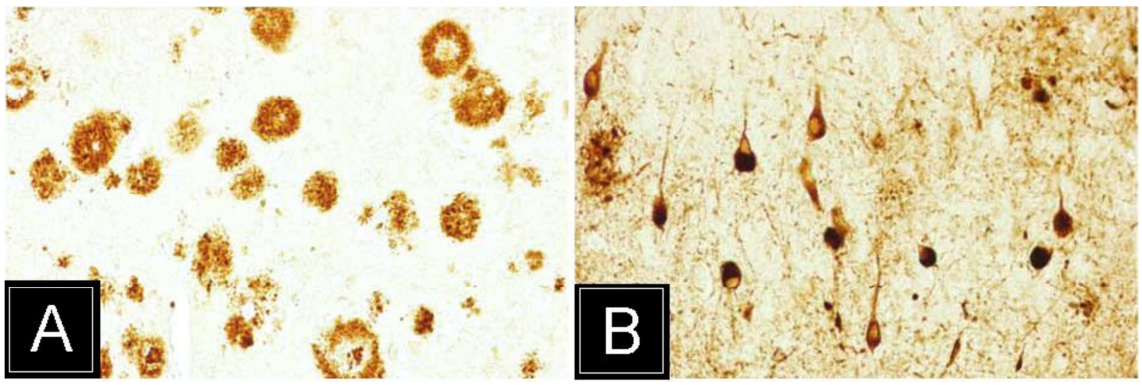

Figure 1.5: Protein Deposits in Alzheimer's Disease
Histopathology imaging of an example brain from a patient suffering from Alzheimer's disease (AD). Following immunohistological staining of post mortem brain tissue, the major protein deposits in the brain can be observed as brown lesions demonstrating **(A)** Amyloid β (Aβ) senile plaques and **(B)** phosphorylated tau (p-tau) tangles.
Figure adapted from reference [5]

1.3.3.1 – Amyloid β

Aβ is one of the major proteins associated with AD, as it is known to form the protein plaque deposits in the brain that are traditionally associated with the disease (Figure 1.5). The full mechanism of Aβ toxicity is unknown, however it has been suggested that once released from APP the protein undergoes conformational changes, which result in the shift from a soluble form to large fibril clusters which eventually develop into the plaques [73]. Braak and Braak first described the pathology and progression of amyloid deposition in AD. They observed initial

deposits of Aβ accumulating in the basal regions of the cortex, with subsequently spreading in a gradual pattern to the most associative neocortical areas with the sensory and motor areas being significantly affected in late stage AD [74]. As well as accumulation of Aβ in brain tissue, observations have also been made reporting Aβ deposits in blood vessels in the brain, which are termed cerebral amyloid angiopathy [75].

Aβ isomers range from Aβ39-42 and differ in their tendency to form plaques, with $Aβ_{42}$ identified as the least soluble and therefore considered the most prone to plaque initiation in brain tissue [76, 77]. However, interestingly, it has been reported that $Aβ_{40}$ is the isomer form that is most prone to aggregation in cerebral amyloid angiopathy [78]. The Aβ plaques have been reported to be neurotoxic causing neuronal death in the brain [79, 80], hence the gradual decline in cognition associated with the disease.

As Aβ I plays such a pathological role in AD isomers of the protein have been investigated as biomarkers for the disease. To date, analysis of Aβ levels in plasma and urine have been inconsistently reported in the literature [81, 82], with the most promising findings obtained from analysis of CSF [56, 83-85]. Although CSF is not a perfect biofluid due to the difficulties and discomfort experienced by patients during collection, it is the closest biofluid to the brain and therefore, is likely to better reflect brain pathology than more peripheral fluids.

Interestingly, studies have reported a decrease in CSF $Aβ_{42}$ in those patients with AD when compared with controls [83-85]. This reduction is thought to be because of the plaque formation of $Aβ_{42}$ in AD patient brain, and therefore is not available for circulation in the CSF [83]. The use of $Aβ_{42}$ levels has been reported to provide sensitivity and specificity values of up to 85%. However, its use in a diagnostic

environment has been hampered due to the fact that a reduction in values has also been observed in other variants of dementia, for example Lewy body dementia [86], vascular dementia [87] and frontotemporal dementia [84].

1.3.3.2 – Tau

The protein tau is also known to form deposits in the brains of AD patients when it becomes abnormally phosphorylated. These are described as neurofibrillary tangles, as they take on a more fibril structure (Figure 1.5). Tau deposits are found inside neuronal cells, again highlighting why complete diagnosis can only occur post mortem. Links between tau and Aβ are unclear but it has been suggested that abnormal ionic homeostasis and an increase in oxidative stress following Aβ plaque formation alters the balance of those enzymes responsible for the regulation of tau [5, 88]. This has been shown to lead to tangle formation followed by synaptic dysfunction and axonal loss [89]. It is therefore no surprise that tau and phosphorylated tau (p-tau) have been investigated as a biomarker for AD and is currently regarded as a lead candidate.

Again CSF has demonstrated the most promising results, with a number of publications reporting increases in both tau [83, 87, 90, 91] and p-tau [87, 91-94] in the CSF of patients suffering from AD, with sensitivity and specificity shown to reach levels of up to 90% and 80% respectively when compared with controls and other forms of dementia [93]. However, the literature raises concerns about the use of tau in a diagnostic capacity as it has been identified at significantly increased levels in patient CSF in other conditions including variations of dementia [87, 90], stroke [95], multiple sclerosis [96] and those patients with brain tumour [97].

To overcome the previously discussed disadvantages encountered when using Aβ and tau as individual biomarkers, analytical results of the two proteins has often

been combined in an attempt to improve the diagnostic sensitivity and specificity, with promising outcomes [98]. An assay that utilises Aβ, tau and p-tau has made it to the market and manufactures claim a sensitivity of 90% and a specificity of 80% [56].

However despite the commercial availability, uptake of the procedure has been reported to be poor [56], and this is likely to be caused by two main factors. Firstly, as previously mentioned, CSF is not an ideal biofluid, requiring collection via a procedure requiring specialist personnel, whilst being extremely uncomfortable for the patient. Furthermore the commercial assay is extremely expensive at 1075USD per sample (as quoted in reference [56]). However, this is likely to be an inflated cost estimate, due to the commercial nature of the for profit American private healthcare market. Typically, ELISA techniques have a far lower "cost" price, and may be an affordable option if adapted for a hospital/clinical testing environment.

This report suggests a growing need for more accessible biomarkers, for example in urine or circulating blood that can be collected and analysed at a much lower cost.

1.3.3.3 – Blood or Urine Based Biomarkers

Biomarker research in non-invasive tissues such as blood or urine has thus far not been as promising as those identified via the approaches described in brain and CSF. $A\beta_{42}$ is one of the most frequent references in the literature, appearing in both plasma [82, 99] and urine [81] based studies, but publications have returned inconclusive results. For example, some groups have reported an increase in $A\beta_{42}$ in the plasma of AD patients [82, 100], whilst others have noted no significant change [101-103] and a recent publication has even reported a reduction in plasma $A\beta_{42}$ [104].

The conflict in results described above is interesting and highlights the need for preliminary results to be confirmed by an independent laboratory. However, when comparing different publications, such as these, the design of the study should be scrutinised. Recently, there have been discussions in the literature with regard to the evolution of study design in AD [105]. Predominantly in the literature, studies are completed in a traditional case(AD)-control design, with distinct patient classes, termed cross sectional. However, recently, alternative approaches have been presented for the identification of biomarkers that aim to reflect disease state [105]. These alternatives are of particular importance in diseases such as AD, which develops over a long preclinical phase, and therefore there is a growing consensus that a proportion of controls are likely to have some degree of the early stages of AD pathology even in the absence of clinical symptoms [105].

An example of an alternative approach is termed longitudinal study design. In this instance patient samples are collected at the first visit (termed baseline) and then at various time points throughout disease progression, thus enabling a picture to be painted of potential markers over time.

Studies that employ traditional case-control and longitudinal study designs can produce alternative interpretations using the same biomarker candidate. An example of this can be found when comparing the previously cited publications regarding plasma levels of $A\beta_{42}$. As previously mentioned the majority of cross sectional publications report no statistical differences when comparing AD patient plasma with control plasma [101-103], however when analysed using a longitudinal approach higher plasma concentrations of $A\beta_{42}$ were found in those patients who started the study as a control, but subsequently developed AD, than those who

remained as controls [82]. A similar result was reported in a second more recent longitudinal study [100].

Further plasma based candidate biomarkers include the proteins clusterin [106], complement factor H (CFH) precursor [107] and $_{\alpha 2}$macroglobulin ($_{\alpha 2}$M) [107], all of which have demonstrated promising potential. However, in follow up studies the results have been disappointing with a recent publication reporting plasma clusterin as having no diagnostic potential [108].

Again however, the reported conflicting results are perhaps related to issues of study design previously discussed. However, despite the longitudinal studies described above offering an alternative to the traditional cross sectional design, they still employ a classic case-control classification scheme, extended over multiple time points. Therefore, there still exists the possibility that age matched controls may exhibit early AD pathology. Therefore, recent studies have begun to correlate potential markers to known disease pathology, such as brain atrophy and brain Aβ concentration via PET scan [109, 110]. This offers a further development in study design and moves away from rigid case-control structure.

The conflicting plasma concentrations of the clusterin, discussed above are an example of this in action. In classic case-control experiments plasma clusterin has been reported to hold no diagnostic benefit when directly comparing between control, MCI or AD patient groups [108]. However, when investigating plasma clusterin using alternative disease progression points, the protein has been demonstrated to be associated with atrophy and Aβ burden in the entorhinal cortex, hippocampal volume and the rate of cognitive decline [106].

The implications of study design on result outcome are interesting, and highlight some of the challenges faced in the search for reliable markers of AD. In addition to research groups beginning to innovate in study design, work is being completed combining marker panels in an attempt to improve accuracy of diagnosis. A recent example of such is a biomarker panel of 18 markers incorporating both proteins (including ApoE, epidermal growth factor receptor (EGFR) and haemoglobin), and smaller molecules (including cortisol, calcium and zinc) [111]. However, a recent discussion piece in the Journal of American Medical Association (JAMA) has raised concerns regarding the use of this biomarker panel [112], due to the fact that an overlap of AD, MCI and controls was still observed, meaning no definitive classification could be achieved. Further to this, with a panel of 18 biomarkers, concerns were raised regarding the over fitting of data [112]. In addition, the panel was only validated between control, MCI and AD, therefore for progression into routine clinical use, there is a requirement for further validation against other forms of dementia and neurodegenerative disorders.

Another publication uses a similar biomarker panel approach. Coincidently, a 18 marker assay is again used as a predictor tool for AD. In this occasion the approach employs 18 signalling proteins such as interleukin-3 (IL-3), 1α (IL-1α) and 11 (IL-11), intercellular adhesion molecule-1 (ICAM-1) and platelet derived growth factor BB (PDGF-BB) [113]. The assay reported an accuracy of diagnosis of 90%. However once again early promise has not progressed to the routine clinical diagnosis environment, and a follow up study by an independent research group found a much lower rate of diagnosis of 63%, and, importantly, could not distinguish AD from other dementias [114].

1.4 – Small Molecule Biomarkers

As previously discussed, despite the extensive research already undertaken into biomarker discovery, currently no candidate, either individually or as a group, has been successful in fulfilling the required role and currently there is no laboratory test for the definitive diagnosis of AD in regular clinical use. Therefore, it is a reasonable conclusion that a different angle of investigation is worth pursuing. The answer may be found in a growing field in biomarker discovery which employs the use of small molecules as markers of disease.

1.4.1 – Definition of Small Molecules

Small molecule biomarkers (SMB) are classed as molecules of approximately <1.5KDa in size and generally involve metabolite molecules such as amino acids, lipids and sugars. In theory, small metabolites are ideal biomarkers due to the mechanisms of systems biology. A simplistic explanation for this is depicted in Figure 1.6. In summary, a single gene coding for a protein, for example an enzyme, can be transcribed to mRNA multiple times. In turn, each strand of mRNA can be translated many times into the relevant proteins. Finally, each resultant enzyme molecule could potentially lead to the catalysis of a large number of metabolic reactions resulting in an increase of small molecule metabolites. Due to the various levels of amplification in the process, any imbalances at any stage of the cascade may be highlighted, resulting in the discovery of SMB capable of disease diagnosis.

A simplified example of SMB in a clinical setting is in the case of type II diabetes mellitus. To briefly summarise, in the disease a resistance to the hormone insulin develops. Under normal circumstances in the liver, insulin levels regulate glucose levels by inhibiting glucose metabolism and its release from cells. However, in

patients with insulin resistance, the liver inappropriately releases glucose into the blood amplifying the signal, which can then be measured and used in a clinical environment to diagnose the disease [33].

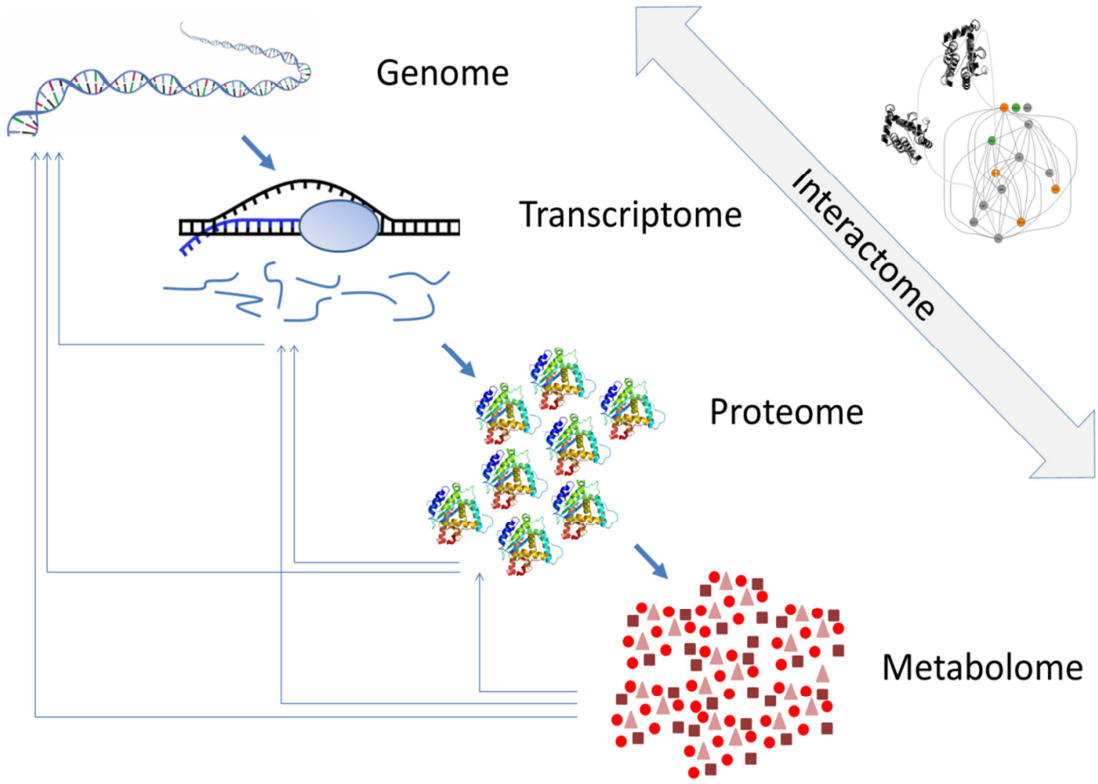

Figure 1.6: Overview of Systems Biology

A simplified overview of systems biology, highlighting the potential advantages of small molecules. At each stage of the process amplification can occur.

In addition the products of the metabolome can interact upstream, with genetic processes or with proteins, for example signalling. Identifying these interactions and imbalances within the metabolome may lead to the discovery of biomarker candidates suitable for the diagnosis of diseases such as AD.

A further potential advantage of the discovery of plasma SMB, especially in AD, is with regard to the blood brain barrier (BBB). Despite evidence in the literature to suggest the BBB is more permeable in patients with AD [115-117], the BBB is still an important consideration when investigating plasma based biomarkers of AD, as the primary disease site is the brain. Therefore, for any candidate molecule to

accurately reflect brain pathology it may be advantageous for markers to be able to cross the BBB. Small molecules are considered advantageous for this compared with larger protein molecules, especially those lipophilic molecules which are more suited to crossing [118].

1.4.2 – Targeted Biomarker Discovery

Method development for biomarker discovery tends to take one of two approaches. Firstly, a targeted (hypothesis driven) approach can be made where the study is designed using a hypothesis based upon a specific molecule or group of molecules. These then undergo specific analysis with a methodology designed with a target in mind.

1.4.3 – Non-Targeted Biomarker Discovery

Secondly, a non-targeted or top-down strategy can be used, which sets out to analyse a biofluid non-discriminately, identifying any differences in the concentrations of molecules detected.

This hypothesis generating style of analysis has become increasingly important, especially as over recent years our traditional view of metabolism has altered from a simple linear structure to a more complex network, with many intracellular outcomes still not fully understood. As non-targeted metabonomics/olomic studies improve and the discipline becomes commonly practised, data will be ideally combined with parallel genetic and proteomic studies to give us an overall picture of systems biology and the whole network processes (Figure 1.6).

In order for a non-targeted approach to be interpreted in a reliable and useful manner the analysis of the raw data is heavily reliant on rigorous data processing methods followed by a series of mathematical models, for example partial least

squares [119], which are capable of grouping samples dependant on the severity of a disease differences, and highlighting any metabolite differences between the disease classification groups.

These differences can then be identified, leading to the potential discovery of novel marker metabolites related to disease states. An extremely informative table describing the various forms of data treatment and chemometric approaches available in metabolomic studies was compiled in a review by Madsen et al [120] and can be found in Table 1.1.

Technique	Typical use	Description and comments
Univariate Testing [121]	Identification of potential biomarkers	Univariate analysis where the corresponding p-values are the standard scientific measure of significance. Multiple testing is prone to false positives unless corrected significance limit is used
Principal component analysis (PCA) [122]	Data overview	Standard multivariate analysis method to provide an overview of a large dataset. Useful for identifying outliers, clusters and trends in the data. Is not a classification method
Soft independent modeling of class analogy (SIMCA) [123]	Classification (supervised method)	PCA model of each class, good prediction capabilities especially for inhomogeneous classes (class size and variance). Less straight forward interpretation of potential biomarkers compared with LDA, PLS-DA or OPLS-DA
Linear discriminant analysis (LDA) [124]	Classification and biomarker identification	Discrimination method related to multiple linear regression. Number of variables must be smaller than the number of observations
Partial least squares discriminant analysis (PLS-DA) [125, 126]	Classification and biomarker identification	Classification variant of PLS. Works best with homogeneous classes. Biomarker identification possible, but not as straight forward as with OPLS-DA.
Orthogonal projection to latent structures discriminant analysis (OPLS-DA) [127]	Classification and biomarker identification	Classification variant of OPLS method. Ability to separate between-class from within-class variability. Straight forward interpretation and identification of potential biomarkers
Neural networks (NN) [128]	Classification (non-linear)	High flexibility in modeling non-linear data, but prone for overfitting. Potential biomarker identification more complicated
Self organizing maps (SOM) [129]	Clustering method	A neural network based method for identifying trends and clusters in the data. Can account for non-linearities in the data. - not there in the other descriptions.
Support vector machines (SVM) [130]	Classification (non-linear)	High flexibility in modeling non-linearities. Careful model selection reduces possibility of overfitting. Potential biomarker identification more complex compared with linear methods,, except when linear variant is used (LS-SVM)

Table 1.1: Data Analysis Methods in Metabolomics
Data analysis methods frequently employed for disease diagnosis and biomarker identification in metabolomic experiments. Table and references obtained from reference [120].

Non-targeted approaches are becoming more popular, with an increase in demand for hypothesis generating results. Many publications are now available covering different conditions and disorders. However, it is still a relatively new technique and disadvantages exist. Firstly, the greatest issue is the problem of interference. The concept of the non-targeted approach is to extract and analyse a wide range of molecules as possible. However, due to the nature of biological systems, metabolites exist at a wide range of concentrations and exhibit a number of physiochemical properties. This can make extraction and analysis difficult, for example the extraction of highly abundant molecules may require a dilution step for accurate analysis, but those molecules at a low concentration will be diluted to below the limit of detection. This can result in features being masked and overlooked. Additionally, when extracting samples in a non-targeted manner, problems can arise in the LC-MS analysis, with co-elution of features resulting in mass spectrometry effects such as ion suppression.

To counter this, improved separation techniques are required, for example by use of chromatography, or by specialised extraction techniques (See Chapter 4 for further investigations in this area).

Further drawbacks include the cost, which can be elevated due to the increased time of project compared with targeted approaches. This additional time comes in the form of the increased data treatment and statistical modelling required. In addition, further adding to the time of the study is the length of time required to confirm any molecules of interest. To date few groups have attempted non-targeted techniques in AD biomarker discovery, although this is changing rapidly.

The following sections contain an overview of the analytical techniques employed to investigate small molecule variation within AD, and examples of how they have

been applied to both targeted and non-targeted study designs, with a summary of the results reported.

1.5 – Analytical Techniques in Small Molecule Biomarker Discovery

The investigation of small molecules with regard to AD is a rapidly growing field. A wide range of techniques have been published with the aim of investigating small molecule variation in AD, with vast improvements in recent years in the sensitivity and selectivity of analytical technologies including nuclear magnetic resonance (NMR), ultra-high performance liquid chromatography (UHPLC) and mass spectrometry (MS). Not one technique is perfect and often a compromise has to be taken depending upon a range of criteria including speed, cost, properties of the analytes, sensitivity and the biofluid employed. These approaches are now discussed below, with advantages and disadvantages with regard to each technique and are summarised in Table 1.2 found at the end of the section.

The subsequent sections 1.6 and 1.7 then discuss examples of how these techniques have previously been applied to investigating small molecule variation in AD. A summary table of these findings can be observed later in Table 1.3.

1.5.1 – Nuclear Magnetic Resonance (NMR)

NMR has become a highly useful and widely used analytical technique. It works on the principle that individual atoms absorb a specific frequency of electromagnetic radiation when under the influence of a magnetic field. The basic theory behind the technique is based upon a property that certain common atomic nuclei, such as ^{1}H, ^{13}C, ^{15}N, ^{19}F, ^{29}Si and ^{31}P have, enabling them to "spin". This "spin" property also results in the nuclei alignment when placed under a magnetic field. Radio frequency radiation is then applied to the sample which has the effect of providing energy that is absorbed, and therefore excitis the atoms, switching the nuclei between aligned and non-aligned states. The frequency required for exciting each

nuclei is highly specific for certain chemical structures, which can then be measured and recorded allowing structural elucidation and the chemical identification of molecules present.

A further advantage of NMR is that it is capable of analysing tissues in a non-destructive and highly reproducible nature, often without the requirement of pre-treatment such as metabolite extraction.

However, the technique has some disadvantages which currently restrict NMR research. The first and most important of which is its relative insensitivity, especially when compared with mass spectrometry methods (discussed in Section 1.5.3), which can impose heavy restrictions on the range of molecules that can be analysed.

A second disadvantage is that although the technique is capable of whole sample non-destructive analysis, in some instances pre-processing of the samples is still required. For example those samples which contain high concentrations of water and are being analysed via ^{1}H NMR technology can sometimes require water removal prior to analysis, as the high number of hydrogen atoms otherwise present in water molecules interfere with the spectra [131]. However, use of variations of NMR such as ^{13}C, ^{15}N, ^{19}F, ^{29}Si and ^{31}P, is not effected by water content as they are not focused on ^{1}H atoms, and therefore do not require this pre-treatment.

A further significant weakness of NMR is that within biological samples concentrations of molecular components are naturally variable. As NMR generally analyses whole samples, the molecules found at high concentrations can overlap

those present at much smaller concentrations, meaning many potential biomarker candidates can be overlooked.

Moreover, the high cost of purchasing and maintaining an NMR can mean the approach is an expensive option. Couple this with the fact that it can be difficult to interpret NMR spectrum unless specially trained expertise is employed, then the cost can escalate dramatically.

However, despite these limitations the technique is still an extremely valuable biomarker tool, providing fast non-destructive analysis, which can lead to reliable structural elucidation of marker molecules.

1.5.2 – Magnetic Resonance Spectroscopy (MRS)

MRS is a similar technique utilising the theory of NMR combined with magnet resonance imaging (MRI), enabling quantification of metabolites in vivo via a scan of the live patient (usually the brain). An interesting review of the MRS technology with a view to small molecule and biomarker discovery has been compiled by Gujar et al [132] and describes the approach in further detail. MRS is a useful technique for the identification of marker molecules as it is relatively non-invasive and no biofluids have to be collected; however there are also limitations to the technique. Interference is a major problem, particularly when scanning adjacent tissues which have major differences in magnetic susceptibility, for example brain tissue and bone, therefore scans of areas such as the base of the skull are very difficult to obtain [132]. The technique also has difficulties in producing spectra from mobile tissues such as peripheral blood or cardiac muscle and therefore is of no use in identifying peripheral biomarkers for AD [132]. As the brain, however, has a mainly homogenous construction and lacks any real movement a spectrum is achievable [132].

1.5.3– Mass Spectrometry (MS)

1.5.3.1 – Direct Infusion Mass Spectrometry (DI-MS)

Mass spectrometry (MS) is a widely used technology which offers unequalled sensitivity in small molecule analyte detection, and can enable metabolite identification and quantification. Initially, the mass spectrometer provides the analyte with a charge, via a process known as ionisation, which occurs in what is termed as the source. Following this, the ions produced are transferred to a gas phase. If samples are injected into the DI-MS in solvent a drying gas is applied to evaporate any liquid.. This enables the manipulation of the ions by the application of either electric or magnetic fields to enable separation within a mass analyser. A mass analyser can come in many forms, for example time-of-flight (TOF), triple quadrupole (QQQ) or ion trap (TRAP). Mass analysers are able to separate ions by their mass to charge ratio (m/z). Finally, a detector records the electronic current generated when a charged particle hits the detector to obtain a mass spectrum. Mass spectrometry is a highly useful technique due to its high specificity, sensitivity and ability to identify biomarker candidates, either through database matching, fragmentation patterns or via comparison to external or internal standards.

However, there are some disadvantages which are associated with MS. One such disadvantage of the technique is known as ion-suppression, which occurs in the ionisation stage of the analysis. This is an analytical effect which can occur when a large number of different species enter the source and consequently compete for charge and ionisation. This can inhibit the ionisation efficiency of some molecules in the mixture, meaning they can go to waste, without undergoing detection. However, it should be noted that ion suppression is not a certainty and depends on

the competing analyte in the source, the design of the source and other variables such as mobile phase used and ionisation polarity. Often this is overcome by the addition of a separation technique such as chromatography prior to MS detection (discussed below Section 1.5.3.2).

A second disadvantage when compared with NMR is that whole samples cannot be analysed without extensive pre-treatment. It is a requirement of the technique that analytes must be extracted from the biofluids into a compatible solvent prior to analysis, which can lead to an increase in analytical variation [133].

Within the literature, MS is widely used in targeted small molecule and metabolite biomarker identification due to its sensitivity, relative ease of use for quantitation and ability to detect a wide range of analytes. The technique can be utilised as standalone and referred to as direct infusion (DI) [134], or coupled to a chromatographic system such as gas chromatography (GC) [135, 136] or liquid chromatography (LC) [137-139].

1.5.3.2 – Chromatographic Separation Prior to Mass Spectrometry

LC utilises a solid stationary phase housed within a stainless steel column (typical length ≤150mm and ID ≤5mm). The column is filled with porous particles, normally consisting of a silica bead base with a bonded molecular side chain on the surface. This side chain is selected depending on the mixture of analytes for separation. For example, C_{18} or C_8 are commonly selected for the separation of non-polar compounds. This is termed reversed-phase chromatography.

Liquid solvent is then passed through the column at a high pressure. Components of a molecular mixture travel down the column at different rates depending on their interaction with both the stationary solid phase and the mobile liquid phase.

For example, in reversed-phase LC a polar compound will interact with a mobile phase with a high percentage aqueous content, rather that the non-polar carbon chain stationary phase. Therefore the transition through the column is relatively quick. Conversely a non-polar compound, for example a lipid with a long carbon side chain, will interact more with the non-polar stationary phase, and its transition along the column will be slower. Hence the two compounds elute off of the column for MS detection at different times and a separation is achieved.

GC works in a similar way, however, the liquid mobile phase is replaced with an inert gas (helium or nitrogen are typical) and the stationary phase column is replaced with a longer stainless steel or glass column which contains either a stationary solid or a stationary liquid phase. The separation occurs within an oven and is based upon analyte volatility, with the more volatile compounds eluting faster. Separation can be refined by ramping the temperature from low to high. Therefore, those compounds that are more volatile at lower temperatures will progress along the column and elute earlier.

Complex mixtures require greater separation and this can be achieved by increasing the analysis time or by using a solvent gradient in LC or a temperature gradient in GC which introduces variable separation conditions enabling greater control of component elution. However, the introduction of a separation technique does have the disadvantage of adding time to sample analysis.

With GC a further step of analysis is required as it is only suitable for volatile compounds, therefore often an extra derivatisation step is required, increasing analyte volatility. This is a disadvantage to the technique as it introduces a further step in the sample preparation which not only increases analysis time but increases the chance of analytical variation.

However, the increased sensitivity of the techniques makes separation a necessity in SMB analysis, especially due to the low trace levels and varied concentration range involved in the nature of the work. The technology is continually advancing, in particular recent advances in LC have greatly improved speed, resolution and sensitivity [133]. This is discussed in further detail in Chapter 4.

1.5.4 – Alternative Small Molecule Analytical Techniques

1.5.4.1 – Chromatography with Alternative Detection

Despite reducing costs mass spectrometry is still generally considered to be an expensive approach. However there are alternative detectors available which can be coupled to LC instruments that are often more affordable and still capable of investigating small molecules from biological tissues.

An example is ultra violet (UV) detection. UV light is absorbed when molecules that contain a chromophore region in their structure pass though the detector. The higher the concentration of molecules, the more UV light is absorbed and therefore the greater the response recorded. Generally UV detectors are very cost effective and easy to obtain. However they have two major disadvantages compared with MS methods: less sensitivity and specificity. Further examples of LC detection include electrochemical (EC) and fluorescence.

Due to the low specificity that alternative detectors possess, methods developed using them are only suitable for targeted analysis.

1.5.4.2 – Immunoassay

Immunoassays come in a variety of formats however the theory behind them is similar. They employ an antibody labelled by the addition of a fluorescent or radioactive tag. The antibody is specific for the molecule of interest and binds to

any molecules which are present. The sample is then washed to remove excess material and viewed under the appropriate detector, with the intensity of detection directly related to the concentration of target molecule present.

A wide range of immunoassay technology and design is available. One of the most widely used is termed an enzyme-linked immunosorbent assays (ELISA). ELISAs work on the principle of binding an enzyme to an antibody designed for a specific target. Examples of enzymes used include horseradish peroxidase, alkaline phosphatase or glucose oxidase. Following antibody binding to a target, the enzymes allow for detection because of an observable colour change in the reagents which are catalysed by the bound enzyme. In some cases these enzymes are exposed to reagents which cause them to produce light or chemoluminescence. An example of the principle behind ELISAs can be found in Figure 1.7.

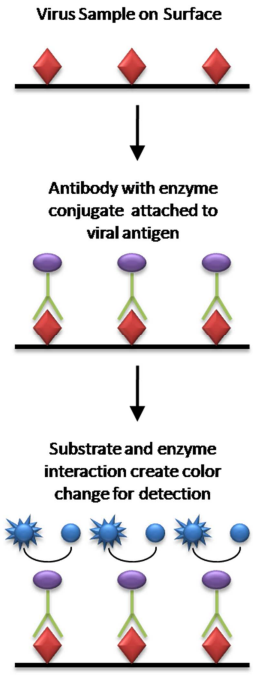

Figure 1.7: Example of ELISA Immunoassay
Principle theory behind an ELISA immunoassay. An enzyme covalently bound to an antibody is prepared for a specific target. The antibody binds to its target, and a reagent is added to the plate. The enzyme catalyses a conformation change of the reagent, resulting in a detectable colour change. Image reproduced from [140].

Alternatives to enzyme linked immunoassays include antibodies bound to radio-isotope and fluorescent tags. The same principle applies, however detection is via radioisotope detection, or measurement of fluorescence.

In addition to the variety of detection tags, there are a number of different antibody methods that can be used in immunoassay analysis. For example, in Figure 1.7, the target virus is found on the surface of the plate. The enzyme bound antibody is then added and binds to the target, and is termed a direct immunoassay. Alternatives include indirect, where a secondary antibody is first introduced and binds to the target molecule. Finally a tagged antibody then is added to the assay and targets the initial antibody/target complex. This is referred in the literature as indirect immunoassay.

A further approach that is found in the literature is termed sandwich immunoassay and involves "capture" antibodies bound to the plate surface. When molecules in solution are added, the targets are bound to the "capture" antibodies. The plate undergoes a wash step to remove undesired molecules, before the tagged antibody is added, and detection and measurement is made.

The highly specific nature of immunoassays enables their use as a suitable technique for targeted metabolite biomarker identification; furthermore, the assays are capable of quantification analysis when coupled to the labelled tags. Despite incurring some disadvantages, including the high cost of some forms of commercial assays and the relatively slow development and low throughput of analysis, there are instances within the literature where immunoassays have been used to quantify small molecules in biological samples from AD patients.

Due to their nature immunoassays are only suitable for targeted biomarker discovery.

Analytical Technique	Targeted or Non-targeted Analysis	Strengths	Limitations
Nuclear Magnetic Resonance (NMR)	Both	• Provides detail on chemical structure • Good for metabolite identification • Can analyse whole biological samples • Highly reproducible	• Relatively insensitive • High instrument and operation costs • Specialist operator required • High concentration metabolites can mask those with small concentration
Magnetic Resonance Spectroscopy	Both	• *In vivo* technique – 100% non-invasive • Provides detail on chemical structure • Good for metabolite identification • Highly reproducible	• Interference between adjacent tissues • Cannot produce spectra in mobile tissues (e.g. blood) • Instrumentation can be confusing/frightening for elderly (especially dementia patients) • Relatively insensitive • Highly expensive • Specialist operator required
Direct Infusion Mass Spectrometry (DI-MS)	Both	• Highly sensitive • Fragmentation provides some structural data • Confirmation possible with comparison to standards • High throughput	• Samples must be pre-treated to extract metabolites • Interference and ion-suppression issues • Less structural information than NMR and MRS
Liquid Chromatography-Mass Spectrometry (LC-MS)	Both	• Separation prior to MS reduces interference and ion-suppression • Easy to operate • Highly sensitive • High selectivity • Confirmation possible with comparison to standards • Fragmentation provides some structural data	• Samples must be pre-treated to extract metabolites • Less structural information than NMR and MRS • Separation adds time to analysis, especially with complex non-targeted approaches • Generates high quantities of organic solvent waste – can be expensive to dispose of
Gas Chromatography-Mass Spectrometry (GC-MS)	Both	• Separation prior to MS reduces interference and ion-suppression • Easy to operate • Highly sensitive • High selectivity • Confirmation possible with comparison to standards • Fragmentation provides some structural data	• Samples must be pre-treated to extract metabolites • Extra time consuming derivatisation step also a necessity to increase analyte volatility • Less structural information than NMR and MRS • Due to high temperatures molecule stability issues can arise • Aqueous solutions and salts cannot be injected into the instrument • Separation time can be lengthy
Liquid Chromatography-Non-MS Detection	Targeted	• Considerably cheaper than LC-MS • High throughput methods can be developed • Easy to operate • High selectivity	• Poor sensitivity • Poor specificity • Samples must be pre-treated to extract metabolites • Generates high quantities of organic solvent waste – can be expensive to dispose of • No structural information – must be compared with standards • No non-targeted approach possible
Immunoassays	Targeted	• Highly specific antibody approach • Highly sensitive • Relatively easy to complete • Can pre-buy many "kits" for specific molecule identification	• Can be expensive • Only targeted analysis possible • Low throughput

Table 1.2: Analytical Techniques in Small Molecule Biomarker Discovery

Summary table comparing the various analytical techniques available to small molecule biomarker discovery and Alzheimer's Disease. Discussed are the approaches available to the technique as well as the strengths and limitations of each technology. Table reproduced from publication by Whiley and Legido-Quigley [141].

1.6 – Literature Review of Targeted Alzheimer's Disease Biomarkers

The following section discusses the available literature on AD, which has investigated variations in small molecular species in a variety of tissues and biofluids.

1.6.1 – Nuclear Magnetic Resonance and Magnetic Resonance Spectroscopy

Typically the brain is the main tissue of study when using NMR and MRS in AD research. Due to the nature of the techniques, NMR tends to be used to analyse post mortem brain homogenates, whilst MRS is generally used to scan the brains of living patients. Considering that the brain contains the second highest concentration of lipids in the body (after adipose tissue) it is of no surprise that a constant reoccurring factor in the literature is the apparent abnormal presence of lipids and their metabolites in samples of AD patients.

An example of this in the literature utilised a ^{31}P-NMR approach and reported differences in post-autopsy brain membrane phospholipids. Results suggested significant reductions in total phosphatidylethanolamine (PE) and phosphatidylinositol (PI) compounds, as well as increases in sphingomyelin (SPH) and phosphotidylethanolamine-plasmalogen (PE-P) [142].

Neuronal acids and their metabolites also regularly occur in AD biomarker literature. As discussed in Section 1.3.1, the aspartic acid metabolite, *N*AA, has been suggested to be helpful in the diagnosis of AD in combination with imaging data. Use of *N*AA was investigated as a marker for AD as it is considered a neuronal marker thought to reflect condition and integrity of neurons [143]. This is

a typical approach to designing a targeted analysis investigation. Studies which apply NMR and MRS targeted methodologies have demonstrated a significant decrease in the levels of *N*AA in a number of brain regions [144-146] suggesting neuronal damage.

However, a challenge in using metabolite concentrations such as *N*AA is that it can be difficult to comprehensively quantify in vivo using NMR/MRS as there is no access to an internal standard. To combat this, biomarker studies often focus on *N*AA ratios with creatine [143], although it should be noted that worryingly for the accuracy of studies, creatine has also been identified at increased levels in AD patients [146]. Within the literature, there are a number of examples which demonstrate reductions in the *N*AA/creatine ratio when comparing AD with control subjects in different brain regions [147-151].

A further small molecule metabolite of interest in AD is the carbohydrate myo-inositol (MYO-IN). MYO-IN is abundant within the brain and has been shown to exist at significantly increased levels in the brains of AD patients via the use of MRS [146, 152]. As with *N*AA, when MYO-IN is analysed via MRS, ratios with other small molecules are often used to enable quantification. The ratio between MYO-IN/creatine and *N*AA/MYO-IN has been shown to significantly change in those patients who suffer from AD [148, 151, 153].

Metabolite ratios have also been analysed in a recent ^{1}H-MRS study which identified a reduction in glutamate in the hippocampus region of patients with AD. Three groups of patients underwent analysis; controls, MCI and AD. As with previous targeted methods which employed MRS, metabolite ratios were also calculated reporting decreased glutamate/creatine, glutamate/MYO-IN, glutamate/*N*AA, and *N*AA/creatine ratios in AD compared with control. The article

also reported reduced glutamate/MYO-IN ratio in AD compared with MCI [154]. This finding suggests potential for the metabolites to be used as a marker for AD, particularly if significant changes are observed between AD and MCI.

As previously discussed in Section 1.2.3, an advantage that an accurate laboratory biomarker can provide is the ability to track the response to treatment. An example of this in action is the use of the *N*AA/creatine in the investigation of the effects of Rivastigmine treatment in AD. Rivastigmine is an acetylcholinesterase inhibitor designed for patients with mild to moderate AD. AD is known to have a number of cholinergic deficits, which inhibit the signalling effect of acetylcholine [155]. Treatment with acetylcholinesterase inhibitors prevents the metabolism of acetylcholine, therefore increasing its bioavailability, and improving signalling function.

The ratio of *N*AA/creatine was monitored throughout rivastigmine treatment via MRS of the brain, with results showing a significant increase in the *N*AA/creatine ratio in patients taking the drug compared with those without. The publication concluded that MRS may be suitable for the future monitoring of response of patients undergoing treatment programs [156].

The literature currently contains no targeted studies which use plasma or urine as the source biofluids, possibly because of the relative insensitivity of NMR as an analytical technique and the relatively low concentrations of small molecule biomarkers found in these biofluids; however this may change as NMR technology improves.

1.6.2 – Mass Spectrometry

Examples of MS in the literature are frequent with regard to targeted analysis in AD. Many examples use DI-MS, which has been used to demonstrate a number of lipid abnormalities in AD.

An investigation into a lipid extract of post mortem brain material identified a significant decrease in the subclass of glycerophospholipids known as plasmalogens. This decrease was particularly apparent in extracts of white brain matter where the total plasmalogen level was approximately 40% lower in AD than in control patients. In grey matter a decrease was also witnessed, although not as extreme with a decrease of approximately 10%. Interestingly correlation between disease severity and plasmalogen level was significantly apparent in the grey matter, with levels decreasing in accordance with increased severity. In contrast, in white matter levels quickly decreased and remained relatively constant regardless of AD severity [157]. These findings are of particular note as plasmalogens are a major component of nerve tissue, with the ethanolamine plasmalogens sub-group responsible for approximately 32% of total phospholipids in myelin, the material which forms the outer layer (myelin sheath), around the axon of a neuron. It is essential for the proper functioning of the nervous system [158] suggesting loss within the brain may play a role in AD pathology.

Continuing the lipid imbalance theme, DI-MS analysis was previously completed on a lipid extract from from brain tissue taken from 22 subjects whose cognitive status at time of death varied from no dementia to very severe dementia to analyse levels of sulphatides (sulphated metabolites of the glycosphingolipid, galactocerebroside). Sulphatides are again found in the central nervous system, predominantly as a component of the myelin sheath [159] and were depleted up to

93% in the grey matter and 53% in the white matter of post-mortem confirmed AD patients compared with controls [160]. In the same study, a second potential galactocerebroside metabolite product, ceramide, was found elevated 3-fold in AD patients, further highlighting the irregularities in the metabolism of neuronal glycosphingolipids in the disease pathology [160].

Whilst results from these two brain studies are clearly not transferable to the clinic due to the impracticality of completing a brain biopsy in living patients, it is a clear example of how DI-MS can be used in a biomarker research capacity.

As well as abnormalities in lipid metabolism, disruptions in glucose utilisation [161, 162] and deficiencies in mitochondrial function [163] are thought to occur in AD, subsequently leading to an energy deficit within the brain. A GC-MS based study analysed patient CSF and investigated the concentration of a range of molecules that require mitochondrial metabolism, with results demonstrating that AD patients have an increase in CSF lactate as well as a decrease in CSF succinate and fumarate [164].

The process of oxidative stress, particularly the modification of lipids, is also thought to play a major role in AD pathology [165, 166], therefore GC-MS has been used with this in mind to identify biomarkers formed as a result of this free radical oxidation process. An ideal group of molecules for this purpose are isoprostanes that are chemically stable metabolites formed via the lipid peroxidation of various fatty acids during oxidative stress. GC-MS has been used to demonstrate an elevation of a number of isoprostanes in many biofluids including various brain region homogenates [136, 167], CSF [135, 136, 168-171], plasma [135] and urine [135, 172]. However, interestingly when using an LC-MS approach to analyse F_2-isoprostanes in urine, no significant differences were observed when comparing between AD

and control [139], conflicting with the results identified in the previously mentioned GC-MS study.

Isoprostanes have also been investigated as an example of a biomarker for use in the tracking of the response of a patient to therapeutic treatment. A GC-MS study was designed to monitor the therapeutic effect of antioxidant vitamin supplements on oxidative stress in AD. Those patients who were dosed with increased vitamin E and C showed less signs of isoprostane oxidative damage than those taking no treatment [173].

Oxidation of fatty acids in AD is also the cause of a significant rise in the levels of hydroxyoctadecadienoic acid, found via a GC-MS analysis of both plasma and erythrocyte extracts. Interestingly the level of hydroxyoctadecadienoic acid also correlated with patient clinical dementia ratings [174], again suggesting a possible role in tracking disease progression using this biomarker.

The neurosteroid dehydroepiamdrosterone (DHEA) is also thought to be susceptible to oxidative stress [175]. This theory was examined by applying GC-MS analytical methods to serum samples and resulted in the identification of a significant increase in 7-hydroxylated metabolites of DHEA in AD patients [176].

A further investigation into oxidative stress of lipid species has been completed using an LC-MS method. The method was designed to quantify glutathione conjugates of trans-4-hydroxy-2-nonenal, a known product of lipid peroxidation in oxidative stress. The analysis was completed using a range of post mortem brain regions from control and AD patients. The study found a significant increase of the conjugate in hippocampus and substantia innomina of AD patients [138], providing yet further evidence of oxidative stress, particularly of lipids, playing a major

pathological role within AD. Once again the result was in brain samples, making it impractical to directly transfer to the clinic, however it highlights the potential for LC-MS to be used in biomarker discovery.

Oxidative stress in AD also affects DNA. Wang et al. [177] applied a GC-MS approach to AD brain samples in a targeted attempt aimed at investigating oxidised DNA bases in AD. The study identified a significant increase in 8-hydroxyguanine as well as an increase in multiple oxidised DNA bases. This suggests products of DNA oxidation may be able to play a role as AD biomarkers.

Small molecule products of protein oxidation, glycation and nitration have also been previously investigated with regard to AD [178]. Analysis of the CSF from AD and control patients was completed in a targeted manner. The study identified a number of small molecules at increased levels including 3-nitrotyrosine, Nε-carboxymethyl-lysine, 3-deoxyglucosone-derived hydroimidazolone, N-formylkynurenine, methylglyoxal-derived hydroimidazolone and glyoxal-derived hydroimidazolone, suggesting extensive oxidation, nitration and glycation of protein products occurs in AD pathology.

1.6.3 – Alternative Analytical Methods in Targeted Study Design

1.6.3.1 – Chromatography with Alternative Detection

The first of these examples is LC-UV which has previously been used to report decreases in uric acid [179, 180], vitamin C [179, 180], vitamin A [181], and vitamin E [181] in plasma of AD patients as well as a decrease in the plasma carotenoid antioxidants including lutein, zeaxanthin, α-carotene, and β-cryptoxanthin [181]. Lutein levels were also found at decreased levels in AD plasma in a second study along with another carotenoid, β-carotene [182]. Interestingly, the decrease of these

two antioxidants appeared to correlate with patient MMSE score and disease severity suggesting potential for monitoring disease progression. These findings suggest support for previously reported increases in metabolites of oxidative stress, and it therefore stands to reason that a decrease in antioxidants may play a role in this process.

In continuation of this theme, the antioxidant vitamin A has also been demonstrated to exist at lower concentrations in AD plasma by using LC-fluorescence detection (method described in [180]), whilst a study using LC-EC has reported a reduction in the concentration of antioxidant species (vitamin C and uric acid) in AD [181].

LC-EC was also used to identify a decrease in the CSF concentration of two monoamine metabolites of AD patients; 5-hydroxyindoleacetic acid and homovanillic acid [183]. Homovanillic acid is of particular interest as it can be used as a marker of metabolic stress in relation to irregularities in glucose metabolism, which as discussed previously is pathologically linked to AD.

LC-EC detection methods have determined significantly increased concentrations of phosphatidylcholine (PC) molecules within the CSF of AD subjects compared with controls. Of these, glycerophosphocholine was demonstrated to be significantly increased by 76%, phosphocholine by 52% and free choline by 39% [184]. This result, again, suggests irregularities in membrane phospholipid metabolism potentially playing a role in AD pathology.

1.6.3.2– Immunoassay

One such developed method purified the steroid, dehydroepiandrosterone, using HPLC then quantified the isolated sample using a specific radio-labelled

immunoassay. The results found increased levels in samples taken from various AD brain regions and CSF, with the findings thought to indicate the presence of an alternative metabolic pathway linked to oxidative stress and therefore more common in AD patient brains [175].

An enzyme linked immunosorbant assay (ELISA) method was published capable of quantifying the level of F_2-isoprostanes in human plasma [185], however reported no significant changes between controls and AD. As discussed earlier, different studies have produced conflicting reports about the levels of F_2-isoprostanes in AD, with GC-MS results suggesting a significant elevation in a range of biofluids [168-171] whilst LC-MS results suggested no significant change in urine [139]. Therefore, the immunoassay adds to the conflicting reports, suggesting isoprostanes would not be a reliable biomarker for AD.

The same study also analysed uric acid by a similar immunoassay and found this to be at a significantly lower concentration in AD plasma than in control plasma [185]. This finding complemented results found via LC methodologies discussed previously [179, 181].

One study that tested the hypothesis that within AD there is a down regulation of the adrenal pituitary hormonal axis, used an immunoassay to quantify the levels of the hormone cortisol in the plasma of AD patients [186]. The significantly increased levels of the hormone observed suppored the initial hypothesis. These results present evidence that suggests further investigation into this hypothesis may yield biomarker results, possibly leading to a novel therapeutic target through hormone treatment.

Smith et al. [187] developed an immunoassay that quantified levels of nitrotyrosine, a small molecule product of tyrosine nitration that can act as an indicator of the presence of peroxynitrite, a powerful oxidant molecule which is capable of not only nitrating tyrosine, but also directly oxidising proteins and other macromolecules. Levels of nitrotyrosine were reported to significantly increase in brain homogenates of AD patients when compared with controls suggesting potential to act as biological marker for the disease.

1.6.4 – Targeted Biomarker Discovery in Alzheimer's Disease – Conclusions

There are clearly many different approaches that can be taken when planning a biomarker investigation with a molecular target in mind. Each technique has its own relative advantages and disadvantages depending on the user requirements. For example, approaches involving MS are certainly more sensitive, but do not allow the analysis of whole samples in a way that NMR analysis can achieve. When designing a non-targeted study, the advantages and disadvantages of each technique should be considered.

However, it should be noted that of concern are the discrepancies that have arisen between different publications and the analytical approaches used. For example isoprostane analysis by GC-MS found a significant increase in many biofluids, including various brain region homogenates [136, 167], CSF [135, 136, 168-171], plasma [135] and urine [135, 172], but there was no significant change in LC-MS analysis of urine [139] and an immunoassay analysis of plasma [185]. This is of particular importance as inter technique variability and conflicting results will not lead to the development of a reliable marker molecule.

Whilst not without problems, the technology required for targeted analysis is improving constantly as time progresses. Combine this with the falling costs of accurate instrumentation and it is certain that targeted approaches will play a role in the future of AD small molecule biomarker research. This is likely to be especially apparent if a biomarker progresses to the clinic and therefore requires routine analysis in a diagnostic capacity.

1.7 – Literature Review of Non-Targeted Alzheimer's Disease Biomarkers

1.7.1 – Nuclear Magnetic Resonance and Magnetic Resonance Spectroscopy

A preliminary study comparing patient and control CSF samples by NMR has been published. The method was capable of investigating a wide variety of components, the results of which were processed by principle component analysis (PCA), and was able to partially separate the diagnostic groups (control and AD) based on the concentrations of metabolites found. Further analysis of the data resulted in the identification of citrate as one of the metabolites contributing most to the model classification. It was later demonstrated that citrate existed at significantly decreased concentrations in AD compared with controls [188].

Jukarainen et al [131] also completed a non-targeted CSF metabolite analysis via NMR analysis. Differences in metabolite concentrations were observed in the study, with a significant increase in creatinine concentrations reported in AD compared with controls. This results complement a targeted study discussed earlier (Section 1.6.1) where creatine (the parent molecule of creatinine) was identified at increased concentrations in brain, suggesting possible irregularities in this metabolic pathway in AD [146].

Analysis of AD patient CSF via NMR is a consistent theme in the literature. An investigation by Kork et al [189] took this approach in a proof-of-concept study, and reported promising findings. Following multivariate data-processing, results highlighted various NMR peaks from the spectrum that were of significant influence to the models. Interestingly, the paper took the unusual approach of not

attempting to identify the molecules that the peaks corresponded to. However the authors concluded that ^{1}H-NMR spectroscopy, as an analytical technique, is a capable method for the detection and quantification of features in CSF and may be applied to biomarker marker research, even without the knowledge of molecular structures [189].

Interestingly, the same author more recently utilised NMR raw data peaks as biomarkers for AD. Again no identification was attempted, but the two publications demonstrate the potential for NMR to be utilised as a biomarker discovery tool in AD [190].

A further non-targeted study has been published analysing serum samples via a ^{1}H-NMR method [191]. In this instance the patient population did not contain any AD patients, but consisted of those diagnosed with MCI (as described in Section 1.1.3). The study reported a decrease in the relative amount of ω-3 fatty acids present in MCI, concluding that this irregularity may possibly indicate an increased risk of AD [191].

To date these are the only examples of non-targeted NMR approaches applied to human tissue samples, however there are examples in the literature that investigate samples obtained from animal models of the disease. The first of these investigated small molecule variation in the brain of TgCRND8 mice models developed to produce amyloid deposits in the brain within 2-3 months of birth. Extracts were examined from a variety of brain regions using ^{1}H-NMR methods before data analysis was completed via a multivariate model, producing a principle component analysis and a partial least squared analysis [192].

Reported results from the comprehensive study indicated a decrease in many different small molecule metabolites including *N*AA, glutamate, glutamine, taurine, γ-amino butyric acid, choline and phosphocholine (co-resonance), creatine, phosphocreatine and succinate, as well as an increase in lactate, aspartate, glycine, alanine, leucine, iso-leucine, valine and finally a group of soluble free fatty acids [192]. This mouse study highlighted the ability of non-targeted analysis to identify a wide range of metabolite variations within AD, supporting the potential for NMR to improve our understanding of the disease and to assist the development of biomarker molecules.

NMR and MRS are clearly useful in the discovery of biomarker candidates with regard to AD with numerous candidates already reported in the literature that are discussed above. Currently the most promising approach combines these metabolite data with imaging data. However, as can be seen, the technique still relies on CSF and brain samples, although this should improve as the technology advances and increases its sensitivity.

In contrast, mass spectrometry is known for its sensitivity, the literature examples of which are now discussed below.

1.7.2 – Mass Spectrometry

DI-MS has been used in a non-targeted manner to analyse plasma lipids in AD. Often termed "shotgun" analysis, the publication infused a lipid extract directly into the MS without the application of pre-separation techniques. The results suggested significant variations in sphingolipid species, with eight demonstrating a significant reduction in AD ($p=<0.05$), whilst two ceramide species (C16:0 and C21:0) were significantly higher in AD ($p=<0.05$). Interestingly MMSE scores were correlated with altered mass levels of both SM20:2 and ceramide25:0

($p<0.004$) [193]. This finding demonstrates the potential of DI-MS analysis, as candidate molecules were identified, without the requirement of a lengthy separation method. This saves analytical time, and therefore cost.

A preliminary LC-MS non-targeted study was developed to analyse plasma samples from AD, MCI and control patients [119]. Although a diagnostic model utilising the complete fingerprint could not be validated, the potential of non-targeted LC-MS within AD was demonstrated by the identification of a number of molecules of interest recommended for further investigation. The first, glycerophosphocholine, as discussed previously is a metabolite of the membrane phospholipid phosphatidylcholine, and is thought to play a role in neuronal membrane degradation in AD. To date no link has been determined between AD and the second molecule of interest identified in the study, D-glucosaminide, therefore more work on this molecule could lead to pathological clues about the mechanism of AD disease.

In addition, a trio of bile acids (GCA, GDA and GCDCA) were identified at increased concentrations in the plasma of AD subjects compared with controls. The authors commented that although a trend was noted, due to the small number of patient samples the resultant data could only be treated as a preliminary result, requiring more work before being statistically significant [119].

A GC-MS analysis was combined with multivariate data treatment to analyse serum free fatty acids in a semi-targeted study [194]. Although the study focused upon fatty acids as an area of particular analysis it had no particular target acid, and aimed to analyse a wide selection in a non-biased manner. Following intensive data treatment and the creation of analytical models the paper identified a number of fatty acids that had significantly decreased in samples derived from AD, these

included; myristic acid (C14:0), palmitic acid (C16:0), oleic acid (C18:1), linolenic acid (C18:3) and docosahexaenoic acid (C22:6).

A current approach in experimental design is the initial screen of samples using a non-targeted method in order to identify any biomarker candidates. This can then be followed by the development of a targeted method designed to validate any findings. This study design was applied to a recent plasma analysis using LC-MS technology. From the initial screen results, a decrease in desmosterol in AD plasma versus controls was identified. Following this, an analytical method was established to measure desmosterol and cholesterol. This targeted validation presented findings suggesting that desmosterol and desmosterol/cholesterol ratio are significantly decreased in AD. In addition, the publication reported an observed difference between mild cognitive impairment and control samples. Of particular interest, the decrease of desmosterol was somewhat more significant in females. Statistical analysis using a receiver operating characteristic (ROC) model between controls and AD, using plasma desmosterol as a marker, returned a promising area under the curve (a representation of specificity and sensitivity) of 0.80. Further data mining presented a significant correlation of plasma desmosterol with the Mini-Mental State Examination scores [195].

The development of non-targeted biomarker discovery is constantly evolving and improving as both the technology and the data treatment progresses. This is reflected in a recent publication of note. The article initially utilised both LC-MS and GC-MS results to analyse patient serum in an attempt to identify biomarker candidates for AD. The results reported a number of decreased concentrations of several lipid classes, including PC, SPH, plasmalogens, and sterols [196].

In addition, the publication analysed the serum of MCI patients who were re-visited, with the conversion to AD noted. The authors then set out to develop a model of baseline data in an attempt to find marker candidates capable of predicating conversion from MCI to AD. Initial statistical analysis identified an individual molecule, 2,4-dihydroxybutanoic acid, to be the most promising predictor of conversion. The acid was found to be up regulated in those patients who progressed to AD ($p=0.0048$). The publication statistics were then expanded with the development of metabolite "clusters". These clusters were formed of a combination of three or four individual metabolite features, with the overall changes of the cluster panel accounted for in the predictor model. The most promising of these clusters consisted of four metabolites: PC18:0/18:2 and PC16:0/20:4, lactic acid and ketovaline. In addition, the data was further combined with APOE genotype data. The cluster model provided a specificity and sensitivity of 0.67 and 0.76 respectively. This was an interesting approach in order to combine a vast amount of data taken from seven LC-MS methods and one GC-MS method [196] and goes to highlight the novel methods and progressions in both the analysis of small molecules and the treatment of the data collected.

1.7.3 – Non-Targeted Biomarker Discovery in Alzheimer's Disease – Conclusions

Non-targeted analysis is a relatively new approach to biomarker discovery, hence there is less data available when comparing with those constructed with a molecular target in the design. However it has been demonstrated here that the approach can be successful, with a number or publications already available which can identify small molecules via data modelling approaches.

Currently, investigations based upon a non-targeted approach are generally more time consuming than those with a target. This is because of a combination of requirements including the know-how, longer analysis time, more intensive data treatment, identification involving database searches and finally study confirmation using standards. This extended time obviously has other implications too, including increased man hours and increased cost of analysis.

Despite these disadvantages, the technologies, methods and statistical models are constantly improving, and it is likely that non-targeted approaches will become the starting point for many future discovery studies and may lead the way to small molecule biomarker discovery in AD.

1.8 – Aims

With the findings of this literature review in mind, a project plan was designed to investigate SMB of AD. The research was designed using a case-control strategy, Initially, both mouse model and human bio-samples underwent analysis in a targeted hypothesis driven approach.

As the project progressed, a hypothesis generating non-targeted analysis was also employed, with the aim of identify novel biomarker candidates of AD. At this stage of the project, the focus was on human plasma, again in a case-control design.

LC-MS was selected as the initial analytical technology due to the advantage of sensitivity, and the techniques ability to complete both targeted and non-targeted analysis, covering a wide range of small molecular species.

The overall aim of the project was to identify novel biomarker candidates in circulating plasma, which may be able to play a future role in the diagnosis and progression monitoring of AD. Plasma from control, MCI and AD patients was analysed, with the ideal outcome a marker that can help differentiate between the two pre-clinical phases (control and MCI) and AD.

Molecule or Group of Molecules	Tissue of Identification	Trend in AD	Targeted or Non-targeted	Identifying Technique	Reference
4 Metabolite Cluster	Plasma	N/A	Non-targeted	LC-MS	[196]
2,4-dihydroxybutanoic Acid	Plasma	Increase	Non-targeted	LC-MS	[196]
5-hydroxyindoleacetic Acid	CSF	Decrease	Targeted	LC-EC	[183]
Dehydroepiamdrosterone	Serum	Increase	Targeted	GC-MS	[176]
Dehydroepiamdrosterone	CSF	Increase	Targeted	GC-MS	[137]
8-hydroxyguanine	Brain	Increase	Targeted	GC-MS	[177]
Bile Acids (GCA, GDA, GCDCA)	Plasma	Increase	Non-targeted	LC-MS	[119]
Ceramide	Brain	Increase	Targeted	DI-MS	[160]
Citrate	CSF	Decrease	Non-targeted	^{1}H-NMR	[188]
Creatine	Brain	Increase	Targeted	^{1}H-MRS	[146]
Creatinine	CSF	Increase	Non-targeted	^{1}H-NMR	[131]
Dehydroepiamdrosterone	CSF	Increase	Targeted	GC-MS	[137]
Dehydroepiandrosterone	Brain/CSF	Increase	Targeted	Immunoassay	[175]
Desmosterol	Plasma	Decrease	Non-targeted	LC-MS	[195]
Desmosterol/Cholesterol Ratio	Plasma	Decrease	Targeted	LC-MS	[195]
Fatty Acids	Serum	Decrease	Non-targeted	GC-MS	[194]
Fumarate	CSF	Decrease	Targeted	GC-MS	[164]
Homovanillic Acid	CSF	Decrease	Targeted	LC-EC	[183]
Hydroxyoctadecadienoic Acid	Plasma	Increase	Targeted	GC-MS	[174]
Hydroimidazolone	CSF	Increase	Targeted	LC-MS	[178]
Isoprostanes	Brain	Increase	Targeted	GC-MS	[136, 167]
Isoprostanes	CSF	Increase	Targeted	GC-MS	[135, 136]
Isoprostanes	CSF	Increase	Targeted	GC-MS	[168-171]
Isoprostanes	Plasma	Increase	Targeted	GC-MS	[135]
Isoprostanes	Plasma	No change	Targeted	Immunoassay	[185]
Isoprostanes	Urine	Increase	Targeted	GC-MS	[135, 172]
Isoprostanes	Urine	No change	Targeted	LC-MS	[139]
Lactate	CSF	Increase	Targeted	GC-MS	[164]
Lutein	Plasma	Decrease	Targeted	LC-UV	[181, 182]
Myo-inositol	Brain	Increase	Targeted	^{1}H-MRS	[146, 152]
Myo-inositol/Creatine Ratio	Brain	Increase	Targeted	^{1}H-MRS	[148, 151, 153]
Myo-inositol/*N*AA Ratio	Brain	Decrease	Targeted	^{1}H-MRS	[151, 153]
*N*AA	Brain	Decrease	Targeted	NMR/MRS	[144-146]
*N*AA /Creatine Ratio	Brain	Decrease	Targeted	^{1}H-MRS	[148-151]
Nε-carboxymethyl-lysine	CSF	Increase	Targeted	LC-MS	[178]
N-formylkynurenine	CSF	Increase	Targeted	LC-MS	[178]
Nitrotyrosine	Brain	Increase	Targeted	Immunoassay	[187]
Nitrotyrosine	CSF	Increase	Targeted	LC-MS	[178]
Phosphatidylcholine	CSF	Increase	Targeted	LC-EC	[184]
Phosphatidylcholine	Plasma	Decrease	Non-targeted	LC-MS	[196]
Phosphatidylethanolamine	Brain	Decrease	Targeted	^{31}P-NMR	[142]
Phosphatidylethanolamine-P	Brain	Increase	Targeted	^{31}P-NMR	[142]
Phosphatidylinositol	Brain	Decrease	Targeted	^{31}P-NMR	[142]
Phospholipid Plasmalogens	Brain	Decrease	Targeted	DI-MS	[157]
Sphingomyelin	Brain	Increase	Targeted	^{31}P-NMR	[142]
Sphingolipids	Plasma	Decrease	Non-targeted	DI-MS	[193]
Succinate	CSF	Decrease	Targeted	GC-MS	[164]
Sulphatides	Brain	Decrease	Targeted	DI-MS	[160]
Uric Acid	Plasma	Decrease	Targeted	LC-UV	[179]
Uric Acid	Plasma	Decrease	Targeted	LC-EC	[179, 181]
Uric Acid	Plasma	Decrease	Targeted	ELISA	[185]
Vitamin A	Plasma	Decrease	Targeted	LC-UV	[181]
Vitamin A	Plasma	Decrease	Targeted	LC-F	[179]
Vitamin C	Plasma	Decrease	Targeted	LC-UV	[179]
Vitamin C	Plasma	Decrease	Targeted	LC-EC	[181]
Vitamin E	Plasma	Decrease	Targeted	LC-UV	[181]
Zeaxanthin	Plasma	Decrease	Targeted	LC-UV	[181]
α-carotene	Plasma	Decrease	Targeted	LC-UV	[181]
β- carotene	Plasma	Decrease	Targeted	LC-UV	[182]
β-cryptoxanthin	Plasma	Decrease	Targeted	LC-UV	[181]

Table 1.3: Small Molecule Biomarkers Previously Reported in the Literature
Summary table presenting previously published SMB candidates of Alzheimer's disease. It is particularly interesting to note the high number of lipid based species in the literature. Of further interest is the reported finding of isoprostanes that have conflicting reports depending on technique used, with GC reporting an increase, but LC and immunoassay reporting no change. Table reproduced from a publication by Whiley and Legido-Quigley [141]

Chapter 2:
Fatty Acids in Alzheimer's Disease – A Targeted Study

2.1 – Introduction

2.1.1 – Introduction to Fatty Acid Species

Fatty acids (FA) are highly abundant molecules throughout all of living systems, and are found everywhere from cell membranes to peanut oils. Structurally, FA consist of a carboxylic head group, attached to varying length side chains consisting of a carbon backbone (Figure 2.1).

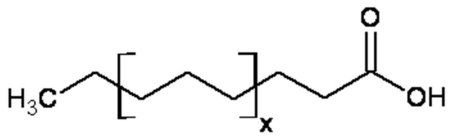

Figure 2.1: Structural Features of Fatty Acids

The fatty acid structure can be seen with a carboxylic head group (COOH) attached to a carbon backbone tail. The tail can vary in length, and finalises in a methyl (CH_3) end group. Carbon atoms in the backbone can either be linked by a single bond (-CH2-CH2-) or a double bond (-CH=CH-).

FA nomenclature can become complex due to a variety of terms an individual species can be referred as. The most widely used of these is the "common name". These are non-systemic names, and are the most frequent referred to in the literature. FA are also designated a systemic name, and is the official name referred to by the International Union of Pure and Applied Chemistry (IUPAC), the organisation responsible for officially naming organic and inorganic compounds. In addition each FA also can be named by the number of carbon chains in its backbone, along with the total number of double bonds, i.e. a FA with 20 carbons and 4 double bonds would be named 20:4. The initial double bond is also added to the description and is counted from the methyl carbon at the tail. For example a double bond between the third and fourth carbons counting from the tail on the backbone, would be termed 20:4ω3. These FA would be referred to as being part

of the ω3 family. Table 2.1 includes some FA examples and the nomenclature associated with each one. From here onwards the thesis will use the "common name" in order to maintain consistency, however the discussion of nomenclature is important as different referenced articles may employ alternative names in their work, particularly between the common name and numerical name.

Structure	Common Name	IUPAC Name	Numerical Reference
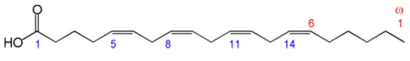	Arachidonic Acid	(5Z,8Z,11Z,14Z)-5,8,11,14-eicosatetraenoic acid	20:4(ω6)
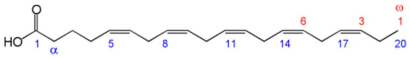	Eicosapentaenoic acid	(5Z,8Z,11Z,14Z,17Z)-5,8,11,14,17-icosapentaenoic acid	20:5(ω3)
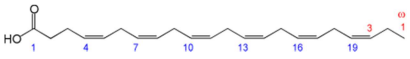	Docosahexaenoic acid	(4Z,7Z,10Z,13Z,16Z,19Z)-docosa-4,7,10,13,16,19-hexaenoic acid	22:6(ω3)

Table 2.1: Nomenclature of Fatty Acids

Three examples of fatty acids and the options that can be applied to name them. The common name is most often found in the literature but the other two examples can be used, and are perfectly acceptable when describing FA. The thesis has employed the common name from this point forward to avoid confusion.

It is commonly known that FA are vital for mammalian system function, for example they are major components of cell membrane structures [197], cell signalling pathways [198, 199], and a mammalian source of energy via β-oxidation [200]. Furthermore they are key components of larger mammalian molecules such as PC and PE.

2.1.1 – Terminology: Free and Bound Fatty Acids

It is important to note the differences in terminology used to describe FA when discussed in the literature. Due to the nature of FA, they can be found as described below:

- Free Fatty Acids (FA_{FREE}): FA_{FREE} are the FA molecules present in a tissue or biofluid in their simple standard FA form.
- Bound Fatty Acids (FA_{BOUND}): FA_{BOUND} occur when FA are found as part of a larger lipid molecule, for example membrane triglycerides or phosphatidylcholines. FA_{BOUND} play important roles in many cellular processes, particularly cellular membranes, and are therefore target for many investigations. In order to analyse FA_{BOUND} a hydrolysis reaction is often completed prior to quantification in order to release the FA from the larger parent lipid.
- Total Fatty Acids (FA_{TOTAL}): FA_{TOTAL} is the combination of FA_{FREE} and FA_{BOUND} and is the complete sum analysis of FA within a tissue or biofluid.

2.1.2 – Fatty Acids in Alzheimer's Disease

The apparent irregular metabolism of lipid species within AD pathology was previously discussed Chapter 1. As expected with the abundance of FA and their metabolites throughout lipid biochemistry, there are a great number of publications, discussing FA in AD, covering a plethora of research areas including:

- FA levels correlating with reduced risk of AD
- Abnormal levels of FA in biological samples
- Abnormal levels of FA metabolites

Most significantly from the perspective of biomarker research, a major population study in 899 patients has previously demonstrated that having a high baseline level of an important brain FA, docosahexaenoic acid (DHA), reduces the risk of progressing to AD. Initially, at visit one, all 899 patients showed no signs of dementia. Levels of DHA_{BOUND} to PC parent species were extracted from plasma using a multi-stage process. Initially chloroform was used to extract total lipid content. This was followed by a HPLC method designed to isolate PC species. Finally, DHA_{BOUND} were released from the PC via a hydrolysis reaction, and derivatised prior to GC analysis. Patients had a follow up visit on average 9.1 years later, where mental cognition was assessed. Patients were divided into quartile groups based on baseline plasma DHA_{BOUND} to PC levels, with those in the upper quartile found to have a 47% reduced chance of progressing to a dementia case [201]. This is an important observation, as it provides evidence that baseline FA in plasma could be influenced by disease state, and therefore could potentially play a role in a biomarker capacity for AD.

Interestingly the publication also reported dietary habits for a subset of the cohort, with 488 patients completing a dietary questionnaire. Results suggested that fish consumption correlated with plasma DHA_{BOUND} to PC levels ($p=<0.001$). In addition, those who ate fish twice a week had a 50% reduction in the relative risk of developing AD [201]. This finding is interesting, because although it suggests dietary habits may effect baseline levels of FA_{BOUND}, those levels still correlate to AD progression, and it is this property that suggests their potential as baseline predictors for AD.

More support is provided throughout the literature with regard to the potential of FA molecules to act as biomarker molecules, with many examples of specific FA

species observed to vary in AD when compared with controls. These observations have been reported in a variety of biofluids, from both human and mouse models. Sanchez-Mejia et al. [202] investigated FA metabolism in brain samples from human amyloid precursor protein (hAPP) in J20 mouse models. J20 hAPP mice are transgenic mice that are specifically designed to over-express hAPP, leading to an increase in Aβ, one of the major features in human AD pathology, thereby modelling aspects of AD pathology [203]. The study reported an increase in free arachidonic acid (AA_{FREE}), a ω6 FA, and its metabolites in the hippocampus of those mice with the mutation compared with wild-type mice. This analysis was completed using an LC-MS targeted analysis. In addition Sanchez-Mejia et al. linked this change to an increase in the activity of a group IV isoform of the phospholipase A_2 (PLA_2) enzyme, responsible for releasing the fatty acid from larger membrane phospholipids. This was found to be due to an increase in the activation of the PLA_2 in the hippocampal region of the mice identified using a targeted immunoassay approach,

The same group IV PLA_2, (also referred to in literature as cytosolic PLA_2), has also been shown to increase in activity in human AD brain cerebral cortex regions [204] and human AD brain glial cells [205]. Additionally the presence of Aβ proteins associated with AD pathology, has been shown to directly activate group IV PLA_2 in astrocytes [206].

In direct contrast, Prasad et al. [207] reported significant decreases in AA in human brain. The study looked at both AA_{FREE}, as well as AA_{BOUND} existing as components of larger lipid molecules, including PC, PE and, PI. Significant decreases were observed in the hippocampus and inferior pareto lobule. AA_{FREE} analysis was completed using a targeted GC method, whilst AA_{BOUND} included a preliminary step

using thin-layer chromatography (TLC) designed to separate the individual parent lipid classes, followed by a hydrolysis step designed to release the AA_{BOUND} for analysis. Significant decreases in the hippocampus brain region were found with the AA_{FREE} and AA_{BOUND} to both PE and PI parent lipids (p=<0.005). No significant differences were observed in AA_{BOUND} to PC parent species.

In addition the publication also investigated levels of both FA_{FREE} and FA_{BOUND} of four further FA: Palmitic (PA), stearic (SA), oleic (OA) and docosahexaenoic acid (DHA). Observations included significant decreases in the hippocampus of FA_{BOUND} to PI parent lipids (OA) and PE parent lipids (SA, OA, DHA).

FA have also been investigated in the plasma of human AD patients. As discussed in Chapter 1, plasma is an ideal biofluid for any predictive biomarker molecule due to its relative non-invasive nature and ease of collection. Conquer et al. [208] investigated levels of FA_{BOUND} to total plasma phospholipids. Patient groups included those suffering from AD (n=19), Controls (n=19), other dementia (n=10) and non-demented but loss of mental cognition (n=36). Results reported a reduction in AD patient plasma of the levels of EPA_{BOUND}, DHA_{BOUND} and lignoceric $acid_{BOUND}$ (LGA_{BOUND}) to total plasma phospholipid species. Further analysis revealed reductions in total ω3 FA_{BOUND} and ω3/ω6 FA_{BOUND} ratio in AD patients compared with the other groups.

Additionally the publication also analysed FA_{BOUND} to individual subgroups of phospholipids, including parent PC, PE and lyso-phosphatidylcholine (LysoPC). In order to achieve this individual lipid classes were isolated using TLC. Again FA_{BOUND} were released from the parent lipids via the use of a hydrolysis reaction step. Results suggested significant reductions (p<=0.05) in those FA_{BOUND} to PC (EPA, DHA, total ω3 and ω3/ω6 ratio) and PE (EPA, DHA and total ω3) [208].

A recent publication investigated a range of FA species from both plasma and brain samples via the use of GC analysis. The paper compared matched plasma and brain samples from control, MCI and AD subjects, and reported levels of FA_{FREE} and FA_{BOUND} to PC and PE parent lipids species. Total plasma FA_{FREE} reduced 43% in MCI patients and 52% in AD subjects compared with controls. Particular reductions were reported in plasma OA_{FREE} (70% in MCI and 80% in AD) and LA_{FREE} (50% in MCI 80% in AD). Reductions in AD compared with controls were also observed in Plasma FA_{BOUND} to total phospholipid parent species, with significant reductions reported in PA_{BOUND}, EPA_{BOUND} and DHA_{BOUND} ($p=<0.05$). In brain tissue (matched to the plasma) differences were less apparent between disease groups. However, DHA_{BOUND} to phosphatidylserine (PS) was reported at significantly reduced concentrations ($p=<0.05$) in AD patients compared with controls [209].

As discussed in Chapter 1, for a biomarker to be used in a clinical environment for diagnostic purposes, a sample that is obtainable from patients, often suffering from reduced mental cognition, is required. As the pathology of AD and MCI is brain related , it suggests a biomarker candidate capable of crossing the BBB would be advantageous.

Although the exact mechanism is unknown it has been previously demonstrated that FA are capable of crossing the BBB, with a detailed review of current literature findings published by Hamilton et al [210]. This mechanism has also been hypothesised to be a two-way transport system, suggesting equilibrium is maintained [211]. It has also been demonstrated that daily turnover of AA and DHA in mammalian brain is 3-5% and 2-8% respectively, and in human brain AA is

0.3% [212]. This would imply levels of FA in plasma are influenced by brain levels, therefore suggesting that they could have potential as biomarker candidates.

It is clear from the literature that FA and the biological pathways surrounding them are altered in AD, suggesting their potential use as biomarkers of AD. Therefore, considering the existing conflicting findings on the relationship between FA levels and AD, and with no previous known investigation into FA_{TOTAL} in AD, a pilot study was designed to investigate FA_{TOTAL} in both mouse brain and human plasma.

2.1.3 – Study Design

The study was designed with a targeted approach. As discussed in Chapter 1 targeted approaches employ a hypothesis and select specific molecules for analysis. In this instance a method was adapted from a previously published and validated an LC-MS method by Salm et al. [213]. The method was ideal for adaptation as it was focused on AA_{TOTAL}, DHA_{TOTAL} and EPA_{TOTAL}, all three of which have been discussed in AD literature in either their $_{FREE}$ or $_{BOUND}$ forms [202, 208, 209]. The method had already been fully validated in the original publication, meaning it could be applied to AD samples.

2.1.4 – Sample Selection

Two available samples sets (described in more detail in Section 2.2.3) were selected for analysis by the method published by Salm et al.[213].

- Mouse Brain – Mice brain samples were collected from n=1 hAPP transgenic mouse, and n=1 wild-type control. Six brain regions were isolated from each mouse for analysis. The initial objective was to investigate the variation of AA_{TOTAL}, DHA_{TOTAL} and EPA_{TOTAL} between brain regions. FA

concentrations for each brain regions were compared between the transgenic and wildtype control mice. From this point forward the analysis of mouse brain samples will be referred to as MB2. For method testing and validation purposes, mouse brain was replaced with more readily available pig brain.

- Human Plasma – Plasma samples from (n=30) patients were selected for analysis based on age and gender matching. The initial objective here was to investigate the variation of AA_{TOTAL}, DHA_{TOTAL} and EPA_{TOTAL}, i.e. total FA_{FREE} combined with FA_{BOUND} bound to larger lipid molecules. This differs from other work in the area as previous publications have focused either on FA_{FREE} in plasma or FA_{BOUND} from particular lipid parent fractions. Further to this the analysis includes patients diagnosed with MCI, in an attempt to evaluate whether AA_{TOTAL}, DHA_{TOTAL} and EPA_{TOTAL} changes in this condition, as well as comparing AD with Controls. From this point forward to avoid confusion the analysis of human plasma will be referred to as HP30.

2.1.5– Method Testing (MTEST)

In order to ensure the method was transferable to the available analytical setup a series of tests were employed to examine reproducibility and linearity. The first of these involved a replica extraction (n=6) of a pool of human plasma, and pig brain. Pig brain was selected as a substitute for mouse brain for method testing.

MTEST was designed to ensure batch reproducibility across repeat extractions using biological tissues employed in later stages of analysis. The second aspect of suitability testing, involved extracting the three FA standards at a range of concentrations as described in the original manuscript, to ensure linearity across

an expected range. This was to ensure that any response observed between biological extracts is a true linear reflection of FA levels.

Figure 2.2 shows the study outline.

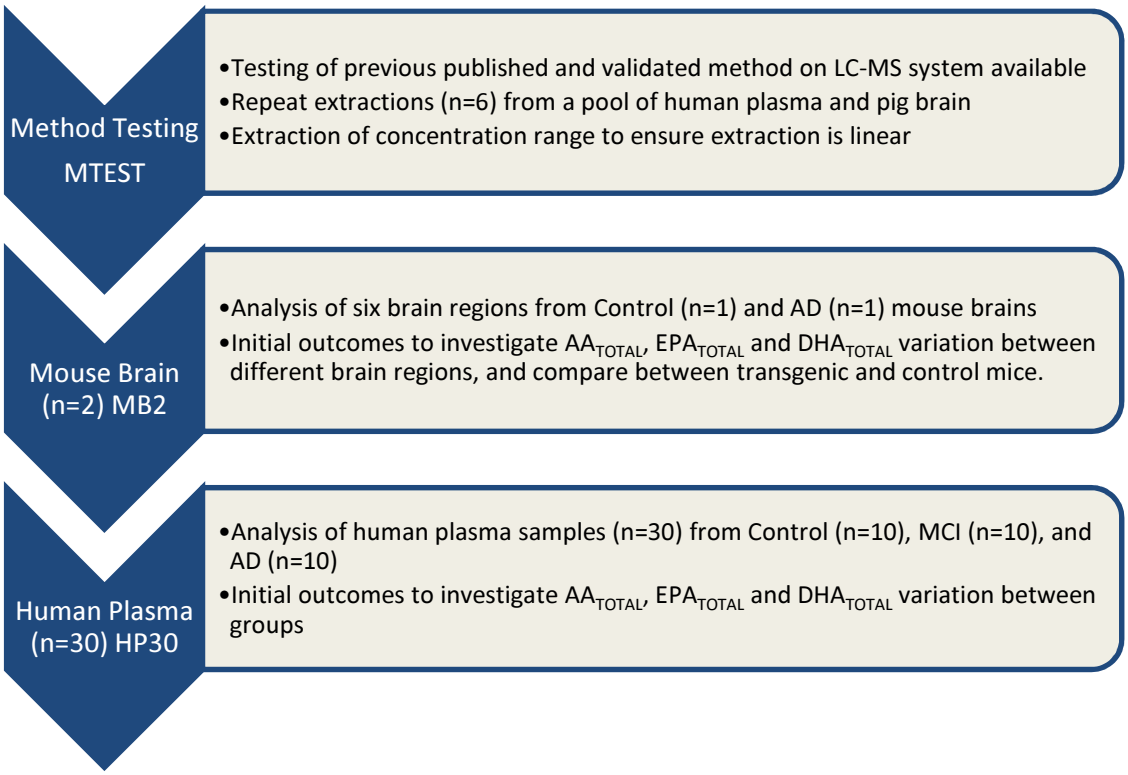

Figure 2.2: Study Experimental Design

An experimental pipeline, providing an overview of fatty acid analysis in a mixture of samples related to Alzheimer's disease. Initially a previously published method was tested on an available LC-MS system to ensure cross system compatibility. This sample set is referred to as MTEST. Secondly mouse brain samples were analysed to investigate total arachidonic acid (AA_{TOTAL}), total docosahexaenoic acid (DHA_{TOTAL}) and total eicosapentaenoic acid (EPA_{TOTAL}) variation between brain regions. This sample set is referred to as MB2. Finally n=30 plasma samples were analysed, investigating variation in Alzheimer's disease patients plasma. This sample set is referred to HP30.

2.2 – Materials and Methods

The method was adapted from a previously developed publication by Salm et al.[213].

2.2.1– Materials

LC-MS Grade methanol was purchased from VWR (Leicestershire, UK) and high purity water deionised water was obtained from an in house Millipore filtration system (EMD Millipore, MA, USA). AA, DHA and EPA standards, were purchased from SIGMA-ALDICH (Gillingham, Dorset, UK). Deuterated AA (d_8-AA) was purchased as an internal standard from Cambridge Bioscience (Cambridge, UK). Formic acid, hydrochloric acid, ammonium acetate, chloroform and HPLC grade acetonitrile were purchased from Fisher Scientific (Loughborough, UK). Crimp top HPLC vials for the extraction were purchased from Chromacol (Cambridge, UK).

2.2.2 – Instrumentation

Instrumentation settings were constant for all three sample sets (MTEST, MB2, HP30).

LC-MS analysis was completed using a Waters Acquity® LC (Waters, Milford, USA) coupled to a Waters Xevo® MS (Waters, Milford, USA). The column used was a Thermo HyPURITY™ Elite C_{18}, (50mm x 2.1mm, 3µm), which was maintained at 30°C. The separation utilised a linear gradient composed of 15% 2mM ammonium acetate in 0.1% formic acid/water and 85% methanol. Solvent was passed through the column at a rate of 0.4mL/min, with an overall runtime of 3.5 minutes.

Mass spectrometry analysis was completed in negative ionisation mode with a capillary voltage of 3.2kV. A cone voltage was employed at 35V, with the extractor setting set at 2.0. Capillary temperature was 120°C, and gas desolvation

temperature was 400°C. Desolvation gas flow was 900L/min and the cone gas was set at 50L/min. Data was collected between 100Da and 1000Da, with a scan time of 0.1sec. A reference solution (leucine enkephalin) was infused at regular intervals (every 15 seconds), and use to update accurate mass to charge ratio (m/z) data values.

2.2.3 – Sample Collection

2.2.3.1 – MTEST Samples

For the MTEST segment of study, both a pool of plasma and pool of brain was employed. The plasma pool was created by using spare plasma from a healthy volunteer. Brain samples were obtained from a pig, and were donated by Sillfield Farm Foods (Kendal, UK).

A concentration range of standards of AA, DHA and EPA in acetonitrile/water (75:25) also underwent extraction (0.625, 1.25, 2.5, 5, 10, 20, 40, 80, 160, 320µg/mL) as described in the initial validation [213]. This involved 25µL of the standards in acetonitrile/water undergoing the same extraction procedure as described in 2.2.4.

2.2.3.2 – MB2 Samples

Mouse brain samples were collected from a collaboration project based a King's College London, Denmark Hill, UK.

Heterozygote TASTPM transgenic mice over expressing both the hAPP695swe mutation (TAS10) and the presenilin-1 M146V mutation (TPM) were generated by standard techniques as previously described [214]. Wild type animals were of the C57BL/6 line. Animals were maintained and euthanized at King's College London under appropriate Personal and Project Home Office Licenses.

Six brain regions were harvested from two mice (n=1 wildtype, n=1 TASTPM AD model): Hippocampus, cerebellum, olfactory bulb, cortex, thalamus and striatum. After collection, the individual brain regions were treated with phosphate buffered saline (PBS) and placed at -80°C until extraction.

2.2.3.3 – HP30 Samples

Human plasma samples (n=30) were acquired from the Institute of Psychiatry, Denmark Hill, London, UK, sample store. The samples consisted of Controls (n=10), MCI (n=10) and AD (n=10).

Plasma samples were collected from two clinical cohorts, AddNeuroMed and the King's College London Dementia Case Register (DCR), which are described in detail in Figure 2.3. All patients from the cohorts underwent standardised assessments, which included collection of general demographic and medical data as well as cognitive assessment. Internationally recognised cognition tests are completed including the MMSE, ADAS-Cog and CERAD. Further to the cognition tests, scales were conducted on function, behaviour and global levels of severity, including the Clinical Dementia rating (CDR).

Patients were diagnosed with probable AD and amnesic MCI according to criteria from NINCDS-ADRDA [27].

Normal elderly controls were defined as having no evidence of cognitive impairment, and had MMSE scores of >28. Their recruitment was initiated from primary care patient lists.

For each patient 10mL of blood was collected in tubes coated with sodium ethylenediaminetetraacetic acid (EDTA). Prior to blood collection patients were required to fast for 2 hours. Post collection blood samples underwent

centrifugation, to produce a plasma supernatant. Plasma was split into aliquots and frozen at -80°C until further use. Ethical approval was awarded for all cohorts in the corresponding countries of collection. Full details on AddNeuroMed and DCR cohorts can be found in publications [106, 107, 215, 216].

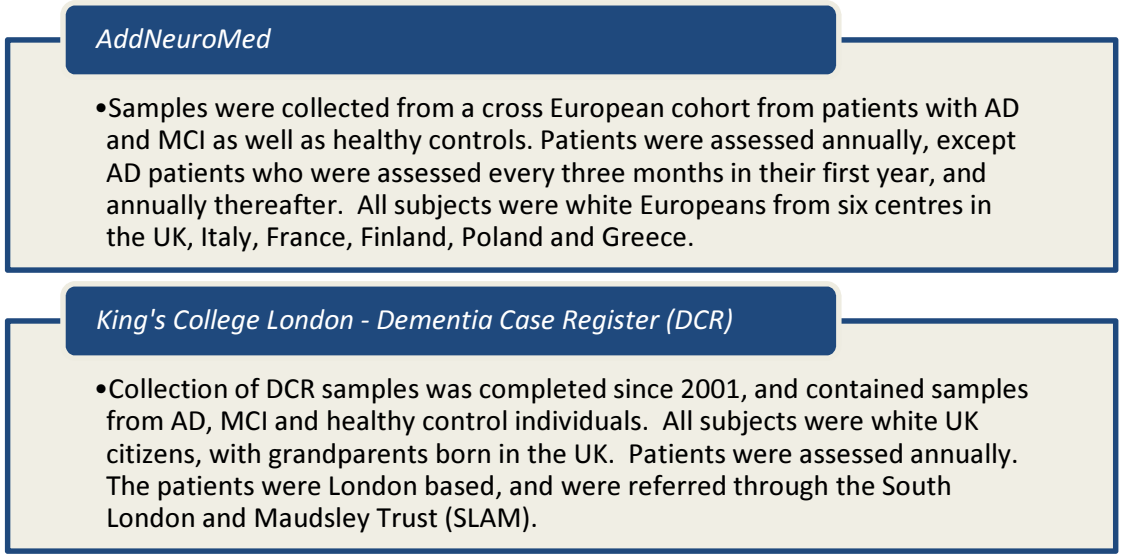

Figure 2.3: Overview of Clinical Plasma Cohorts

Two clinical cohorts were used to collect the human plasma samples, the details for each one are described here

Samples were selected to ensure age and gender matching across the disease groups. A summary of patients selected can be seen in Table 2.2.

	Control	MCI	AD
Total Samples	10	10	10
Male/Female	5/5	5/5	5/5
% Male/%Female	50/50	50/50	50/50
Age Mean	77.30	83.64	83.32
Age Stan Dev	6.37	6.56	8.11
MMSE Mean	28.9	24.7	15.4
MMSE Stan Dev	1.60	2.98	5.72

Table 2.2: Patient Data for Study HP30

Summary of patient data of plasma samples included in the study HP30. Samples were age and gender matched as much as possible to reduce external influences of analysis. Mini Mental State Exam (MMSE) results are also presented.

2.2.4 – General Sample Extraction

Brain samples were prepared by adding 10µL of 0.1% ammonium acetate buffer (pH7) per 1µg of wet brain mass as used by Matyash et al in lipid brain extractions [217], followed by vortex mixing. 25µL of this mix was added to a crimp top glass 2.5mL HPLC vial for the extraction procedure.

Plasma samples simply underwent a vortex mix after defrosting. 25µL was added to a crimp top 2.5mL HPLC vial for the extraction procedure.

The following applies for both tissue types:

50µL of 5N hydrochloric acid was added to the HPLC vial containing samples. To this 500µL of acetonitrile was added containing 2µg/mL of d_8-AA to be used as an internal standard. Vials were tightly crimp-top capped and placed at 100°C in a water bath for 1 hour. This stage initiated the hydrolysis reaction required for releasing all of the FA_{BOUND} from parent lipids.

Samples were allowed to cool, before de-capping and the addition of 500μL of chloroform and 500μL of high purity water. Samples were re-capped and vortex mixed for 10 minutes, before centrifugation at 2500g for 5 minutes.

Samples were de-capped, the upper aqueous phase removed, and 500μL of high purity water again added. Samples again underwent re-capping, and vortex mixed for 10 minutes, before centrifugation at 2500g for 5 minutes. The addition of chloroform step extracts the FA present. Both FA_{FREE} and the previously FA_{BOUND} and released from parent lipid in the hydrolysis step are extracted, meaning FA_{TOTAL} undergoes extraction.

100μL of the lower phase was extracted and transferred to a fresh HPLC vial containing a glass insert (Chromacol, Cambridge, UK). This was dried under a stream of nitrogen, and re-suspended in mobile phase. 5μL was injected onto the LC for analysis.

For both tissue types samples were extracted and analysed by LC-MS in random order. Pooled samples made from corresponding tissue samples were included as quality controls. These were extracted and analysed at regular intervals (before, consistent middle intervals, and after).

2.2.5 – Data Treatment

Raw mass spectrometry data was collected using MassLynx v4.1 (Waters, Milford, USA). FA peaks were extracted using QuanLynx software included in MassLynx v4.1 (Waters, Milford, USA). Statistical independent two tailed t-test validation was calculated by SPSS v20 (IBM, Portsmouth, UK)

2.3 – Results

2.3.1 – MTEST Samples

Initially repeats were completed on pooled human plasma and pig brain. Ratios were calculated for FA/internal standard (d8-AA) peak areas. Mean peak areas, standard deviation and relative standard deviations (RSD) figures were calculated and can be seen in Table 2.3 (a) and (b). RSD of the three FA in the plasma were AA_{TOTAL} (0.97%), DHA_{TOTAL} (1.41%) and EPA_{TOTAL} (2.45%). RSD of the two major FA in brain were AA_{TOTAL} (4.03%) and DHA_{TOTAL} (4.21%). EPA_{TOTAL} is far less prevalent in brain, and was not at a sufficient concentration to be detected.

A linearity study was also completed on the MTEST samples. FA standards (0.625, 1.25, 2.5, 5, 10, 20, 40, 80, 160, 320µg/mL) in ACN/H_2O were extracted using the method described. Linear plots can be seen in Figure 2.4 (a), (b) and (c), with R^2 values of 0.9982 (AA), 0.9980 (DHA) and 0.9963 (EPA) being reported.

Quality Control Human Plasma Pool (n=6)									
Fatty Acid	**1 (µg/ml)**	**2 (µg/ml)**	**3 (µg/ml)**	**4 (µg/ml)**	**5 (µg/ml)**	**6 (µg/ml)**	**Mean (µg/ml)**	**Std Dev**	**RSD (%)**
AA_{TOTAL}	271.9	272.9	276.4	277.4	273.9	278.4	275.1	2.6	1.0
DHA_{TOTAL}	20.6	20.2	20.6	21.5	21.3	20.9	20.9	0.5	2.2
EPA_{TOTAL}	149.1	152.3	142.3	152.3	148.2	149.3	148.9	3.7	2.5

Quality Control Pig Brain Pool (n=6)									
Fatty Acid	**1 (µg/ml)**	**2 (µg/ml)**	**3 (µg/ml)**	**4 (µg/ml)**	**5 (µg/ml)**	**6 (µg/ml)**	**Mean (µg/ml)**	**Std Dev**	**RSD (%)**
AA_{TOTAL}	475.4	516.4	519.9	509.4	525.4	533.9	513.4	20.4	4.0
DHA_{TOTAL}	197.9	213.3	216.5	212.6	221.2	223.3	214.1	9.0	4.2
EPA_{TOTAL}	BLQ	BLQ	BLQ	BLQ	BLQ	BLQ	N/A	N/A	N/A

Table 2.3: Extraction Reproducibility Study

Results from a study to investigate extraction reproducibility in (a) Pooled Plasma and (b) Pooled Brain. Concentration values (µg/mL) for the three fatty acids of interest (arachidonic acid – AA, docosahexaenoic acid – DHA and eicosapentaenoic acid – EPA) along with values for mean concentration, standard deviation (Std. Dev) and relative standard deviation (RSD). EPA was not detected in brain samples using this method and is therefore labelled BLQ (below limit of quantitation (2.5µg/ml)).

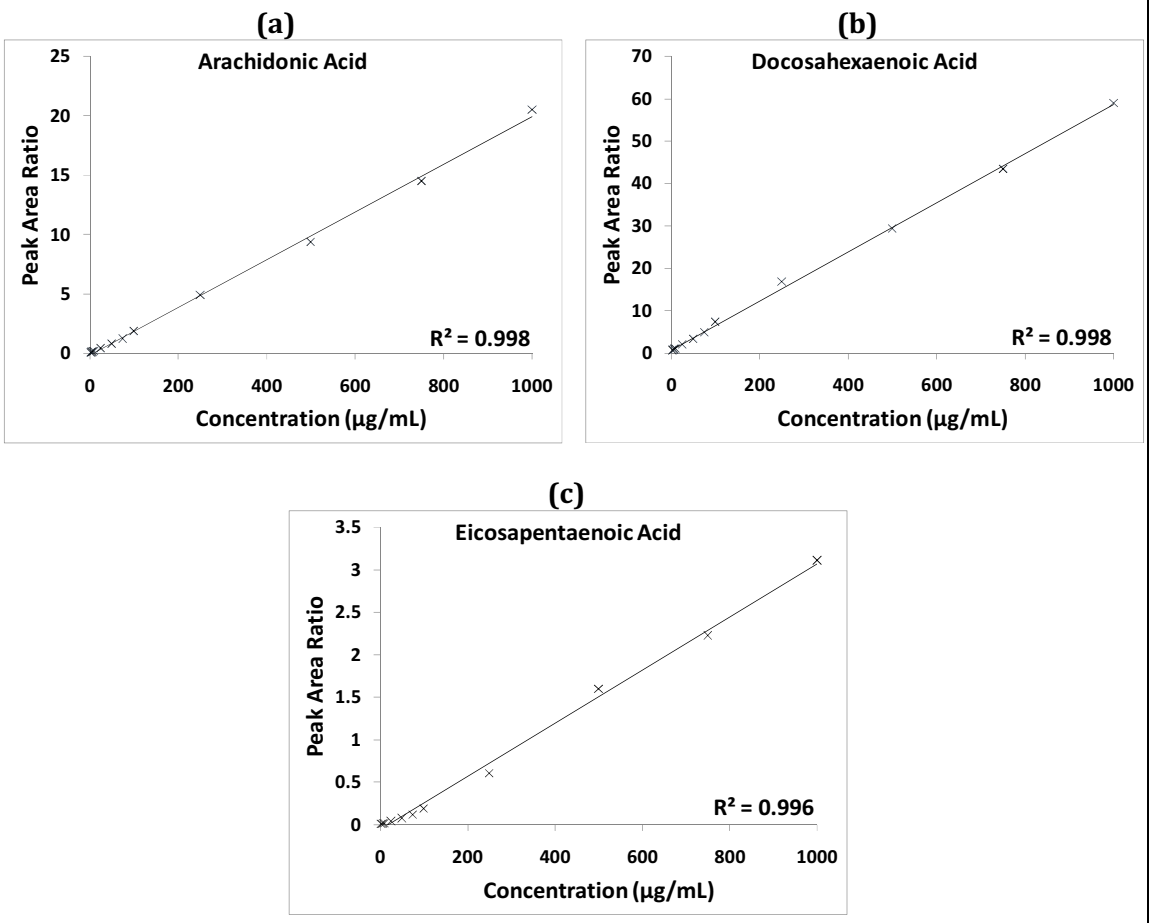

Figure 2.4: Extraction Linearity Plots of Individual Fatty Acids

Linearity plots for **(a)** arachidonic acid (AA), **(b)** docosahexaenoic acid (DHA) and **(c)** eicosapentaenoic acid (EPA). Figure values are a ratio of FA peak area over internal standard (d_8-AA) peak area. Concentrations extracted were 0.625, 1.25, 2.5, 5, 10, 20, 40, 80, 160 and 320µg/mL. Acceptable R^2 values of 0.9982 (AA), 0.9980 (DHA) and 0.9963 (EPA) were achieved for all three FA species.

2.3.2 – MB2 Samples

2.3.2.1 – Quality Control

Quality control (QC) samples were analysed at regular intervals during the analytical run. Before (n=2), every four injections (n=1) and after (n=2) (total n=6). Reproducibility was calculated in the same manner as section 2.3.1. Peak area ratios and corresponding concentration values were calculated for the individual FA. Values for RSD (%) across the analytical run were, 4.93% (AA_{TOTAL}) and 3.02% (DHA_{TOTAL}). As in the MTEST section EPA_{TOTAL} was not detected at a quantifiable concentration.

2.3.2.2 – Fatty Acids in Brain Tissue

EPA_{TOTAL} was below the limit of quantification in all brain regions within the brain samples. Peak areas for AA_{TOTAL} and DHA_{TOTAL} were extracted using QuanLynx package in MassLynx (Waters, Milford, USA). Concentration values were then calculated for each of the six brain regions, the results of which can be seen in Table 2.4 and visualised in Figure 2.5.

Arachidonic Acid$_{TOTAL}$ Concentrations in Mouse Brain		
Brain Region	**Wild Type (µg/mL)**	**AD Model (µg/mL)**
Cerebellum	420.05	458.63
Cortex	543.60	589.12
Hippocampus	562.53	513.71
Olfactory	418.77	399.08
Striatum	326.35	472.65
Thalamus	372.72	465.04

Docosahexaenoic Acid$_{TOTAL}$ Concentrations in Mouse Brain		
Brain Region	**Wild Type (µg/mL)**	**AD Model (µg/mL)**
Cerebellum	269.52	321.05
Cortex	294.15	330.33
Hippocampus	262.40	259.80
Olfactory	285.07	270.94
Striatum	148.31	241.63
Thalamus	192.01	264.21

Table 2.4: Arachidonic Acid and Docosahexaenoic Acid in Mouse Brain Regions
Concentration values for (µg/mL) of Arachidonic Acid (AA_{TOTAL}) and Docosahexaenoic Acid (DHA_{TOTAL}) in six brain regions from two mice. These results are visually displayed in Figure 2.5.

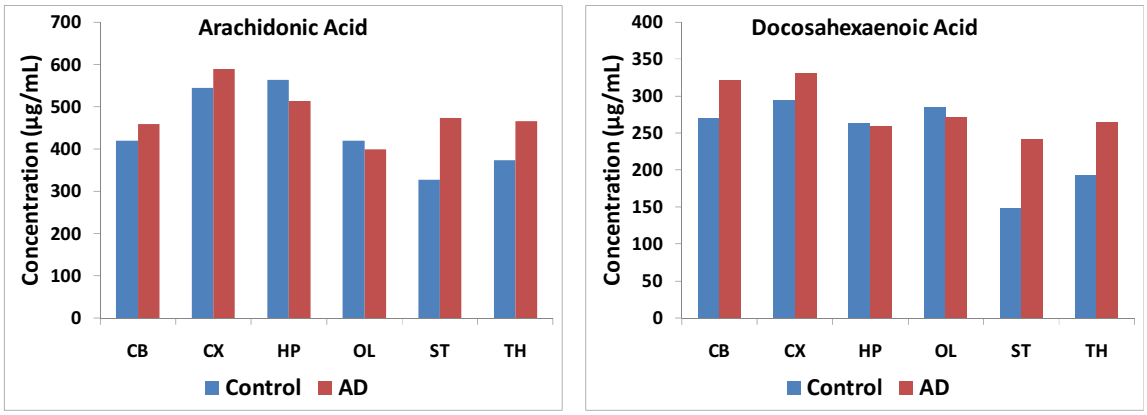

Figure 2.5: Arachidonic Acid and Docosahexaenoic Acid in Mouse Brain Regions
Concentration values of the two major fatty acid species in six mouse brain regions – Arachidonic (AA_{TOTAL}) and Docosahexaenoic acid (DHA_{TOTAL}). Brain regions included are Cerebellum (CB), Cortex (CX), Hippocampus (HP), Olfactory (OF), Striatum (ST) and Thalamus (TH).

2.3.3 – HP30 Samples

2.3.3.1– Quality Control

Quality control (QC) samples were analysed at regular intervals during the analytical run. Before (n=2), every six injections (n=1) and after (n=2). Reproducibility was calculated in the same manner as section 2.3.1. Peak area ratios to internal standard (d_8-AA) and the corresponding concentration values were calculated for the three individual FA. Values for RSD (%) across the analytical run were, 2.55% (AA_{TOTAL}), 2.40% (DHA_{TOTAL}) and 2.78% (EPA_{TOTAL}) respectively.

2.3.3.2 – Fatty Acids

Concentration values for AA, DHA and EPA were determined by comparing FA/d_8-AA peak area ratios to a known calibration curve. Samples were grouped by disease status, with the results presented in Figure 2.6. Statistical significance was calculated by comparing FA mean concentration values in an independent samples t-test using SPSS v20 (IBM, UK).

Comparison of EPA_{TOTAL} levels between the control and AD groups provided a statistically significant difference (p=0.023). The concentration of EPA_{TOTAL} was recorded as Control (708.31µg/mL), MCI (684.36µg/mL) and AD (456.86µg/mL). No other comparison revealed any significant differences.

Mean concentration values of AA_{TOTAL} were consistent across all three groups – Control (426.82µg/mL), MCI (425.70µg/mL) and AD (423.73µg/mL).

DHA_{TOTAL} was reported to decrease in AD samples compared with control and MCI groups, however this change was not statistically significant (p=0.107 Control →

AD and p=0.075 MCI → AD). Results reported concentration values of: Control (48.52µg/mL), MCI (50.35µg/mL) and AD (35.39µg/mL.

Ratios between each of the FA were also calculated. AA_{TOTAL}/DHA_{TOTAL} = Control (2.52), MCI (2.57), AD (3.23). AA_{TOTAL}/EPA_{TOTAL} = Control (4.68), MCI (5.46), AD (7.07). DHA_{TOTAL}/EPA_{TOTAL} = Control (1.80), MCI (2.04), AD (2.20).

Control → AD (AA_{TOTAL}/EPA_{TOTAL}) was a significant increase (p=0.05).

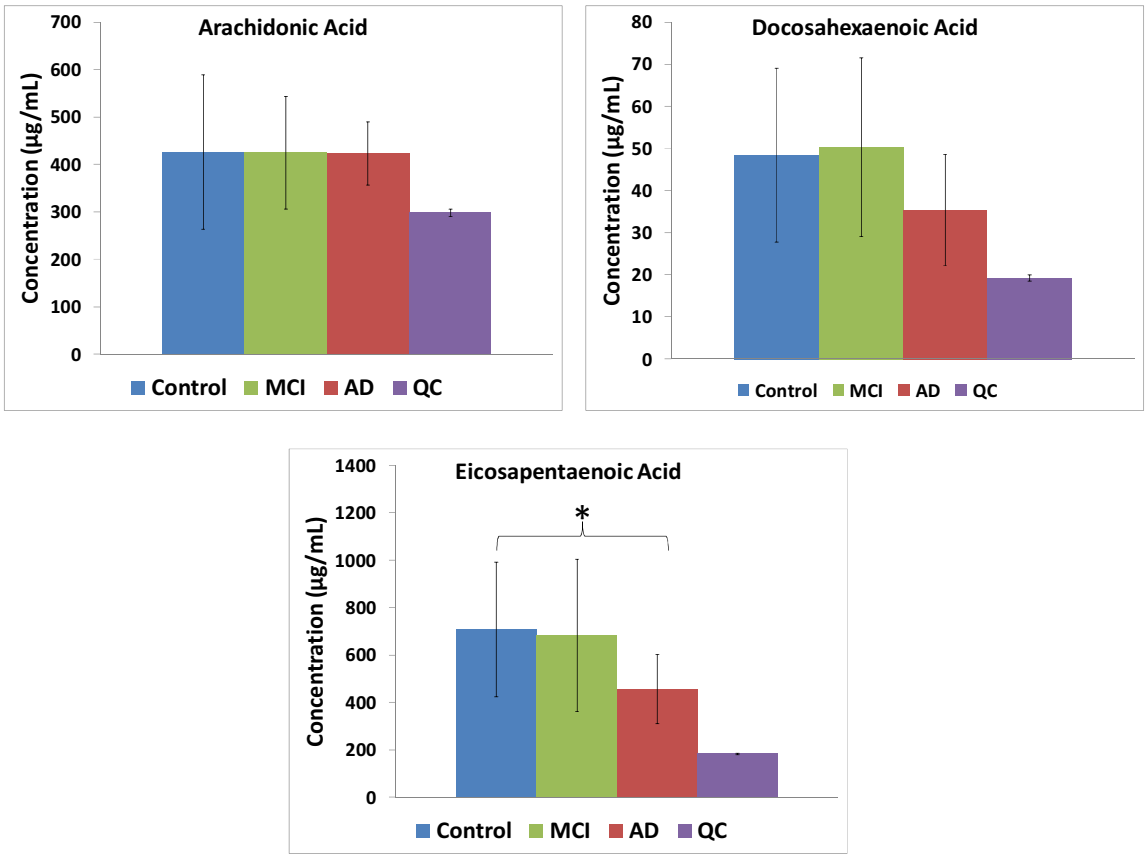

Figure 2.6: HP30 Results Overview

Overview of results from investigation into total fatty acid levels in human plasma sample set HP30. Sample numbers are Alzheimer's disease (AD) n=10, mild cognitive impairment (MCI) n=10, and control n=10. * signifies statistical significance of p=0.023. No other comparisons provided significant results. Values for Quality Controls (QC) were taken from a replicate extraction of a pool of plasma (n=8). Error bars signify standard deviation of samples.

2.4 – Discussion

2.4.1 – MTEST Samples

Although the study employed a previously published and fully validated method [213] it was vital that it underwent re-evaluation on the available laboratory setup and LC-MS instrumentation. The original authors utilised an analytical setup comprising of an Agilent 1100 Series LC (Agilent Technologies, Waldbronn, Germany) coupled to a 4000 QTrap linear ion trap quadrupole mass spectrometer (Applied Biosystems/MDS Sciex Instruments, Concord, Canada). This contrasts to the Waters Acquity® LC and Waters Xevo® MS utilised here.

Column selection was altered slightly due to laboratory availability, with a Thermo HyPURITY™ Elite C_{18}, (50mm x 2.1mm x 3µm) being used in place of the published Varian Pursuit™ C_{18} (50mm x 2mm x 3µm), however due the similarity of phases and dimensions this did not have a major impact on method transferability.

Similarly LC systems were programmed to apply the reported isocratic flow rates and column oven temperatures (isocratic 0.4mL/min and 40°C respectively), well within their maximum constraints, and therefore it was expected to have no major impact on the overall chromatography.

This was reflected in comparison of retention times, with the initial publication reporting AA (2.4min), DHA (2.4min) and EPA (1.9min). The analytical set up reported here recorded retention times of AA (2.11min), DHA (2.01min) and EPA (1.57min) and are sufficient in comparison (see Figure 2.7). As can be seen in the figure, peaks AA, DHA and d8-AA co-elute. This is due to their similar structure, carbon chain length, and physiochemical properties. Despite this co-elution, from both the original manuscript and in the findings reported here, there was found no

effect on linearity, or reproducibility of analysis. Major modifications to the original method would have been required to obtain a complete separation of the three FA species, and would have required time intensive testing and validation. The authors reported no problem in their validation due to the co-elution, therefore similar linearity values were achieved on the Waters Xevo® instrumentation.

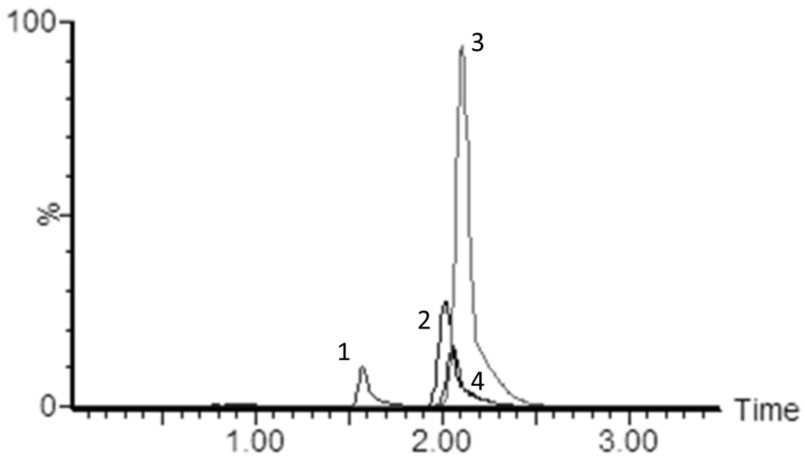

Figure 2.7: Overlaid Chromatogram of Extracted Fatty Acids

Three fatty acids extracted from plasma: (1) Eicosapentaenoic acid (EPA) (Retention time – 1.57) (2) Docosahexaenoic acid (DHA) (RT – 2.01) (3) Arachidonic acid (AA) (RT – 2.11). Also included is a deuterated internal standard (4) d8-arachidonic acid (d_8-AA) (RT – 2.11). Chromatography closely reflects the original manuscript by Salm et al.[213]. Peak co-elution occurs due to similar carbon chain lengths and properties and has no adverse effect on analysis.

To test the Waters Xevo® MS, six replicate extractions were completed on individual pools of plasma and brain tissue homogenate. Variation (RSD %) in plasma for the three extracts were all well below 5% (AA_{TOTAL} 0.97%, DHA_{TOTAL} 1.41% and EPA_{TOTAL} 2.45%). Similarly variation (RSD %) in pooled brain for the two detected extracts was also lower than 5% (AA_{TOTAL} 4.03% and DHA_{TOTAL} 4.21%).

This demonstrates a high level of reproducibility between extractions and was deemed acceptable to progress onto sample analysis.

EPA was below the limit of quantification in brain samples. In an attempt to detect the FA a four-fold increase of brain material underwent attempted extraction (100µL). However, although a small peak of EPA was detected it was below the level of quantification required. It was not possible to extract more material, due to the small sample sizes of the mouse brain, and therefore EPA was classed as below the limit of detection for the brain samples.

To test the linearity on the Waters analytical set up a range of FA standards in ACN/H_2O were extracted. This approach was employed in the original manuscript to demonstrate linearity across the expected range of endogenous FA. When tested on the Waters Xevo® QTOF the three FA provided acceptable R^2 values across a range 0.625-320µg/mL – AA (R^2=0.998), DHA (R^2=0.998) and EPA (R^2=0.996).

These R^2 values demonstrate that the extraction and analysis on the QTOF instrumentation are more than acceptable over the required range. Peak areas for each FA from the plasma samples from the pool fell comfortably within the peak areas for the range. These observations combined with the highly reproducible findings in the pooled extraction repeats of plasma and brain suggest that the method is suitable for use investigating changes of total FA, with application to different tissue samples in AD.

2.4.2 - MB2 samples

The examples discussed in Section 2.4.2 are summarised in Table 2.5.

MB2 was designed as a preliminary pilot study, in order to see if any major changes in FA_{TOTAL} were apparent in individual brain regions of wild type and TASTPM AD model mouse. In the study sample availability was low (n=1 per group). Therefore the project was treated as a proof of concept study.

TASTPM mouse models were used as a comparison in study MB2. The model is an amyloid based transgenic model, with a double APP mutation on the APP_{swe} and the PS1.M146V genes. This double mutation enables the early detection of amyloid deposits within three months, leading to cognitive impairment comparable to that in AD within six to eight months [214]. The advantage of using this double mutant model is that not only are Aβ protein deposits found in the brain, but there is also a decline in cognitive impairment, both aspects of which are not always observed in single APP transgenic mice models [214]. This property makes the samples used in study MB2 ideal to explore FA disruption as brain pathology relates to AD disease in human cases.

The TASTPM mice are designed to model AD pathology, with Aβ plaques forming in the cerebellum [214], similar to that described by Braak and Braak [74], who first described the stages of Aβ proliferation in human AD brain. They reported initial deposits in the cerebral regions, particularly the isocortex (Braak stage A), and spreading throughout the frontal and parietal lobe (Braak stage B), before finally spreading to the striatum, thalamus and hypothalamus (Braak stage C). This progress is also observed in the TASTPM models, with Howlett et al. reporting Aβ deposits mainly observed in the cortex regions [214].

Reference	Mouse Model (Biofluid)	Fatty Acid	Free or Bound	Observed Effect in AD	FA_{TOTAL} Effect in MB2
[218]	TASTPM (Plasma)	AA	Free	Decrease	N/A
[218]	TASTPM (Brain)	AA	Free	NSC	Increase
[202]	hAPP (Brain HC)	AA	Free	Increase	NSC
[202]	hAPP (Brain CX)	AA	Free	Increase	Increase
[219]	SAMP8 (Brain HC)	AA	Bound (TPL)	NSC (Aging)	N/A
[219]	SAMP8 (Brain HC)	DHA	Bound (TPL)	Decrease	N/A

Table 2.5: Summary of Fatty Acids in Alzheimer's Disease Mouse Model Literature
The above table highlights the fatty acids of interest in the literature. Examples are provided for arachidonic acid (AA) and docosahexaenoic acid (DHA) to enable comparison with the results reported in study MB2.
Ref = reference, TPL = total phospholipid, NSC = no significant change, HC = Hippocampus, CX = Cortex

Results from study MB2 appear to reflect the Aβ deposition pathology reported by Howlett et al. in the TASTPM mouse model [214] with an increase of AA_{TOTAL} and DHA_{TOTAL} in AD compared with controls in the cortex, thalamus and striatum regions. The results of the analysis in the hippocampus region analysis reported no change in FA_{TOTAL} levels between the wild type and AD TASTPM model. .

Concentration values of AA_{TOTAL} were reported to be increased in AD model mouse brain in the thalamus, cortex, striatum and cerebellum regions. The largest increase was found in the striatum and the thalamus.

The TASTPM models used in study MB2 have also been employed in a metabonomic non-target analytical publication, which analysed whole brain homogenate extracts, alongside those of plasma. Although the study was not specifically designed to target AA_{FREE}, the FA was investigated. Results reported

that AA did not significantly change between wild-type and TASTPM model brain homogenates [218]. Interestingly however, a decrease in AA_{FREE} in the plasma of the transgenic AD mice was observed. As the results were reported in whole brain homogenate extracts rather than specific isolated regions, it is difficult to directly compare with the findings of MB2 reported here, however an interesting future study would be to compare individual and total brain region AA_{TOTAL} to see if it correlated to the finding of AA_{FREE} reported in [218].

A further relevant publication, analysed AA_{FREE} levels in brain regions from an alternative mouse model (J20 hAPP mice). The J20 model utilises a strain of mice with single hAPP gene mutation. The data showed an increase in AA_{FREE} in both the hippocampus and cortex regions [202]. This outcome was discussed to be due to a difference in the activity of phospholipase A_2, the enzyme responsible for the release of AA from larger lipid species. This contrasts with the findings of MB2, which showed no variation in the hippocampus. However this could be due to a number of reasons, for example a difference in the mouse model used. An expansion to the study could be employed using a range of mice models in order to see if FA levels are consistent between different strains of mice model.

It is also interesting to note the decrease identified in the plasma of the AD mice models. This perhaps suggests that an imbalance exists between brain and plasma, with an increase in brain levels of AA, countered by a decrease in that of plasma.

FA have also been investigated in other AD mouse models. Petursdottir et al. [219] analysed FA in SAMP8 mice, a line of mice selectively bred, to have over expression of Aβ, compared with the wildtype, and thus is thought to model aspects of AD pathology [220]. The study reported concentrations of a number of FA, including DHA_{BOUND} and AA_{BOUND}. This was achieved by the completion of a pre-separation

by TLC that allows isolation of individual large molecule lipid species followed by the hydrolysis release of the FA_{BOUND}. This study reported levels of FA in both the hippocampus and amygdala regions of SAMP8 mice brains, focusing on FA changes with aging rather than comparing AD and Control mice. The results presented, show that DHA_{BOUND} decreases in hippocampus regions during aging of the AD model mice, indicating that FA metabolism perhaps plays an important role in mammalian aging, and it may be this effect that is observed in studies regarding AD, not as a response to AD pathology.

MB2 was developed as a proof of concept pilot study, and returned interesting observations regarding the level of FA_{TOTAL} in six mouse model brain regions. Despite the low sample size, differences of AA_{TOTAL} and DHA_{TOTAL} were apparent, supporting a justified expansion of the project to a larger sample set.

2.4.3– HP30 Samples

A summary table of the findings discussed in the following sections can be found at Table 2.6.

2.4.3.1– Quality Control

QC samples were included as replicate extractions of a pool of plasma (n=8). During the extraction procedure, samples were included at random, to ensure no group bias. These samples underwent analysis at regular intervals across the analytical run, 2x before, 1x every six injections during the run and 2x at the end of the run. Three FA molecular species (AA_{TOTAL}, DHA_{TOTAL} and EPA_{TOTAL}) were extracted as per patient samples, and the corresponding concentration values were calculated. Variation was found to be >3% in all cases, suggesting the method was highly reproducible across the run and any differences observed in HP30 groups is therefore due to differences in patient physiology as opposed to analytical variation.

Ref	Biofluid	Fatty Acid	Free or Bound	Observed Effect in AD	FA_{TOTAL} Effect in HP30
[209]	Plasma	AA	Bound (TPL)	NSC	NSC
[208]	Plasma	AA	Bound (TPL)	NSC	NSC
[208]	Plasma	AA	Bound (PC, PE, LysoPC)	NSC	NSC
[221]	Plasma	AA/DHA Ratio	Free	High Ratio	NSC
[221]	Plasma	AA	Free	NSC	NSC
[209]	Plasma	DHA	Bound (TPL)	Decrease	NSC
[209]	Plasma	DHA	Free	NSC	NSC
[208]	Plasma	DHA	Bound (TPL)	Decrease	NSC
[222]	Serum	DHA	Bound (PC)	Decrease	NSC
[223]	Plasma	DHA	Bound (TPL)	NSC	NSC
[201]	Plasma	DHA	Free	Low Baseline	NSC
[224]	Plasma	DHA	Free	Low Baseline	NSC
[209]	Plasma	EPA	Bound (TPL)	Decrease	Decrease
[208]	Plasma	EPA	Bound (TPL)	Decrease	Decrease
[208]	Plasma	EPA	Bound (PC, PE, LysoPC)	Decrease	Decrease
[221]	Plasma	AA/EPA Ratio	Free	NS	Increase
[225]	Serum	EPA	Free	Aging Decrease	N/A

Table 2.6: Summary of Fatty Acids in Alzheimer's Disease Human Literature

The above table highlights the fatty acids of interest in the literature. Examples are provided for arachidonic acid (AA), docosahexaenoic acid (DHA) and eicosapentaenoic acid (EPA) to enable comparison with the results reported in study HP30.

Ref = reference, TPL = total phospholipid, PC = phosphatidylcholine, PE = phosphatidylethanolamine, LysoPC = lysophosphatidylcholine, NSC = no significant change

2.4.3.2 – Arachidonic Acid

AA, along with DHA is one of the most predominant FA in the human brain, and therefore is a major metabolite at the centre of AD pathology. The findings here reported no significant change of plasma AA_{TOTAL} between any of the diagnostic groups (AD, MCI, Control) with a relatively consistent concentration between all three. This finding appears to complement previous studies of human plasma. Cunnane et al. investigated a range of plasma AA_{BOUND} in control, MCI and AD patient groups. The study found that no significant differences of AA_{BOUND} to phospholipids, despite demonstrating a slight decreasing trend in AA_{BOUND} concentrations (Control → MCI → AD) [209]. FA levels in plasma were then correlated to levels in corresponding human brain samples, however in the case of AA no significant patterns emerged.

A further study investigated the variation of plasma AA_{BOUND} between four groups of patients; normal controls, AD, cognitive impairment but non-demented and other non-AD dementia cases [208]. The study looked at AA_{BOUND} to plasma phospholipid species, and of AA_{BOUND} to individual lipid classes including PC, PE and LysoPC. AA_{BOUND} was found not to vary significantly in any of the extractions from different groups.

A large population study (n=1214) that recorded baseline polyunsaturated FA_{FREE} levels at an initial visit, and two follow up visits, two and four years later to check for progression of dementia, identified plasma AA_{FREE} as a risk factor. Those patients who exhibited a high ratio of AA_{FREE} to DHA_{FREE} were shown to have an increased risk of progressing to AD over the 4 years ($p=0.004$). AA_{FREE} on its own was demonstrated to be non-significant ($p=0.45$) [221]. This result appears to show that it is an imbalance of AA_{FREE} compared with other FA_{FREE} that alters more in

dementia cases. When data in study HP30 was analysed in a similar manner, using FA ratios, the only ratio to provide significance was AA/EPA (p=0.05), which increased in samples from the AD patient cohort. Ratio AA/DHA showed no significant differences between controls and AD (p=0.08), contradicting the findings in the larger population study.

In general previously published examples correlate to findings reported here in the HP30 study. This would suggest that despite AA being shown to vary significantly in human (temporal cortex) [226] and mouse model brain (hippocampus) [202] as well as previously being shown to cross the BBB [212], the trend does not apply to human plasma, and therefore results suggest that AA_{TOTAL} is unable to distinguish between disease groups in plasma.

2.4.3.3 – Docosahexaenoic Acid

Along with AA, DHA is also one of the major FA found in the brain. In the HP30 samples the mean concentration values of DHA_{TOTAL} were found to decrease between control → AD and MCI → AD, however this was not found to be significant when comparing means using the student's t-test.

This result relates to a previous study that investigated the plasma DHA of individuals in control, MCI and AD patient groups, where it was reported that DHA_{FREE} displayed no significant differences between disease groups. However in contrast, the same study also demonstrated a significant decreasing trend between control → AD and MCI → AD, when comparing DHA_{BOUND} to phospholipid species (p=<0.05) [209]. A decreasing trend was also observed for DHA_{BOUND} to total plasma lipids, however this was non-significant. Interestingly the same study found that DHA_{BOUND} in human brain was significantly lower as a % of total phospholipids. It

was found to be reduced by 14% in the mid-frontal region and 12% in the temporal cortex.

Of particular interest from a biomarker perspective is that the study investigated the correlation between plasma and brain fatty acid compositions, however only identified one significant trend, reporting %DHA_{BOUND} to total plasma lipids, compared with % DHA_{BOUND} to brain PE. These reported findings in both plasma and brain appear to suggest that brain changes can be reflected in the plasma of individuals, increasing the chance that they may play a role as suitable biomarkers.

A further study into human plasma has found that DHA_{BOUND} to phospholipids is present at significantly lower concentrations in cases of AD, cognitive impairment but non-demented and other non-AD dementia cases ($p=<0.05$). This significant reduction is also observed in DHA_{BOUND} to plasma PC and plasma PE ($p=0.05$) [208].

Providing further support to this finding, serum DHA_{BOUND} to PC has been shown to be present at significantly lower concentrations in dementia cases. 193 patients were organised into five different patient groups; controls, AD (MMSE upper quartile), AD (MMSE second quartile), AD (MMSE third quartile) and AD (MMSE lower quartile), with significant reductions in DHA_{BOUND} to PC being observed when comparing controls with each of the MMSE quartiles ($p=<0.001$ for all quartiles) [222]. However, the article found a significant difference when comparing the ages of the MMSE quartiles with those from the control group ($p=<0.001$). This could potentially affect the outcome of the results and should be considered when judging the reported observations.

A non-significant result was observed in a cross sectional population study. DHA_{BOUND} to phospholipids were quantified, with comparisons between patients in

groups of controls, cognitively impaired but non-demented and AD. What is interesting with regard to this study is that a sub-group of these patients were also revisited on average four years later, with those progressing from control to AD having a 30% higher baseline level of DHA_{BOUND} to phospholipids, however this was statistically non-significant (p=0.07) [223]. This provides evidence that a cross sectional study like HP30 might not provide significant differences, but longitudinal studies, may be more informative.

A further study that investigated 899 initially dementia free men and women quantified DHA_{FREE} levels at visit one to record a baseline reading, and at a follow up visit on average 9.1 years later. It was shown that those with plasma baseline of DHA_{FREE} in the upper quartile had a 47% lower chance of progressing to AD [201]. Although the results of HP30 were not significant, a decrease in DHA was observed in the cognitively impaired groups (MCI and AD) compared with controls, which would complement the results in the large cohort follow up study.

In a similar study, Lopez et al. also found a trend of increased DHA_{FREE} plasma with a reduced risk of progressing to Alzheimer's disease or other dementia types [224]. The study took plasma levels of DHA from 266 individuals. The study reported that those with DHA_{FREE} levels in the upper tertile were found to have 65% reduced risk of being an all type dementia case, and 60% reduced odds of being an AD case. Although results in HP30 were non-significant, the overall trend is again in agreement with these findings, with a decrease of DHA_{TOTAL} identified in patients with AD.

In addition, another study reported baseline DHA_{FREE} in 1214 patients, who were re-visited after two and four years to track for progression to AD. No significant relationship between baseline DHA_{FREE} levels, and the progression to AD was

reported [221]. However, the ratio of AA_{FREE} to DHA_{FREE} was found to lead to a significant reduction of risk, where those with lower ratio tended to have a reduced risk of AD progression (p=0.004). This was not the case in HP30 with ratios of AA_{TOTAL}/DHA_{TOTAL}, found to be non-significant between the disease groups (p=0.08).

Despite a number of studies reporting significant changes in both DHA_{FREE} and DHA_{BOUND}, the result presented here in HP30 of combined DHA_{TOTAL} suggests that it does not significantly change between the patient groups of control, MCI and AD. Therefore it would seem that it is not suitable for progression in a biomarker capacity in AD.

2.4.3.4 – Eicosapentaenoic Acid

EPA was the only FA of the three analysed in HP30 to demonstrate a significant change in concentration values for Control → AD (p=0.023), with an overall trend of diminishing levels observed for Control → MCI → AD.

A recent study, investigated plasma and brain FA profiles in both MCI and AD. A significant decrease was observed when comparing EPA_{BOUND} to phospholipids in Control → AD (p=<0.05) and MCI → AD (p=<0.05) [209]. A similar trend was also seen in HP30 with a decrease in EPA_{TOTAL} between Control → AD as well as MCI → AD, however in this instance only controls and AD comparisons proved significant (p=0.023).

A further study provided more support to these findings [208], reporting significant changes of EPA_{BOUND} when comparing controls with AD (p=<0.05), dementia cases other than AD (p=<0.05), and non-dementia cases with cognitive impairment (p=<0.05). This finding applied to both EPA_{BOUND} as part of total plasma

phospholipids, as well as individual EPA_{BOUND} to PC and PE parent species. The authors went on to hypothesise that this decrease of EPA in the cognitively impaired groups was due to dietary factors, however provided no data to support this discussion.

However, this hypothesis is contradicted by findings from the Chicago Health and Aging Project [227] where dietary intake of EPA was not associated with development of AD in a patient cohort of 815 patients. The study has particular weight due the size of the patient cohort. This would therefore suggest differences in EPA observed in AD could be due to a pathological function of the disease mechanism rather than dietary factors.

Previously it has been demonstrated in a large population study (n=1214) where the patients were visited after two and four years to track progression to AD, that those with a high plasma concentration of EPA had a significantly reduced risk of progressing to AD ($p=0.02$) [221]. This is in agreement with the results in HP30. However, the publication, differed in relation to the findings on ratio analysis, with AA/EPA found to be non-significant, whilst in the study HP30, this ration significantly increased in patients with AD ($p=0.05$).

EPA, as part of serum cholesterol esters has also been demonstrated to decrease in patients with AD. Tully et al. [222] analysed the serum of 193 patients, which were organised into five different patient groups; controls, AD (MMSE upper quartile), AD (MMSE second quartile), AD (MMSE third quartile) and AD (MMSE lower quartile). The study reported a significant reduction in the concentration of EPA extracted from cholesterol esters when comparing each MMSE quartile with the control ($p=<0.05$ quartile 1, $p=<0.001$ quartiles 2-4). Interestingly, as discussed previously (Section 2.4.3.3), the publication reports that the mean age of the

dementia groups was significantly older than the controls (p=<0.001), which could undermine the statistical significance of the finding.

An interesting extract from the *Proceedings of the eighth international symposium on the neurobiology and neuroendocrinology of aging* published in the journal *Experimental Gerontology (2007)* also discussed EPA concentrations in serum, and compared levels between Japanese centenarians (n=200) and gender matched young healthy controls (n=150). Thus reported a significant decrease in serum EPA found in the elder group (p=<0.05). Importantly, the EPA concentrations in the centenarian group, also significantly correlated with MMSE scores (p=<0.05) suggesting that although EPA levels are associated with age, they are also associated with cognitive state [225].

2.5 – Conclusions

2.5.1 – MTEST

The method adapted from a previous literature source was proven to be suitable for the analysis of three FA species in human plasma and mouse brain. It was demonstrated that the extraction was reproducible and linear across the range observed in the two studies, and therefore was useful in determining any changes that occur between sample groups.

2.5.2 – MB2

Despite the small samples size of the study (n=2), DHA_{TOTAL} and AA_{TOTAL} variation was demonstrated across brain regions of each individual mice, highlighting that each individual brain region is likely to hold different metabolic pathways. These results appeared to correlate to AD related progression of Aβ throughout the brain, with the largest FA differences shown to be in regions known to be most at risk of Aβ development. Although the small sample size makes it difficult to discuss with any statistical significance, important questions are raised, leading the way to hopeful future investigations and collaborations.

2.5.3 – HP30

Numerous studies have linked abnormal levels of FA both in human brain and plasma to AD. Despite this, to the author's knowledge this is the first time the three FA have been considered in their entirety (free and bound) with regard to AD. However the results only showed significant decreases in EPA_{TOTAL}. Literature sources on FA in the circulatory system often contradict one another, with no clear pattern emerging.

It is clear that there is conflicting information in the literature, some that supports the finding of HP30, and some that directly contradicts it. This could be due to a number of factors such as effects relating to general cognitive function, or even general aging differences.

With this finding in mind, there is a suggestion that a requirement for AD predictive markers is that they are more specific to the pathology of AD. Therefore the strategy of biomarker discovery was progressed to a non-targeted lipid analysis, in an attempt to identify novel small metabolite markers of disease, which perhaps have yet to be reported in the literature (see chapter 3).

A decision was made to focus directly on human plasma samples due to better sample availability and because of the greater relevance if future findings show promise and progress to a clinical environment.

Chapter 3:

Preliminary Non-Targeted Biomarker Screen

3.1 – Introduction

Chapter 2 described a targeted approach in order to observe the total plasma levels of three abundant FA species. Despite the observation of a significant reduction in EPA_{TOTAL} ($p=0.023$), and a significant increase in the ratio AA_{TOTAL}/EPA_{TOTAL} ($p=0.05$) in AD patients compared with controls, a decision was made to adjust the project strategy in an attempt to identify a novel biomarker previously not published in the literature.

Therefore, the next step of the investigation was to perform non-targeted biomarker discovery. An overview and comparison with targeted approaches can be observed in Figure 3.1.

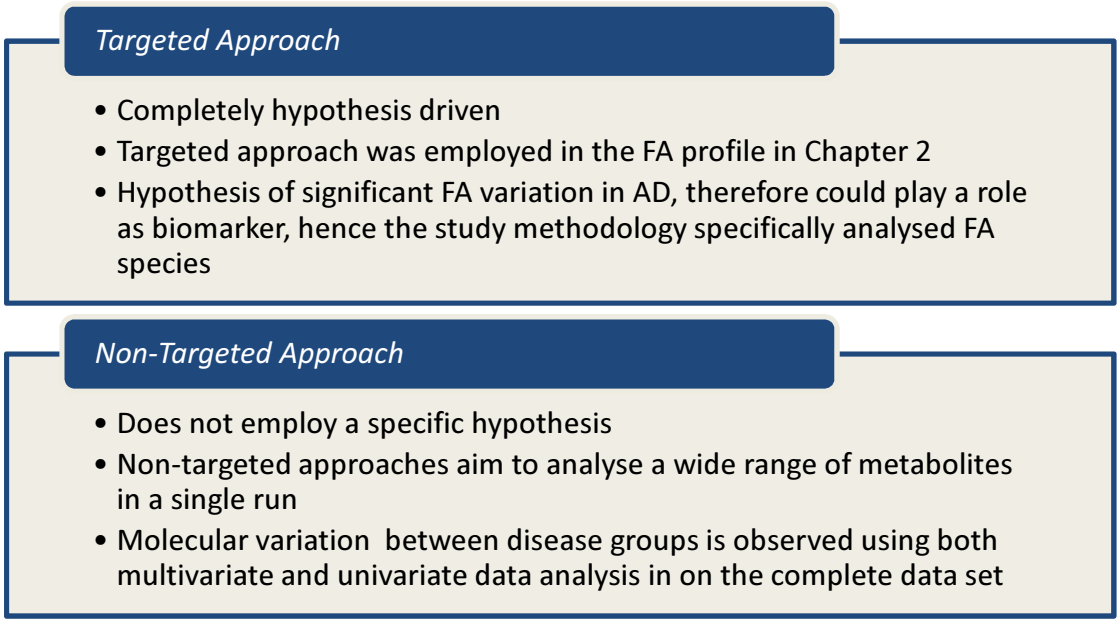

Figure 3.1: Comparison of Non-Targeted to Traditional Target Approaches

3.1.1 – Terminology

When discussing non-targeted approaches the terminology employed can become confusing due the large number of definitions found in the literature, with the most common of these being metabolomics and metabonomics.

Recently, a definition structure has begun to take shape, with metabolomics now commonly defined as the "comprehensive detection and quantitation of all the low-molecular-weight molecules and metabolites present in cells, tissues or organisms under a set of given conditions", and metabonomics described as the "quantitative analysis of the metabolic response of living systems to pathophysiological stimuli or genetic modification over time" [228].

Further common terms that are encountered in the literature and add to the confusion include, metabolic profiling, metabolic fingerprinting and metabolic phenotyping. Although referenced literature examples discussed herein may refer to any one of these terminologies, they will be referred to as non-targeted analytical approaches.

A further important terminology that is commonly used when it comes to non-targeted analysis includes what is known as a molecular "feature". A feature is an individual molecular species. For example in LC-MS non-targeted approaches, an unidentified molecular structure is often referred to as a feature, meaning a specific mass at a specific retention time.

3.1.2– Non-Targeted Literature Examples in Alzheimer's Disease

A review of non-targeted approaches employed in biomarker research with regard to AD is presented in the main introduction to the thesis and can be found in Section 1.7. However, to summarise briefly, a number of publications are available in the literature that utilise NMR [131, 188, 191, 192], GC-MS [229] and LC-MS [119, 193, 196] techniques in a range of biofluids, from both human patients and animal AD models.

Important findings included a significant reduction in particular plasma bile acids [119], CSF citrate [188] and creatinine [131], an increase in plasma ceramide (CER16:0) levels and a decrease in plasma sphingolipid (SP16:0) levels [193] and a significant variation of serum FA between MCI and control patients [191].

A high number of these findings, particularly by NMR approaches, identified many polar metabolites such as citrate and creatinine. However, as discussed in Chapter 1 and Chapter 2, there is a bulk of literature linking lipid abnormalities to AD.

Examples of non-polar candidate to come from non-targeted methods include bile acids [119], ceramide 16:0 [193], sphingomyelin C16:0 [193], as well as those in a publication by Oresic et al [196], who statistically grouped three or four similar metabolites in what was termed "clusters", with the most promising cluster containing one non-polar PC. Further to this, the application of LC-MS techniques to AD biomarker discovery in a non-targeted manner is in its infancy, with only a handful of publications to date.

Therefore, with this in mind, an LC-MS study was designed to encapsulate a wide range of plasma molecular species, with a consideration on the non-polar element of the extraction, and the aim of identifying novel biomarker candidates for AD. In addition, MCI samples underwent comparison, with the aim of identifying any biomarkers that may be intermediate between the condition and AD or control.

3.2 – Materials and Methods

The screening method discussed within this chapter was adapted and modified from a publication previously published by Raineville *et al*. [230].

3.2.1– Materials

LC-MS Grade acetonitrile was purchased from VWR (Leicestershire, UK) and high purity water deionised water was obtained from an in house Millipore filtration system (EMD Millipore, MA, USA). Analytical grade ammonium formate was purchased from Fisher Scientific (Loughborough, UK).

3.2.2 – Instrumentation

LC-MS analysis was completed using a Waters Acquity UPLC® (Waters, Milford, USA) coupled to a Waters Xevo® G1 QTOF (Waters, Milford, USA). Analysis was completed in both positive and negative ionisation. Both LC and MS settings were specifically designed for each phase and are described below.

3.2.2.1 – Positive MS Ionisation Analysis

The chromatographic column used was a Waters UPLC-BEH C_{18} (2.1×100mm, 3µm) maintained at 60°C. Mobile phase A was H_2O (10mM ammonium formate) and B was acetonitrile (10mM ammonium formate). A gradient analysis was employed as follows: 0min (30%B); 15min (100%B). A 5min re-equilibration at the initial 30%B was employed before injection of the next sample. Solvent was passed through the column at a rate of 0.6mL/min.

The Waters Xevo® MS was operated in the positive ion mode with a capillary voltage of 3.2kV and a cone voltage of 35V. The extraction cone was set to 2.0V. The desolvation gas flow was 900L/hour and maintained at 350°C. The source temperature was 120°C and cone gas was set to 50L/hour. All analyses were

acquired using the reference solution to ensure accuracy and reproducibility; leucine enkephalin was used as a reference mass (m/z 556.2771 and 278.1141) at a concentration of 500ng/mL and a flow rate of 10µL/min. Data was collected in the centroid mode over the mass range 50–1000Da with an acquisition time of 0.1 seconds per scan.

3.2.2.2 – Negative MS Ionisation Analysis

The chromatographic column used was a Waters UPLC-BEH C_{18} (2.1×100mm, 3µm) maintained at 60°C. Mobile phase A was H_2O (10mM ammonium formate) and B was acetonitrile (10mM ammonium formate). A gradient analysis was employed as follows: 0min (30%B); 2min (60%A); 10min (100%B). A 5min re-equilibration at initial 30%B was employed before injection of the next sample. Solvent was passed through the column at a rate of 0.35ml/min.

The Waters Xevo® G1 QTOF MS was operated in the negative ion mode with a capillary voltage of -2.6kV and a cone voltage of 45V. The extraction cone was set to 2.0V. The desolvation gas flow was 800L/hour and maintained at 350°C. The source temperature was 120°C and the cone gas was set to 20L/hour. All analyses were acquired using the lock spray to ensure accuracy and reproducibility; leucine enkephalin was used as a lock mass (m/z 554.2615 and 276.0985) at a concentration of 500ng/mL and a flow rate of 10µL/min. Data was collected in the centroid mode over the mass range 50–1000Da with an acquisition time of 0.1 seconds per scan.

3.2.3 – Waters MS^e Data Collection

In both polarities data was collected using Waters MS^e technology, meaning data was collected at two constantly interchanging collision cell energy ranges. This enables data collection in two “levels”. Level one is acquired using a low collision

energy (4V) enabling MS data with parent molecular ionisation. Level two applies a high collision energy (50V) within the MS collision cell, which has the effect of causing molecular fragmentation, meaning accurate mass fragmentation data can be collected simultaneously to accurate mass parent ion data. Importantly, this can assist with structural elucidation (discussed later in Chapter 5 – Section 5.3.3) with only a single analytical run required, thus preventing the need for repeat extractions and analyses, vital for valuable sample preservation and also reducing analytical time and cost.

3.2.4 – Sample Preparation

Human plasma samples were acquired from the Institute of Psychiatry, Denmark Hill, London, UK. The samples were obtained from the two clinical cohorts AddNeuroMed and DCR. These cohorts are described in full detail in Chapter 2, Section 2.2.3.3.

Sample sets were selected based on age and gender. Full details of each of the sample sets used for the analysis can be found in Table 3.1.

QC samples were prepared by creating a pool of aliquots taken from all samples. Lipids were extracted from patient plasma by precipitating the plasma protein with acetonitrile (ratio 1:3 plasma:acetonitrile). Samples were centrifuged at 2500g for 5mins. The supernatant was removed and 5µL was injected for LC-MS analysis.

	Positive Ionisation			Negative Ionisation		
	Control	MCI	AD	Control	MCI	AD
Age(years) Mean	78.05	84.57	81.69	79.19	83.73	78.17
Age Std Dev	6.35	6.45	8.56	7.44	6.63	6.76
MMSE Mean	28.87	25.50	16.40	28.3	25.1	17.1
MMSE St Deviation	1.46	2.95	6.80	2.7	3.3	5.6
Total Samples	15	10	10	12	10	7
Number of Male/Female	5/10	5/5	5/5	5/7	5/7	3/4
% Male/Female	33/66	50/50	50/50	42/58	50/50	43/57

Table 3.1: Patient Data for The LC-MS Screening Study

Summary of patient data of plasma samples included in the study. Samples were age and gender matched as much as possible to reduce external influences of analysis. Mini Mental State Exam (MMSE) results are also reported here.

3.2.5 – Data Processing

Following LC-MS analysis of the samples, the mass spectrometry raw data underwent feature alignment using Waters MarkerLynx software, a package within Waters MassLynx 4.1 (Waters Corporation, Milford, USA).

The alignment procedure results in an output of peak height values, which in turn are normalised. The MarkerLynx software applies a normalisation algorithm which takes into account total ion counts of each chromatogram, and adjusts all marker intensities so that the sum of intensities within each sample is the same.

The alignment procedure was completed separately for each ionisation sample set (positive and negative). The marker outputs of these, was then transferred to SIMCA-P+ 12.0 (Umetrics, Umeå, Sweden), where they were subjected to

multivariate data modelling, including pareto scaled principle component analysis (PCA) and orthogonal partial least squares discriminate analysis (OPLS-DA).

QC samples were included in the PCA models for each ionisation mode to demonstrate reproducibility across the sample run. If QC samples grouped within 15% of the total t[1] and t[2] on the unsupervised PCA model, then the run was considered to be acceptable for further use.

Once the models had been accepted the two data sets progressed to and underwent OPLS-DA modelling. An OPLS-DA model was initially created for Control vs. MCI vs. AD. The completion of a corresponding S-plot analysis then enabled those features that had the highest magnitude of variation between groups, therefore influencing the OPLS-DA models, to be isolated.

These individual metabolite features were then individually re-extracted from the raw data using Waters QuanLynx, a package within Waters MassLynx 4.1 (Waters Corporation, Milford, USA). These features then underwent univariate means testing and were analysed for significance using a standard "students" t-test in IBM SPSS (IBM, Portsmouth, UK).

3.2.6 – Putative Identification of Features

All features that were observed to influence the models and therefore underwent univariate data analysis, were also preliminarily identified using the human metabolome database (HMDB) [231-233] and the equivalent METLIN (METabolite LINk) database [234]. Using the HMDB allowed an indication of the molecular classes, enabling a decision on the progression of the project.

Due to the high number of database hits generally returned by the database search, a number of rules were enforced in the identification database searching process

in order to be as consistent as possible. These rules are listed and explained below:

- 0.05 Dalton (Da) error:
    - The error of the search on the database searches was set to 0.05Da error, as this was well within the accuracy of the Waters Xevo® MS and confirmed by our external calibration.
- Polarity:
    - The feature in each instance must realistically ionise in the polarity being observed. For example FA, are generally only observed in negative ionisation mass spectrometry (unless they have formed adducts in the ionisation source).
- Human biology:
    - Features in the search must be metabolites from human biology and have been observed in human biology, preferably in the circulatory system, for example plasma or whole blood. HMDB lists instances where the molecules have been extracted from human tissue and previously reported in the literature.
- Retention Time
    - Retention time of each feature is considered, for example molecules with a similar structure often elute in the same region of the chromatogram, and this was taken in consideration when completing the database search.

3.3 – Results

Results from the positive ion screen are discussed in Section 3.3.1, whilst the results of the negative ionisation screen are discussed later on in Section 3.3.2.

3.3.1– Positive Ionisation Screen

Following adaptation of the chromatographic method, combined with positive ionisation MS detection, a final 15 minute chromatogram was developed that was suitable for a screening analysis. Following alignment of all of the data using Waters MarkerLynx software, a final list of 950 features (m/z at a retention time) was produced. Figure 3.2 presents an example positive ionisation chromatographic trace.

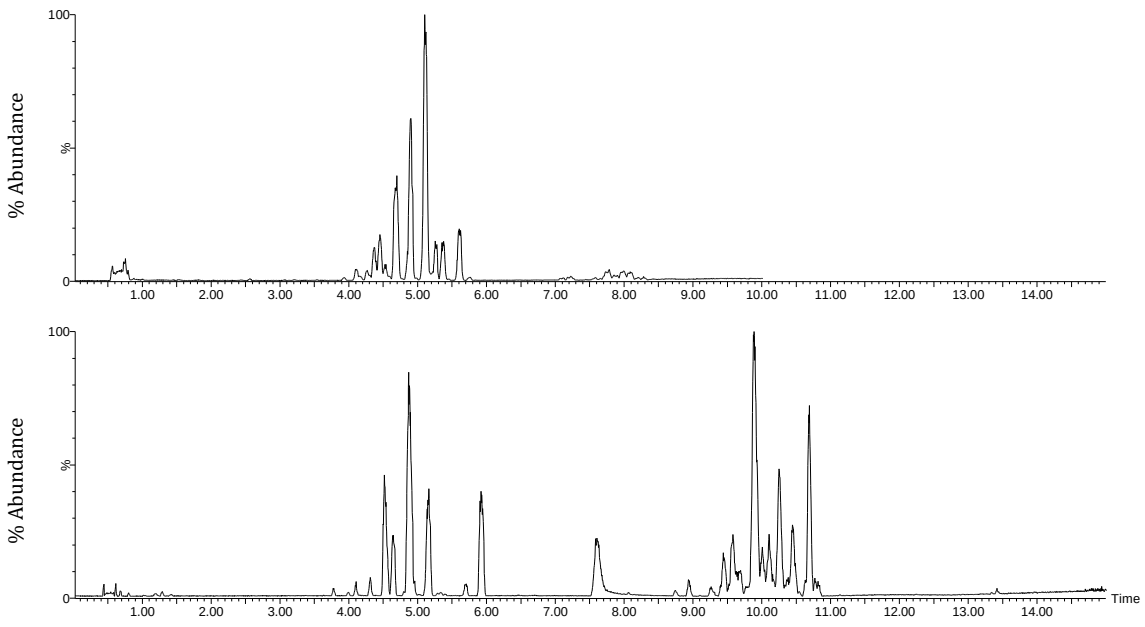

Figure 3.2: Example Screen Chromatograms of QC Samples

The upper figure presents a total ion chromatogram (TIC) of a QC sample analysed under negative ionisation chromatographic and mass spectrometry settings. A 10 minute gradient was applied, which gave a rapid LC-MS plasma screen. The gradient time had to be increased due to the increased number of features in the positive ionisation mode (lower TIC), resulting in a 15 minute plasma metabolite screen. Both methods were fully reproducible as demonstrated by QC clustering on the relevant PCA models (Figure 3.3a Figure 3.7a).

3.3.1.1– Principle Component Analysis to Demonstrate Reproducibility of Intra-Run QCs for Acquired Positive Ionisation Data

Following the alignment of the raw positive ionisation data, an unsupervised pareto scaled PCA model was produced in SIMCA-P+ (Umetrics, Sweden), to show QC grouping and reproducibility across the analytical run (Figure 3.3a). Clustering of the QC samples was required to be within 15% of the total model (both t[1] and t[2]).

From the PCA it could be observed that the QCs grouped within the model as expected from a reproducible run. Therefore the data was accepted for further analysis. As would also be expected in age and gender matched samples in a complex matrix such as human plasma, no obvious disease groupings or separations occurred on the PCA model (Figure 3.3b). This also suggests no inter-group differences due to analytical or extraction irregularities or patterns. This would also be expected from a randomised run.

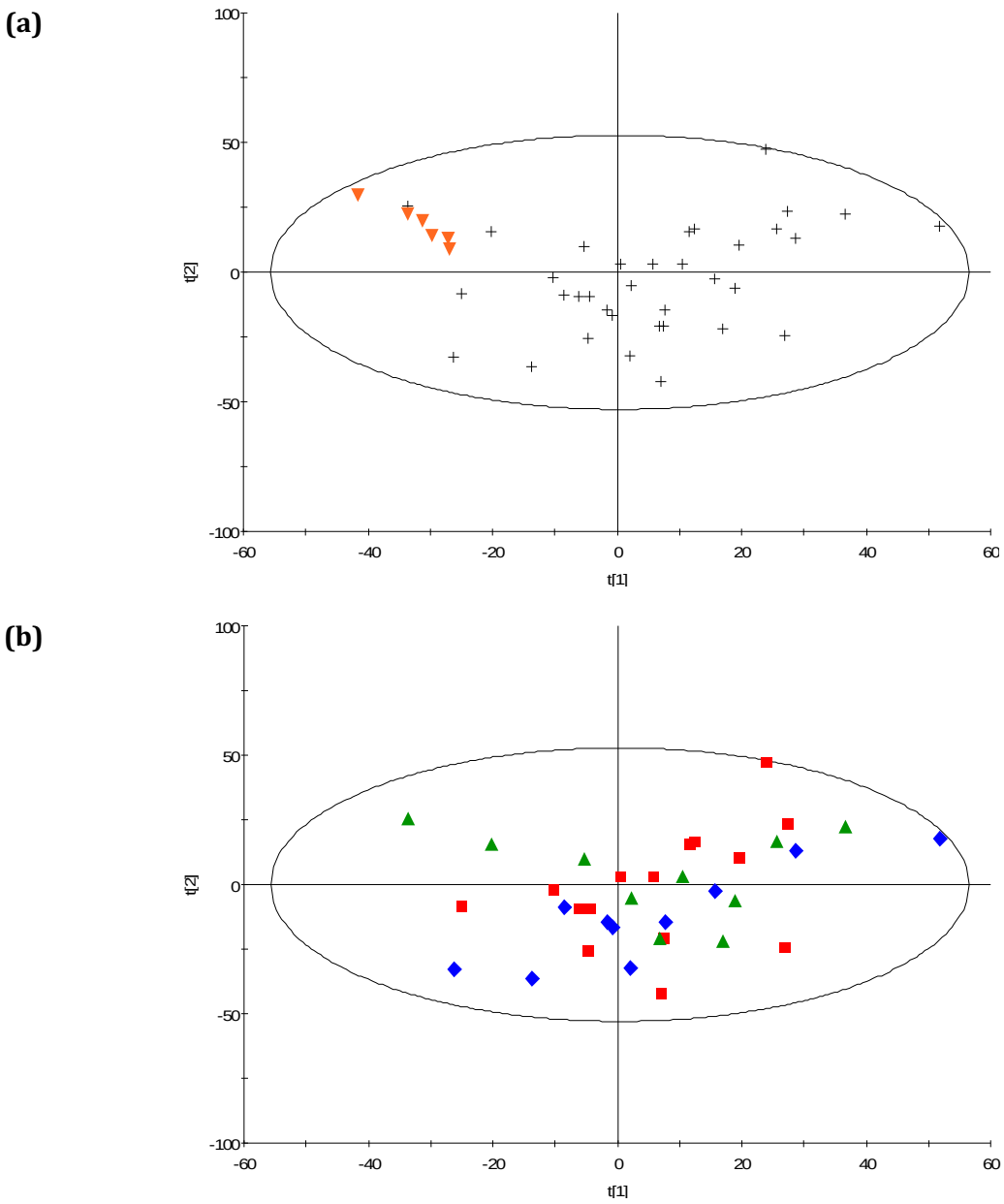

Figure 3.3: Principle Component Analysis of Positive Ionisation Screen Study Data

Unsupervised Principle Component Analysis (PCA) positive mass spectrometry dataset (n=41 respectively).

(A) Quality control (QC) samples can be seen as orange inverted triangles. QCs were excepted if clustering on the PCA =<15% for the total t[1] and t[2].

(B) PCA with diagnostic class colour coded. No outliers were observed.

The PCA model demonstrates no diagnostic group clustering. This would also indicate no differences or patterns of an analytical nature or batch effect, and is as expected from a randomised sample analysis.

3.3.1.2 – Orthogonal Partial Least Squares Discriminate Analysis of Positive Ionisation Data

Pareto scaled OPLS-DA models were produced for the positive ionisation data. The samples were grouped by class (Control or MCI or AD), with an initial model to compare all three within the same model (Figure 3.4a). A clear separation was observed between AD samples and the rest of the sample set (MCI and Control).

SIMCA-P+ software assigns each model it produces two values as an assessment of the models validity – R^2 and Q^2. The R^2 value represents the models ability to separate into classified groups whilst the Q^2 value is a figure designed to represent the prediction capabilities of an unknown feature into the model. The perfect predictive model score would be $R^2 = 1.0$, $Q^2 = 1.0$. Umetrics recommend that when using SIMCA-P+ an acceptable biological PCA model for use as a fully validated predicative tool, should return scores of $R^2 = 0.5$, $Q^2 = 0.4$. A negative Q^2 value means the model has no predictive capabilities at all [235].

The OPLS-DA created from the positive data returned an R^2 and Q^2 value of 0.321 and 0.298 respectively. This figure is below recommendations for a validated predictive model, however, in the case of this study, the aim is to identify potential candidate biomarkers, and therefore, for use as a data-mining tool the values are acceptable.

From the OPLS-DA model an S-plot was produced (Figure 3.4b) to illustrate the features that varied the most between disease classes. Features were selected that had a magnitude of variation value (p[1]) of >0.15 in the model. The models for positive ionisation produced 8 eight such features.

(a)

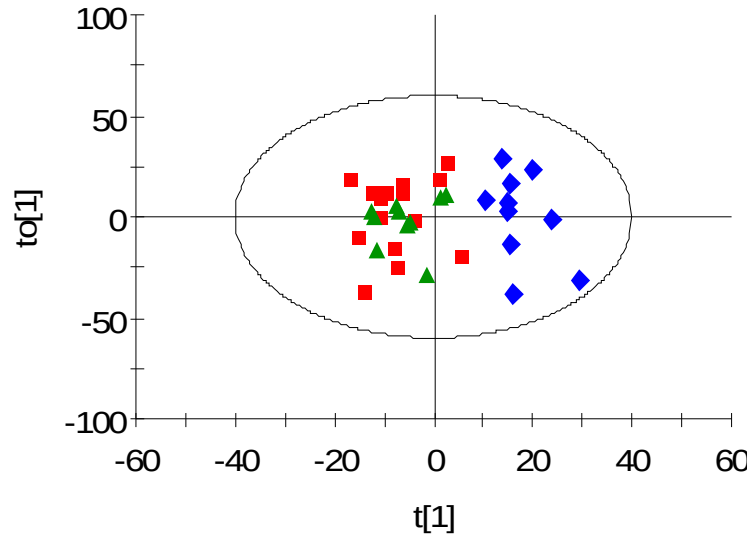

(b)

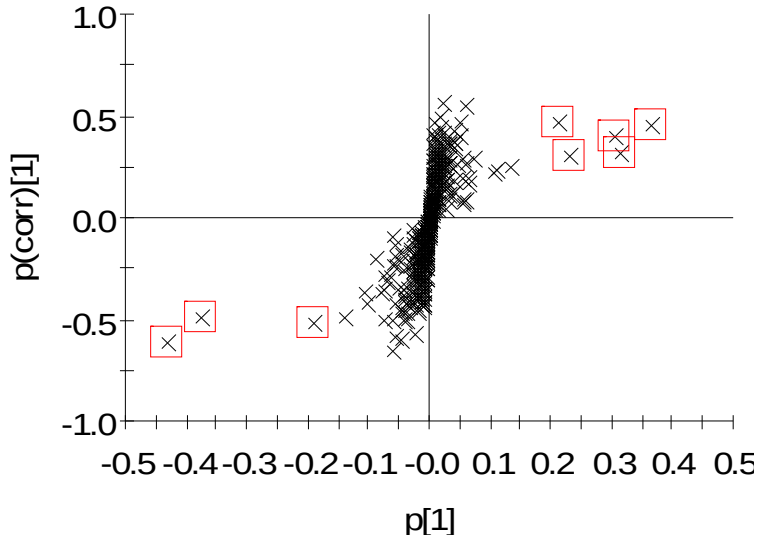

Figure 3.4: OPLS-DA model of Positive Ionisation Data

The figure presents supervised pareto scaled OPLS-DA model **(a)** for positive data.

A clear visual separation of groups was achieved between AD and both Control and MCI with model validation values of $R^2 = 0.298$ and $Q^2 = 0.034$.

S-plot analysis **(b)** highlights those features which had the greatest magnitude of variation (p[1]) within the corresponding OPLS-DA model **(a)**. Features with a p[1] value >0.15 are highlighted and underwent further investigation. These features can be found in Table 3.2.

As a further data mining approach, models were also created for individual disease comparisons. Again visual separation was observed in each comparison (Figure 3.5). Results returned the following R^2 and Q^2 values.

- Control vs. MCI: $R^2 = 0.660$ and $Q^2 = -0.475$
- Control vs. AD: $R^2 = 0.708$ and $Q^2 = 0.214$
- MCI vs. AD: $R^2 = 0.763$ and $Q^2 = 0.257$

Again, the values are below the recommended value for use as a validated predictor tool, but are acceptable for use a data-mining tool for biomarker discovery.

S-plot analysis was completed for each model, which again revealed those features that varied most in the model (p[1]>0.15). Many of these features overlapped with those from the initial model; however some new features were presented.

Table 3.2 lists the highlighted features of interested obtained from the positive ionisation S-plot analysis.

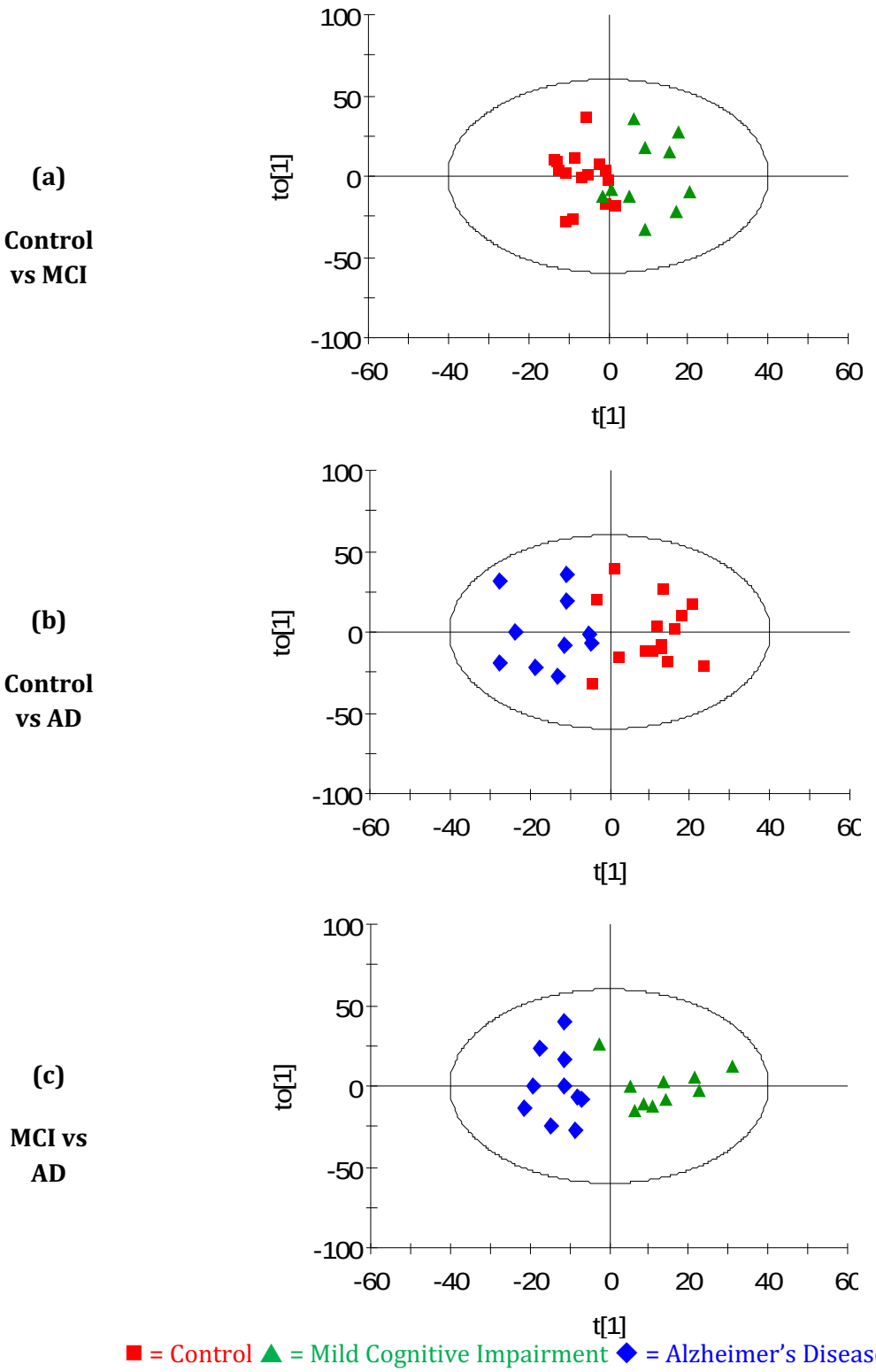

Figure 3.5: Individual OPLS-DA Models of Positive Data

The above figure displays OPLS-DA of positive ionization data, illustrating the intergroup separation of each disease class. R^2 and Q^2 values for each model are as follows:

- Control vs. MCI = $R^2 = 0.660$ and $Q^2 = -0.475$
- Control vs. AD = $R^2 = 0.708$ and $Q^2 = 0.214$
- MCI vs. AD = $R^2 = 0.763$ and $Q^2 = 0.257$

m/z	Retention Time (min)	Three Way Model	Control vs MCI	Control vs AD	MCI vs AD	MPA Control (Counts)	MPA MCI (Counts)	MPA AD (Counts)	Putative Identification
494.3248	4.07	-	✓	-	-	158.78 ±71.11	110.58 ±28.69	157.71 ±114.12	LysoPC
515.4132	10.66	✓	-	✓	✓	2301.83 ±577.46	2133.11 ±688.48	2419.63 ±248.70	TAG
522.3555	5.09	-	✓	-	-	1276.27 ±266.98	1136.76 ±291.67	1273.95 ±457.97	LysoPC
532.4417	10.66	✓	-	✓	✓	1357.4053 ±410.24	1239.98 ±489.28	1455.05 ±153.16	TAG
542.3221	4.00	-	-	✓	-	76.57 ±29.39	81.56 ±72.29	37.72 ±22.00	LysoPC
544.342	4.51	-	✓	-	-	314.03 ±106.76	269.92 ±67.91	292.35 ±60.26	LysoPC
568.3408	4.51	-	-	✓	-	119.87 ±42.73	108.27 ±36.00	78.16 ±29.80	LysoPC
703.5784	9.42	-	✓	-	-	571.44 ±52.49	603.58 ±52.50	564.78 ±27.96	SPH, DAG, PE
734.5718	10.09	-	✓	-	-	100.4161 ±20.73	115.74 ±23.88	104.68 ±13.79	PC, PE, DAG
758.5725	9.85	✓	✓	✓	✓	3948.08 ±568.02	4130.14 ±818.00	4452.22 ±705.75	PC, PE, DAG
760.5878	10.23	✓	✓	✓	-	1986.68 ±386.06	2187.63 ±530.13	2241.05 ±824.00	PC, PE, DAG
780.5578	9.53	✓	✓	✓	✓	1075.91 [(c)] ±278.29	1172.05 [(a)] ±683.88	645.64 [(a,c)] ±263.60	PC, PE
782.5747	9.89	-	✓	-	-	1044.75 ±678.45	2002.38 ±565.27	2018.86 ±464.19	PC, PE
784.5887	10.02	-	-	✓	-	923.55 ±215.49	973.90 ±224.33	1040.68 ±215.55	PC, PE
786.6029	10.41	-	✓	✓	-	1215.56 ±166.49	1225.94 ±253.35	1326.72 ±241.96	PC, PE
806.5746	9.81	✓	-	✓	✓	1416.81 [(b)] ±274.86	1044.22 ±709.96	1061.87 [(b)] ±382.33	PC, PE
834.6026	10.41	✓	-	-	✓	292.33 [(b)] ±79.68	267.86 [(a)] ±113.59	146.01 [(a,b)] ±133.58	PC, PE

Table 3.2: Features of Interested from Positive Ionisation Models

The table presents those features that have the largest influence on the positive ionisation orthogonal partial least squares discriminate analysis (OPLS-DA) models. Features were extracted from the corresponding S-plots which exhibited a magnitude of variation value (p[1]) of >0.15, for example those features highlighted in red squares in Error! Reference source not found..C.

Each feature is linked to a specific model, for example if it provided influence to the Control vs. AD analysis, a ✓ is placed in the relevant column.

Peak areas for each feature were extracted from the raw data and are also presented here. These peak areas then underwent testing for significance by univariate mean analysis using "Student's" t-test in SPSS.

Putative identification was provided for each feature of interest using the Human Metabolome Database (HMDB). A number of rules were applied in order to filter the search results in the HMDB, these are discussed in greater detail in the methods section (Section 3.2.6 (Page 119)).

MPA = Mean Peak Area, DAG = Diacylglyceride, TAG = Triacylglyceride, LysoPC = Lysophosphatidylcholine, PC = Phosphatidylcholine, PE = Phosphatidylethanolamine and SPH = Sphingomyelin.

The most promising features were m/z 780.5578, 806.5746 and 834.6026, which indicated a significant decrease in AD compared with controls ((a) p=<0.05, (b) p=<0.01, (c) p=<0.001). These features returned a putative identification of phosphatidylcholines or phosphatidylethanolamines.

3.3.1.3 – Univariate Data Mining of Acquired Positive Ionisation Data

In addition to the multivariate modelling, univariate analysis was also completed on those features shown to have a high magnitude of variation in the S-plot models. Those features that p[1] = >0.15 from each of the S-plot models underwent extraction from the raw chromatographic data using Waters QuanLynx, a package found in MassLynx 4.1 (Waters, Milford, USA). After extraction the data underwent means analysis in SPSS (IBM, Portsmouth, UK), the overall results of which are summarised in Table 3.3.

Three features provided a significant change between each of the disease groups. These are displayed in Table 3.3. found below. Example extracted ion chromatograms can be found in Figure 3.6.

m/z (±0.005)	Retention Time	Control [counts] (Std Dev)	MCI [counts] (Std Dev)	AD [counts] (Std Dev)	Putative Database Identification
780.5578	**9.5325**	1075.91[(c)] (278.29)	1172.05[(a)] (683.88)	645.64[(a,c)] (263.60)	PC, PE
806.5746	**9.8105**	1416.81[(b)] (274.86)	1044.22 (709.96)	1061.87[(b)] (382.33)	PC, PE
834.6026	**10.4127**	292.33[(b)] (79.68)	267.86[(a)] (113.59)	146.01[(a,b)] (133.58)	PC, PE

Table 3.3: Significant Features From Positive Ionisation Data

The mean peak areas (MPA) presented here were extracted from the raw data using Waters QuanLynx Software. The three features (molecular m/z at a retention time) were found to be significantly reduced in Alzheimer's disease (AD) compared with mild cognitive impairment (MCI) and controls. (a) p=<0.05, (b) p=<0.01, (c) p=<0.001. Putative identification was completed via database matching using the accurate mass. This indicated the three features were phosphatidylcholine (PC) or phosphatidylethanolamine (PE) molecules. Example extracted ion chromatograms can be found in Figure 3.6.

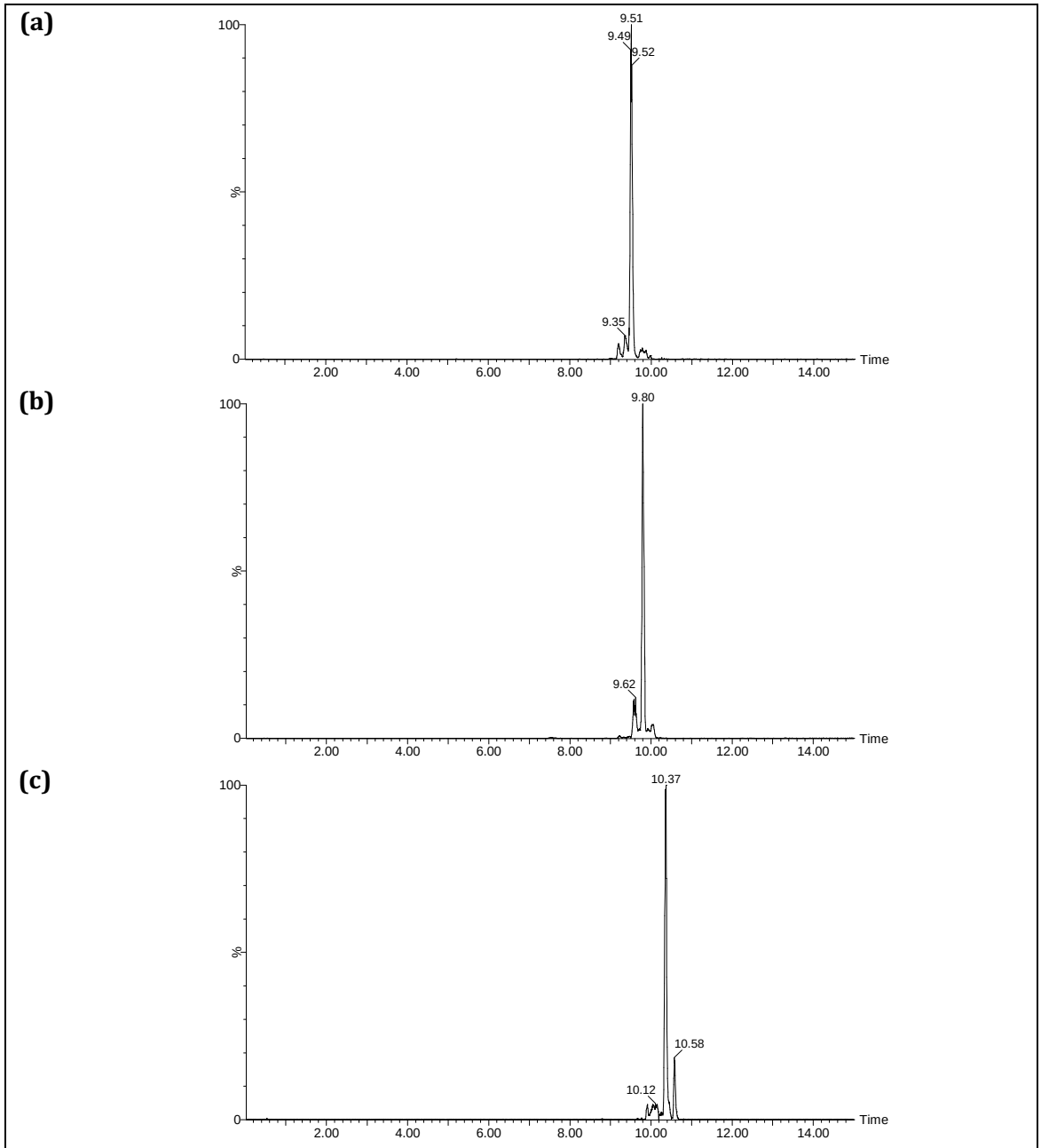

Figure 3.6: Example Extracted Ion Chromatograms

(a) Feature with m/z 780.5578 at 9.51 minutes

(b) Feature with m/z 806.5746 at 9.80 minutes

(c) Feature with m/z 834.6026 at 10.37 minutes

3.3.1.4 – Putative Identification of Features from Positive Ionisation Models and Analysis

Features that were found to influence the OPLS-DA models, listed in Table 3.2 , also underwent putative identification. The results of which are also included in the tables.

Identification was achieved by database accurate mass searching. The databases often provide multiple options for the identification per m/z, therefore the identification is only preliminary as an aim to generalise the type of molecules thought to alter in the disease groups. Listed in the table are general molecule classes that the m/z refers to.

The three significant features after univariate analysis underwent further identification at a later stage, however this is discussed in more detail alongside further validation work in Chapter 5 (Section 5.3.3).

Positive ionisation MS produced a number of different classes of molecule that affected the model. Most commonly phosphatidylcholine (PC) and phosphatidylethanolamine (PE) molecules were identified. It was from these two molecular classes that the molecules of most interest were observed. As previously reported in section 3.3.1.3, three m/z were observed to significantly decrease in AD compared with controls, and initial database identification pointed at PC and PE.

Further lipid classes that demonstrated an influence in the multivariate models were diacylglyceride (DAG), triacylglyceride (TAG), sphingomyelin (SPH) and lysophosphatidylcholine (LysoPC).

3.3.2 – Negative Ionisation Screen

Following adaptation of the chromatographic method, combined with negative ionisation MS detection, a final 10 minute chromatogram was developed that was suitable for a screening analysis. Following alignment of all of the data using Waters MarkerLynx software, a final list of 420 features (m/z at a retention time) was produced. Figure 3.8 presents an example negative ionisation chromatographic trace.

3.3.2.1 – Principle Component Analysis to Demonstrate Reproducibility of Intra-Run QCs for Acquired Negative Ionisation Data

Following alignment of the negative ionisation data, an unsupervised pareto scaled PCA model was produced in SIMCA-P+, to show the clustering of QC samples and therefore reproducibility across the analytical run (Figure 3.7a). On visual inspection of the PCA it demonstrated clear QC grouping at the centre of the model. This would be the expected result from a reproducible run and therefore was accepted for further analysis. As would also be expected in age and gender matched samples in a complex matrix such as human plasma, no obvious disease groupings or separations occurred on the PCA model (Figure 3.7b).

Upon observation of the PCA however, it is clear that one sample (highlighted inside a red box) is a major outlier compared with the rest of the samples within the model (Figure 3.7b). The outlier is a sample extracted from a control patient. Following further investigation and inspection of the raw data it was clear that the chromatogram was at a significantly reduced signal compared with QC samples and other typical chromatograms from the disease classes (Figure 3.8). Therefore based on these two items of information the individual sample in question did not progress to OPLS-DA modelling.

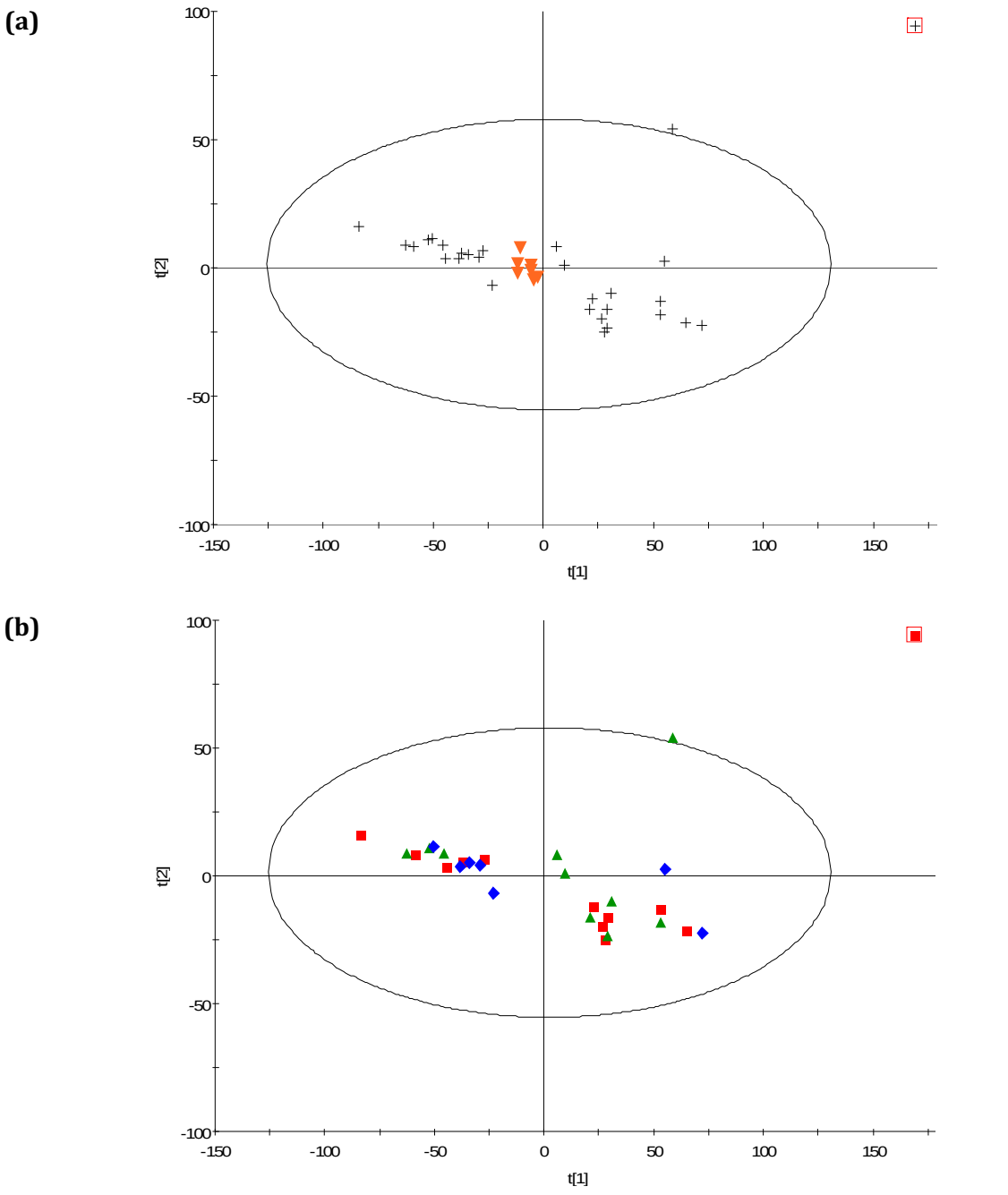

Figure 3.7: Principle Component Analysis of Negative Ionisation Screen Study Data

Unsupervised Principle Component Analysis (PCA) negative Mass Spectrometry Dataset (n=36 respectively).
(A) Quality control (QC) samples can be seen as orange inverted triangles. QCs were excepted if clustering on the PCA =<15% for the total t[1] and t[2].
(B) PCA with diagnostic class colour coded. The PCA contains a major outlier, highlighted by a red box. Upon investigation of the raw data, this sample was excluded from further analysis due to the poor quality of the chromatographic data, suggesting analytical error (Figure 3.8).
The PCA model demonstrates no diagnostic group clustering. This would also indicate no differences or patterns of an analytical nature or batch effect, and is as expected from a randomised sample analysis.

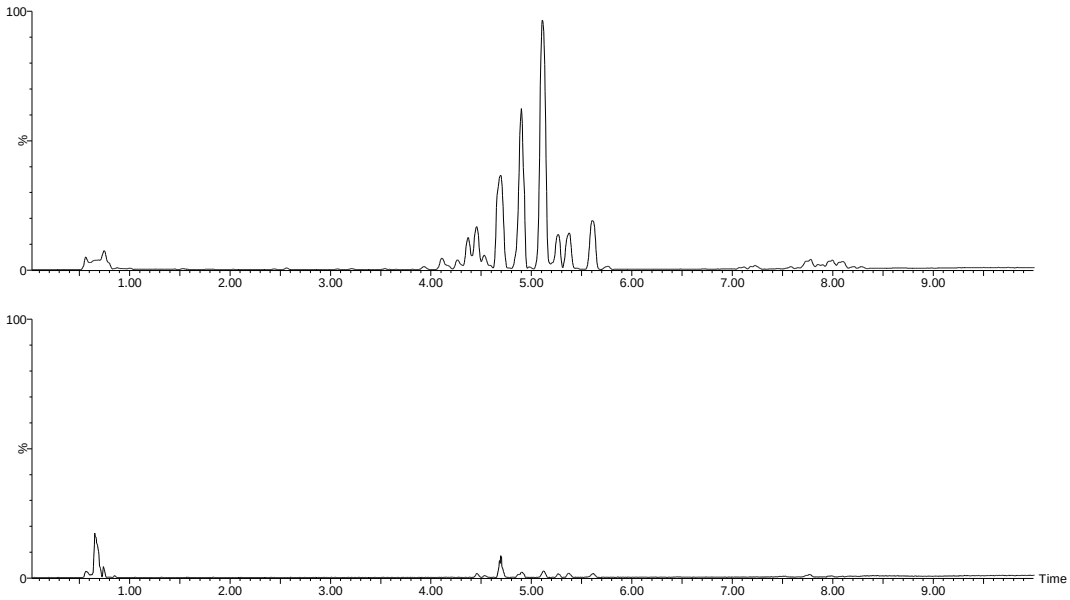

Figure 3.8: Negative Ionisation Mass Spectrometry Chromatogram (Outlier)

Chromatograms from the raw negative ionisation mass spectrometry. The upper chromatogram is of a QC sample and demonstrates typical intensities of peaks. The lower chromatogram is on the same axis scale and is of the control sample identified as an outlier in the initial PCA analysis (Figure 3.9). It is clear that there has been an analytical error, for example a miss injection of sample, or an irregularity during the sample extraction.

3.3.2.2– Orthogonal Partial Least Squares Discriminate Analysis of for Acquired Negative Ionisation Data

A pareto scaled OPLS-DA model was produced with the remaining samples. These samples were grouped by class (Control or MCI or AD), with an initial model made comparing all three (Figure 3.9a). It can be seen that separation on the model was not as distinct as when using positive ionisation, however MCI appear to separate from both AD and control class groups. R^2 and Q^2 values reported at 0.341 and -0.170 respectively.

An S-plot analysis was completed in order to isolate those features which varied the most in magnitude (p[1]) between groups in the models (Figure 3.9b). Features were selected that had a p[1] value of >0.15 in the model. The models for negative ionisation produced 14 such features.

(a)

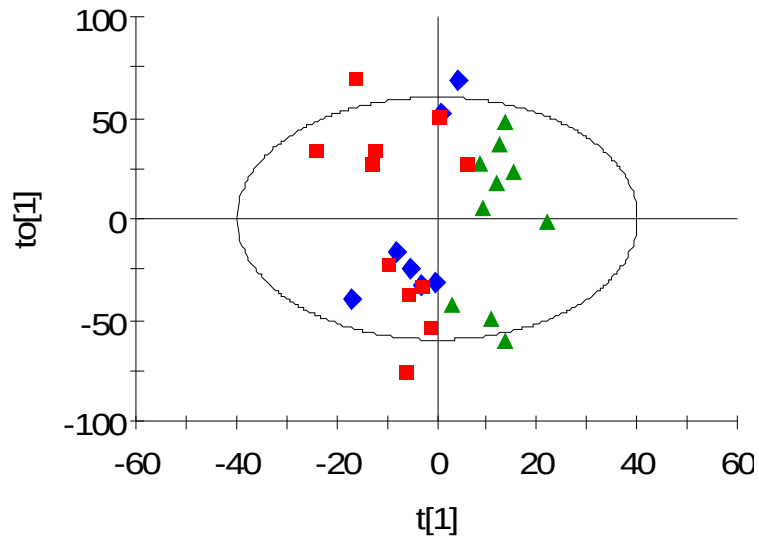

■ = Control ▲ = Mild Cognitive Impairment ◆ = Alzheimer's Disease

(b)

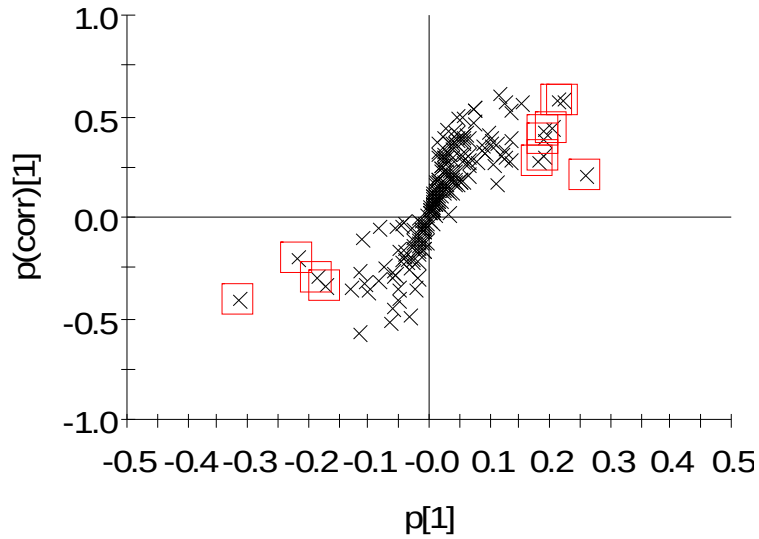

Figure 3.9: OPLS-DA model of Negative Ionisation Data

The figure presents supervised pareto scaled OPLS-DA model **(a)** for negative data.

A visual separation of groups was achieved between MCI and both Control and AD with model validation values of R^2 = 0.341 and Q^2 = -0.170.

S-plot analysis **(b)** highlights those features which had the greatest magnitude of variation (p[1]) within the corresponding OPLS-DA model (a). Features with a p[1] value >0.15 are highlighted and underwent further investigation. These features can be found in Table XX.

Once again, to increase the data mining output of the investigation models were produced for individual comparisons (Control vs. MCI, Control vs. AD and MCI vs. AD).

Visual separation was observed in each comparison (Figure 3.10), however as with the initial all three group OPLS-DA, low R^2 and Q^2 values suggested overall poor model properties.

- Control vs. MCI: $R^2 = 0.426$ and $Q^2 = 0.203$
- Control vs. AD: $R^2 = 0.523$ and $Q^2 = -0.147$
- MCI vs. AD: $R^2 = 0.662$ and $Q^2 = -0.255$

Again, the values are below the recommended value for use as a validated predictor tool, but are acceptable for use a data-mining tool for biomarker discovery.

S-plot analysis was completed of each model, which again revealed those features that most varied in magnitude between groups in the model (p[1]>0.15). Many of these features overlapped with those from the initial three disease group OPLS-DA model; however some new features were presented. A summary of the findings from the S-plot analysis can be found in Table 3.4.

(a) Control vs. MCI

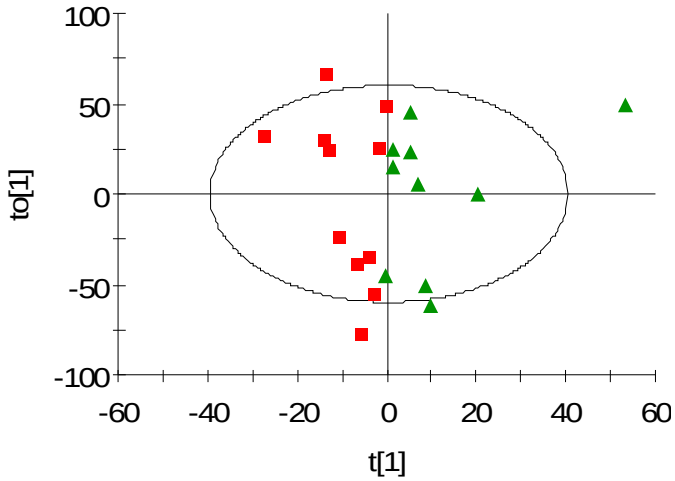

(b) Control vs. AD

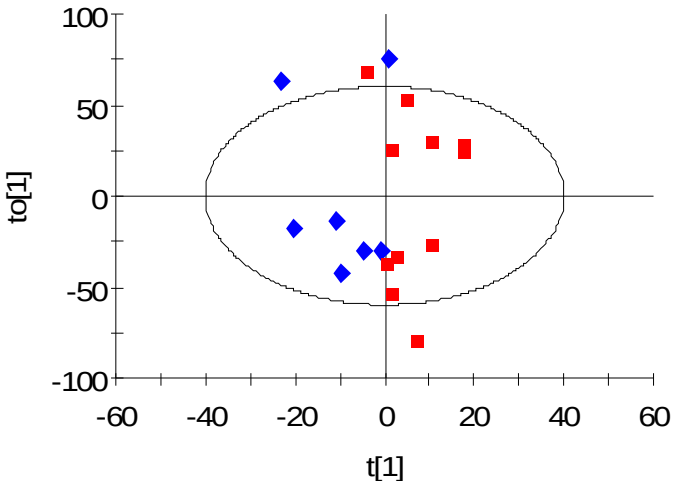

(c) MCI vs. AD

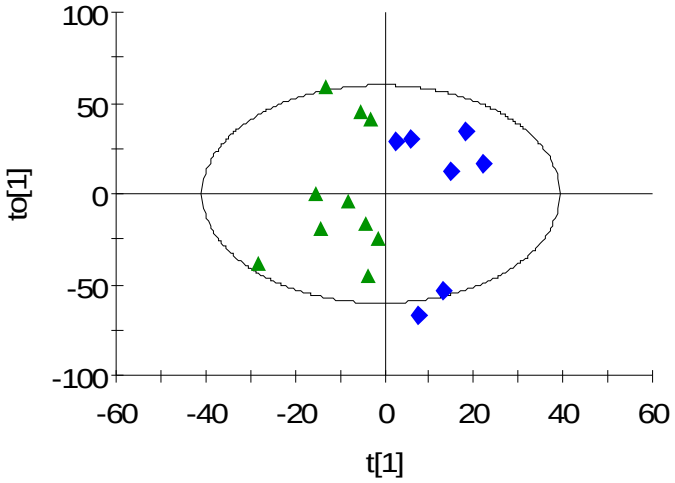

■ = Control ▲ = Mild Cognitive Impairment ◆ = Alzheimer's Disease

Figure 3.10: Individual OPLS-DA Models of Negative Data

The above figure displays OPLS-DA of positive ionization data, illustrating the intergroup separation of each disease class. R^2 and Q^2 values for each model are as follows:

- Control vs. MCI = Negative ionisation $R^2 = 0.426$ and $Q^2 = 0.203$
- Control vs. AD = Negative ionisation $R^2 = 0.523$ and $Q^2 = -0.147$
- MCI vs. AD = Negative ionisation $R^2 = 0.675$ and $Q^2 = 0.255$

m/z	Retention Time (min)	Three Way Model	Control vs MCI	Control vs AD	MCI vs AD	MPA Control (Counts)	MPA MCI (Counts)	MPA AD (Counts)	Putative Identification
255.2294	4.89	-	-	✓	-	1311.55 ±885.09	967.13 ±591.86	1321.90 ±654.82	FA
269.2488	5.27	✓	✓	✓	-	309.20 ±103.25	244.55 ±94.09	278.05 ±62.75	FA
277.2149	4.27	-	✓	✓	✓	128.41 ±98.63	75.15 ±65.56	137.55 ±108.79	FA
279.2312	4.69	✓	-	✓	-	815.35 ±647.92	634.62 ±481.15	933.24 ±534.03	FA
281.2434	5.11	-	-	✓	✓	2229.60 ±1737.71	1795.28 ±1319.14	2465.12 ±1267.59	FA
283.2636	5.61	✓	✓	-	-	534.06 ±312.47	378.76 ±190.36	575.94 ±263.71	FA
303.2302	4.67	-	-	✓	-	66.61 ±40.49	40.35 ±20.26	52.04 ±18.52	FA
480.3073	4.68	✓	✓	-	✓	712.49 ±237.00	619.61 ±213.20	746.81 ±82.73	LysoPC
504.3081	4.45	-	-	✓	-	312.85 ±153.59	223.15 ±80.98	382.46 ±126.97	LysoPC
506.3241	4.86	-	-	✓	✓	239.85 ±95.60	201.09 ±82.18	293.01 ±112.05	LysoPC
742.5277	7.77	✓	✓	-	✓	127.11 ±32.95	115.26 ±35.40	145.04 ±23.56	PE, PS
744.5400	7.98	✓	✓	-	✓	110.44 ±30.14	102.17 ±35.11	121.72 ±21.47	PE, PS, Cer
764.5181	7.58	✓	✓	-	✓	36.29 ±14.23	38.64 ±18.71	29.25 ±9.93	PE, PS
790.5332	7.70	✓	✓	-	-	61.36 ±21.62	62.79 ±23.37	62.15 ±14.46	PE, PS
802.5570	7.77	✓	✓	-	-	29.33 ±6.96	26.61 ±7.42	33.82 ±5.52	PE
804.5704	8.00	✓	✓	-	-	40.27 ±9.22	37.59 ±11.09	44.22 ±6.65	PE
818.5770	7.99	✓	✓	-	-	119.68 ±33.69	114.65 ±40.46	128.07 ±25.78	PE, PS
824.5424	7.58	✓	✓	-	-	8.15 ±3.58	10.03 ±4.34	7.32 ±2.81	PE
838.5541	7.58	✓	✓	-	-	32.09 ±12.98	33.66 ±17.60	24.04 ±9.36	PE

Table 3.4: Features of Interested from Negative Ionisation Models

The table presents those features that have the largest variation in magnitude between groups on the negative ionisation orthogonal partial least squares discriminate analysis (OPLS-DA) models. Features were extracted from the corresponding S-plots, for example those features highlighted in red squares in Error! Reference source not found..D.

Each feature is linked to a specific model, for example if it provided influence to the Control vs. AD analysis, a ✓ is placed in the relevant column.

Peak areas for each feature were extracted from the raw data and are also presented here. These peak areas then underwent testing for significance by univariate mean analysis using "Student's" t-test in SPSS. No features returned significant differences between disease groups during the univariate data analysis.

Putative identification was provided for each feature of interest using the Human Metabolome Database (HMDB). A number of rules were applied in order to filter the search results in the HMDB, these are discussed in greater detail in methods section (Section 3.2.6 (Page 119)).

MPA= Mean Peak Area, FA = Fatty Acid, MAG = Monoacylglyceride, LysoPC = Lysophosphatidylcholine, LysoPE = Lysophosphatidylethanolamine PE = Phosphatidylethanolamine, PS = Phosphatidylsphingomyelin and Cer =

Ceramide.

3.3.2.3 – Univariate Data Mining of Negative Ionisation Data

Those features that were obtained from the S-plot analysis from each of the models underwent univariate extraction from the raw chromatographic data using Waters QuanLynx, a package found in MassLynx 4.1. After extraction the data underwent means analysis using SPSS, the overall results of which are summarised in Table 3.4.

None of the features provided significant mean value alterations between disease groups.

3.3.2.4 – Putative Identification of Features from Negative Ionisation Models and Analysis

Features that were found to influence the OPLS-DA models listed in Table 3.4, also underwent putative identification. The results of which are also included in the table.

As with the positive ionisation analysis, identification was achieved by database accurate mass searching. The databases often provide multiple options for the identification per m/z, therefore the identification is only preliminary as an aim to generalise the type of molecules thought to alter in the disease groups. Listed in the table are general molecule classes that the m/z possibly refers to.

The negative ionisation screen produced a number of lipid families in the database identification process. On this occasion no feature provided a significant variation in any disease group in the univariate statistics, but preliminary identification was completed nonetheless.

The database search returned hits for FA, LysoPC, PE, PS and Ceramide (CER).

3.4 – Discussion

3.4.1 – Biological Observations

From the results in Table 3.2 and Table 3.4 the it can be seen that preliminary identification suggests that all of the features of major influence to the models are lipid molecules. The findings of these and their previous links to AD are discussed below.

3.4.1.1 – Phosphatidylcholines and Lysophosphatidylcholines

Following the HMDB preliminary identification of those features isolated in the S-plot model, one of the most common returns from the search was a group of molecules termed phosphatidylcholines (PC) and their metabolites lysophosphatidylcholines (LysoPC).

PC and LysoPC molecules have been previously shown to be detected using positive ionisation [236], however sensitivity in negative mode is poor, often producing no detectable ions [237]. It is for this reason that PC species were filtered from the HMDB negative ionisation search and only appear in Table 3.2 from the positive screen.

PCs are a class of glycerophospholipid, consisting of a choline head group and fatty acid side chains (Figure 3.11). They are an essential component of cell membranes, and make up ~ 95% of total choline containing compounds in the majority of tissues [238, 239]. They have a common zwitterionic structure, with the variation in the length and saturation of their hydrophobic side chains defining their structural roles since chain length differences can affect cell membrane fluidity [240]. Along with their structural roles, they are also found as components of lipoproteins, in particular of high-density lipoproteins (HDL). PCs interact with

ApoE as part of the HDL group, and are implicated in cholesterol transport [241]. This is of interest as ApoE is heavily linked with AD [242, 243], and the ε_4 allele of the ApoE gene is a well-established predictor and is often considered one of the most significant risk indicators of AD [244].

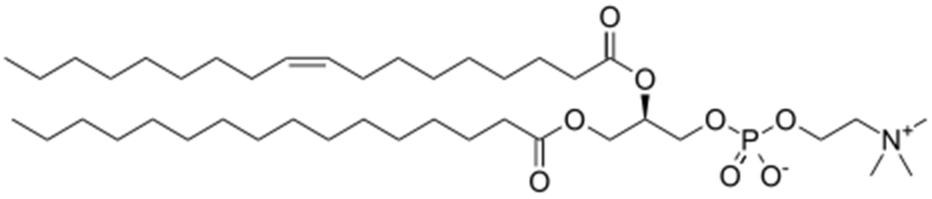

Figure 3.11: Phosphatidylcholine Structure

An example figure of a phosphatidycholine (PC) molecule. PC consist of a choline head group and two FA side chains.

Gaudin et al identified two PCs - 32:0 and 34:1, which were decreased in the presence of senile plaques, when extracted from post-mortem AD brain compared with controls. The group concluded that PC regulation was affected in AD and that it could be linked to the roles of PLA2 and PLD1 in Aβ activation [245]. This result complements previous findings where total PC species were found decreased in the frontal and parietal cortex of AD patient brain by 12-15% ($p=<0.05$) [246].

A previously published metabolomic based study employed a cluster style analysis which investigated the use of groups of similar molecules, rather than individual species as markers for conversion from MCI to AD [196]. The most promising cluster identified in the analysis, consisted of three molecules that demonstrated significant changes in the progression from MCI to AD. These included a PC16:0/16:0, alongside 2,4-dihydroxybutanoic acid and an unidentified molecule [196].

A further PC molecule, PC16:0/20:5 was included in a separate cluster analysis, however in that example, no significant prediction properties (p=0.27) as a group were found [196].

LysoPC (Figure 3.12) are metabolites formed by partial hydrolysis of one of the FA side chains of PCs by the phospholipase family of enzymes. Irregularities in this family of enzymes in AD has previously been demonstrated in AD mouse models, where an increase in arachidonic acid was attributed to an over activity of phospholipase enzymes [202].

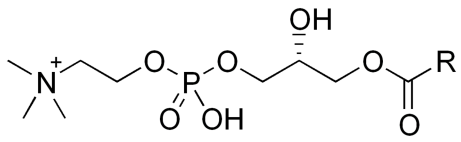

Figure 3.12: Lysophosphatidylcholine Structure

An example figure of a lysophosphatidycholine (LysoPC) molecule. LysoPC consist of a choline head group and a single FA side chain. They are formed by hydrolysis release of a FA from a PC.

The ratio of total LysoPC to PC has been shown to significantly vary when comparing the CSF obtained from controls and AD patients, although no significant changes of total PC and LysoPC on their own were observed [247].

Interestingly, LysoPC have also been demonstrated to enhance Aβ plaque formation by decreasing the required threshold for Aβ coagulation into fibrils, as well as enabling the increasing of Aβ fibril length [248]. As Aβ is one of the major protein deposits in AD brain, it perhaps is no surprise that abnormal LysoPC metabolism is therefore linked to AD. This would lead to the hypothesis that an increase in LysoPC may occur in AD brain, and therefore result in an increase in

the deposit of Aβ plaques, however no current publication has reported this trend as yet.

The results reported here from the LC-MS data set, present five possible LysoPC features, and nine PC features, suggesting these families of molecules as candidates for biomarkers of AD, which would complement those findings reported in previous publications.

3.4.1.2 – Sphingomyelin and Ceramide

As with PC and LysoPC, SPH species consist of a choline head group (Figure 3.13), and therefore also ionise in positive ionisation mode [249]. SPH are found in cell membranes, particularly those that make up the myelin sheath in neuronal cells, and is also thought to act as a secondary cell messenger [250].

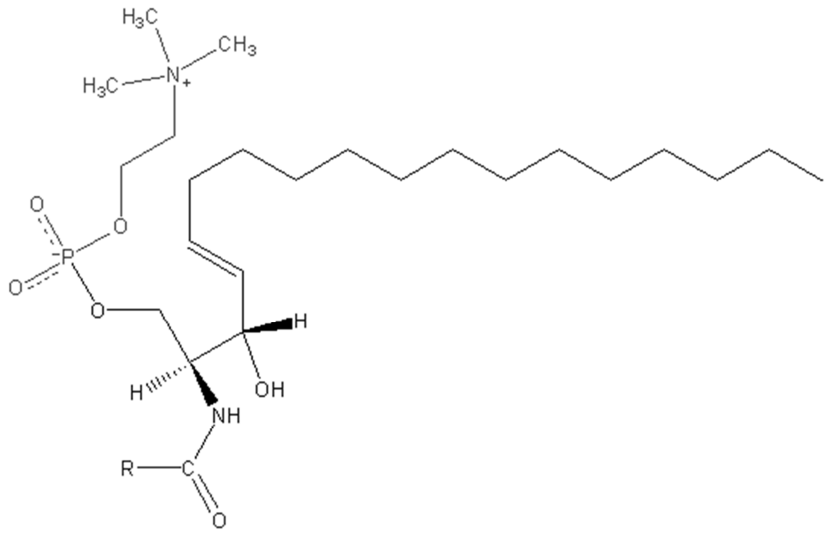

Figure 3.13: Sphingomyelin Structure

An example structure of a sphigomyelin (SPH) molecule. SPH consist of a choline head group, and a FA sidechain. SPH also consist of a sphingosine side chain alongside the FA.

CER are a molecular group that are structurally similar to SPH, but do not have the phosphocholine head group (Figure 3.14). They have been shown to be detected by both positive and negative ionisation mass spectrometry [251].

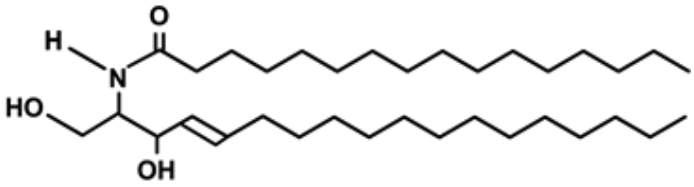

Figure 3.14: Ceramide Structure

An example structure of a ceramide (CER) molecule. CER consist of a FA and a sphingosine. Unlike SPH molecules, CER do not have choline head groups.

SPH have been shown to vary in AD patients. A study that utilised ^{31}P NMR technology demonstrated a significant increase in SPH in brain samples of AD patients compared with controls [142]. These findings were complemented by those in a publication that identified significant increases of SPH in AD brain, particularly in the middle frontal gyrus (MFG) region. Increases in SPH C16:0, C18:0, C22:0 and C24:0 were observed in the grey matter of the MFG regions. No differences were reported in white matter. Interestingly the paper also reported patient ApoE data, and found that the presence of the ε4 allele of the ApoE gene is not associated with irregular brain sphingolipid biochemistry, unless patients already had an underlying neurological disorder such as AD. These suggest it is not just the polymorphism in the ApoE gene that contributes to abnormal lipid metabolism within the brain [252].

This elevation in AD of SPH and metabolites is complemented by a publication reporting significantly increased SPH levels ($p=0.003$) in the CSF from individuals with prodromal AD compared with cognitively normal controls. However, no changes in the CSF SPH levels between mild and moderate AD groups and

cognitively normal controls were observed [253]. This result of increased SPH in AD CSF was also reflected in another publication [254]. This suggests that brain variation of SPH is reflected in other biofluids other than brain, an important consideration when investigating candidate biomarker molecules.

These findings appear to correlate to results published that suggest increased levels of plasma SPH correspond to a reduced rate of progression in AD, and a reduction in cognitive decline [255].

Further work has also been reported in AD patient plasma with a non-targeted "shotgun" lipidomics designed study. In shotgun lipidomics, lipid extracts undergo direct MS injection followed by statistical analysis. It was reported that eight SPH molecules, particularly those with 22 and 24 carbon atom side chains, significantly decreased ($p=<0.05$) in AD patient plasma. Further to this two ceramide molecules (C16:0 and C21:0) were shown to significantly increase ($p=0.05$). Interestingly the paper correlated these significant findings to two "categories" of AD, mild (MMSE >20) and moderate (MMSE <20) reporting a correlation for SPG C20:2 ($p=0.003$) and CER C25:0 ($p=0.004$) [193].

SPH metabolites have also come under investigation, with reported findings of abnormal sulphatide variation in AD brain. Sulphatides are sulphated metabolites of galactocerebrosides, a form of glycosphingolipid, and are present in the central nervous system (CNS) as a component of the myelin sheath [159]. The publication reported a depletion of sulphatides of up to 93% in brain grey matter and up to a 53% depletion in the white matter of autopsy confirmed AD brains compared with controls [160]. The same publication also examined a further group of SPH metabolites, CER that were reported to be elevated threefold in the brain samples of AD patients compared with controls [160].

Therefore SPH have been shown to generally increase in a variety of biofluids (brain, plasma and CSF) in patients suffering from AD. Due to the differences in variation in metabolites of SPH molecules (CER elevated, Sulphatides depleted), it would suggest irregularities in particular metabolic pathways potentially playing a role in the pathogenesis of the disease, and/or perhaps general cognition.

Some work has been published regarding these pathways in an attempt to identify any abnormal pathways in the disease. He et al. [256] reported the levels of brain SPH and some of its metabolites, along with the activity of a number of lipid related enzymes. The publication reported elevated activation of the enzymes acid sphingomyelinase (ASM) and ceramidase, leading to a reduction in SPH, an increase in CER as well as the elevation of the metabolite sphingosine, and the reduction of the metabolite sphingosine-1-phosphate. The elevated ASM enzyme and reduced S1P levels in AD were highly correlated with the levels of Aβ and hyperphosphorylated tau protein. The publication also reported that the addition of Aβ to neuronal cell cultures mimicked the sphingolipid changes and induced apoptosis [256]. These findings suggest, that it is the presence of Aβ plaque deposits that result in the activation of the enzymes responsible for SPH metabolism, and therefore SPH markers could play a role as tracking AD progression and the progression of Aβ deposits.

3.4.1.3 – Phosphatidylserines, Phosphatidylethanolamines and Lysophosphatidylethanolamines

PS and PE are a class of phospholipid found as structural components of cell membranes. PE (Figure 3.15a) make up approximately 20% of mammalian phospholipids, and importantly with regard to AD are found at high concentrations in cells of the CNS, particularly in the white matter of the brain, where they form

45% of all phospholipids [257]. PS (Figure 3.15c) make up approximately 3-15% of mammalian phospholipids, and again are particularly abundant in the brain [257].

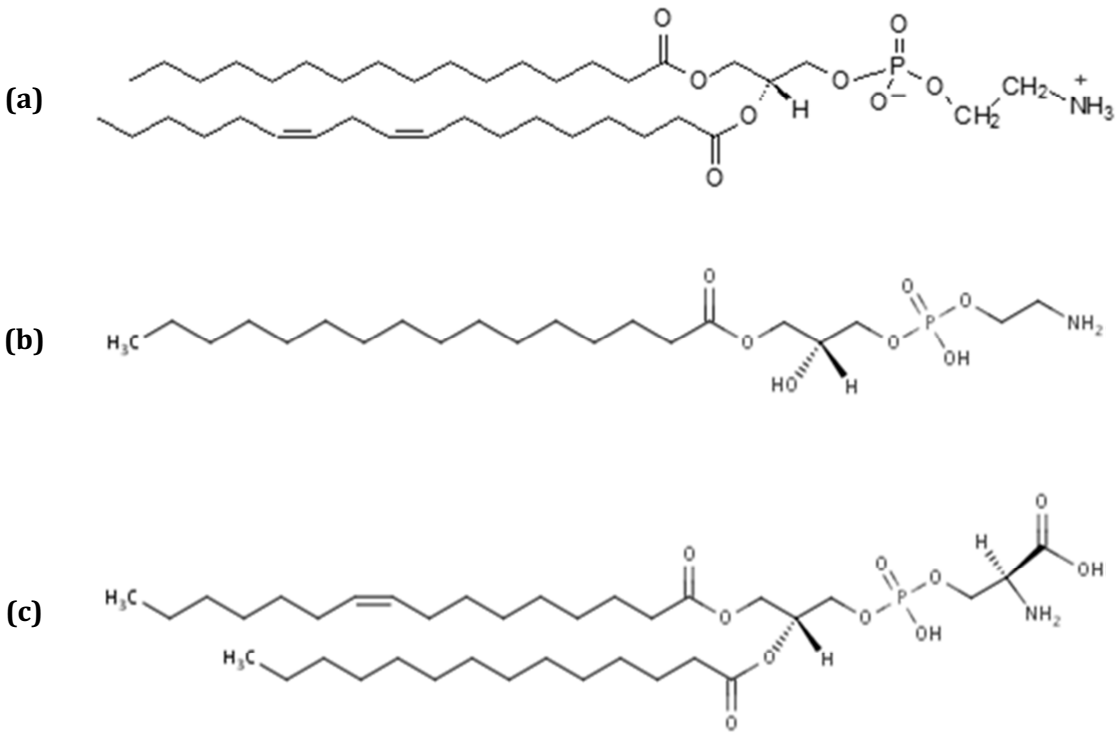

Figure 3.15: Example PE, PS and LysoPE Structures

(a) An example structure of a phosphatidylethanolamine (PE) molecule. PE consist of an ethanolamine headgroup, and two fatty acid sidechains. **(b)** An example structure of a lysophosphatidylethanolamine (LysoPE). LysoPE consist of an ethanolamine headgroup and a single FA sidechain. **(c)** An example structure of a phosphatidylserine (PS). PS consist of a serine headgroup and two fatty acid sidechains.

LysoPE (Figure 3.15b) are metabolites of PE that have undergone a hydrolysis reaction and a release of a fatty acid side chain. LysoPE can also act as precursor molecules to PE, and therefore are also involved in PS biosynthesis [257].

PE and LysoPE have previously been shown to ionise readily in positive ionisation mode [236], whilst PE and PS have also both been shown to ionise in negative ionisation [258], and therefore appear in the appropriate preliminary identification tables presented previously.

Many examples exist of decreased PE in AD brain samples, with a decrease being observed in frontal and parietal cortex of AD patient brain compared with controls (p=<0.05) [246]. Further to this, a targeted method which employed an NMR analytical approach to brain samples described a significant reduction in PE (p=0.007) when comparing AD brain homogenates with age matched control samples, specifically in the superior temporal gyrus region of the brain (p=0.01) [142]. The same publication also identified a significant increase in the metabolite PE-plasmalogen (p=0.0006) [142]. This finding would suggest a possible abnormality in the metabolism of PE, resulting in decreased PE and increase metabolites of the cell membrane lipid.

This result was reflected in an animal model study that employed an LC based method to analyse brain phospholipid levels. The study investigated the hypothesis that the accumulation of Aβ had a direct influence on the distribution of phospholipids within the brain. In order to achieve this the group analysed phospholipid content including PE in transgenic mouse model of AD expressing both mutant hAPP and human PSEN-1 genes. The results were compared with brains from wild-type mice after four months and nine months. Results demonstrated a significant reduction in PE after nine months (p=<0.01), but no statistically significant changes were observed after four months [259].

The study also reported significant decrease in PS species after nine months. Again after four months, no significant differences were observed. This would suggest that Aβ accumulation over the longer time period could be directly responsible for abnormal PE and PS levels in AD brain..

However, this result was not reflected in a study of human CSF comparing AD with controls, with no significant differences observed for PE species [254] providing

possible evidence that the physiological changes of PE species in the brain may not be detected in CSF.

The previously discussed reports of decreased PS in mouse brain [142] contradicts that of a publication investigating various lipid fractions from human brain. The study reported significant increases of a group of lipids it describes as serine glycerophospholipids, in membrane fractions from synaptosomes ($p=0.0011$) and a combination of glial and neuronal cell bodies ($p=0.016$). Results regarding PE complemented those discussed above, with a significant decrease observed in both fractions in AD brain ($p=0.0041$ and $p=0.0001$) [260], suggesting potential differences between the disease in humans and corresponding mouse models.

Work has been published investigating potential reasons for the decrease in PE species in AD brain with a recent article examining the role of the enzyme phosphatidylethanolamine-N-methyltransferase (PE-N-MT). Findings reported that the activity of PE-N-MT was decreased in the frontal cortex of brain samples affected with AD [261]. PE-N-MT catalyses the synthesis of PC via the stepwise transfer of methyl groups to the amino head group of PE. However, as can be seen from the literature previously published and reported here, generally PE species are reported to decrease in AD, as are PC species. With this finding of PE-N-MT activity decreasing in AD, it would be expected that although PC may decrease, PE would not be transformed as rapidly and therefore may increase. This would suggest a more complex imbalance occurring in AD brain than just the decrease in activity of PE-N-MT.

Although it appears PE therefore may be able to play a role as candidate biomarkers in AD the majority of the work published reports PE as a total non-specific value. However, as with PC species, it would certainly be of interest to see

if any specific PE with particular fatty acid side chains is present at abnormal concentrations in AD. It would appear from the findings presented here in Chapter 3 that a number of different PE species are presented, suggesting expansion of the LC-MS screen may present further answers toward PE in AD.

3.4.1.4 – Mono-, Di- and Tri-acylglycerol

Acylglycerol are a family of lipids that consist of a glycerol head unit, and can contain one, two or three FA side chains, hence mono, di and tri-acylglycerol (MAG, DAG and TAG) (Figure 3.16). They play a role in mammalian physiology as secondary cell signalling molecules, and are often an intermediate stage in PC, PE and PS synthesis and metabolism [262].

They have all been shown to commonly ionise in positive MS [263], however negative ionisation has a low sensitivity and ionisation success and therefore is excluded from the results table.

Acylglycerols are not as commonly linked to AD as the previously discussed phospholipids, however a few examples exist in the literature regarding the disease. An investigation into the synaptic plasma membranes isolated from the cerebral cortex of adult rats reported findings that observed a non-significant reduction of DAG species after the introduction of Aβ peptides. The paper concluded that the pathway being influenced by the Aβ was the degradation of PI, particularly those with side chain consisting of AA [264]. The paper presents evidence that the enzymes affected by Aβ are those in the Ca^{2+} and cholinergic receptor mediated pathways via phospholipase C.

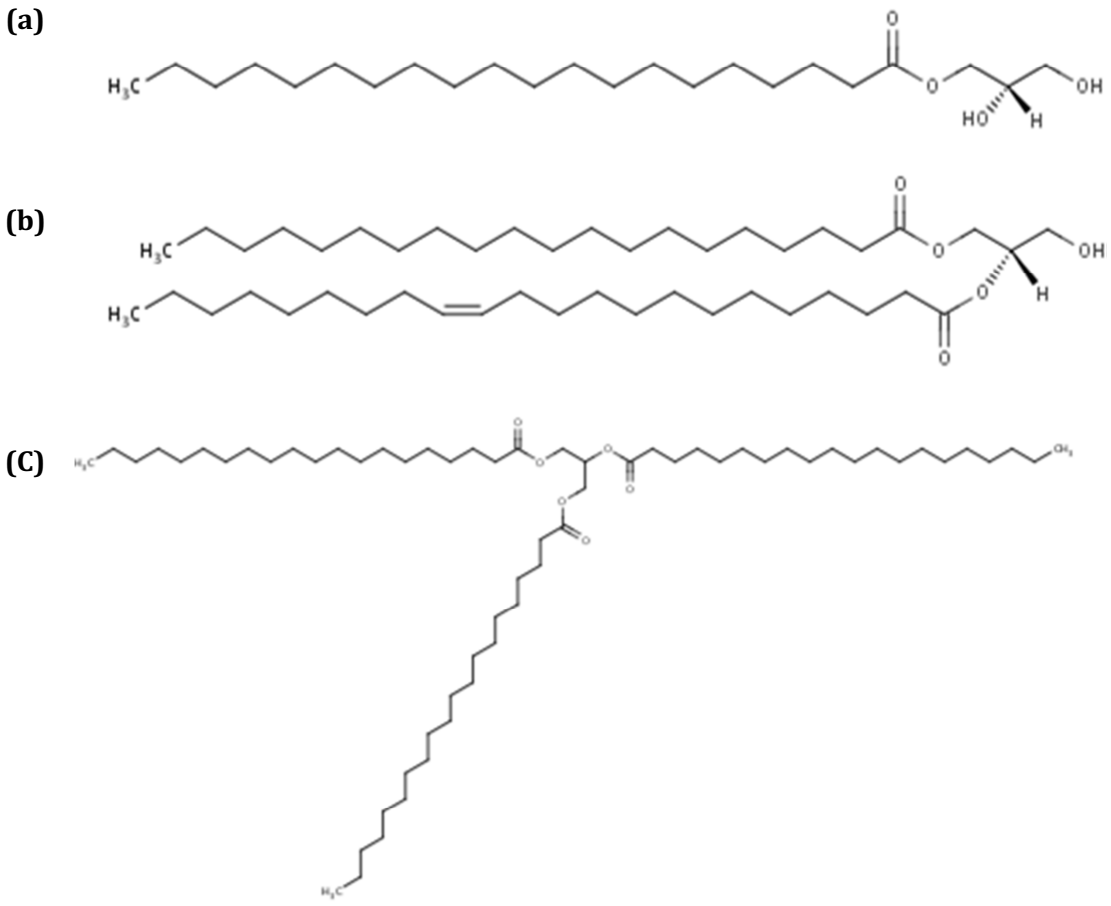

Figure 3.16: Mono-, Di- and Tri- acylglycerol Structures

(a) An example of a monoacylglycerol (MAG) structure. MAG consist of a single fatty acid sidechain and a glycerol headunit. **(b)** An example of a diacylglycerol (DAG) structure. DAG consist of two fatty acid sidechains and a glycerol headunit. **(c)** An example of a triacylglycerol (TAG) structure. TAG consist of three fatty acid sidechains and a glycerol headunit

Further studies into the enzyme pathways regarding acylglycerols have also been shown to alter in AD. Differences in the activity of monoacylglycerol lipases (MAG-Lip) and diacylglycerol lipases (DAG-Lip) were identified in specific brain regions when comparing AD brain to normal controls. MAG-Lip was shown to decrease in activity in the nucleus basalis ($p=<0.01$), frontal cortex ($p=<0.05$), occipital cortex ($p=<0.05$) and hippocampus regions ($p=0.01$). DAG-Lip activity decreased in nucleus basalis ($p=<0.01$) and hippocampus ($p=<0.01$), whilst it was increased in

the parietal cortex (p=<0.05) and occipital cortex (p=<0.05) [265]. This provides further support that a specific lipid metabolism pathway is affected in AD, and this suggests that MAG, and DAG molecules may have suitable properties enabling them to act as biomarker candidates, reflecting any pathway irregularities.

As previously discussed in 3.4.1.2, a shotgun lipidomics approach was applied to plasma lipids in AD patients. As part of this investigation TAG species were also investigated for alterations in AD, however no significant differences were reported between controls, mild AD (MMSE >20) and moderate AD (MMSE <20) [193].

Although major differences in MAG, DAG and TAG species in AD are not reported in the literature, the observations discussed above regarding enzymatic pathway abnormalities, combined with the results presented here, with five features returning DAG, or TAG putative identification, suggests that they should not be discounted at this stage.

3.4.1.5 – Fatty Acids

Fatty acids were discussed in great detail in Chapter 2, and are therefore not discussed here.

3.4.2– Analytical Observations

The LC-MS parameters used for the positive ionisation screen resulted in a reproducible chromatogram suitable for preliminary non-targeted biomarker discovery. A 15 minute runtime provided 950 aligned features using the Waters MarkerLynx data processing package.

In contrast, only a 10 minute analytical run was required for negative ionisation. This reduction in time is possible because of fewer species ionising in the negative

mode. For example, the larger DAG and TAG do not ionise successfully, and therefore do not require separation time. Using these parameters, the MarkerLynx data processing package aligned 420 features.

In both ionisation modes, the MS analysis was set to record m/z from 50Da to 1000Da. The analysis was a general chromatographic method utilising a C_{18} column and a wide ranging gradient that in both cases progressed from 30%B to 100%B meaning that a variety of molecules with a range of structures, properties and polarities were catered for.

In the pareto scaled PCA models both methods provided acceptable QC clustering, suggesting good overall reproducibility across the course of the analysis. QC samples consisted of a pool of plasma extracted concurrently with the patient samples, and analysed at regular intervals throughout the LC-MS worklist. As a PCA model is unsupervised, high quality reproducible runs will cluster. This is because, in theory each extract will contain exactly the same molecular features as each one comes from the same identical pool. This approach to ensuring non-targeted analytical methods are reproducible is commonly used in a number of previous plasma based publications [266-268].

The chromatographic separation time of both the positive and the negative ionisation stages of the analytical procedure are similar to a previously published article, which was previously successfully used in the non-targeted analysis of plasma [230]. However, despite this, it can clearly be seen from the results Table 3.2 and Table 3.4 that a number of features of influence in the multivariate models shared the same retention time. A particular example of this is observed in Table 3.3.. Two of the features which were reported to significantly decrease in AD

patient plasma had co-eluting retention times, with m/z 780.5578 and 806.5746 eluting at 9.53 and 9.81 minutes respectively.

Co-elution in LC-MS can cause detector effects, for example ionisation suppression or enhancement. As features from the chromatographic separation elute off of the column they enter the MS source, where they become charged. If an un-resolved mixture of molecules enter the source at the same time then they are competing for charge, and therefore ionisation effects can occur. This effect may not always be consistent, and therefore may skew the data and subsequent analysis.

It should, however, be noted that these in-source effects of co-eluting peaks are not necessarily always an issue, for example the publication adapted for use in Chapter 2 [213] encountered no quantification issues when two of the analysed FA species co-eluted, and were able to report linear calibration ranges. Furthermore an approach often taken in non-targeted biomarker strategies is direct infusion mass spectrometry where tissue extracts are directly injected into a MS source without prior chromatographic separation. Although this obviously greatly increases the risk of ionisation effects, direct infusion has previously been successful in identifying plasma biomarker candidates for Alzheimer's disease, identifying significant differences in circulating plasma sphingolipids [193]. Further to this, direct infusion has been used in specific metabolite target driven methodologies, demonstrating abnormal concentrations of lipid plasmalogen, sulphatide and ceramide metabolites from Alzheimer's disease brain samples [157, 160].

Despite these exceptions, general recommendations in the literature suggest an optimised LC separation in order to reduce any ionisation effects in the MS source [269, 270] and therefore, in order to improve the confidence in the reported findings of this screen, a longer analytical method with increased component separation an

therefore less co-elution was sought and developed. The full details of this analytical development can be found in Chapter 4, and the results when applied to a high-throughput project discussed in Chapter 5.

3.5 – Conclusions

An LC-MS screen was successfully completed comparing Control, MCI and AD plasma. The multivariate data treatment highlighted a number of features of interest that progressed to putative identification using a combination of database matching combined with a number of rules employed to filter results. Of these features three were of particular interest, as after univariate statistical analysis, significant reductions were reported. These were 780.5578 (p=<0.001), 806.5746 (p=<0.01) and 834.6026 (p=<0.01). Of these two were also significantly reduced when comparing MCI with AD, 780.5578 (p=<0.05) and 834.6026 (p=<0.05). These were putatively identified as being PC or PE species, both of which have been heavily linked to AD previously, and therefore provided further investigation.

From these it is clear that lipid species are the small molecule features most likely to be altered in AD pathology, particularly when considering it has been published that the common trend is that Aβ concentrations in the brain appear to correlate to lipid abnormalities [248, 256, 264]. This finding would suggest a possible role for biomarkers in AD, with the potential to track disease progression as Aβ accumulates.

However, it is clear that although the employed method was suitable as a screening technique a number of co-eluting peaks occurred. Therefore to support the findings with further evidence an improved method is required. Further to this a larger sample set would also provide greater significance to any reported findings.

With this in mind, a collaboration was proposed with the Centre for Metabolomics and Bioanalysis (CEMBIO) at the Universidad San Pablo in Madrid, Spain. A six

month exchange project was undertaken with the aim of developing a lipidomic method. The findings of this are discussed in Chapter 4.

Chapter 4:
Comprehensive Lipidomics Method Development

4.1 – Introduction

Due to the vast variations in the chemical properties of analytes, current methodology can only identify subsets of the metabolic content of biological samples. Most comprehensive approaches use a combination of technologies, for example LC-MS, NMR and GC-MS. For example, recent work by the previously mentioned HMDB project utilised these approaches to comprehensively profile human serum metabolites (<1500Da) resulting in the confirmation of 4600 individual components [231-233].

Although this multi-pronged approach can provide a wealth of data, analysis time and cost are greatly increased. However, perhaps of more importance in current biomarker research is the limitation of available biofluids, with valuable fluids at a premium. Therefore, for the research field to progress efforts must be made to increase metabolite coverage within each analytical technique.

LC-MS (along with NMR) is currently one of the main techniques used to profile metabolites from biological samples. The technique can boast the benefit of on column separation of molecules prior to mass spectral analysis, ensuring it is able to provide a broad metabolic picture of the sample [271]. However issues still arise, for example components that are not fully resolved can undergo ion effects such as suppression or enhancement in the mass spectrometer source, meaning non-separated components compete with one another for ionisation and therefore detection, which can lead to a reduction in selectivity and accuracy. Further to this, matrix components, for example endogenous phospholipids, are a significant source of imprecision in analyses conducted by LC-MS/MS. Present at relatively high concentrations, they are heavily associated with influencing ion suppression and enhancement effects, thus introducing analytical variation [272]. This is of

particular importance when considering the results reported in Chapter 3, which putatively identified a number of phospholipid classes as varying between AD, MCI and control groups, suggesting an improvement in extraction and separation would be valuable. Therefore, an improved small molecule profile will provide valuable data on phospholipids and their interactions and roles in Alzheimer's disease.

Traditional LC-MS approaches to non-targeted metabolic fingerprinting typically tend to employ a simple protein precipitation extraction designed to remove protein, avoiding column degradation and blockage. Following this, extracts are injected onto an LC system and analysed by a reversed-phase gradient [119, 273, 274]. However, when utilising this general approach, the extremes of the metabolite spectrum are overlooked and potentially important biomarker candidates are lost. For example, highly polar compounds wash off in the solvent front of the chromatogram as they undergo little to no retention, whilst highly non-polar species can be insoluble in the extraction solvents used in metabolite studies, (methanol and acetonitrile are common), and are either not efficiently extracted or remain on column, unable to undergo elution.

Increasing the metabolite coverage by optimisation of sample pre-treatment has been investigated previously. For example, one recent publication by Yanes et al [275] examined a range of seven extraction protocols, combined with a range of modified chromatographic and MS detection methods. The paper concluded that to extend the best range of extraction coverage an improved single-phase "all-in-one" extraction was developed whereby the coverage of analysed molecules from *E. Coli* samples was increased. The approach employed an extraction protocol using ethanol mixed with ammonium acetate, and found this combination of

extraction solvents to be most successful when extracting a mixture of polar and non-polar compounds.

Conversely, a second approach in expanding the coverage of metabolite extractions can employ a combination of dual extractions, one designed for polar molecules, the other for non-polar has previously been reported [276]. In this investigation, a number of methods underwent comparison that either extracted polar metabolites prior to non-polar extraction, or used a two phase extraction using two solvents which are non-miscible and therefore separate (dichloromethane and methanol). Analysis was then completed via UPLC-MS with the findings suggesting that the optimal protocol for profiling both polar and non-polar metabolites utilised an aqueous extraction with water/methanol prior to an organic extraction with dichloromethane/methanol [276].

It is becoming more common in the literature for publications to focus on specific subsets of the metabolome, rather than attempting to cover it all in one extraction. For example, a major research area currently is termed lipidomics. Lipidomics represents a subset of metabolomics, focused of the lipid fraction of tissues, and is becoming particularly prevalent in biomarker studies as a large number of disease states are associated with irregularities in lipid metabolism. These include neurological diseases such as AD [142], schizophrenia [277] and Parkinson's disease [278]; cardiac disease such as atherosclerosis [279]; viral infection [280] and bacterial infection [281]; as well as obesity [282] and type 1 [283] and type 2 [284] diabetes. Furthermore, it is well known that lipids play vital roles in cellular functions, including membrane regulation [285], source of reserve energy within vacuoles [286] and cell signalling transduction processes [287].

In addition to the challenges faced when considering approaches to take with sample extraction method development, it is also of critical importance that when extracting metabolites for fingerprinting, no "false" metabolites are introduced to the sample via the pre-treatment process. A common known fact, which highlights this, is that unsaturated fatty acids and unsaturated lipid species can undergo oxidation when exposed to atmospheric conditions including UV light exposure combined with atmospheric oxygen [288]. Therefore care must be taken when drying or transferring any extracts, to avoid these modifications. Again, other systematic errors introduced by extraction protocols such as loses when transferring sample between vials and tubes during extraction. It stands to reason that, because of this, the more stages of transfer within a procedure, the more chances there are of introducing these errors.

The results in Chapter 3 highlighted a number of non-polar lipid classes of particular interest from the models. This information, combined with the ever increasing need of developing methods that expand the metabolite coverage of extraction approaches, lead to the development of a novel two phase metabolic fingerprinting method. The method developed here produces both a lipophilic non-polar extract, combined with a hydrophilic polar extract from 20µL of plasma.

The complete extraction and analysis was designed to be completed within the same LC-MS vial, therefore reducing extraction steps and analytical variation. Each phase was individually analysed using LC- MS, using an optimised gradient for the metabolites present in each layer. The method was designed to increase the component coverage from a small sample aliquot and to improve the reproducibility of the overall process. Further to this, metabolites remain

constantly suspended in solution; therefore reducing the risk of modification due to external influences such as drying loses.

The method was named “in-vial dual extraction” (IVDE), a direct injection metabolic fingerprinting method which both increases metabolite coverage whilst decreasing the analytical variability, making it ideal for comprehensive metabolic profiling and biomarker discovery. In addition, particular relevance was placed upon the upper phase of the extraction, as it specialises in non-polar lipid components, making it an ideal tool to analysis an extended AD sample set, reducing the limitations encountered in Chapter 3.

The developed method presented here in Chapter 4 consists of two major components. The first stage of progression focused on the method development and employed human plasma from healthy volunteers. The in-vial approach was designed to improved reproducibility and therefore underwent comparison with a traditional style approach involving vial transfers, evaporation to dryness, and re-suspension in mobile phase.

Once the method development was completed, it underwent a validation procedure. When developing a novel biomarker method it is useful to demonstrate its successful implementation in a sample set of known major metabolic irregularities. If the method can not determine known differences, it is unlikely that it will be of use in an unknown sample set. Therefore a sample set of animal models for diabetes was employed as it is widely accepted that metabolic differences, particularly in lipid metabolism, are widely apparent, and therefore, should be a suitable test set in order to validate the method. An overview of the investigation can be observed in Figure 4.1.

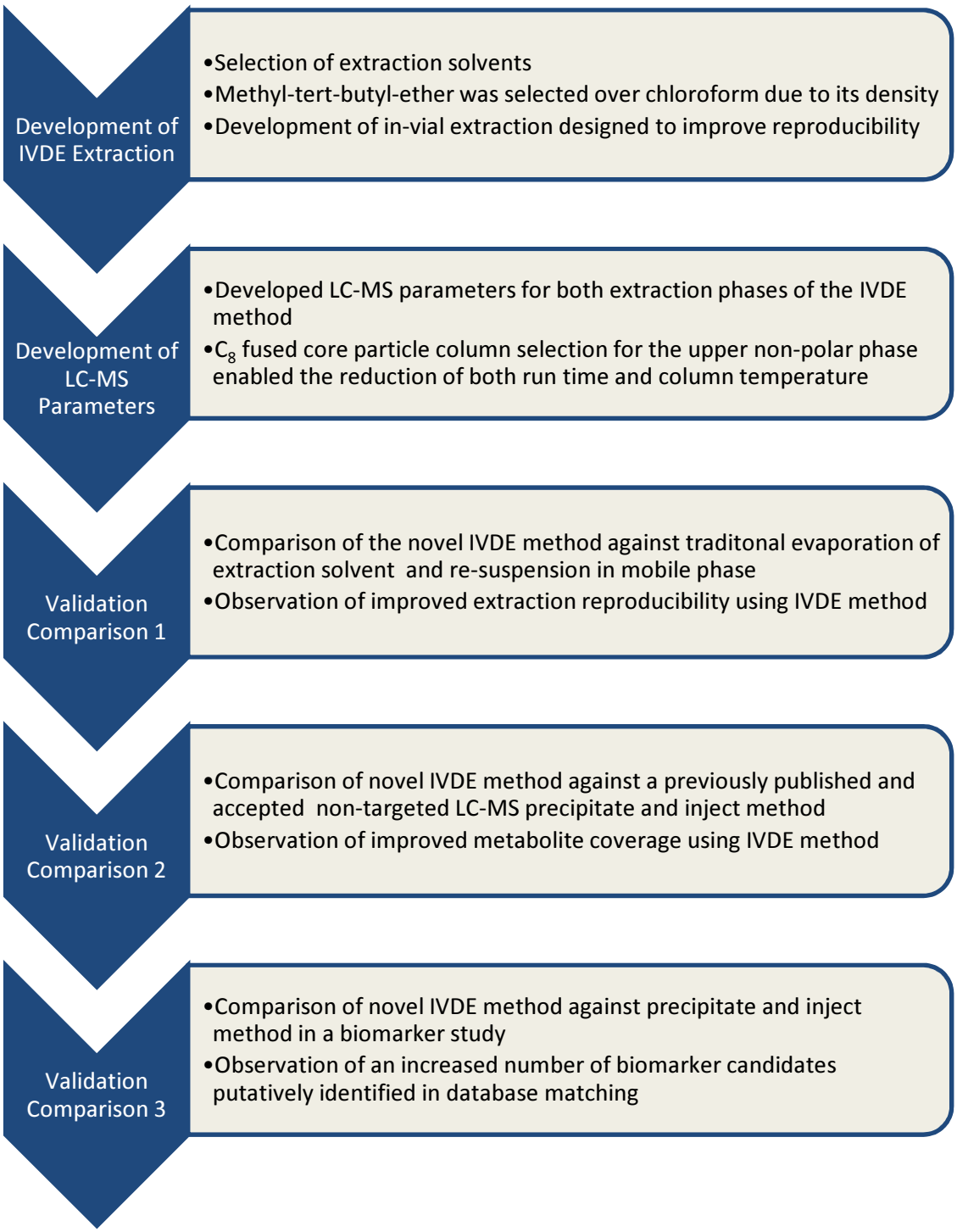

Figure 4.1: Overview of Chapter 4 Progression

The above figure presents the progression of the IVDE method development, and the tests completed to ensure its validation.

4.2 – Materials and Methods

4.2.1 – Materials

Ultrapure water, used to prepare all the aqueous solutions was obtained from an in house Milli-Q+ 185 filtration system (Millipore, Billerica, MA, USA). LC-MS grade methanol, acetonitrile and analytical grade formic acid were purchased from Fluka Analytical (Sigma-Aldrich Chemie GmbH, Steinheim, Germany). Analytical grade ammonium hydroxide was acquired from Panreac Quimica SA (Barcelona, Spain) and analytical grade methyl-tert-butyl-ether (MTBE) was from Sigma-Aldrich Chemie GmbH (Steinheim, Germany). A C15 triacylglycerol (tripentadecanoin) with m/z 764.6894 ($C_{48}O_6H_{92}$) purchased from Larodan Fine Chemicals AB (Malmö, Sweden) was used as an internal standard. Chromacol 03-FIV HPLC vials with fixed 0.3mL glass inserts (Chromacol - Welwyn Garden City, UK) were chosen.

4.2.2 – Instrumentation

The analysis was completed using an HPLC system (1200 series, Agilent Technologies, Waldbronn, Germany) coupled to an Agilent MS (6520 series, Agilent Technologies, Waldbronn, Germany) equipped with an electrospray ionisation source. The HPLC system consisted of a degasser, two binary pumps, temperature controlled autosampler and column oven. During all analysis two reference m/z were used: m/z 121.0509 ($C_5H_4N_4$) and m/z 922.0098 ($C_{18}H_{18}O_6N_3P_3F_{24}$) for positive ionisation mode and m/z 112.9856 ($C_2O_2F_3(NH_4)$) and m/z 1033.9881 ($C_{18}H_{18}O_6N_3P_3F_{24}$) for negative mode. These m/z are continuously infused to the system to allow constant mass correction.

4.2.3 – Samples

The extraction method and analytical conditions for analysis were developed using human plasma from a healthy volunteer.

The study designed to test the biomarker discovery capabilities of the obtained method was performed using rat plasma from streptozotocin (STZ) diabetic and control (age and sex matched).

Sprague-Dawley male rats, 12 ± 2 weeks of age, from the animal quarters of University San Pablo-CEU, were used. Throughout the experiments the animals were kept in collective cages (less than 7 animals per cage) and controlled conditions (22 ± 2 ºC and 55 ± 10% relative humidity). Animals had free access to tap water and diet (Harlan Global Diet 2014, Harlan Interfauna Ibérica, Madrid, Spain).

Samples were obtained from rats that came from two experimental groups: Animals that received an intraperitoneal dose (50 mg/kg, dissolved in 50mM citrate, pH=4.5) of streptozotocin and showed blood glucose levels over 200mg/dL 4 days after treatment (diabetics, D; n=9) were sacrificed at 14 days after the STZ administration. Sex and age-matched rats that did not receive STZ were studied in parallel (controls, C; n=7).

The experiments were approved by the Ethical Committee of the University San Pablo-CEU and they are in agreement with Amsterdam Treaty and Spanish legislation (RD 223/1988).

More information can be found and the same animal models used as in the publication [289].

4.2.4 – Sample Extraction Methods

The novel IVDE method underwent a comparison with two further traditional extraction approaches, to investigate if an in-vial approach improved reproducibility across an analytical run.

4.2.4.1 – Sample Extraction Method 1: In Vial Dual Extraction Followed by Direct Injection to Liquid Chromatography-Mass Spectrometry

The IVDE method uses MTBE as an organic phase solvent, originally presented as an alternative to the commonly used chloroform by Matyash et al. [217]. During this procedure the whole plasma extraction and separation of the two phases (ether and water) was performed within a HPLC vial (Figure 4.2). The volumes of the method were adapted to suit the size of the vial inserts. 20µL of plasma was mixed with 10µL of MilliQ water. Proteins were precipitated with 40µL of methanol and vortex-mixed for 2 min. Then 200µL of MTBE containing 10µg/mL of internal standard (TGC15) were added, prior to mixing of the whole mixture via vortex at room temperature for one hour. After adding 50µL of MilliQ water, the sample was mixed and centrifuged at 3,000g for 10 min. The upper MTBE and lower methanol-water phases were then injected onto the LC-MS system directly from the vial by adjustment of the instruments needle height in two separate runs, at 5 or 15 mm from the bottom (positions -5 and +5 in the autosampler settings), with the same drawing and ejecting speed (200 µL/min).

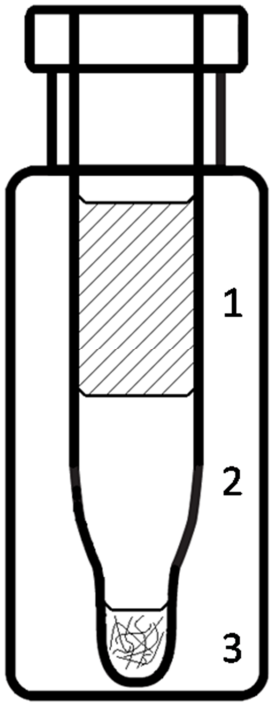

Figure 4.2: In Vial Extraction Overview

A schematic diagram of the in vial extraction. 20µL of plasma is added to the vial, followed by water, methanol and ether. After centrifugation the final result can be seen in the above three layers.

1) Upper phase consisting of ether containing the non-polar compounds, particularly lipids
2) Lower phase consisting of water containing the polar compounds
3) A solid pellet consisting of precipitated protein

Layers 1 and 2 can then progress to LC-MS analyses specialised for each phase. Injection onto the LC-MS is achieved by adjusting the needle height of the autosampler, and therefore removes any requirement for the extraction to undergo any transfer or drying stages.

4.2.4.2 – Sample Extraction Method 2: Ether Extraction, Evaporation and Re-Suspension in Traditional Liquid Chromatography Compatible Solvents

Traditional extraction methods often involve the transfer of sample between extraction and LC-MS vials, as well as the evaporation of extraction solvent, followed by the re-suspension in a typical LC-MS compatible solvent. Therefore a study was designed in order to compare this traditional approach with the developed IVDE method, to see if removal of transfer, evaporation and re-suspension stages of the extraction improved overall reproducibility.

The use of MTBE as an extraction solvent was previously presented as a solvent suitable for lipid extraction by Matyash et al [217], however, described here is the method was adapted for use within an LC-MS sample vial. To summarise, 20µL of plasma was added to glass tubes along with, 10µL of MS-grade water and 40µL of MS-grade methanol prior to a vortex-mix for 2min. Following this 200µL of MTBE (containing 5µg/mL internal standard) was added. The capped tube was vortex-mixed for 1hour, 50µL MS-grade water was added and vortex-mixed for 2min. Tubes were centrifuged at 3000g for 10min. From the upper phase 50µL of MTBE was removed and transferred to new glass tubes. Samples were evaporated to dryness at 35°C in a vacuum evaporator (Thermo Fisher Scientific, Waltham, MA, USA) and finally re-suspended (vortex for 2min) in 50µL of isopropanol (IPA), before being transferred to a HPLC vial and injected onto the LC-MS system.

4.2.4.3 – Sample Extraction Method 3: Precipitate and Inject

Precipitation of protein using an organic solvent such as methanol or acetonitrile is a widely accepted and used approach in non-targeted metabolite profiling. Therefore, a previously published precipitate and inject method was applied to the

same plasma pool as a comparative control to observe if the IVDE method increased metabolite coverage.

The extraction method has been previously described and employed for the purpose of plasma metabolic fingerprinting, and therefore is an ideal comparison tool [274, 289]. This method consisted of protein precipitation with 3 volumes of cold (maintained on ice) methanol:ethanol mixture (1:1) to 1 volume of plasma. Samples were vortex-mixed and then incubated on ice for 5 min, and centrifuged at 3000g at 4°C for 20min. Collected supernatant was filtered through a 0.22µm nylon, syringe filter and passed to a HPLC vial for the analysis.

4.2.5 – Instrumental Conditions

Two sets of instrumental conditions were used for the comparisons. The first was specifically designed for the non-polar upper ether phase. It was used to compare the IVDE method 1, described in Section 4.2.4.1, with the evaporation and re-suspension method 2, described in Section 4.2.4.2.

The second set of conditions has previously been published [274, 289] alongside the precipitate and inject extraction. The method consists of a typical reversed-phase gradient employed to cover a wide range of polarities. In the comparison study reported here, the analytical set up was employed to analyse the extracts from the precipitate and inject method as a comparative control. The method was also used to analyse the lower water phase from the IVDE extraction method as a tool to expand overall metabolite coverage.

4.2.5.1 – Instrumental Condition Set 1 – Non-Polar Upper Ether Based Phase

Analysis was completed at 60°C using an Agilent Poroshell 120 EC-C_8 column (150 x 2.1mm, 2.7µm). A gradient was employed consisting of mobile phase A (10mM

ammonium formate in MilliQ water) and mobile phase B (10mM ammonium formate in methanol) pumped at 0.5mL/min. Initial conditions were 75%B, increasing 96%B in 23min. This was then held until 45min. The gradient then increased to 100%B by 46min and held until 50min. Starting conditions were returned by 51min and a 9min re-equilibration time was included taking the total run time to 60min. Chromatographic conditions were previously optimised as described below.

Mass spectromic detection was performed in both positive and negative ESI mode in full scan from 50 to 1200 m/z. The mass spectrometer source conditions consisted of a capillary voltage of 3500V (positive mode) or 4500V (negative mode), whilst both ionisation modes used a scan rate of 0.2 seconds per scan, a nebulizer gas flow rate of 10.0L/min, a source temperature of 350°C and a source pressure of 40psig. The same instrumental conditions were applied when comparing the evaporation method described above

4.2.5.2 – Instrumental Condition Set 2: Polar Lower Water Based Phase and Traditional Precipitate and Inject

Conditions were as previously described [274, 289]: 10µL of extracted sample was injected onto a reversed-phase C_{18} column (Discovery HS C_{18} 150 x 2.1mm, 3µm; Supelco) with a guard column (Discovery HS C_{18} 20 x 2.1mm, 3µm; Supelco). Separation was performed in 40°C at the flow rate 0.6mL with solvent A composed of water with 0.1% of formic acid, and solvent B consisted of acetonitrile with 0.1% of formic acid. Metabolites were eluted using general gradient started from 25% B to 95% B in 35 min, and returned to initial conditions in 1 min, with 9 min re-equilibration time.

Mass spectromic detection was completed in both positive and negative ESI mode in full scan from 50 to 1000 m/z for positive mode and from 50 to 1000 m/z for negative mode. The capillary voltage was accordingly 3kV for positive polarity and 4kV for negative ionisation. Scan rate of 0.2 seconds per scan, and nebulizer gas flow rate 10.5L/min, temperature 325°C, pressure 52psig were the same for both ionisation modes.

4.2.6 – Data Treatment

Data from all analytical runs were processed and treated in the same manner, to ensure comparison between methods was consistent.

The raw data collected by the analytical instrumentation were cleaned of background noise, and unrelated ions by the Molecular Feature Extraction tool in the MassHunter Qualitative Analysis Software (B.04.00, Agilent Technologies). The MFE algorithm uses the accuracy of the m/z measurements to group ions related by charge-state envelope, isotopic distribution, and/or the presence of adducts and dimmers. The MFE then creates a listing of all possible components as represented by the full MS data. Each compound is described as a feature and contains m/z, retention time and abundance.

For data extraction the pre-set "small molecules (chromatographic)" algorithm was applied, with 200 counts as a limit for the background noise. In addition, the algorithm was set to find co-eluting adducts of the same feature. For this, adduct settings were applied for the lower aqueous phase (+H, +Na, +K, neutral loss of water) in positive ionisation and (-H, +HCOO) for negative ionisation. Due to the ammonium formate in the mobile phase, for the upper lipid phase the adduct settings (+H, +Na, +K, neutral loss of water, +NH4) for positive ionisation applied

and (-H, +CH_3COO) for negative ionisation were applied. For the upper phase the option for "salt dominated ion" was also applied.

Due to subtle retention time shifts, samples need alignment to ensure the same metabolite is listed as the same feature within each sample analysis. Therefore samples were aligned using MassProfiler Professional (B.02.01, Agilent). Alignment applied retention time correction as well as correction of the m/z.

To filter the data matrix from background signals and data Agilent's filter by frequency algorithm was applied. The process works by filtering only those features present in all samples per group. For example in a disease classifier study, the feature must be present in all controls or all disease samples to be included for further analysis. The theory behind this approach is that sporadic features which are only in one or two samples have increased likelihood that they are background or an exogenous compound present in a test tissue.

In the "Comparison 3" study between control and diabetic rats, univariate data analysis was completed to identify those features that vary significantly between groups. After logarithmic transformation student´s t-test ($p \leq 0.05$) was competed.

4.2.7 – Databases for identification

Metabolites were identified by searching by m/z against the online available databases such as the METLIN [234], HMDB[231-233], and the Mass Translator into Pathways (MassTRIX) database [290]. For the database search the error mass used for was adjusted to 7 ppm.

4.3 – Results

4.3.1 – Comparison One

4.3.1.1 – In Vial Dual Extraction Compared with Evaporation and Re-Suspension

Initially a comparison was completed between the novel IVDE approach and a more typical approach which involves removal of the extraction solvent via evaporation and replacing it with a conventional LC-MS compatible solvent such as methanol, acetonitrile or isopropanol. More on this selection of solvent is examined in the discussion (Section 4.4.1 (Page 183)).

The results from the comparison are presented in Table 4.1 and can be visualised in Figure 4.3. It can clearly be seen from the table that the IVDE method is more reproducible. Initially it can be seen that the total number of features in all samples (n=3) is increased in the IVDE method (2280 compared with 603). Further to this the number of features exhibiting a lower %RSD between extracts is also increased, for example the number of features with a %RSD <5 were 821 for IVDE, but only 86 for evaporation and re-suspension. In addition, an increase in both total signal and total useable signal can also be observed.

Parameter	IVDE	Evaporation
Number of features present in all samples	2280	603
RSD<30%	1912	338
RSD<20%	1738	280
RSD<10%	1358	182
RDS<5%	821	86
RSD<30% [%]	83.86	56.05
RSD<20% [%]	76.23	46.43
RSD<10% [%]	59.56	30.18
RDS<5% [%]	36.01	14.26
TS	2.95E+09	2.24E+09
TUS	2.88E+09	1.95E+08

Table 4.1: Comparison 1: In Vial Dual Extraction and Evaporation/Re-Suspension

The above table displays the results from the comparison between the IVDE method (upper ether phase only) and the traditional evaporation and re-suspension method when used to extract the same pool of human plasma (n=3). The apparent compatibility of the MTBE and LC-MS allowed the direct injection of the extraction solvent for analysis. The data are for positive ionisation detection only.

The improvement in reproducibility can clearly be seen, with both more features in all samples and more features present at a lower %RSD in the direct injection method. Further to this an increase in both total signal and total useable signal can also be observed.

TS (total signal): sum of signals for all features detected in all replicates.

TUS (total useful signal): sum of signals only for features common for all three samples.

[%]: percent of features with expected RSD among number of features present in all samples.

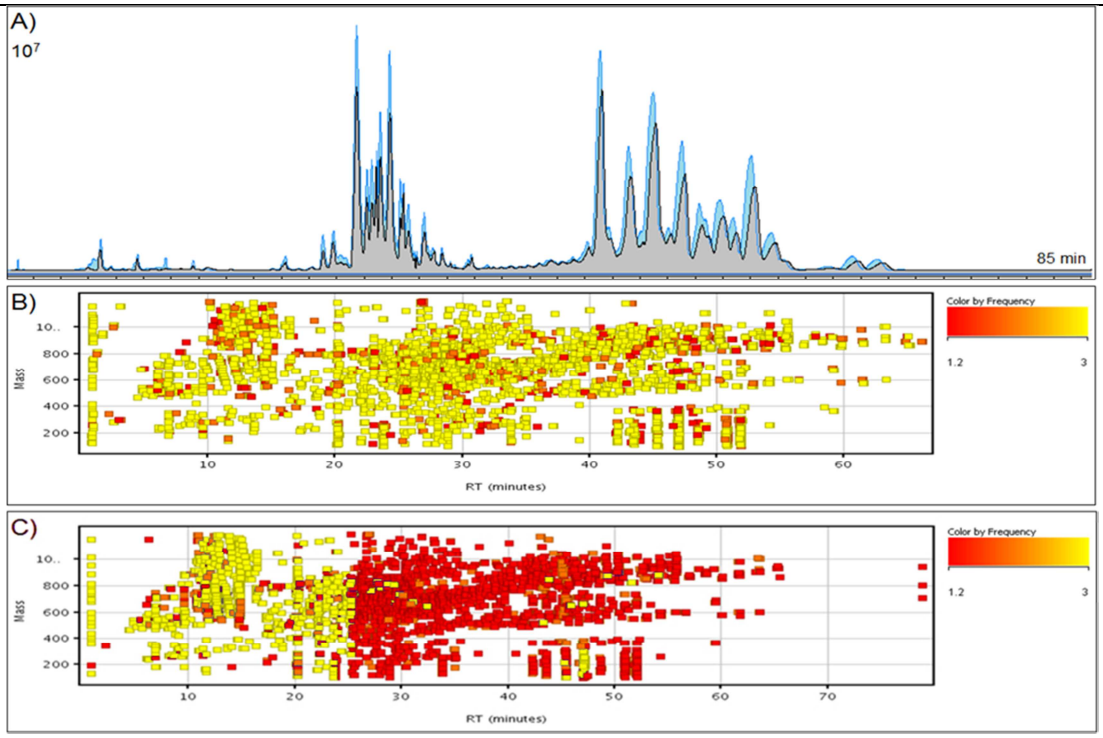

Figure 4.3: Comparison of In Vial Dual Extraction and Evaporation/Re-Suspension

The above figure highlights the comparison between the IVDE extraction (upper ether phase only) and the traditional evaporation and re-suspension method when used to extract the same pool of human plasma (n=3).

A) Extracted compound chromatograms (ECC) for IVDE (blue) and for the evaporation approach (grey). The increase in overall signal can be seen for the blue IVDE method.

B) LC-MS feature map of data collected using the IVDE method. An LC-MS feature map is a visual plot of m/z (y-axis) and retention time (x-axis). Each feature is coloured by frequency of detection in each of the three plasma replicates. (Red = 1, Orange = 2, Yellow = 3).

C) LC-MS feature map of data collected using the evaporation and re-suspension approach.

From this figure, reproducibility for IVDE can be seen, with greater signal intensities in (A) and more yellow features on the feature map of IVDE (B), suggesting improved extraction reproducibility.

4.3.2 – Comparison Two

4.3.2.1 – In Vial Dual Extraction Compared with Precipitate and Inject

To further test the capabilities of the IVDE method, it underwent comparison alongside a previously published precipitate and inject method [274, 289]. Particular interest in this instance was on the total number of features extracted from each method.

The IVDE approach consisted of two phases, and underwent MS analysis in positive and negative ionisation. The precipitate and inject approach only consisted of the single phase, but was also analysed using positive and negative ionisation.

The improvement in the metabolite coverage when using the IVDE extraction can be observed in Table 4.2.

In positive ionisation detection, 3636 reproducible features were observed in the upper and lower positive ionisation phase of the IVDE, with only 1020 features observed in the precipitate and inject method.

More features are also observed in the IVDE combined approach in negative ionisation, with 826 features, compared with 636 in the precipitate and inject method.

The two extraction methods were also compared by the number of features that returned database hits following a search. Again it can be seen that an increase is apparent in the IVDE approach, with 1425 (positive) and 314 (negative) features observed, compared with 493 (positive) and 283 (negative) in the precipitate and inject method.

Parameter	IVDE (Both Phases)		Precipitate and Inject	
	Positive	Negative	Positive	Negative
Features present in all samples	3636	826	1020	636
RSD<30%	3120	696	916	418
RSD<20%	2762	556	852	310
RSD<10%	1738	348	698	126
RDS<5%	637	210	489	38
RSD<30% [%]	85.81	84.26	89.80	65.72
RSD<20% [%]	75.96	67.31	83.53	48.74
RSD<10% [%]	47.80	42.13	68.43	19.81
RDS<5% [%]	17.52	25.42	47.94	5.97
Features identified	1425	314	493	283

Table 4.2: Comparison 2: In Vial Dual Extraction and Precipitation and Injection

The above table displays the results from the comparison between the IVDE method and the previously published precipitate and inject method when used to extract the same pool of human plasma (n=3).

The improvement in the metabolite coverage can be observed from the table with 3636 reproducible features observed in the upper and lower positive ionisation phase of the IVDE, and only 1020 features in the precipitate and inject method.

More features are also observed in the IVDE combined approach in negative ionisation, with 826 features, compared with 636 in the precipitate and inject method.

The Features Identified row represents those features that returned a database search hit. Again it can be seen that an increase is apparent in the IVDE approach.

4.3.3 – Comparison Three

4.3.3.1 – In Vial Dual Extraction Compared with Precipitate and Inject in a Non-Targeted Biomarker Discovery Study

In order to ensure the IVDE method performed well in a realistic biomarker discovery scenario, it underwent a validation investigation using control rat plasma along with diabetic rat plasma.

The results of which were run in parallel with the previously published precipitate and inject method [273, 274].

The analysis using the IVDE extraction method produced more reproducible features present in all samples, in both positive and negative ionisation detection modes. Following this filtration of features present in all samples, the features underwent univariate analysis, via means analysis with student's t-test. Again the IVDE method produced more significant features in both positive and negative ionisation MS detection modes.

Finally the significant features underwent analysis using the MassTRIX pathway generator [290]. The algorithm analyses the m/z and produces a model metabolic map. Following this MassTRIX pathway search algorithm, once again the IVDE method returned a higher number of significant than the precipitate and inject approach.

Parameter	IVDE (Both Phases)		Precipitate and Inject	
	Positive	Negative	Positive	Negative
Features present in all samples	3568	908	1361	446
Statistically significant m/z	536	165	140	79
Identified features	293	102	99	72
Pathways	46	33	28	16
Significant pathways	13	16	11	5

Table 4.3: Comparison 3: In Vial Dual Extraction and Precipitation and Injection

The above table displays the results form a comparison between the novel IVDE method and the precipitate and inject method when applied to a biomarker discovery scenario. Plasma from control (n=6) and diabetic (n=6) rats underwent analysis by both methods. Features were filtered and had to be present in all samples. An increase in the number of features was observed when using the IVDE method.

Following univariate data analysis the number of significant (Welch's t-test) features that differentiated between control and disease groups also increased using the IVDE method.

Features also underwent analysis using the MassTRIX pathway translator [290]; again more pathways of interest were observed using the IVDE method.

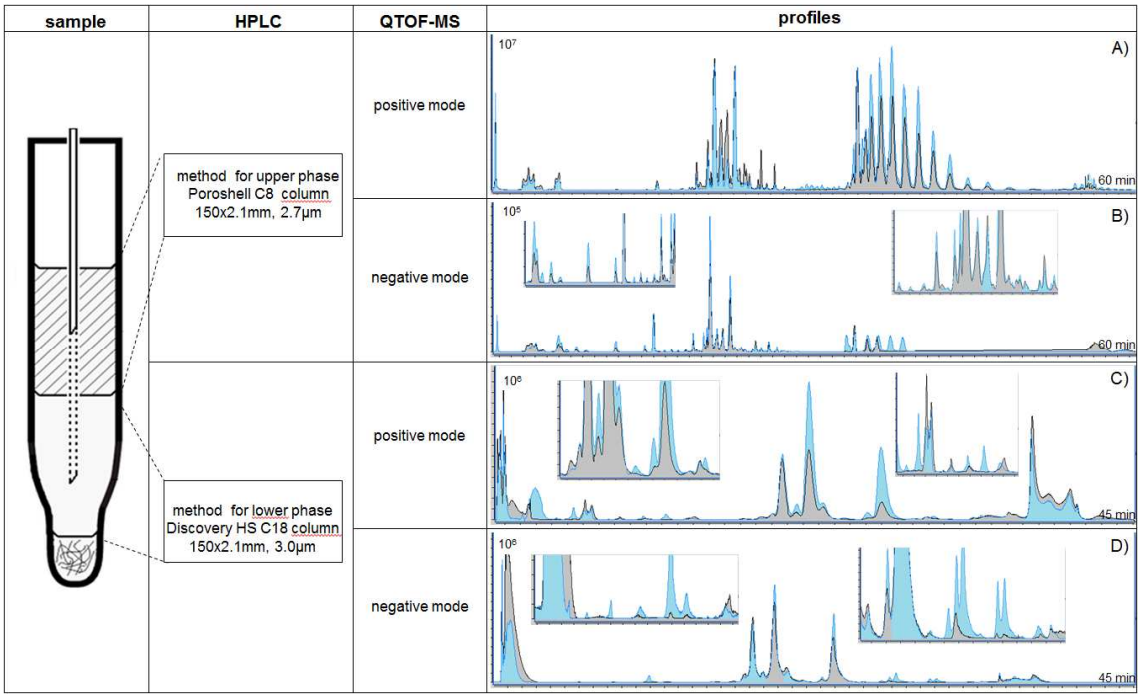

Figure 4.4: Overview of Finalised Chromatography

The above figure presents chromatograms from each of the IVDE extraction phases. Both positive and negative ionisation chromatograms are presented.

The schematic displays the IVDE method with two different specialised chromatographic conditions and two polarity modes. Extracted compound chromatograms (ECC) are displayed for

A) Upper phase analysed in positive mode
B) Upper phase analysed in negative mode.
C) Lower phase analysed in positive mode
D) Lower phase analysed in negative mode.

Chromatograms in grey are representative for controls whilst those in blue are for diabetic rat model plasma.

4.4 – Discussion

IVDE extraction consists of adding two non-miscible solvents to 20µL of plasma in a 300µL vial insert. The procedure leads to a separation of analytes that disperse into either phase, meaning successive re-extractions with solvents of different polarities will not be necessary to improve the detection of less polar compounds. Two different chromatographic methods optimised for each type of metabolites were employed with the aim of decreasing matrix effects, increasing resolution and improving compound identification.

4.4.1 – Selection of Solvents for In Vial Dual Extraction

The IVDE method selected MTBE as extraction solvent over a number of published alternatives, especially the more commonly accepted Folch method [291], due to its density and polarity.

The Folch method is a widely accepted gold standard of lipid extraction that employs chloroform as an organic solvent. Figure 4.5 demonstrates the advantage of using the MTBE based extraction employed in the IVDE approach compared with the Folch chloroform extraction. Importantly, the MTBE method produces two layers of solvent above the protein precipitate, which forms a solid pellet of protein in the base of the vial. This is in contrast to the traditional Folch lipid extraction, which results in the lipid phase sitting below the floating protein precipitate. Traditional analysis of this dense phase requires careful collection, following the removal of both the upper aqueous and protein layers. When working with small volumes, such as the IVDE method described here (20µL of plasma is required) this is a delicate operation increasing the risk of analytical errors and the introduction of variation.

As previously described above, the IVDE method results in a protein pellet at the base of the vial. This enables the easy injection of the two phases, whilst removing the risk of column blockages caused by the precipitate.

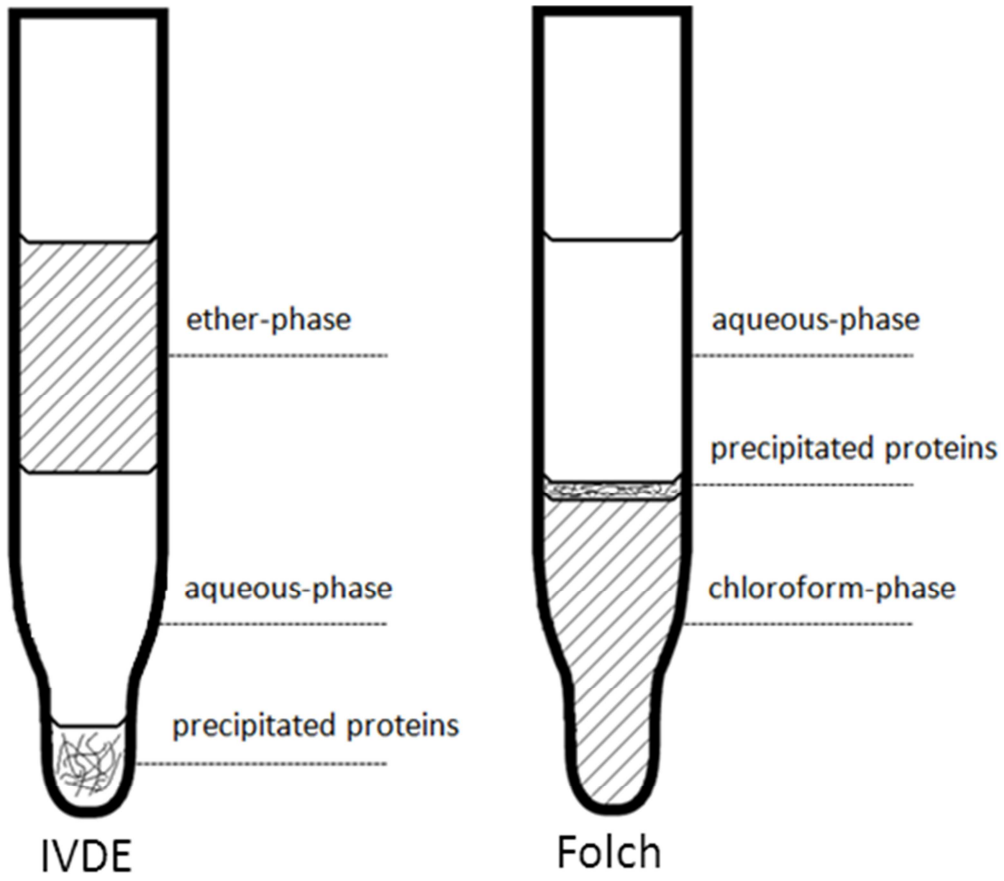

Figure 4.5: Solvent Dispersion in Extraction Using Ether or Chloroform

The above schematic view demonstrates the resulting phase dispersion after the completion of the novel IVDE and the classical Folch procedure. The IVDE method employs methyl-tert-butyl-ether (MTBE), whilst the Folch procedure utilises the more dense chloroform to extract lipid components.

On the left IVDE example, the lipid containing MTBE layer is the top most phase, enabling easy analysis. A further important aspect of the procedure is the fact that the protein forms a solid pellet at the bottom of the extraction vial. This enables the direct injection onto LC-MS analytical systems, as the risk of protein injection and therefore blockages within the LC-MS system is removed.

The ether extraction method was first described by Matyash et al [217] and has been extensively tested against the Folch method resulting in comparable if not favourable extraction recoveries.

A further advantage of the completion of the extraction using the method described here was that MTBE was found to be suitable for direct injection onto the LC-MS gradient. Traditionally, the injection of 100% organic solvent is not advised when completing LC separation due to the adverse effect it can have on early eluting peaks. However, as the separation described here is completed over the course of an hour long gradient, the direct injection of MTBE was found to have no effect on the reproducibility and separation achieved. This observation included the early eluting peaks. Therefore in using MTBE as an extraction solvent, not only is the extraction method and collection procedure simpler, but it removes a drying and re-suspension stage from the protocol, reducing the risk of drying losses, analytical variation, and potentially oxidative conditions to dried unsaturated lipid species, such as UV light and atmospheric oxygen exposure.

Arguably the greatest benefit to using the described IVDE extraction is the ability to complete the extraction and analysis in one simple in-vial procedure. It was found that by adding the plasma and extraction solvents to a capped LC vial the extraction could be completed prior to direct injection. The ability to manually adjust the injector needle enabled both the upper and the lower phase could be directly injected onto column in separate runs.

4.4.2 – Development of Liquid Chromatography – Mass Spectrometry

Specific LC-MS methods and parameters were developed for each extraction phase of the IVDE method. These are discussed in detail below:

4.4.2.1 – Upper Phase of the In Vial Dual Extraction

A selection of different columns, gradients and temperatures were tested to optimise the chromatographic separation for the upper phase. Starting conditions were adapted from Sandra et al [292]. Chromatographic methods were compared by injecting the same extract onto the LC-MS analytical set up. Resulting chromatograms from the method development process were compared in terms of:

- Visual inspection of chromatograms looking at the intensity of the signal, number and aspect of the peaks;
- The total number of features obtained following feature extraction and alignment
- The number of features extracted, aligned and observed in every sample of a triplicate series of injections;
- The relative standard deviation (%RSD) of those features present in each sample of a triplicate injection to check method repeatability;
- The quality of the separation for two phospholipids: PE(36:2) and PC(34:1) that differ in m/z by 0.0364 Da to inspect chromatographic resolution. This approach was previously employed in the previous publication by Sandra et al [292];
- The number of features identified in a database search to test the biological usefulness of the method;

Figure 4.6 summarises initial and final conditions as well as the extracted compound chromatograms (ECC) (Figure 4.6, panels A, C and E) and extracted ion chromatograms (EIC) showing PE(36:2) and PC(34:1) traces (Figure 4.6, panels B and D).

A number of modifications were made from the original conditions. The most significant of which was the change in column stationary phase particles from totally porous to fused core with a porous outer layer.

The use of superficially porous stationary phases can provide a number of advantages. These are highlighted in Figure 4.7. As can be seen in the figure, fused core stationary phases reduce the dispersion distance of analytes, therefore helping to reduce band broadening and to improve peak shape and resolution.

A second advantage of the phase is due to the design of the solid core. This enables a more uniform peak shape, and therefore improves its packing within the column, helping to remove dead volumes and voids. Again, this can lead to improved peak shape, and an increase in resolution.

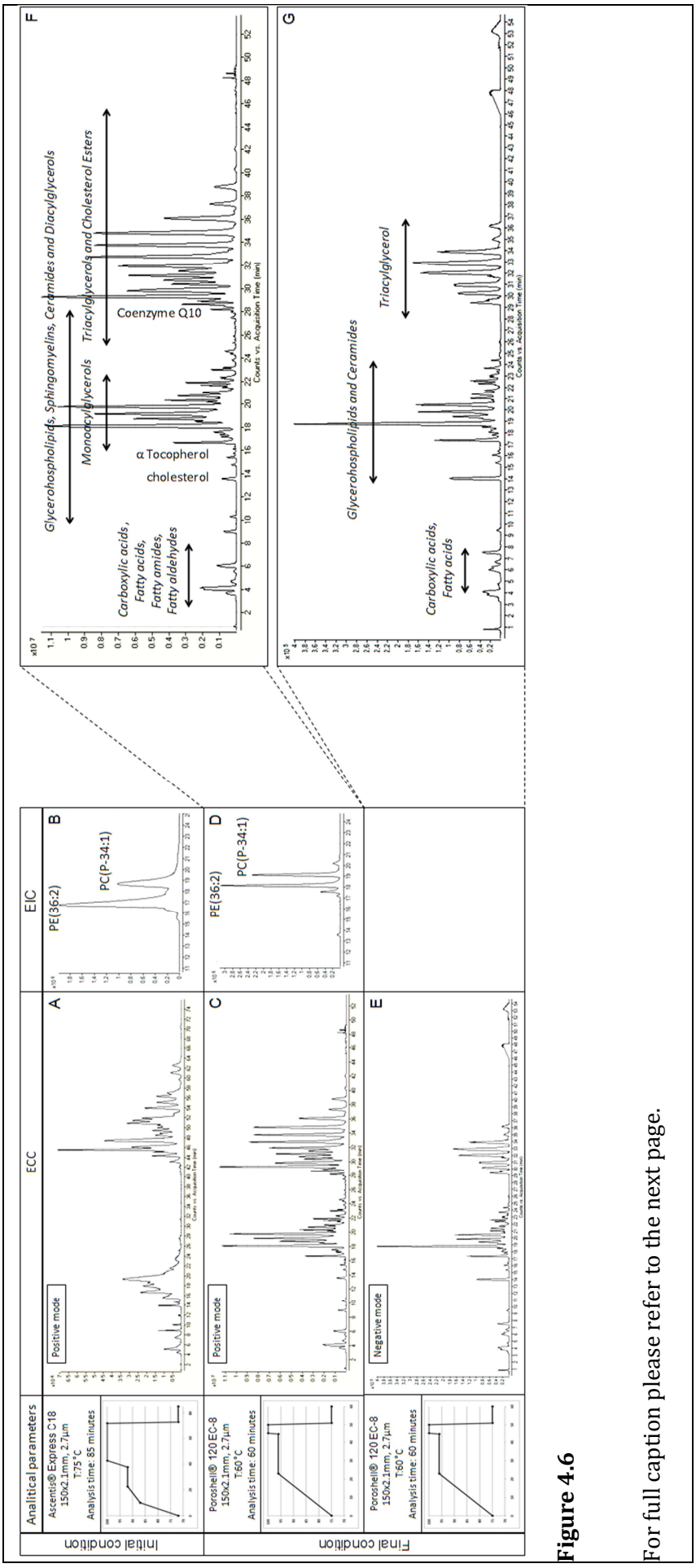

Figure 4.6

For full caption please refer to the next page.

Figure 4.6: Chromatographic Development Overview

Figure on previous page.

Initial and optimised chromatographic conditions for the IVDE upper phase extract of human plasma.

A) Extracted Compound Chromatograms (ECC) for initial conditions in positive ionisation mode. The conditions employed a Supelco Ascentis® Express column with a C_{18} stationary phase. The overall runtime was 85min.

B) Extracted Ion Chromatogram (EIC) for PE(36:2) and PC(P-34:1) when using the starting conditions in (A)

C) ECC for the final optimised conditions in positive ionisation mode. The final conditions employed an Agilent Poroshell® column with a C_8 stationary phase. The overall runtime was reduced from the original conditions to 60min.

D) EIC for PE(36:2) and PC(34:1) when using the optimised conditions in (C)

E) ECC for optimised conditions in negative ionisation mode. The same chromatographic conditions were used for both ionisation polarities, and again an Agilent Poroshell® column with a C_8 stationary phase was used for the separation.

F) Enlarged C

G) Enlarged E

Stationary Particle Type	Schematic of the Particle	Band Spread Effect In Column	Chromatographic Result
Superficially Porous (Fused Core)	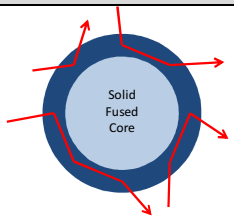	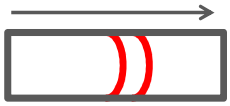	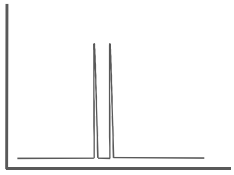
Fully Porous	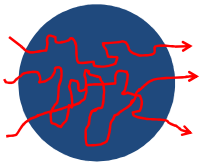		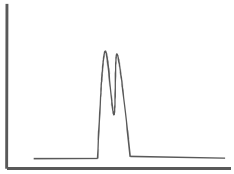

Figure 4.7: Schematic Comparison of Fused Core Stationary Phases

The above figure demonstrates the key differences between traditional porous LC stationary phase particles and those stationary phases that consist of superficially porous particles.

The superficially porous particles are manufactured by applying typical stationary phase to a solid inner particle. The advantage of this is a reduction in the distance that analytes have to disperse through the stationary phase. This can lead to a reduction in band broadening, and lead to improved peak shape and resolution

A further advantage of the fused core approach is a more uniform particle size, which enables better stationary phase packing, and reduction of void volumes, again improving peak shape and resolution.

A further modification to stationary phase selection was made via a switch to a C_8 phase. These changes combined enabled the reduction of column temperature from 75ºC to 60ºC, whilst still providing an efficient separation of lipid features, protecting the column lifetime. Further to this, the optimised gradient developed on the C_8 phase enabled a reduction in the overall runtime from 85 to 60min.

For the LC-MS analysis of the IVDE lower phase analysis, a gradient with reversed-phase chromatography previously optimised for total plasma [273, 274] was employed under the hypothesis that after eliminating non-polar compounds, ion suppression would decrease and a higher number of compounds could be identified with an appropriate sensitivity and reproducibility. Furthermore, the method has performed well when analysing the polar compounds of urine [289].

4.4.3 – Comparison One

4.4.3.1 – In Vial Dual Extraction Compared with Evaporation and Re-Suspension

Once the chromatographic conditions were optimised, a separate experiment compared a direct injection of the IVDE upper phase with a traditional transfer, evaporation and re-suspension approach common in many profiling methods [292].

Reproducibility of both methods was examined by comparing the RSD% values for features detected in all three replicate extractions of the same plasma pool. Table 4.1 clearly demonstrates a higher number (378% increase) of molecules extracted using the IVDE method with an acceptable RSD% value compared with the evaporation approach.

Other comparison parameters which were used to examine the methods were: Total Signal (TS), which is the sum of signals for all features detected in all three

replicates, and Total Useful Signal (TUS), being the sum of signals only for those common features which are found in all three sample replicates.

The TS obtained with both type of sample treatments is relatively similar, with little difference between the two, whilst the TUS differs significantly (Figure 4.3). The difference between TS and TUS is very small for the IVDE approach, but for the evaporation method the difference is comparatively large, further confirming the superior reproducibility of sample treatment when performing IVDE direct injection.

Due to the observations in the results, the benefit of completing the IVDE method as opposed to a typical evaporation and re-suspension is thought to be a result of the reduction of sample preparation steps, and therefore reducing the number of instances that variation can be introduced to samples. The approach also avoids drying and transfer losses, however the exact reason of this loss of metabolites is difficult to identify.

4.4.4 – Comparison Two

4.4.4.1 – In-Vial Dual Extraction Compared with Precipitation and Injection

Further testing and validation of the IVDE method was demonstrated by the completion of an evaluation study designed to compare the novel IVDE approach to that of a currently accepted method [273, 274] employing a single phase precipitate and inject to LC-MS approach.

As can be seen in Table 4.2, splitting the sample extraction into two phases using the IVDE approach gave a 256% increase in reproducible features (positive ionisation) and 30% (negative ionisation) compared with the precipitate and inject method, meaning a total increase of reproducible features of 269%.

The results presented suggest that the implementation of the IVDE method has successfully increased the metabolite coverage when compared with tradition precipitate and inject methods. The use of two injection phases, from the same 20µL plasma extract also provides the advantage of expanding the coverage whilst preserving valuable sample.

4.4.5 – Comparison Three

4.4.5.1 – In Vial Dual Extraction Compared with Precipitation and Injection in a Biomarker Discovery Model

As the IVDE method was developed with the aim for use in future biomarker identification studies, it had to undergo validation for its capabilities for completing this role. In order to achieve this, a non-targeted biomarker study was developed comparing control rats with those treated to show signs of diabetes. This model is a preliminary test for a method such as one like the IVDE, as it is commonly accepted that lipid abnormalities are apparent in both forms (type 1 and type 2) of the disease [283, 284].

Plasma samples were obtained from rats in two groups; rats that received STZ (D group), and their corresponding sex and age-matched controls (C group). It is known that STZ selectively destroys the beta cells of the Langerhans islets from pancreas, and therefore insulin cannot be further synthesised, mimicking the complications of type 1 diabetes [293]. Additionally, STZ treated rats are of interest as they have previously been used as a model for AD. This is due to the development of an insulin resistant brain state which is thought to possibly proceed Aβ pathology in the brain [294, 295].

Table 4.3 shows the results for a comparison of coverage between the two groups of samples. Again the samples were prepared via both IVDE and the precipitate and inject method. In the IVDE method, results from upper and lower phase were combined to provide a comprehensive overview.

To evaluate the two analytical approaches the total number of features present in all samples for each group was compared, with results showing an increase in the number of statistically significant and identified features in the IVDE method compared with the precipitate and inject method. The IVDE method increased the number of reproducible features by 162% in positive MS and 103% for negative MS compared with traditional precipitate and inject.

Following multivariate modelling the total number of statistically significant features found to be responsible for the separation between samples from control and diabetic animals also increased in the IVDE method compared with precipitate and inject, by 283% in positive MS and 109% for negative MS.

These statistically significant molecules then underwent putative database identification, with the IVDE method again providing an increase with 196% and 42% more features identified in positive MS and negative MS respectively compared with the precipitate and injection method.

In addition to this, the MassTRIX [290] metabolic pathway translator was employed to analyse both approaches, with the two phase method providing information on approximately twice the number of pathways, than the traditional single method.

4.5 – Conclusions

Over the course of the study presented here in Chapter 4, an IVDE followed by LC-MS analytical method has been developed that was designed to decrease analytical variation and expand the global coverage of metabolite identification. The end result was a method capable of the analysis of >4500 reproducible features from a 20μL plasma extract.

This was achieved by the development of an in-vial two phase extraction, taking advantage of the non-miscible properties of the interaction between MTBE and water. The extraction solvent was then able to undergo direct analysis via LC-MS. The method was robustly tested and provided data that demonstrated an increase in the overall number of features and a decrease in the variability observed between injections when compared with two typically previously accepted methods.

Finally the IVDE method was applied to an animal model of diabetes – a model well accepted as having plasma metabolic differences. Following univariate data mining, data suggested that the IVDE held an advantage for fingerprinting over traditional precipitate and inject approaches.

The results complemented the aims set from Chapter 3, by improving metabolite coverage, particularly chromatographic separation in the lipid component of the extraction. The method was then progressed to a biomarker study with regard to plasma from control, MCI and AD patient groups, expanding on the findings reported in the initial LC-MS screen in Chapter 3.

Chapter 5:
Comprehensive LC-MS Lipidomics

5.1 – Introduction

From the results discussed in Chapter 3, it was apparent that non-polar lipid species were of high influence to the multivariate models and subsequent data analysis. The methodology in Chapter 3 employed a rapid LC-MS screen type approach, and putatively identified a number of lipid based features. Three features significantly reduced from control to AD patient groups. However, a high amount of co-elution was observed, therefore introducing potential ion suppression effects, which may have affected this result.

Further to the findings in Chapter 3, there is a plethora of previously published studies (either targeted or non-targeted) that identified abnormal concentrations of lipids or lipid groups in AD, with much of this evidence suggesting a role for HDL and related proteins in plasma [106, 193, 196, 296, 297]. Other studies pointing towards metabolic markers of AD include, in particular, the genetic studies confirming ApoE as a susceptibility factor [19] and both genome wide studies and plasma proteomics identifying apolipoprotein J (clusterin) in association with AD [106]. Clusterin is found as a component of HDL and is thought to be a chaperone of amyloid protein, heavily involved in the pathology of AD [106, 107].

In addition, two recent plasma fingerprinting studies discovered AD-linked alterations in lipid metabolism. The first study found an increase in ceramide (CER C16) levels and a decrease in sphingolipid (SP16) levels in the plasma of AD patients [193]. A second investigation identified a phosphatidylcholine (PC 16:0/16:0) as one of a cluster of three metabolites, thought to be predictive markers of AD development in people with MCI [196].

Therefore with these literature examples in mind, along with the initial result from Chapter 3, a novel comprehensive lipidomic method was developed, focused on the non-targeted biomarker discovery of lipid species in plasma (Chapter 4).

To briefly summarise, the developed method consisted of a lipid specific extraction using ether within an LC vial. This was followed by a direct injection from the vial onto the LC-MS system. The idea behind this was to minimise the transfer steps of the process, thereby improving reproducibility.

Four separate phases and LC-MS methods were employed to make it a fully comprehensive approach, as both the non-polar ether phase and the polar aqueous phase were developed and analysed in both positive and negative ionisation.

However due to the high number of samples presented here in Chapter 5 (n=141 + 20QC) combined with the extended run time of the improved method, it was not feasible with financial and time resources available to complete all analyses for the sample set size. Therefore, in an attempt to produce the highest chance of biomarker discovery, a decision was made to analyse only in positive mode which, based on, the results in Chapter 3, produced better analytical results. In addition the three features of significance were identified in the positive ionisation conditions.

The database search returned hits for PC compounds, suggesting a non-polar lipid extraction would be best suited. Therefore, with these considerations in mind the sample set was subjected to ether based lipid extraction followed by the positive lipidomic analysis described in Section 4.2.

5.2 – Materials and Methods

The method used is the upper phase positive ionisation analysis described in detail in Chapter 4 (Section 4.2). As previously discussed, the method described in Chapter 4 was developed with an Agilent 1200 LC in combination with an Agilent 6520 QTOF mass spectrometer. Upon return to King's College London the method was transferred to the equivalent Waters Acquity® LC connected to a Waters Xevo® QTOF mass spectrometer, therefore the methods are summarised below.

5.2.1 – Materials

LC-MS grade methanol was purchased from VWR (Leicestershire, UK) and high purity water deionised water was obtained from an in house Millipore filtration system (Millipore, MA, USA). Analytical grade ammonium formate was purchased from Sigma UK (Gillingham, Dorset, UK). Analytical grade MTBE was purchased from Fisher Scientific (Loughborough, UK). The internal standard, (triacylglyceride C15:0/C15:0/C15:0 [TG15:0]), was purchased from Larodan fine chemicals (Sweden).

5.2.2 – Instrumentation

LC-MS analysis was completed using a Waters Acquity UPLC® (Waters, Milford, USA) coupled to a Waters Xevo® G1 QTOF (Waters, Milford, USA). Analysis was completed in positive ionisation mode.

Chromatographic separation was achieved using an Agilent Poroshell 120 EC-C_8 column (150mm × 2.1mm, 2.7μ m), maintained at 60°C. A gradient was employed consisting of 10mM ammonium formate (A) and 10mM ammonium formate in methanol (B). The solvent was delivered at a flow rate of 0.5mL/min. The gradient consisted of 0min (75%B), 23min (96%B), 45min (96%B), 46min

(100%), 50min (100%). The column was re-equilibrated at 75%B for 9min prior to each injection.

The Waters Xevo® QTOF MS was operated in the positive ion mode with a capillary voltage of 3.2kV and a cone voltage of 60V. The desolvation gas flow was 800L/hour and the source temperature was 120°C. All analyses were acquired using the reference solution spray to ensure accuracy and reproducibility; leucine encephalin were used as lock mass (m/z 556.2771 and 278.1141) at a concentration of 500ng/mL and a flow rate of 10µL/min. Data were collected in the centroid mode over the m/z range 100–1000Da with an acquisition time of 0.1 seconds a scan.

5.2.3 – Waters MS^e Data Collection

As discussed in Chapter 3 (Section 3.2.3), the Waters Xevo QTOF MS employs a technique referred to MS^e, enabling the application of a high collision energy to ions, resulting in their fragmentation. This is of particular use, as fragment data can assist with identification of unknown species. As with the screen phase discussed in Chapter 3, level one data was acquired using a low collision energy of 5V, whereas level two acquired the data at a high collision energy of 50V.

5.2.4 – Samples Used for Analysis

Samples were collected and obtained from the two cohorts (AddNeuroMed and DCR) that make up the Institute of Psychiatry sample bank. These have been discussed previously in great detail in Section 2.2.3.3.

N=141 age and gender matched samples underwent analysis by the method described above. A summary of the samples can be viewed in Table 5.1.

A pool of plasma was used as a quality control sample. This was extracted alongside patient plasma, and underwent LC-MS analysis at regular time points across the run (n=20). Patient samples were analysed in a randomised order.

Due to the large number of samples, and therefore the extended analytical run time, samples were analysed in four evenly distributed separate batches (n=40). In addition, before each analytical run a pool of plasma was extracted and injected onto the column n=5 times. This ensured maximum column equilibration recommended when analysing biofluids in a metabolomic or lipidomic approach [298]. This resulted in approximately a total run time of 45hr per batch.

	Control	MCI	AD
Total Samples	49	50	42
Age (years) Mean	78.27	78.91	78.27
Age Std Dev	6.57	5.48	7.78
MMSE Mean	28.88	26.60	21.33
MMSE Std. Dev	1.17	2.16	5.06
Male/Female	24/25	24/26	22/20
% Male/Female	49/51	48/52	52/48

Table 5.1: Summary of Plasma Samples Used in Comprehensive Lipidomics

Table presenting the age and gender matched samples used for lipidomics analysis. Compared with the screen study discussed in Chapter 3, sample numbers were increased to n=141.

5.2.5 – Data Processing

Data was analysed in two ways. Firstly multivariate data analysis was completed by aligning the data set using the MarkerLynx package within MassLynx 4.1 (Waters, Milford, USA). Data was normalised according to internal standard (TGC15:0) to adjust for inter batch runs.

Following this a pareto scaled PCA model was created using SIMCA-P+ (Umetrics, Sweden) to ensure QC samples grouped, providing evidence for the reproducibility of the study. As with the PCA models in Chapter 3, grouping within <15% of both t[1] and t[2] of the total model was used as an arbitrary cut off value. The clustering of QCs was particularly important when considering the analysis was completed over four separate batches.

PC molecule m/z were extracted from the raw LC-MS data from all samples (n=141) using Waters QuanLynx software, a package within MassLynx 4.1 (Waters Corporation, Milford, USA). Following this each feature was normalised via peak area ratio to peak area of internal standard TG15:0. This was completed in Microsoft Excel 2010 (Microsoft, Reading, UK).

Univariate analysis for each PC ratio was then completed using SPSS statistical software (IBM, Portsmouth, UK) via "Students" t-test mean analysis.

This approach of raw data alignment in MarkerLynx, followed by multivariate data analysis in SIMCA-P+ → univariate data analysis → identification using database matching and fragmentation patterns has successfully been employed in a previous metabolomics publication [268].

Finally a predicative receiver operating characteristic (ROC) analysis was completed. Logistic regression was used to investigate the association of each of the three features with disease status after adjusting for the number of *ApoE* ε4 alleles. The three features were log transformed prior logistic regression analysis. Different models using different predictor combinations were tested and the best predictor combination was selected by step-wise regression using the Akaike's information criterion. ROC curves, were completed, with the area under the curve

(AUC) values reported for each model. Analyses were performed in STATA 10 (StataCorp. 2007. Stata Statistical Software: Release 10. College Station, TX: StataCorp LP.). The ROC analyses were completed in collaboration with Petroula Proitsi, a bioinformatician based at the Institute of Psychiatry with the required STATA 10 licensed software.

5.2.6 – Structural Elucidation and Feature Identification

Initially, putative identification was achieved using databases. Accurate m/z extracted from the raw data underwent database searching using the HMDB [232] and METLIN [234].

To enable the confirmation of features from the database matching, MS fragment patterns were analysed. Fragment patterns for each molecule were collected using Waters MS^e technology within the MS collection parameters. The technology allows a rapidly alternating mode of data collection grouped in levels (Section 5.2.3 (Page 200)). This approach has been employed in a previous publication by Rainville et al. [230].

5.3 – Results

5.3.1 – PCA to Demonstrate Reproducibility

Data from the n=141 test and n=20 QC samples underwent feature alignment using Waters MarkerLynx. A pareto scaled PCA analysis was completed using SIMPCA-P+ to demonstrate intra and inter batch overall reproducibility (Figure 5.1.A). Although the QCs generally grouped in the centre of the PCA, the distribution was slightly skewed. This observation was due to a slight batch effect (Figure 5.1.B) between samples run on different days. However, as with the PCA analyses in

Chapter 3, a cut off value of <15% of the total model (both t[1] and t[2]) was required. QCs clustered within this cut off.

As with the screen phase of the thesis discussed in Chapter 3, the three disease classes demonstrated no grouping in the PCA (Figure 5.1.C). This is as expected in a randomised extraction and analytical run and suggests no analytical trends between the groups, and therefore differences identified are more likely to be biologically related.

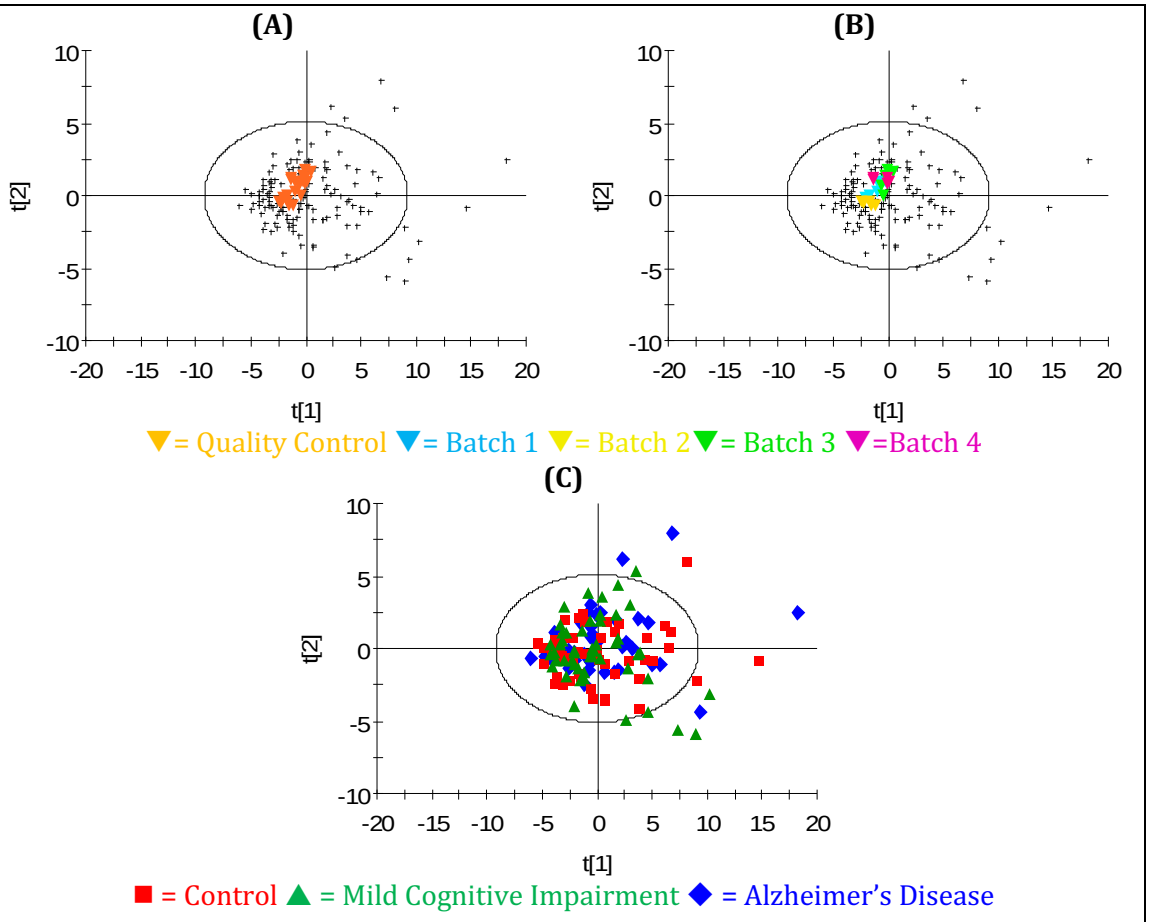

Figure 5.1: Principle Component Analysis of Comprehensive Lipidomics

Analysis of all samples (n=141 + n=20 QC) analysed as part of the human plasma lipidomic study.

(A) Displays quality controls (QC) clustering in the centre of the model. There is a minor batch effect as samples had to be split into four batches, however clustering (<15% of total model) can still be seen to be centralised in the model and has an acceptable grouping.

(B) A summary PCA of the batch effect observed in QC sample clustering displayed in (A). Each day has been designated a separate colour, and it can be seen that days two and four in particular show batch grouping.

(C) A demonstration of all samples coloured by disease class. The PCA shows no obvious grouping, as would be expected from a randomised extraction and analysis protocol and suggests no analytical trends in the data between disease classes.

5.3.2 – Univariate Feature Confirmation

Peak area values for features highlighted in the positive ionisation screen experiment previously discussed in Chapter 3 were extracted from the raw chromatographic data. Of these, three features that were previously identified as undergoing significant change between groups in the screen study, these were found to be significantly reduced in intensity in AD samples (Table 5.2 and Figure 5.2). Example extracted ion chromatograms for the features can be found in Figure 5.3.

m/z (M+H) [Da]	Mean PAR Control (SD)	Mean PAR MCI (SD)	Mean PAR AD (SD)
779.5465 (780.5543)	0.2122 (0.1210)[a][c]	0.1589 (0.1210)[a]	0.1261 (0.0692)[c]
805.5622 (806.5700)	0.5996 (0.2429)[a]	0.5268 (0.2429)	0.4715 (0.2030)[a]
833.5935 (834.6013)	0.2362 (0.1079)[b]	0.2082 (0.1108)	0.1729 (0.0812)[b]

Table 5.2: Peak Area Ratio Values for Features of Significance from Lipidomic Data
Mean peak area ratios of features demonstrated to significantly change between disease classes in the comprehensive lipidomic analysis. Peak areas for each m/z were extracted from the raw data using Waters QuanLynx, and were then normalised using an internal standard (Triacylglyceride C15:0/15:0/C15:0) resulting in a peak area ratio.
Significance was calculated by performing a "student's" t-test on the mean peak area ratio values. [a] p=<0.05, [b] p=<0.005, [c] p=<0.001.
In column "m/z" the m/z of the PC molecule is also shown, alongside that of the m/z detected by the LC-MS (in brackets). In the remaining columns the standard deviation (SD) is provided.

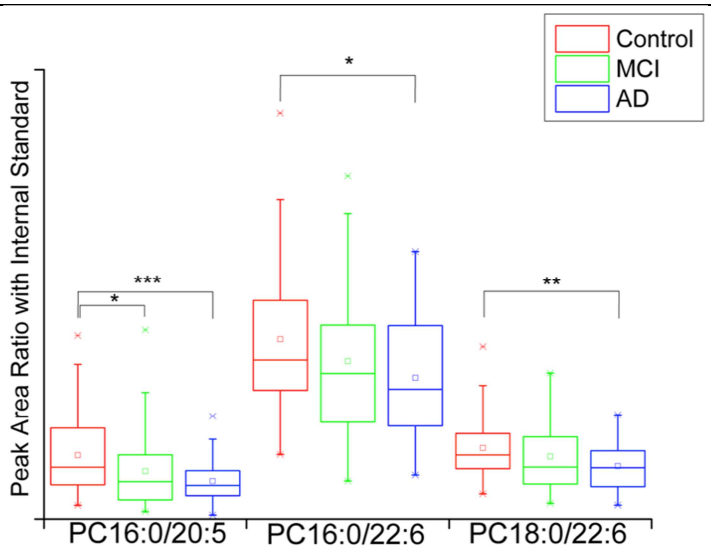

Figure 5.2: Box Plot Analysis of Features of Significance from Lipidomic Data

Box plot analysis for the three significant molecules highlighted in the comprehensive lipidomic analysis. Disease group data was tested for statistical significance by analysing the mean values using "Students" t-test. Interestingly, the overall trend was a reduction from Control → MCI → AD

* $p<0.05$, ** $p<0.01$, *** $p<0.001$.

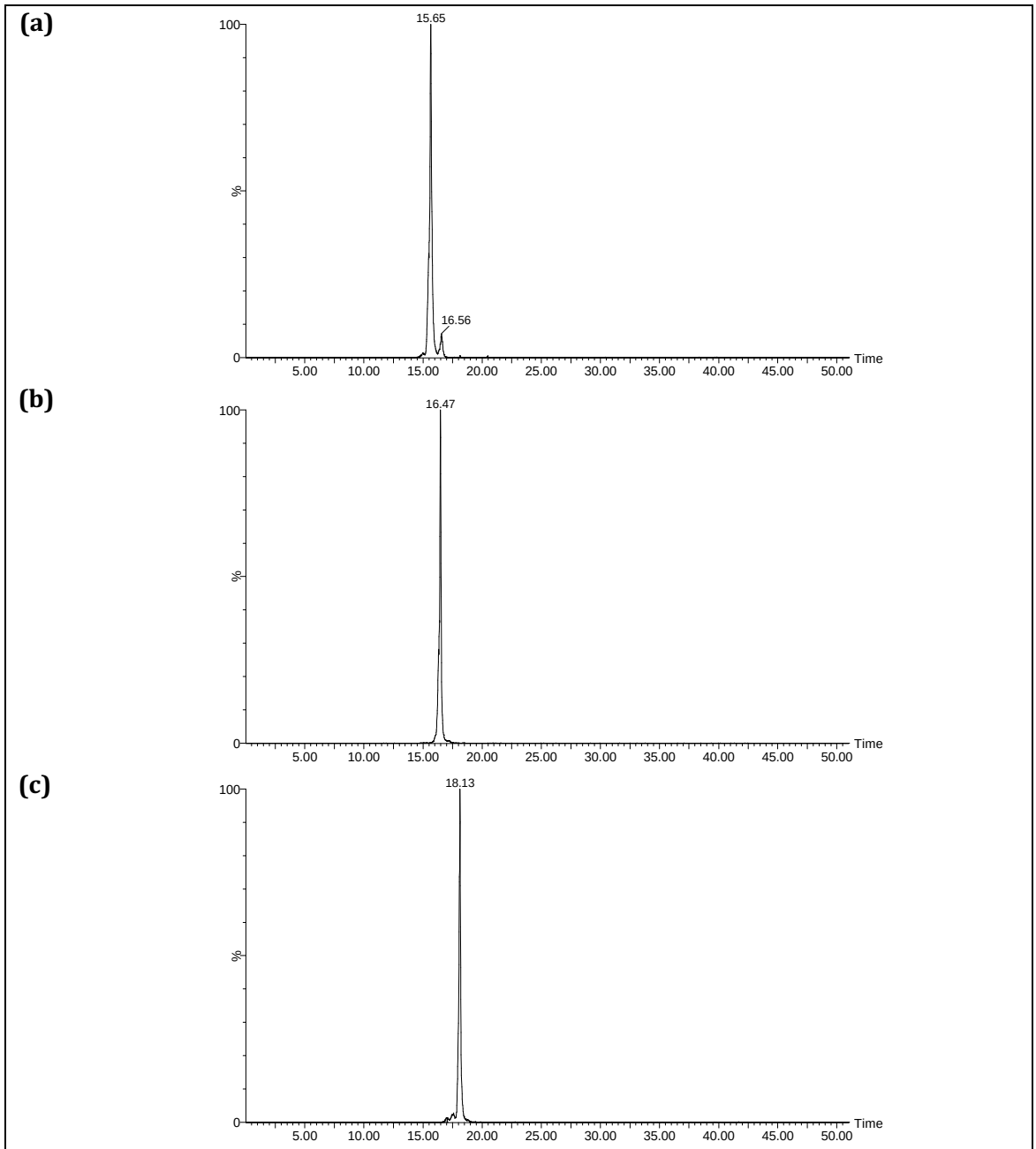

Figure 5.3: Example Extracted Ion Chromatograms

(a) Feature with m/z 780.5578 at 15.65 minutes

(b) Feature with m/z 806.5746 at 16.47 minutes

(c) Feature with m/z 834.6026 at 18.13 minutes

5.3.3 – Structural Identification of Features

Once the three features had been shown to demonstrate significant reductions in AD, structural identification and elucidation was required.

As described in section 5.2.6 above, level two data was analysed from the MS^e technology on the Waters Xevo instrument. Fragments were analysed enabling the structures to be identified.

Initial observations demonstrated a fragment ion in each m/z at 184.0773Da, which is indicative of the choline head unit common in both phosphatidylcholine PC and SPH species. However when observing the results from the vast databases in both HMDB and METLIN, no sphingomyelin species were associated with the relevant m/z, providing a strong indication that the species of interest are PC molecules.

PC molecules consist of a choline head unit bound to two FA side chains. These side chains were elucidated by observing fragments lost, for example a loss of 302.2246 indicates a structure consisting of $C_{20}H_{30}O_2$ suggesting a chain loss of C20 with 5 unsaturated double bonds, otherwise known as eicosapentaenoic acid. This approach using fragmentation patterns has been used previously for phosphatidylcholine elucidation [236], and also in particular with Waters MS^e technology [230].

Final identification resulted in three phosphatidylcholine species PC16:0/20:5, PC16:0/22:6 and PC18:0/22:6. Figure 5.4, Figure 5.5 and Figure 5.6 present the structural elucidation of each molecule, and Table 5.3 displays each fragment, its exact m/z and the m/z observed in the MS data.

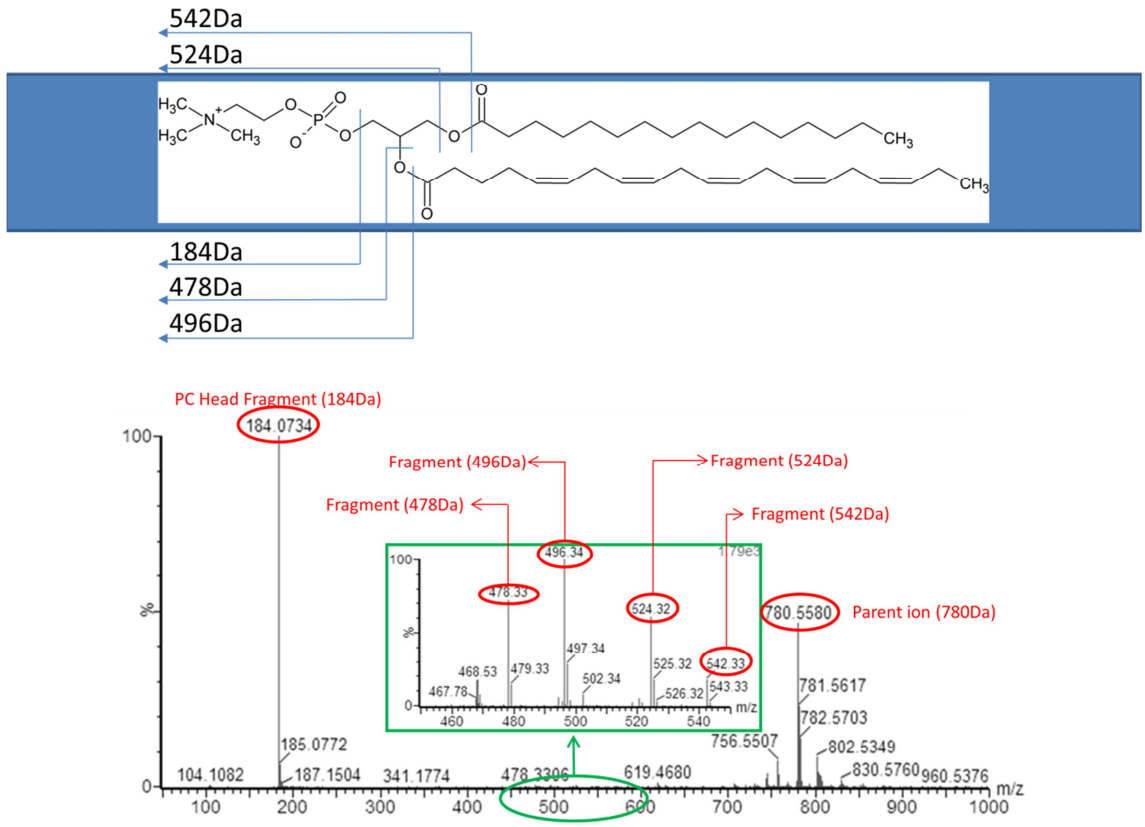

Figure 5.4: MS^e Fragmentation Pattern for Parent Ion m/z 780.5538Da

MS^e spectrum for feature m/z 780.5538Da. The identification of phosphatidylcholine (PC) molecular class was confirmed by the presence a fragment m/z at 184.0773Da, indicative of PC species. As the MS was completed in positive mode and therefore requires the PC head group for ionisation, the identification focused on side chains lost. For example, m/z 478.3292Da is the combination of the PC head unit and side chain C16:0. The m/z that is lost compared to the parent ion is 302.2264Da, indicating a loss of side chain 20:5. Two fragments that differ by 18Da indicated a fragmentation that has occurred on either side of an oxygen bond, further assisting with the structural confirmation.

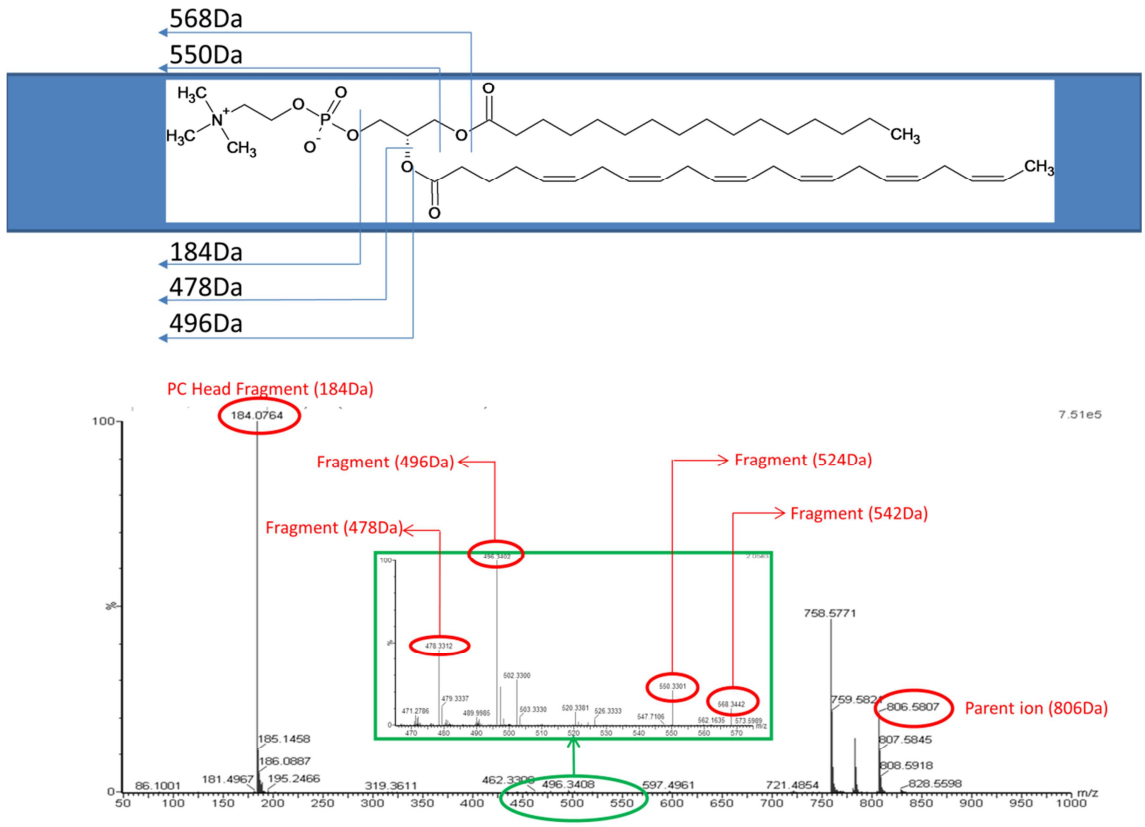

Figure 5.5: MS^e Fragmentation Pattern for Parent Ion m/z 806.5694Da

MS^e spectrum for feature m/z 806.5694Da. The identification of phosphatidylcholine (PC) molecular class was confirmed by the presence a fragment m/z at 184.0773Da, indicative of PC species. As the MS was completed in positive mode and therefore requires the PC head group for ionisation, the identification focused on side chains lost. For example, m/z 478.3292Da is the combination of the PC head unit and side chain C16:0. The m/z that is lost compared to the parent ion is 302.2264Da, indicating a loss of side chain 20:5. Two fragments that differ by 18Da indicated a fragmentation that has occurred on either side of an oxygen bond, further assisting with the structural confirmation.

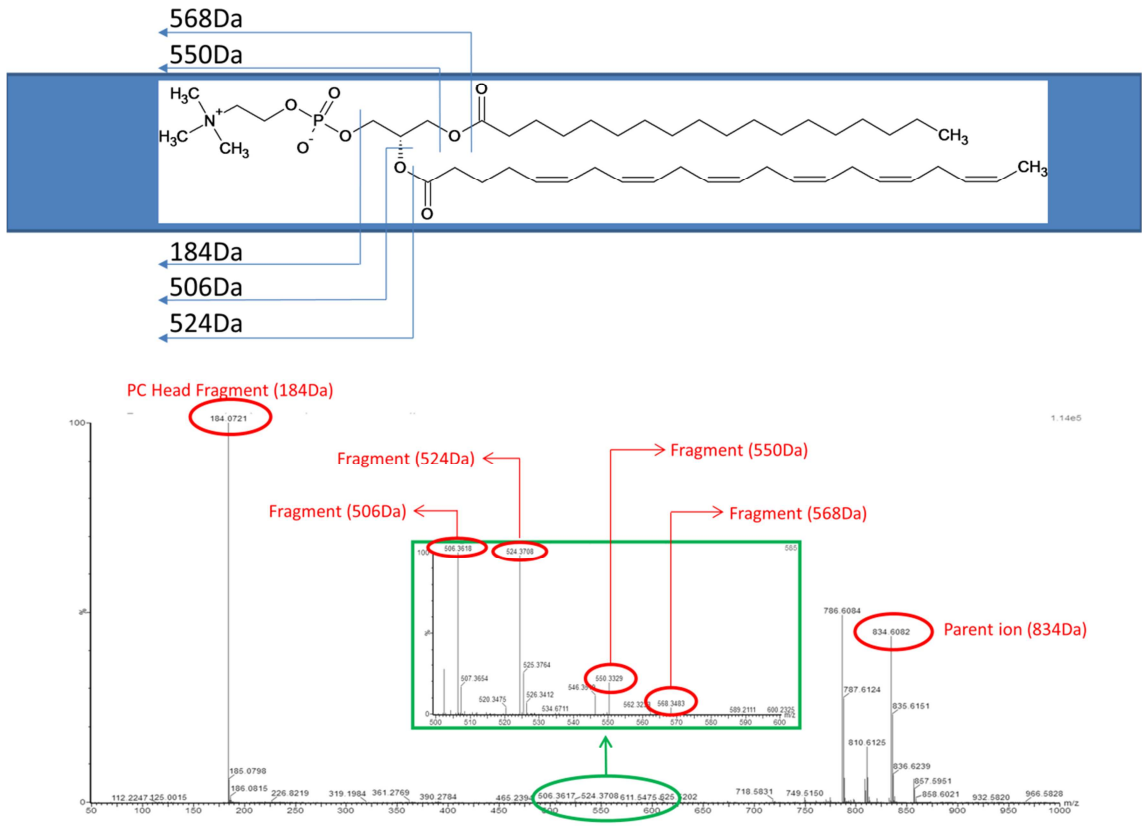

Figure 5.6: MS^e Fragmentation Pattern for Parent Ion m/z 834.6007Da

MS^e spectrum for feature m/z 780.5538Da. The identification of phosphatidylcholine (PC) molecular class was confirmed by the presence a fragment m/z at 184.0773Da, indicative of PC species. As the MS was completed in positive mode and therefore requires the PC head group for ionisation, the identification focused on side chains lost. For example, m/z 506.3605Da is the combination of the PC head unit and side chain C18:0. The m/z that is lost compared to the parent ion is 328.2402Da, indicating a loss of side chain 22:6. As before, two fragments that differ by 18Da indicated a fragmentation that has occurred on either side of an oxygen bond, further assisting with the structural confirmation.

5.3.4 – Support of Findings – Screen Identification

To further provide evidence and support for the findings that three PC species significantly decrease in AD, the matching three features in the screen study also underwent structural fragmentation elucidation.

The three features were also found to be PC16:0/20:5, PC16:0/22:6 and PC18:0/22:6. The results of the fragmentation can be observed in Table 5.3.

This provides confidence in the findings, as now the three molecules have been shown to significantly reduce in AD in two separate methods, using two different sample sets of different numbers and also completed at different time points during the PhD project.

		780.5538	806.5694	834.6007
Molecule		PC(16:0/20:5)	PC(16:0/22:6)	PC(18:0/22:6)
Structure		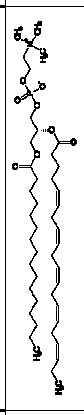	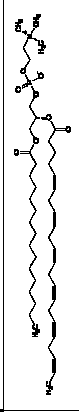	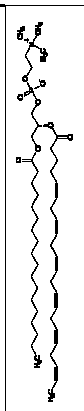
Molecular Formula		$C_{44}H_{78}NO_8P$	$C_{46}H_{80}NO_8P$	$C_{48}H_{84}NO_8P$
Monoisotopic Mass of Parent Molecule (+H)		780.5538	806.5694	834.6007
Retention Time of Feature	Pilot	9.62	9.9	10.35
	Confirmation	15.65	16.4	18.05
Extracted Mass of Parent Peak	Pilot	780.5599	806.5764	834.6086
	Confirmation	780.5491	806.562	834.5969
Mass Difference (Da)	Pilot	0.0061	0.007	0.0079
	Confirmation	-0.0047	-0.0074	-0.0038
Mass Difference (ppm)	Pilot	7.8	8.7	9.5
	Confirmation	-6.0	-9.2	-4.6

Table continued on the next page

Table 5.3: Fragmentation Data for Phosphatidylcholine Molecules

The above table presents MS^e data of the three PC molecules which demonstrated a significant decrease in AD compared with controls. The table presents both parent and fragment data for all masses that were used to confirm the structure of the molecule. Identification was completed in both the larger lipidomic study discussed in Chapter 5, as well as plasma samples from Chapter 3. The three PC species exhibited a significant reduction in two separate studies, providing support to the overall result. Table continues on next page.

		780.5538	806.5694	834.6007
Monoisotopic Mass of Fragment 1 (+H)		184.0773	184.0773	184.0773
Formula of Fragment 1		$C_5H_{14}NO_4P$	$C_5H_{14}NO_4P$	$C_5H_{14}NO_4P$
Structure of Fragment 1		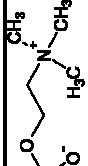	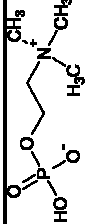	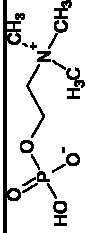
Extracted Mass of Fragment 1	Pilot	184.0721	184.0707	184.0724
	Confirmation	184.0706	184.0736	184.0617
Mass Difference (Da)	Pilot	-0.0052	-0.0066	-0.0049
	Confirmation	-0.0067	-0.0037	-0.0156
Mass Difference (ppm)	Pilot	-28.2	-35.9	-26.6
	Confirmation	-36.4	-20.1	-84.7
Monoisotopic Mass of Fragment 2		478.3292	478.3292	506.3605
Formula of Fragment 2		$C_{24}H_{48}NO_8P$	$C_{24}H_{48}NO_8P$	$C_{26}H_{52}NO_8P$
Structure of Fragment 2		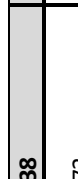	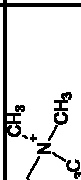	
Extracted Mass	Pilot	478.331	478.3308	506.362
	Confirmation	478.3296	478.33	506.3582
Mass Difference (Da)	Pilot	0.0018	0.0016	0.0015
	Confirmation	0.0004	0.0008	-0.0023
Mass Difference (ppm)	Pilot	3.8	3.3	3.0
	Confirmation	0.8	1.7	-4.5

Table continued on the next page

Table 5.3: Fragmentation Data for Phosphatidylcholine Molecules (Continued from Previous Page)

The above table presents MS^e data of the three PC molecules which demonstrated a significant decrease in AD compared with controls. The table presents both parent and fragment data for all masses that were used to confirm the structure of the molecule. Identification was completed in both the larger lipidomic study discussed in Chapter 5, as well as plasma samples from Chapter 3. The three PC species exhibited a significant reduction in two separate studies, providing support to the overall result. Table continues on next page.

		780.5538	806.5694	834.6007
Monoisotopic Mass of Fragment 3		496.3398	496.3398	524.3711
Formula of Fragment 3		$C_{24}H_{50}NO_7P$	$C_{24}H_{50}NO_7P$	$C_{26}H_{54}NO_7P$
Structure for Fragment 3			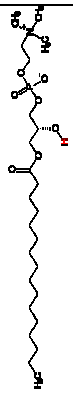	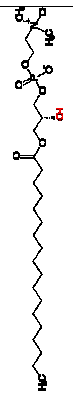
Extracted Mass of Fragment 3	Pilot	496.3402	496.3391	524.3716
	Confirmation	496.3404	496.3416	524.3691
Mass Difference (Da)	Pilot	0.0004	-0.0007	0.0005
	Confirmation	0.0006	0.0018	-0.0020
Mass Difference (ppm)	Pilot	0.8	-1.4	1.0
	Confirmation	1.2	3.6	-3.8
Monoisotopic Mass of Fragment 4		524.3136	550.3292	550.3292
Formula of Fragment 4		$C_{28}H_{46}NO_6P$	$C_{30}H_{48}NO_6P$	$C_{30}H_{48}NO_6P$
Structure for Fragment 4			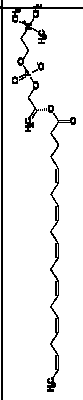	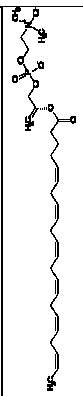
Extracted Mass of Fragment 4	Pilot	524.3157	550.3302	550.3334
	Confirmation	524.3143	550.3283	550.3301
Mass Difference (Da)	Pilot	0.0021	0.0010	0.0042
	Confirmation	0.0007	-0.0009	0.0009
Mass Difference (ppm)	Pilot	4.0	1.8	7.6
	Confirmation	1.3	-1.6	1.6

Table continued on the next page

Table 5.3: Fragmentation Data for Phosphatidylcholine Molecules (Continued from Previous Page)

The above table presents MS^e data of the three PC molecules which demonstrated a significant decrease in AD compared with controls. The table presents both parent and fragment data for all masses that were used to confirm the structure of the molecule. Identification was completed in both the larger lipidomic study discussed in Chapter 5, as well as plasma samples from Chapter 3. The three PC species exhibited a significant reduction in two separate studies, providing support to the overall result. Table continues on next page.

			780.5538	806.5694	834.6007
Monoisotopic Mass of Fragment 5			542.3241	568.3398	568.3398
Formula of Fragment 5			$C_{28}H_{46}NO_6P$	$C_{30}H_{50}NO_6P$	$C_{30}H_{50}NO_6P$
Structure for Fragment 5			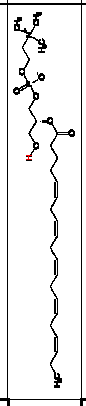	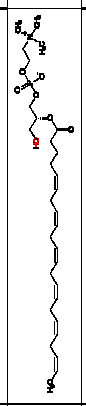	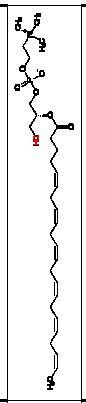
Extracted Mass of Fragment 5	Pilot		542.3258	568.3428	568.3442
	Confirmation		542.3301	568.34	568.3315
Mass Difference (Da)	Pilot		0.0017	0.0030	0.0044
	Confirmation		0.0060	0.0002	-0.0083
Mass Difference (ppm)	Pilot		3.1	5.3	7.7
	Confirmation		11.1	0.4	-14.6

Table 5.3: Fragmentation Data for Phosphatidylcholine Molecules (Continued from Previous Page)

The above table presents MS^e data of the three PC molecules which demonstrated a significant decrease in AD compared with controls. The table presents both parent and fragment data for all masses that were used to confirm the structure of the molecule. Identification was completed in both the larger lipidomic study discussed in Chapter 5, as well as plasma samples from Chapter 3. The three PC species exhibited a significant reduction in two separate studies, providing support to the overall result. Table continues on next page.

5.3.5 – Further Investigation into Phosphatidylcholine Molecules

Due to the findings reported above, further PC molecules that were both present in the MS raw data and also shared similar side chain arrangements also underwent extraction from the raw data. Again peak area ratios were calculated, and the means underwent "student's" t-test analysis for significance, however these molecules did not show significance (Table 5.4).

Mass of PC [Da] (Detected m/z (M+H))	PC Molecule	Mean PAR Control	Mean PAR MCI	Mean PAR AD
781.5621 (782.5699)	PC(16:0/20:4)	0.8589 (0.3529)	0.7995 (0.3504)	0.7806 (0.0556)
831.5778 (832.5856)	PC(18:1/22:6)	0.0346 (0.0153)	0.0323 (0.0154)	0.0292 (0.0145)
809.5935 (810.6013)	PC(18:0/20:4)	0.5784 (0.2484)	0.5459 (0.2755)	0.5145 (0.2468)

Table 5.4: Further Phosphatidylcholine Molecule Analysis

The above table presents peak area ratio figures for three further phosphatidylcholine (PC) species. Their selection was based upon availability from the in the raw mass spectrometry data and also sharing similar side chains to the three significant features discussed previously. PC species were confirmed by accurate m/z matching to databases as well as side chain elucidation using fragmentation patterns. No significant variations were observed between the disease classes.

5.3.6 – Receiver Operating Characteristic Analysis

To test the sensitivity and specificity of the three phosphatidylcholine species as a biomarker predictor for the disease, a ROC was completed. Peak area ratio data for each of the three PC species was analysed both individually (Figure 5.7) as well as when combined with patient ApoE gene data (Figure 5.8), a well established risk factor for predicting the disease [244].

For the n=141 sample set, ApoE data on its own gave an initial reference AUC of 0.667. Individually, both PC16:0/20:5 and 16:0/22:6 provide increased AUC

scores of 0.722 and 0.680 respectively. PC16:0/22:6 returned an AUC of 0.662, slightly below that of the ApoE benchmark for the sample set.

The combination of each of the individual PC peak area ratios along with patient ApoE data improves the AUC score for the analysis. PC16:0/20:5 + ApoE returns an AUC of 0.782 + ApoE, PC16:0/22:6 returned 0.746 and finally PC18:0/22:6 + ApoE returned an AUC of 0.756. Combined peak area ratios for all three PC molecules, used in combination with ApoE patient data for the analysis returned the most promising result, with an AUC of 0.8279 (Figure 5.7 and Figure 5.8).

ROC analyses were also completed in order to observe the predictive properties of Control vs. MCI and MCI vs. AD. These were less promising, yet still provided an increase compared with using ApoE patient data alone. For example combining the PAR data along with ApoE data as opposed to ApoE data alone, increased the AUC from 0.570 to 0.672 (Control vs. MCI) and from 0.593 to 0.651 (MCI vs. AD) respectively. A full AUC summary of the ROC analyses can be found in Table 5.5.

	Control vs. AD	Control vs. MCI	MCI vs. AD
ApoE Only Data	0.667	0.570	0.593
PC16:0/20:5	0.722	0.625	0.576
PC16:0/22:6	0.622	0.569	0.588
PC18:0/22:6	0.680	0.592	0.594
All Three PC	0.786	0.640	0.588
PC16:0/20:5 + ApoE	0.776	0.665	0.638
PC16:0/22:6 + ApoE	0.739	0.624	0.629
PC18:0/22:6 + ApoE	0.754	0.637	0.631
All Three PC + ApoE	0.827	0.672	0.651

Table 5.5: Area Under the Curve from Receiver Operated Characteristic

The above table presents the area under the curve (AUC) values which were observed following a receiver operated characteristic (ROC) analysis. ROC analyses were completed comparing all disease groups (including Control vs. AD, Control vs. MCI). This enables the observation of the predictive properties of each phosphatidylcholine (PC) molecule and for each disease state. The most promising approach involved combining data from all three PC peak area ratios with ApoE gene data. The end result of which was an AUC of 0.827 when comparing Control and AD patients.

Example ROC analyses can be observed in Figure 5.7 and Figure 5.8.

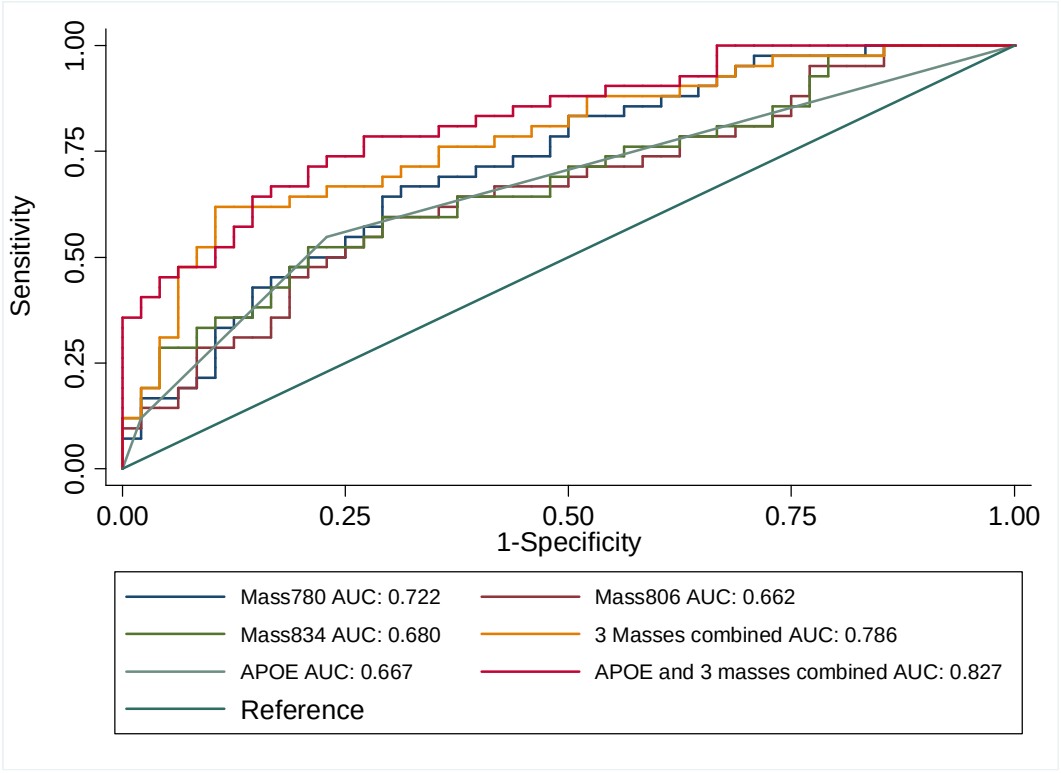

Figure 5.7: Receiver Operating Characteristic Analysis

Peak area ratios (PAR) for each phosphatidylcholine molecule (PC) were used to produces this receiver operated characteristic (ROC) analysis.

ApoE data was initially used on its own as a start comparison point and provided an area under the curve (AUC) of 0.667.

Each PC PAR was then used individually in order to observe its predictive properties. Both PC 16:0/20:5 (m/z 780) and PC 18:0/22:6 (m/z 834) returned AUC scores of greater than ApoE on its own (0.722 and 0.680 respectively). PC 16:0/22:6 (m/z 806) returned an AUC of 0.662, slightly below that of ApoE.

When combining the PAR data of all three PC species, the AUC was 0.786.

A combination of all three PC molecules and ApoE data returned the most promising result with an AUC of 0.826, making it comparable to many lead markers in AD biomarker research.

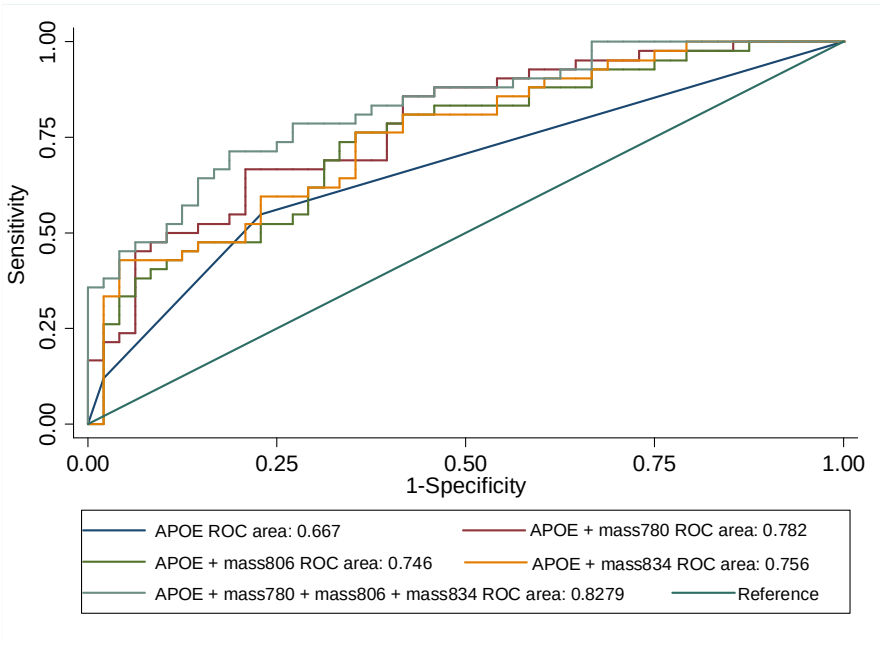

Figure 5.8: Receiver Operating Characteristic Analysis with ApoE Data

Peak area ratios for each phosphatidylcholine molecule (PC) were combined with patient ApoE gene data to produce this receiver operated characteristic (ROC) analysis.

ApoE data was initially used on its own as a start comparison point and provided an area under the curve (AUC) of 0.667. Each PC molecule combined with ApoE improved this AUC with PC16:0/20:5 (m/z 780) returning 0.782, PC16:0/22:6 (m/z 806) returning 0.746 and PC18:0/22:6 (m/z 834) returning and AUC of 0.756.

A combination of all three PC molecules and ApoE data returned the most promising result with an AUC of 0.8279, making it comparable to many lead markers in AD biomarker research.

5.4 – Discussion

Lipidomic analysis was completed on an n=141 sample set, to provide clarification and confidence on those results reported in the screen phase of the Ph.D. project discussed in Chapter 3. From the screen, three features were of most interest as they were identified at significantly reduced values in the disease samples after univariate data treatment; 780.5578 (p=<0.001), 806.5746 (p=<0.01) and 834.6026 (p=<0.01).

Following the promising results from the LC-MS screen, an extended LC-MS method underwent development with the aim of reducing co-elution and expanding the number of features analysed. This is discussed in great detail in Chapter 4. The extended LC-MS method was then applied to an increased sample set (n=141). Due to cost constraints the focus was upon lipid species that ionise in the positive mode. This decision was based upon a number of factors.

- Better multivariate model results in the LC-MS Screen from Chapter 3.
- The three significant features from the LC-MS Screen were all identified in univariate analysis of the positive screen.
- Greater sensitivity and overall number of features available in positive ionisation phase, as reported in Chapter 4.

5.4.1 – Quality Control and Batch Analysis

Due to concerns about instrument mass accuracy over a long term analytical run, samples were divided into four batches to enable regular instrument calibrations. Therefore it was of importance to ensure QC repeatability across the four batches. Normalisation using internal standard intensities was completed in the alignment process using MarkerLynx.

Figure 5.1.A presents the breakdown of PCA that were created using the data. As can be seen, QC samples clustered in the middle of the model. Figure 5.1.B presents the n=5 QC samples from each batch as a different colour. A minor batch effect can be observed, however as there were no QC outliers from any batch, the data were progressed to further multivariate analysis. Minor inter-batch variation is common in LC-MS metabolomics, however pooled QC analysis, and the inclusion of an internal standard, is a commonly used and accepted approach in overcoming these problems [299].

5.4.2 – Significant Lipids and their Identification

Findings in the extended LC-MS method reported here, confirmed that the three features of interest from the LC-MS screen in Chapter 3, are also reflected in a larger sample set and using an improved method. To ensure the m/z related to the same molecules, and not just features that share the same molecular m/z, they too underwent identification using fragmentation patterns analysis. The process was described in great detail above in the results section, and follows that of similar publications [230, 236]. Three PC species (PC16:0/20:5, PC16:0/22:6 and PC18:0/22:6) were therefore identified and observed to significantly decrease in AD compared with controls.

Confidence in the reporting of the three PC species is therefore increased. This confidence is obtained from the fact that they were identified at significantly reduced levels in AD in:

- Two completely different LC-MS methods and approaches – the LC-MS screen discussed in Chapter 3 and the extended LC-MS analysis discussed here in Chapter 5. In order to prevent confusion in this discussion piece, the findings in

Chapter 3 will be referred to as screen. The new results presented here in Chapter 5 are referred to as validation LC-MS.

- Two sets of different samples were employed for both the screen and the validation LC-MS, with no overlap of samples.

PC16:0/20:5, PC16:0/22:6 and PC18:0/22:6 were all found to be diminished in AD samples from two LC-MS analytical sample sets, with respective p values of <0.001, 0.011 and 0.004 in the extended LC-MS results discussed here. In the results also the overall trend - i.e. control>MCI>AD - suggested a general decline linked to cognition.

5.4.3 – Phosphatidylcholine species decrease in AD plasma

As previously discussed in Chapter 3, PCs are a class of diacylglycerophospholipids that are an essential component of cell membranes, and make up ~ 95% of the total choline compound pool in most tissues [238, 239]. Figure 5.9 demonstrates their structure, with a choline head group and FA side chains. The length of these side chains can influence PC function and help define their structural roles, since chain length differences can affect cell membrane fluidity, as per reference [240].

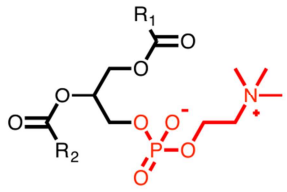

PHOSPHATIDYLCHOLINE (PC)

PC	R_1	Source fatty acids	R_2	Source fatty acids
16:0/20:5	$-(CH_2)_{14}CH_3$	$CH_3(CH_2)_{14}COOH$ (palmitic)	$-(CH_2)_8(CH=CH)_5CH_3$	$CH_3(CH_2)_8(CH=CH)_5COOH$ (eicosapentanenoic)[a]
16:0/22:6	$-(CH_2)_{14}CH_3$	$CH_3(CH_2)_{14}COOH$ (palmitic)	$-(CH_2)_8(CH=CH)_6CH_3$	$CH_3(CH_2)_8(CH=CH)_6COOH$ (docosahexenoic)[b]
18:0/22:6	$-(CH_2)_{16}CH_3$	$CH_3(CH_2)_{16}COOH$ (stearic)	$-(CH_2)_8(CH=CH)_6CH_3$	$CH_3(CH_2)_8(CH=CH)_6COOH$ (docosahexaenoic)[b]

[a]IUPAC nomenclature: (5Z,8Z,11Z,14Z,17Z)-5,8,11,14,17-icosapentaenoic acid
[b](4Z, 7Z, 10Z, 13Z, 16Z, 19Z)-docosa-4,7,10,13,16,19-hexaenoic acid

Figure 5.9: Phosphatidylcholine Structure

The above figure highlights the general phosphatidylcholine (PC) structure, with the key components highlighted. In red is the choline head unit common in all PC structures. This is then connected to two fatty acid (FA) side chains. The attached table highlights the side chains of specific interest, which were shown to significantly decrease in AD disease compared with control patients.

Image provided by a collaborator Dr Arundhuti Sen with permission to reproduce

Along with their structural roles, they are also found as components of lipoproteins, in particular of HDL. PCs interact with ApoE as part of the HDL group, and are implicated in cholesterol transport [241]. This is of interest as ApoE is linked with AD [242, 243], and the ε4 allele of the ApoE gene is a well-established predictor (indeed, considered one of the most significant risk indicators) of AD [244].

A previous publication also expands further knowledge on the genetic background to PC species. A genome-wide association study (GWAS) incorporated the results

from a metabolomic analysis of human serum. The study reported a number of loci associated with the concentration ratios of a number of PCs, for example PLEKHH1, a gene of presently unknown function, and PC36:5 were found to be linked [300]. This finding provides evidence that PC metabolism is genetically linked, and therefore it is possible that irregular PC metabolism may be linked to genetic causes of AD.

Figure 5.10 presents the major metabolic transformations which regulate PC and choline homeostasis. Within the figure there is particular emphasis on those that are thought to be relevant to various neurodegenerative pathologies.

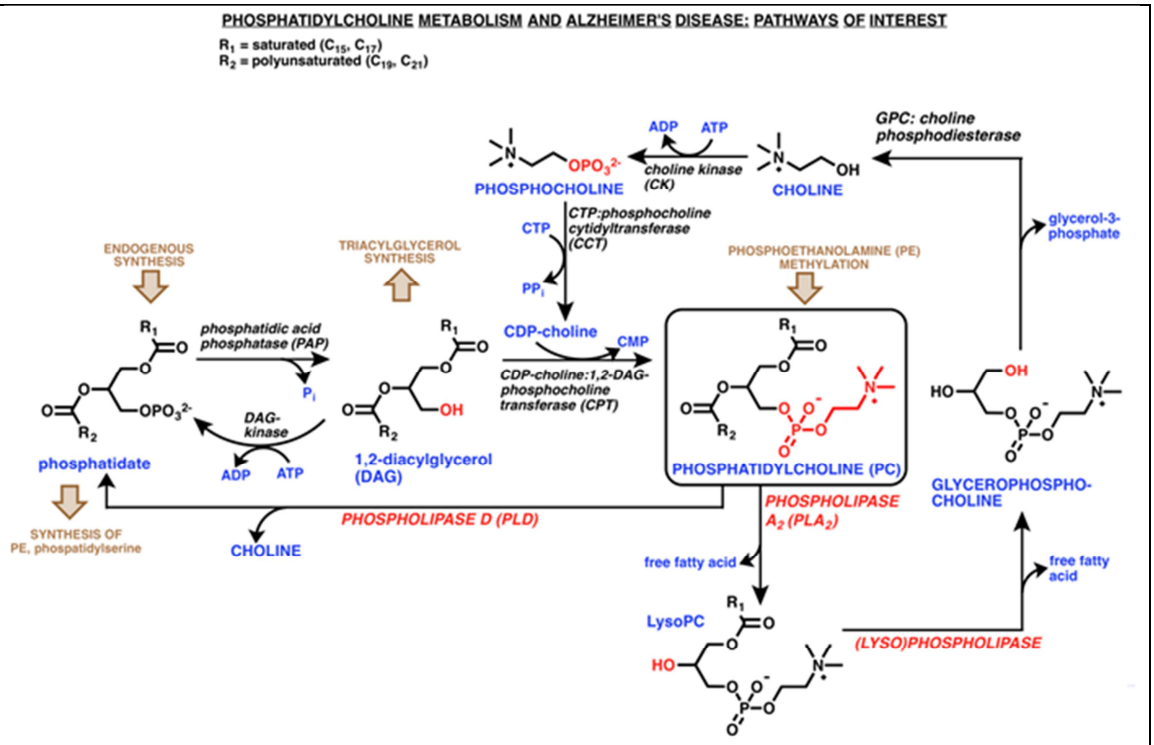

Figure 5.10: Phosphatidylcholine metabolism and Alzheimer's disease

This overview illustrates the major routes to phosphatidylcholine (PC) biosynthesis, with an emphasis on steps involving choline-containing compounds and those that have been previously associated with the pathology of Alzheimer's disease. Phosphatidate (phosphatidic acid (PA)) is synthesised endogenously from glycerol-3-phosphate in most tissues, and is a key signalling molecule and a precursor for other 1,2-diacylglycerophospholipids. PA is converted to 1,2-diacylglycerol (DAG) and then enters the CDP-choline Kennedy pathway to form PC (PC can also be formed in the liver from phosphatidylethanolamine (PE) in a multi-step pathway catalysed by PE-methyl transferase). PC is subject to the action of a variety of phospholipases, two main families of which are the phospholipase D (PLD) and phospholipase A_2 (PLA_2): PLD enzymes hydrolyse PC to yield free choline (Ch) and PA, while PLA_2 enzymes cleave acyl groups from the sn-2 position of PC to yield LysoPC.

Image created by Dr Arundhuti Sen with permission to reproduce.

The most significant pathways involving PC metabolism is the Kennedy pathway, which consists of the enzymes (CK, CCT, CPT in Figure 5.10) and phosphatidic acid phosphatase (PAP). The pathway is involved in the biosynthesis of PC molecules from choline and phosphatic acid (PA), and are associated primarily with cell growth, proliferation and signal transduction cascades [301].

It is this enzyme pathway that catalyses and regulates the general breakdown of PC, to phosphatidate, via use of the phospholipase D (PLD) and to glycerophosphocholine and free fatty acids using the phospholipase A_2 enzymes (PLA_2). PLA_2 enzymes are of particular interest as they have previously been directly associated with AD [301-303].

The PLA_2 family of enzymes is further linked to AD as it has been observed that they undergo increased activation within neurons by Aβ, in turn releasing secondary lipid messengers such as AA [202].

The release of AA has downstream effects that include the stimulation of the sphingomyelinase-ceramide pathway responsible for the metabolism of sphingomyelin (of which PC is a precursor) to phosphocholine and ceramide. This pathway has been previously investigated with regard to AD, with results reporting increases in sphingomyelinase and acid ceramidase activity in the AD brain [255, 256].

Several previous publications [304-308] have reported that PLA_2 activity and expression in the AD brain and CNS. Activity and expression appears to be correlated with the progression of AD, with results reporting reduced activity in the early stages and the up-regulation in the later stages of the disease. These

findings, therefore suggest further support to the importance of lipid and glycerophospholipid pathways in AD pathology [297].

The findings from the extended study here in Chapter 5 reported three PC molecules, PC16:0/20:5, PC16:0/22:6 and PC18:0/22:6, which are diminished in AD plasma. This finding complements numerous previous data on AD-associated differences in phosphoglycerolipid metabolism, some of which have been reviewed elsewhere [141]. In previously published studies sphingomyelins, ceramides and diacylglycerols have been found to be elevated in brain tissue and, more recently, in plasma, serum and CSF of AD patients [160, 193, 309-311]. Since PC is a precursor for sphingomyelin (via the sphingomyelin synthases), our results are in agreement with the observed increase in these molecules. Furthermore, Gaudin et al found that two PCs (32:0 and 34:1) were decreased in senile plaques extracted from the post-mortem AD brain. In the publications the PC species were reported with values representing combined side chains, and were not fully elucidated, for example PC32:0 could relate to PC16:0/16:0 or 18:0/14:0. The group concluded that PC regulation was affected in AD and that it could be linked to the roles of PLA_2 and PLD1 in Aß activation [245].

Interestingly, the results of Chapter 5 identify side chain 22:6 in two PCs, PC16:0/22:6 and PC18:0/22:6, and is therefore linked to the FA DHA. To the best of our knowledge, these two PC species have not been reported previously as being different in AD patient plasma when compared with control samples. DHA with regard to AD was discussed in great detail in Chapter 2.

To investigate the possibility that changes in PLA_2 activity may be causing the observed decrease in PCs, the findings reported here were linked to those reported in Chapter 2. Results reported in the earlier Chapter suggested that the

concentration of DHA_{TOTAL} and EPA_{TOTAL} in circulating plasma provided significance values of p=0.107 and 0.023 respectively (control→AD). This suggests that plasma DHA_{TOTAL} is consistent between groups, and that therefore a possible imbalance exists in the distribution and metabolism of DHA to phospholipid species. In contrast, plasma EPA_{TOTAL} shows a moderate decrease from Control → AD. This concentration of EPA_{TOTAL} could therefore be linked to the depletion of PC 20:5, but interpreting these results in a more quantitative fashion is beyond the scope of this study and would require further work.

While our results are in keeping with the general trend observed in previous studies (i.e. disruptions in glycerophospholipid pathways appear to be correlated with the prevalence of AD), Figure 5.10 all too clearly illustrates the complexity of choline and phospholipid biochemistry. Thus it is difficult to hypothesise about the exact metabolic reasons for the reductions of the three PCs in AD plasma, without more precise knowledge about the links of particular side chains to enzymatic steps and their involvement in the overall pathway.

5.4.4 – Phosphatidylcholine C16:0/20:5

Of the three molecules identified as potential candidates, PC16:0/20:5 was of the greatest significance from the resulting data. The PC16:0/20:5 has previously been discussed with regards to AD, again the result was generated by a non-targeted metabolite analysis. However, the PC was not deemed to significantly alter on its own merits, but was reported in a cluster-style analysis. The study employed a combination of molecules which it termed “clusters”. These consisted of three or four individual markers, the resulting variations of which were combined, resulting in a model of prediction for the conversion of MCI to AD [196]. In the example of the cluster which included PC16:0/20:5 as one of its features, no

significant prediction properties (p=0.27) for the three-molecule cluster as a group were apparent.

Conversely, in the results reported here within the thesis, PC16:0/20:5 showed a highly significant decrease between controls and AD, with p=0.001 and <0.001 for the screen results reported in Chapter 3 and the extended validation LC-MS phase reported in Chapter 5.

When comparing MCI and AD, a significant decrease was also observed in the screen results in Chapter 3 (p=0.038), however in the analysis described here in Chapter 5 a non-significant decrease was observed (p=0.102). This data suggests a potential role for PC16:0/20:5 as a predictor for AD when compared with controls, however not as a converter marker from MCI and is therefore in agreement with the cluster analysis discussed previously [196].

The cluster-style analysis did however find three major molecules which showed promise as predictors of progression from MCI to AD. Interestingly these included a PC (PC16:0/16:0), alongside 2,4-dihydroxybutanoic acid and an unidentified molecule [196]. Of particular relevance and interest was the fact that the identified PC contained two 16:0 side chains, therefore suggesting a potential link with two of the three molecules identified throughout the thesis, which also contained 16:0 side chains (16:0/20:5 and 16:0/22:6).

This result takes on further relevance when considered in conjunction with the consideration that LysoPC16:0 is a precursor of platelet activating factor (PAF). LysoPC16:0 is a metabolite of PC species with a 16:0 side chain and is generated by the previously discussed PLA_2. PAF has a role in mammalian physiology as a mediator in inflammation-related processes. Perhaps more interestingly, the

C16:0 PAF has been shown to be toxic to neurons [312] and therefore it is plausible that neurone death in AD could, in some part be a result of abnormal PC metabolism in the disease.

Further to this, a metabolomics study by Han et al. reported SPH and CER with chains C22:0, C23:0 and C16:0 to significantly vary between AD and controls, with high correlation with AD progression [193]. Of particular relevance is the reported ratio of CER/SPH molecules, which contains the C16:0 side chain, as this provided the highest correlation with AD, providing further evidence to the importance of this particular chain length.

As discussed earlier, abnormalities in the phospholipase pathways have been implicated in the pathology of AD. As illustrated in Figure 5.10, such altered PL activity for selected PCs could very well lead to an over-metabolism of these molecules, and therefore a subsequent diminishment in plasma levels.

Further to this, the link between membrane breakdown, amyloid deposits and neuronal dysfunction has been supported by publications from Dyrke et al.[313] and Pettigrew et al. [314]. These previously published results all support the abnormal PC levels found in AD disease patients in this study, and suggest a relationship with the amyloid deposits associated with the brain pathology of the disease. This would suggest that PCs may have a crucial role in AD biomarker discovery.

5.4.5 – Choline Metabolism and Links to Phosphatidylcholines

In the previous sections above the focus of the discussion was structured around the metabolism of side chains, however the metabolism of the choline component of PCs may also be a cause of the results observed presented throughout the thesis.

Kantarci et al have published findings which correlated the amounts of choline-containing compounds to AD pathology in specific regions of the brain. Using MRS, they measured an increase in choline to creatine ratios in AD patients [315]. They argued that an increase in the membrane turnover of choline during neuronal degeneration led to increased free choline in the brain.

Further discussions have hypothesised an alternative model, which would suggest that Aβ binding to membrane lipids is directly responsible for the disruption of membrane structures [316], and it is this which leads to an increase in free choline throughout the human brain.

5.4.6 – Phosphatidylcholines as Clinical Biomarker Candidates for AD

Perhaps the most clinically relevant aspect of the study and therefore the thesis project on the whole is the overall predictive properties of the three PC molecules of interest. Therefore to test these predictive properties, a number of ROC analyses were completed.

A ROC analysis is essentially a statistical technique which enables the visualisation of classifier values, such as those for the PC molecules. The ROC graph is a two dimensional graph which is the result of plotting a predicative value that incorporates both the sensitivity (the prediction rate of true positives) and specificity (the prediction rate of false positives).

The false positive rate is calculated by dividing the negatives incorrectly classified by total negatives, whilst the true positive rate is the positives correctly classified value divided by the total positives.

In some classifier cases, the model is designed to produce only one class decision for example a Yes or No, and therefore produces a single ROC point. However in

the case of the ROC model employed here, a ROC curve is plotted by the implementation of an arbitrary threshold value. The threshold value changes throughout the plot, for example if it was set at 1, any value >1 would be classed as a positive result and <1 visa versa. As the threshold increases, the risk of a false positive may decrease, but as does the chance of obtaining an actual positive. Therefore the curve model implements a range of arbitrary threshold values, and plots the specificity and sensitivity associated with each, thereby forming a curve shape on the plot area. The area under this curve is often referred to, and represents the probability that a positive patient will rank higher than a randomly chosen negative one. Therefore the higher the value, the better the predictive properties of the marker set. A full review of ROC analyses can be read at the following review by Fawcett [317].

Currently, one of the major genetic markers of AD is the presence of one of the two ApoE gene alleles (ε2 or ε4) [15]. In the case of the extended LC-MS samples set presented here (n=141) using ApoE data alone gave an AUC of 0.667. When combined with the three lipid peak area ratio findings, the AUC rose to 0.828, suggesting a predictive potential of >80%. 80% is an important benchmark as it is currently regarded as a minimum requirement for AD biomarker candidate molecules [318, 319].

AUC scores for other combinations of PC and ApoE data, were not able to match the 0.828 value. Similarly combinations of the data sets in comparisons between MCI and AD and Control and MCI were not as promising, with the highest AUC scores at 0.651 and 0.672 respectively. However, this figure could potentially be improved with a longitudinal study design, where those MCI patients which progress to AD over a number of visits are recorded. This would enable the

differentiation of MCI but stable and MCI that convert to AD. This further study could provide interesting data regarding the progression of the disease.

5.5– Conclusions

The work presented here in Chapter 5, elucidated the structures of three PC species that were identified in the screen phase of the project presented in Chapter 3. The three PC species – 16:0/20:5, 16:0/22:6 and 18:0/22:6, were further tested in a larger dataset of n=141, with an improved profiling methodology, and were shown to significantly reduces following a pattern of Control → MCI → AD.

A series of ROC analyses were employed in order to visualise the predictive classifier properties of the PC molecules, where the most promising approach was to combine peak area ratio data with ApoE data for each patient, which produced an AUC of 0.827 when comparing control and AD. This suggests early promise for the PC species as biomarkers of AD. Further work is required in order to confirm and refine the finding, particularly as ROC results between AD and MCI were less promising, suggesting that MCI markers need to be more specific with progression into AD accounted for. A comparison between various disease states, including other forms of dementia such as Lewy body dementia and vascular dementia would improve the understanding of this.

Chapter 6:
Conclusions and Further Work

AD is rapidly becoming a major global burden. Aging populations and an increased efficacy at treating infectious and acute disease, is resulting in the sharp rise of diagnosed cases. This is having a major impact on both the economic cost of care, and the personal stresses and strains that occur within affected families.

Currently one of the significant challenges facing the management of AD is in the actual diagnosis, with current approaches relying on cognition testing combined with physical assessment and expert opinion. Whilst the process can be effective, inconsistencies occur, particularly when diagnosing between the numerous types of dementia. In addition, AD progression and response to treatment is difficult to track and record, with certain patients capable of performing well in cognition testing even if suffering from moderate to severe dementia. Therefore, a requirement exists for molecular markers that are capable of either (or both) the diagnosis of the disease and the accurate tracking of disease progression and cognitive decline.

A further challenge in the current procedure is that for a diagnosis to be given it is essential for symptoms to be apparent in the patient. However, there is a consensus that the mechanism behind AD pathology potentially begins in the patient 20 years or earlier, prior to the initial observation of symptoms [29, 30]. With this in mind it has been mooted that future pharmaceutical treatments will be designed to be disease modifying, altering the course of the disease from an early time point, before the patient has progressed to signs of cognitive impairment. Again, suggesting a need for a biomarker, especially one that can predict disease state from in pre-symptomatic patients.

Despite numerous candidate markers in the literature, both protein and genetic, current lead candidate biomarkers have proved inconsistent, especially when

diagnosing between AD and alternative dementias. Therefore, in order to expand the field on AD biomarkers and to present an alternative approach work was completed on small molecule biomarker research, in an attempt to identify novel candidate markers in the disease.

6.1 – Fatty Acid $_{TOTAL}$ in Alzheimer's Disease

6.1.1 – Study MB2

The initial study design utilised bio-tissue from both animal mouse model (brain) and human plasma, with a target study designed to investigate the possibility of the use of FA_{TOTAL} as a biomarker for the disease. Despite frequent discussions in the literature regarding FA in AD, to date, the use of FA_{TOTAL} has not previously been reported for AD in a biomarker capacity.

When comparing FA_{TOTAL} concentrations between AD model mouse and wild-type, differences were observed, however, statistical validation was not possible due to a restriction on available sample numbers. In order to provide a statistical interpretation of the findings, future work would be required that would incorporate brain regions from a greater number of animals. An interesting additional aspect which could be included in the study design would be to analyse concentrations in FA_{TOTAL} in the brain regions, along with corresponding plasma or serum. This would enable the observation of metabolite variations across the blood brain barrier, further increasing the understanding of FA_{TOTAL} in AD.

Additionally, if careful consideration was taken in the study design and sample volumes were managed effectively, a battery of analytical procedures could be completed on the different tissues, for example NMR, LC-MS targeted and LC-MS untargeted methods. This would provide a wealth of data, both in the biomarker

discovery phase, as well as metabolite ratios between the brain and the peripheral system. Animal models would be ideal subjects for this, as they exist in an extremely controlled environment. Despite the advantage of this controlled environment, results from a study designed with animal models as sources of tissue and biofluid, should clearly be considered as preliminary in a biomarker discovery workflow, due to the significant differences between animal models and actual human AD pathology. Therefore, any significant biomarker discovery would need to undergo further validation in a human population.

6.1.2 – Study HP30

It was a requirement for clinical relevance which drove much of the project planning presented within the thesis, hence the focus upon human plasma. The initial investigation into plasma concentrations of three major FA_{TOTAL} returned interesting results. Most promisingly, EPA_{TOTAL} was reported to significantly decrease when comparing control patient with AD patient plasma ($p=0.023$). In addition, the ratio of AA_{TOTAL}/EPA_{TOTAL} was demonstrated to significantly increase when comparing control patient with AD patient plasma ($p=0.05$).

Again, expansion of this study could provide further interesting results. Initially the increase of sample numbers would validate the statistical significance over a larger population. In addition, the LC-MS targeted approach could be adapted for a number of further FA_{TOTAL} species for example C16:0 and C18:0, which were associated with the three PC compounds of interest that were discussed in the later chapters.

Additionally, LC-MS targeted work could be completed on the individual fractions of individual FA molecules for example, FA_{TOTAL}, FA_{FREE} and FA_{BOUND} to various lipids and subclasses. This would enable the observation of the distribution ratios

within the disease classes. Despite the fact that other research groups have previously published results reporting the concentration of FA in both FA_{FREE} and FA_{BOUND} forms [208, 209]; as yet no one has published findings reporting the percentage distribution of individual fatty acids in an AD-control comparison.

6.2 – Lipidomics in Alzheimer's Disease

Following the early FA_{TOTAL} result, a decision was taken to continue with the use of human patient plasma. Plasma was selected based upon not only sample availability, but perhaps more importantly, potential clinical relevance and application. As discussed previously, the selection of biofluid is an important consideration, as for a biomarker to be successfully applied in a clinical scenario; ideally it needs to be obtainable from a non-invasive and easy to obtain biofluid.

A non-targeted screening study was developed, aimed at the investigation of small molecules using LC-MS combined with metabolomic data treatment. Results of this were promising, and following multivariate data modelling a number of features of interest were isolated for further investigation. Of particular significance was the observation of three features, later identified as PC molecules, which were demonstrated to be significantly reduced when analysed using univariate statistics in AD plasma, when compared with control patients.

Following this, a comprehensive lipid profiling method underwent development. Once the method had undergone a number of validation procedures, designed to examine extraction reproducibility and metabolite coverage, a study was completed which analysed an expanded AD/MCI/control human plasma sample cohort (n=141). The results of this investigation identified confirmed that three previously unreported PC species (PC16:0/20:5, PC16:0/22:6 and 18:0/22:6)

significantly decreased in AD compared with controls. Results demonstrated that the same three molecules were significantly decreased both in the screen and the comprehensive studies, further providing confidence to the finding. When combining the patient PC data with *ApoE* allele data, a ROC analysis returned an area under the curve of 0.827.

This reported result opens up numerous avenues of progression, and a number of additional studies can be completed to expand the investigation.

One of the major findings in the thesis was the significant decrease of three FA when comparing control plasma with AD plasma. An initial continuation experiment of this of particular interest would be the development and implementation of a fully validated LC-MS targeted study that is designed specifically to quantify the three PC molecules.

Future study design would ideally incorporate a larger cohort, in order to investigate if the observed trends are reflected in increased sample numbers. However, a number of challenges would be presented, the most significant of which would be the completion of the chromatographic separation of the three compounds, using a short as possible analytical run time. The speed of such an analysis would be an important consideration and method development should be focused on achieving a rapid extraction and analysis procedure. This would be an advantage when increasing sample numbers, as the use of an hour gradient employed in the comprehensive non-targeted analysis discussed here, would be unfeasible. A rapid separation would enable the analysis of a large as possible number of samples for a provided budget. The greater the number of samples which can be afforded would provide a greater weight of significance in any resultant findings.

However, the design of such a study should undergo meticulous planning. The reason for this is that study design in biomarker discovery is increasingly coming under scrutiny. Predominantly in the literature, studies are completed such as those described here in the thesis, in a traditional case (AD)-control design, and are often termed "cross sectional". However, recent alternative approaches have started to appear in the literature regarding identification of biomarkers that aim to reflect disease state [105]. This evolution is especially important in a disease such as AD which is the result of a long preclinical phase, and there is a growing consensus that controls are likely to have early signs of AD pathology even in the absence of clinical symptoms, making biomarker discovery challenging [105]. Alternative approaches include longitudinal designs, where patients are monitored at the first visit (termed baseline) and then at fixed time points as the disease progresses. This enables a picture to be painted of potential markers, with their effect observed over time along with increasing disease severity.

One such example of where this approach would be especially useful is in the case of MCI and AD progression. In the results presented within the thesis, the only PC molecule which reported a significant change between control and MCI was PC16:0/20:5. In addition no PC was found to significantly alter between MCI and AD despite the observation of a trend control>MCI>AD. With this in mind, the development of a specific method to quantify the three PC markers could therefore be employed to investigate this further, however, in a longitudinal manner that analyses plasma from control and MCI patients at baseline visit one and from follow up visits. This would enable the tracking of PC concentrations in those patients who convert to AD from MCI and controls and those who are stable over time (effectively two distinct "groups" of MCI). The application of this longitudinal

design would enable the investigation of PCs as a predictor for AD in MCI cases, and may help to identify those patients at most risk in the MCI stage.

However, often this longitudinal study design still employs classic case-control disease classes. Opinions are starting to shift, with recent publications beginning to explore avenues outside of this traditional approach. Examples of such include, correlating potential markers to known disease progression over time, such as brain atrophy and Aβ concentrations in the brain [109, 110]. Opinions in the literature have recently been published to this effect, and there is a consensus that it this more flexible approach, rather than the rigid case(AD)-control subgroups may reveal AD biomarkers that are both sensitive to AD severity and progression [105]. Therefore, an option for further work would be to complete a study in parallel with brain imaging data, to observe if the PC compounds alter with brain atrophy. In addition, it would be interesting to correlate the PC concentrations with Aβ brain levels, which can be achieved using positron emission tomography scans, and therefore it would be interesting to complete a study that ran plasma PC quantification alongside the real time Aβ aggregation values.

The results of this thesis focused upon the biomarker sensitivity and specificity when comparing between disease classes, with a ROC area under to curve of 0.827 when comparing AD with controls. However another important factor when considering the merits of a biomarker is the ability to classify between related dementia cases. There are many examples where biomarkers have appeared promising in case-control experiments, however when compared with a range of further conditions, the specificity of the biomarker has been found to be less effective. Examples of this include levels of $A\beta_{42}$ in CSF which have previously been reported to decrease in AD, providing sensitivity and specificity values of up

to 85% when compared with controls [83-85]. However, its use in a diagnostic environment has been bought into question due to the fact that a reduction in $A\beta_{42}$ concentrations have also been observed to decrease in other variants of dementia, for example Lewy body dementia [86], vascular dementia [87] and frontotemporal dementia [84].

Therefore, an interesting further work pathway would be to compare plasma PC concentrations from AD cases with a range of alternative types of dementia, cognitive impairment and neurological disorders, for example; vascular, frontotemporal and Lewy body dementia, as well as cases of brain tumour and stroke. The results from a study of this design would be important when evaluating the full merits of the three PC molecules as biomarkers of AD. To be useful in a clinical environment, the markers would ideally be unique markers of AD, and able to differentiate not only between controls, but also between dementia types. Therefore, it would be of significant interest to investigate how PC concentrations would perform when compared with a range of conditions.

An additional aspect of further interest would be to investigate whether the PC decrease observed in AD is a primary or secondary response to the disease. This is important as links to lipoprotein abnormalities have been widely reported in the disease, for example ApoE and clusterin [15, 106, 107], therefore, it could be feasible that the differences in PC could be linked to protein abnormalities as opposed to be a direct response to the disease. To investigate, it would be interesting to complete a study design that incorporated both proteomic and targeted PC analysis on parallel sample cohorts. From the resultant data it would be interesting to see if there are any correlations between the PC species and the major lipoproteins linked to AD in the literature.

6.3 – Alternative Avenues in Future Work

The above discussed further work focuses on the use of the three PC species as a marker for the disease. However, an alternative future work direction would be to investigate the actual biochemical pathways and imbalances behind the concentration variations of the PC molecules. An approach such as this could identify novel pathway targets in AD and help improve understanding of the disease, and lead to novel therapeutic treatments.

A starting point for such a study could be the enzyme PLA_2, responsible for the cleavage of FA side chains from PC molecules, with evidence in the literature suggesting a possible role in AD [202]. In order to investigate the role of PLA_2, FA side chains, the products of the enzymatic cleavage reaction, could be investigated with regard to PC species. A preliminary discussion of this was considered in Chapter 5, with the FA_{TOTAL} data of Chapter 2 being combined with the PC data, where it was highlighted that two of the side chains and in circulating plasma provided significance values of p=0.107 and 0.023 respectively (control→AD). This suggested that the concentration of EPA_{TOTAL} could therefore be linked to the depletion of PC 20:5, but interpreting these results in a more quantitative fashion was beyond the scope of the study and needs require further work.

One such approach that would improve the understanding of FA distribution in AD compared with controls was previously discussed above, with individual analyses of FA_{TOTAL}, FA_{FREE} and FA_{BOUND} to individual lipid species, in order to elucidate the metabolic balance within plasma. This could be expanded to include the side chains 16:0 and 18:0 which were not part of the original investigation in Chapter 2, however, were components of the three PC molecules of interest.

A further, more complex investigation in PC metabolism would be to introduce radiolabelled [*methyl*-^{3}H]choline into cell and organ cultures. As choline is a precursor to PC species, over time the [*methyl*-^{3}H]choline becomes incorporated into the PC metabolism pathway. Individual PC species can then be observed using a combination of LC-MS, detection by fluorescent tagging, as well as the use of liquid scintillation detection. This method at monitoring the metabolism of individual PC has previously been applied to rat trachea and lung parenchyma tissue [320]. The paper investigated the composition, the synthesis and release of PC compounds and reported observations that the trachea contained and synthesised more PC16:0/18:1, PC16:0/18:2, PC16:0/20:4 and PC16:0/16:0 than rat parenchyma. This approach could be adapted to investigate PC metabolism in AD brain tissue and a pilot study of this design could initially employ a neuronal cell line *in vitro* model. The radioisotope compounds could be introduced to the cell line, and monitored for effect following the introduction of insoluble Aβ aggregates.

To briefly summarise the project identified a number of biomarker candidates, of particular interest, including EPA_{TOTAL}, AA_{TOTAL}/EPA_{TOTAL} ratio and three previously unreported PC compounds (PC16:0/20:5, PC16:0/22:6 and 18:0/22:6). The results presented herein also open up future directions in both AD biomarker validation, as well as providing leads for future research on the pathways of the disease which could lead to an improvement in the understanding of the underlying mechanism in AD.

References

1. Alzheimer A. (1907). **Uber Eine Eigenartige Erkrankung Der Hirnrinde.** . *Allgemeine Zeitschrift fur Psychiatrie und Phychish-Gerichtliche Medizin*146-148].

2. Alzheimer A., Stelzmann R.A., Schnitzlein H.N., and Murtagh F.R. (1995). **An English Translation of Alzheimer's 1907 Paper, "Uber Eine Eigenartige Erkankung Der Hirnrinde"**. *Clinical Anatomy*. [8:429-431].

3. Ferri C.P., Prince M., Brayne C., Brodaty H., Fratiglioni L., Ganguli M., Hall K., Hasegawa K., Hendrie H., Huang Y., Jorm A., Mathers C., Menezes P.R., Rimmer E., and Scazufca M. (2005). **Global Prevalence of Dementia: A Delphi Consensus Study**. *Lancet*. [366:2112-2117].

4. Hebert L.E., Weuve J., Scherr P.A., and Evans D.A. (2013). **Alzheimer Disease in the United States (2010-2050) Estimated Using the 2010 Census**. *Neurology*. [80:1778-1783].

5. Minati L., Edginton T., Bruzzone M.G., and Giaccone G. (2009). **Current Concepts in Alzheimer's Disease: A Multidisciplinary Review**. *American Journal of Alzheimer's Disease and Other Dementias*. [24:95-121].

6. Hardy J., and Selkoe D.J. (2002). **The Amyloid Hypothesis of Alzheimer's Disease: Progress and Problems on the Road to Therapeutics**. *Science*. [297:353-356].

7. Li R., Lindholm K., Yang L.B., Yue X., Citron M., Yao R.Q., Beach T., Sue L., Sabbagh M., Cai H.B., Wong P., Price D., and Shen Y. (2004). **Amyloid Beta Peptide Load Is Correlated with Increased Beta-Secretase Activity in Sporadic Alzheimer's Disease Patients**. *Proceedings of the National Academy of Sciences of the United States of America*. [101:3632-3637].

8. Fukumoto H., Cheung B.S., Hyman B.T., and Irizarry M.C. (2002). **Beta-Secretase Protein and Activity Are Increased in the Neocortex in Alzheimer Disease**. *Archives of Neurology*. [59:1381-1389].

9. Kaether C., Haass C., and Steiner H. (2006). **Assembly, Trafficking and Function of Gamma-Secretase**. *Neurodegenerative Diseases*. [3:275-283].

10. Wiley J.C., Hudson M., Kanning K.C., Schecterson L.C., and Bothwell M. (2005). **Familial Alzheimer's Disease Mutations Inhibit Gamma-Secretase-Mediated Liberation of Beta-Amyloid Precursor Protein Carboxy-Terminal Fragment**. *Journal of Neurochemistry*. [94:1189-1201].

11. Jankowsky J.L., Fadale D.J., Anderson J., Xu G.M., Gonzales V., Jenkins N.A., Copeland N.G., Lee M.K., Younkin L.H., Wagner S.L., Younkin S.G., and Borchelt D.R. (2004). **Mutant Presenilins Specifically Elevate the Levels of the 42 Residue Beta-Amyloid Peptide in Vivo: Evidence for Augmentation of a 42-Specific Gamma Secretase**. *Human Molecular Genetics*. [13:159-170].

12. Haass C., Lemere C.A., Capell A., Citron M., Seubert P., Schenk D., Lannfelt L., and Selkoe D.J. (1995). **The Swedish Mutation Causes Early-Onset**

Alzheimer's Disease by Beta-Secretase Cleavage within the Secretory Pathway. *Nature Medicine*. [1:1291-1296].

13. Tanzi R.E., and Bertram L. (2005). **Twenty Years of the Alzheimer's Disease Amyloid Hypothesis: A Genetic Perspective**. *Cell*. [120:545-555].

14. Querfurth H.W., and LaFerla F.M. (2010). **Alzheimer's Disease**. *New England Journal of Medicine*. [362:329-344].

15. Ashford J.W. (2004). **Apolipoprotein E Genotype Effects on Alzheimer's Disease Onset and Epidemiology**. *Journal of Molecular Neuroscience*. [23:157-165].

16. Irizarry M.C., Deng A., Lleo A., Berezovska O., Von Arnim C.A., Martin-Rehrmann M., Manelli A., LaDu M.J., Hyman B.T., and Rebeck G.W. (2004). **Apolipoprotein E Modulates Gamma-Secretase Cleavage of the Amyloid Precursor Protein**. *Journal of Neurochemistry*. [90:1132-1143].

17. Ewers M., Zhong Z., Burger K., Wallin A., Blennow K., Teipel S.J., Shen Y., and Hampel H. (2008). **Increased Csf-Bace 1 Activity Is Associated with Apoe-Epsilon 4 Genotype in Subjects with Mild Cognitive Impairment and Alzheimer's Disease**. *Brain*. [131:1252-1258].

18. Harold D., Abraham R., Hollingworth P., Sims R., Gerrish A., Hamshere M.L., Pahwa J.S., Moskvina V., Dowzell K., Williams A., Jones N., Thomas C., Stretton A., Morgan A.R., Lovestone S., Powell J., Proitsi P., Lupton M.K., Brayne C., Rubinsztein D.C., Gill M., Lawlor B., Lynch A., Morgan K., Brown K.S., Passmore P.A., Craig D., McGuinness B., Todd S., Holmes C., Mann D., Smith A.D., Love S., Kehoe P.G., Hardy J., Mead S., Fox N., Rossor M., Collinge J., Maier W., Jessen F., Schurmann B., van den Bussche H., Heuser I., Kornhuber J., Wiltfang J., Dichgans M., Frolich L., Hampel H., Hull M., Rujescu D., Goate A.M., Kauwe J.S.K., Cruchaga C., Nowotny P., Morris J.C., Mayo K., Sleegers K., Bettens K., Engelborghs S., De Deyn P.P., Van Broeckhoven C., Livingston G., Bass N.J., Gurling H., McQuillin A., Gwilliam R., Deloukas P., Al-Chalabi A., Shaw C.E., Tsolaki M., Singleton A.B., Guerreiro R., Muhleisen T.W., Nothen M.M., Moebus S., Jockel K.H., Klopp N., Wichmann H.E., Carrasquillo M.M., Pankratz V.S., Younkin S.G., Holmans P.A., O'Donovan M., Owen M.J., and Williams J. (2009). **Genome-Wide Association Study Identifies Variants at Clu and Picalm Associated with Alzheimer's Disease**. *Nature Genetics*. [41:1088-U1061].

19. Shi H., Belbin O., Medway C., Brown K., Kalsheker N., Carrasquillo M., Proitsi P., Powell J., Lovestone S., Goate A., Younkin S., Passmore P., and Morgan K. (2012). **Genetic Variants Influencing Human Aging from Late-Onset Alzheimer's Disease: A Genome-Wide Association Study**. *Neurobiology of Aging*. [33:1849.e1845-1849.e1818].

20. Van Den Heuvel C., Thornton E., and Vink R. (2007). **Traumatic Brain Injury and Alzheimer's Disease: A Review**. *Progress in Brain Research*. [161:303-316].

21. Geerlings M.I., den Heijer T., Koudstaal P.J., Hofman A., and Breteler M.M. (2008). **History of Depression, Depressive Symptoms, and Medial**

Temporal Lobe Atrophy and the Risk of Alzheimer Disease. *Neurology*. [70:1258-1264].

22. Ownby R.L., Crocco E., Acevedo A., John V., and Loewenstein D. (2006). **Depression and Risk for Alzheimer Disease: Systematic Review, Meta-Analysis, and Metaregression Analysis**. *Archives of General Psychiatry*. [63:530-538].

23. Kamer A.R., Morse D.E., Holm-Pedersen P., Mortensen E.L., and Avlund K. (2012). **Periodontal Inflammation in Relation to Cognitive Function in an Older Adult Danish Population**. *Journal of Alzheimers Disease*. [28:613-624].

24. Koepsell T.D., Kurland B.F., Harel O., Johnson E.A., Zhou X.H., and Kukull W.A. (2008). **Education, Cognitive Function, and Severity of Neuropathology in Alzheimer Disease**. *Neurology*. [70:1732-1739].

25. Johnson S.C., Schmitz T.W., Trivedi M.A., Ries M.L., Torgerson B.M., Carlsson C.M., Asthana S., Hermann B.P., and Sager M.A. (2006). **The Influence of Alzheimer Disease Family History and Apolipoprotein E Epsilon 4 on Mesial Temporal Lobe Activation**. *Journal of Neuroscience*. [26:6069-6076].

26. Jack C.R., Jr., Albert M.S., Knopman D.S., McKhann G.M., Sperling R.A., Carrillo M.C., Thies B., and Phelps C.H. (2011). **Introduction to the Recommendations from the National Institute on Aging-Alzheimer's Association Workgroups on Diagnostic Guidelines for Alzheimer's Disease**. *Alzheimer's and Dementia*. [7:257-262].

27. McKhann G., Drachman D., Folstein M., Katzman R., Price D., and Stadlan E.M. (1984). **Clinical Diagnosis of Alzheimer's Disease: Report of the N.I.N.C.D.S-A.D.R.D.A Work Group under the Auspices of Department of Health and Human Services Task Force on Alzheimer's Disease**. *Neurology*. [34:939-944].

28. Folstein M.F., Folstein S.E., and McHugh P.R. (1975). **"Mini-Mental State". A Practical Method for Grading the Cognitive State of Patients for the Clinician**. *Journal of Psychiatric Research*. [12:189-198].

29. Reiman E.M., Quiroz Y.T., Fleisher A.S., Chen K., Velez-Pardo C., Jimenez-Del-Rio M., Fagan A.M., Shah A.R., Alvarez S., Arbelaez A., Giraldo M., Acosta-Baena N., Sperling R.A., Dickerson B., Stern C.E., Tirado V., Munoz C., Reiman R.A., Huentelman M.J., Alexander G.E., Langbaum J.B., Kosik K.S., Tariot P.N., and Lopera F. (2012). **Brain Imaging and Fluid Biomarker Analysis in Young Adults at Genetic Risk for Autosomal Dominant Alzheimer's Disease in the Presenilin 1 E280a Kindred: A Case-Control Study**. *Lancet Neurology*. [11:1048-1056].

30. Fleisher A.S., Chen K., Quiroz Y.T., Jakimovich L.J., Gomez M.G., Langois C.M., Langbaum J.B., Ayutyanont N., Roontiva A., Thiyyagura P., Lee W., Mo H., Lopez L., Moreno S., Acosta-Baena N., Giraldo M., Garcia G., Reiman R.A., Huentelman M.J., Kosik K.S., Tariot P.N., Lopera F., and Reiman E.M. (2012). **Florbetapir Positron Emission Tomography Analysis of Amyloid-Beta**

Deposition in the Presenilin 1 E280a Autosomal Dominant Alzheimer's Disease Kindred: A Cross-Sectional Study. *Lancet Neurology*. [11:1057-1065].

31. Lopez O.L., Jagust W.J., DeKosky S.T., Becker J.T., Fitzpatrick A., Dulberg C., Breitner J., Lyketsos C., Jones B., Kawas C., Carlson M., and Kuller L.H. (2003). **Prevalence and Classification of Mild Cognitive Impairment in the Cardiovascular Health Study Cognition Study: Part 1**. *Archives of Neurology*. [60:1385-1389].

32. Mitchell A.J., and Shiri-Feshki M. (2009). **Rate of Progression of Mild Cognitive Impairment to Dementia: Meta-Analysis of 41 Robust Inception Cohort Studies**. *Acta Psychiatrica Scandinavica*. [119:252-265].

33. Seino Y., Nanjo K., Tajima N., Kadowaki T., Kashiwagi A., Araki E., Ito C., Inagaki N., Iwamoto Y., Kasuga M., Hanafusa T., Haneda M., and Ueki K. (2010). **Report of the Committee on the Classification and Diagnostic Criteria of Diabetes Mellitus**. *Journal of Diabetes Investigation*. [1:212-228].

34. DeKosky S.T., Carrillo M.C., Phelps C., Knopman D., Petersen R.C., Frank R., Schenk D., Masterman D., Siemers E.R., Cedarbaum J.M., Gold M., Miller D.S., Morimoto B.H., Khachaturian A.S., and Mohs R.C. (2011). **Revision of the Criteria for Alzheimer's Disease: A Symposium**. *Alzheimer's and Dementia*. [7:e1-12].

35. World Health Organization (WHO). (1992). **The I.C.D10 Classification of Mental and Behavioural Disorders: Clinical Descriptions and Diagnostic Guidelines**

36. American Psychiatric Association. (1994). **Diagnostic and Statistical Manual of Mental Disorders Fouth Edition**

37. **Mini-Mental State Examination**. *Guys and St. Thomas NHS Trust*. (www.guysandstthomas.nhs.uk/resources/our-services/acutemedcine-gi-surgery/elderlycare/mini-mental-state-evaluation.pdf). [Last Accessed Online 10 January 2013].

38. Rosen W.G., Mohs R.C., and Davis K.L. (1984). **A New Rating Scale for Alzheimer's Disease**. *American Journal of Psychiatry*. [141:1356-1364].

39. Morris J.C., Heyman A., Mohs R.C., Hughes J.P., van Belle G., Fillenbaum G., Mellits E.D., and Clark C. (1989). **The Consortium to Establish a Registry for Alzheimer's Disease. Part I. Clinical and Neuropsychological Assessment of Alzheimer's Disease**. *Neurology*. [39:1159-1165].

40. Reisberg B., Ferris S.H., de Leon M.J., and Crook T. (1982). **The Global Deterioration Scale for Assessment of Primary Degenerative Dementia**. *American Journal of Psychiatry*. [139:1136-1139].

41. Berg L. (1988). **Clinical Dementia Rating**. *Psychopharmacology Bulletin*. [24:637-639].

42. Alexopoulos G.S., Abrams R.C., Young R.C., and Shamoian C.A. (1988). **Cornell Scale for Depression in Dementia**. *Biological Psychiatry*. [23:271-284].

43. Mayer L.S., Bay R.C., Politis A., Steinberg M., Steele C., Baker A.S., Rabins P.V., and Lyketsos C.G. (2006). **Comparison of Three Rating Scales as Outcome Measures for Treatment Trials of Depression in Alzheimer Disease: Findings from Diads**. *International Journal of Geriatric Psychiatry*. [21:930-936].

44. Fox L.S., Olin J.T., Erblich J., Ippen C.G., and Schneider L.S. (1998). **Severity of Cognitive Impairment in Alzheimer's Disease Affects List Learning Using the California Verbal Learning Test**. *International Journal of Geriatric Psychiatry*. [13:544-549].

45. Hogervorst E., Combrinck M., Lapuerta P., Rue J., Swales K., and Budge M. (2002). **The Hopkins Verbal Learning Test and Screening for Dementia**. *Dementia and Geriatric Cognitive Disorders*. [13:13-20].

46. Barzotti T., Gargiulo A., Marotta M.G., Tedeschi G., Zannino G., Guglielmi S., Dell'Armi A., Ettorre E., and Marigliano V. (2004). **Correlation between Cognitive Impairment and the Rey Auditory-Verbal Learning Test in a Population with Alzheimer Disease**. *Archives of Gerontology and Geriatrics*. [9:57-62].

47. Cahn D.A., Salmon D.P., Monsch A.U., Butters N., Wiederholt W.C., Corey-Bloom J., and Barrett-Connor E. (1996). **Screening for Dementia of the Alzheimer Type in the Community: The Utility of the Clock Drawing Test**. *Archives of Clinical Neuropsychology*. [11:529-539].

48. Crutch S.J., Rossor M.N., and Warrington E.K. (2007). **The Quantitative Assessment of Apraxic Deficits in Alzheimer's Disease**. *Cortex*. [43:976-986].

49. Lim A., Tsuang D., Kukull W., Nochlin D., Leverenz J., McCormick W., Bowen J., Teri L., Thompson J., Peskind E.R., Raskind M., and Larson E.B. (1999). **Clinico-Neuropathological Correlation of Alzheimer's Disease in a Community-Based Case Series**. *Journal of the American Geriatrics Society*. [47:564-569].

50. Petrovitch H., White L.R., Ross G.W., Steinhorn S.C., Li C.Y., Masaki K.H., Davis D.G., Nelson J., Hardman J., Curb J.D., Blanchette P.L., Launer L.J., Yano K., and Markesbery W.R. (2001). **Accuracy of Clinical Criteria for Alzheimer's Disease in the Honolulu-Asia Aging Study, a Population-Based Study**. *Neurology*. [57:226-234].

51. Varma A.R., Snowden J.S., Lloyd J.J., Talbot P.R., Mann D.M., and Neary D. (1999). **Evaluation of the N.I.N.C.D.S-A.D.R.D.A Criteria in the Differentiation of Alzheimer's Disease and Frontotemporal Dementia**. *Journal of Neurology, Neurosurgery and Psychiatry*. [66:184-188].

52. Kazee A.M., Eskin T.A., Lapham L.W., Gabriel K.R., McDaniel K.D., and Hamill R.W. (1993). **Clinicopathologic Correlates in Alzheimer Disease:**

Assessment of Clinical and Pathologic Diagnostic Criteria. *Alzheimer Disease & Associated Disorders*. [7:152-164].

53. Dubois B., Feldman H.H., Jacova C., Dekosky S.T., Barberger-Gateau P., Cummings J., Delacourte A., Galasko D., Gauthier S., Jicha G., Meguro K., O'Brien J., Pasquier F., Robert P., Rossor M., Salloway S., Stern Y., Visser P.J., and Scheltens P. (2007). **Research Criteria for the Diagnosis of Alzheimer's Disease: Revising the N.I.N.C.D.S-A.D.R.D.A Criteria**. *Lancet Neurology*. [6:734-746].

54. Plassman B.L., Khachaturian A.S., Townsend J.J., Ball M.J., Steffens D.C., Leslie C.E., Tschanz J.T., Norton M.C., Burke J.R., Welsh-Bohmer K.A., Hulette C.M., Nixon R.R., Tyrey M., and Breitner J.C. (2006). **Comparison of Clinical and Neuropathologic Diagnoses of Alzheimer's Disease in 3 Epidemiologic Samples**. *Alzheimer's and Dementia*. [2:2-11].

55. Bullock R. (2004). **Future Directions in the Treatment of Alzheimer's Disease**. *Expert Opinion on Investigational Drugs*. [13:303-314].

56. Sunderland T., Hampel H., Takeda M., Putnam K.T., and Cohen R.M. (2006). **Biomarkers in the Diagnosis of Alzheimer's Disease: Are We Ready?** *Journal of Geriatric Psychiatry and Neurology*. [19:172-179].

57. Hardy J. (2009). **The Amyloid Hypothesis for Alzheimer's Disease: A Critical Reappraisal**. *Journal of Neurochemistry*. [110:1129-1134].

58. Convit A., De Leon M.J., Tarshish C., De Santi S., Tsui W., Rusinek H., and George A. (1997). **Specific Hippocampal Volume Reductions in Individuals at Risk for Alzheimer's Disease**. *Neurobiology of Aging*. [18:131-138].

59. Schuff N., Woerner N., Boreta L., Kornfield T., Shaw L.M., Trojanowski J.Q., Thompson P.M., Jack C.R., Weiner M.W., Alzheimer's t., and Initiative D.N. (2009). **Magnetic Resonance Imaging of Hippocampal Volume Loss in Early Alzheimer's Disease in Relation to Apoe Genotype and Biomarkers**. *Brain*. [132:1067-1077].

60. Bobinski M., de Leon M.J., Convit A., De Santi S., Wegiel J., Tarshish C.Y., Saint Louis L.A., and Wisniewski H.M. (1999). **Magnetic Resonance Imaging of Entorhinal Cortex in Mild Alzheimer's Disease**. *Lancet*. [353:38-40].

61. Hampel H., Teipel S.J., Bayer W., Alexander G.E., Schwarz R., Schapiro M.B., Rapoport S.I., and Moller H.J. (2002). **Age Transformation of Combined Hippocampus and Amygdala Volume Improves Diagnostic Accuracy in Alzheimer's Disease**. *Journal of the Neurological Sciences*. [194:15-19].

62. Laakso M.P., Lehtovirta M., Partanen K., Riekkinen P.J., and Soininen H. (2000). **Hippocampus in Alzheimer's Disease: A 3-Year Follow-up Magnetic Resonance Imaging Study**. *Biological Psychiatry*. [47:557-561].

63. Schuff N., Amend D., Ezekiel F., Steinman S.K., Tanabe J., Norman D., Jagust W., Kramer J.H., Mastrianni J.A., Fein G., and Weiner M.W. (1997). **Changes of**

Hippocampal N-Acetyl Aspartate and Volume in Alzheimer's Disease. A Proton Magnetic Resonance Spectroscopic Imaging and Magnetic Resonance Imaging Study. *Neurology*. [49:1513-1521].

64. Du A.T., Schuff N., Amend D., Laakso M.P., Hsu Y.Y., Jagust W.J., Yaffe K., Kramer J.H., Reed B., Norman D., Chui H.C., and Weiner M.W. (2001). **Magnetic Resonance Imaging of the Entorhinal Cortex and Hippocampus in Mild Cognitive Impairment and Alzheimer's Disease**. *Journal of Neurology, Neurosurgery and Psychiatry*. [71:441-447].

65. Catani M., Cherubini A., Howard R., Tarducci R., Pelliccioli G.P., Piccirilli M., Gobbi G., Senin U., and Mecocci P. (2001). **H^1-Magnetic Resonance Spectroscopy Differentiates Mild Cognitive Impairment from Normal Brain Aging**. *Neuroreport*. [12:2315-2317].

66. Klunk W.E., Engler H., Nordberg A., Wang Y., Blomqvist G., Holt D.P., Bergström M., Savitcheva I., Huang G.-F., Estrada S., Ausén B., Debnath M.L., Barletta J., Price J.C., Sandell J., Lopresti B.J., Wall A., Koivisto P., Antoni G., Mathis C.A., and Långström B. (2004). **Imaging Brain Amyloid in Alzheimer's Disease with Pittsburgh Compound-B**. *Annals of Neurology*. [55:306-319].

67. Mosconi L. (2005). **Brain Glucose Metabolism in the Early and Specific Diagnosis of Alzheimer's Disease. Fdg-Pet Studies in Mci and Ad**. *European journal of nuclear medicine and molecular imaging*. [32:486-510].

68. Mayeux R., Saunders A.M., Shea S., Mirra S., Evans D., Roses A.D., Hyman B.T., Crain B., Tang M.X., and Phelps C.H. (1998). **Utility of the Apolipoprotein E Genotype in the Diagnosis of Alzheimer's Disease. Alzheimer's Disease Centers Consortium on Apolipoprotein E and Alzheimer's Disease**. *New England Journal of Medicine*. [338:506-511].

69. Saunders A.M., Strittmatter W.J., Schmechel D., George-Hyslop P.H., Pericak-Vance M.A., Joo S.H., Rosi B.L., Gusella J.F., Crapper-MacLachlan D.R., Alberts M.J., and et al. (1993). **Association of Apolipoprotein E Allele Epsilon 4 with Late-Onset Familial and Sporadic Alzheimer's Disease**. *Neurology*. [43:1467-1472].

70. Farrer L.A., Cupples L.A., Haines J.L., Hyman B., Kukull W.A., Mayeux R., Myers R.H., Pericak-Vance M.A., Risch N., and van Duijn C.M. (1997). **Effects of Age, Sex, and Ethnicity on the Association between Apolipoprotein E Genotype and Alzheimer Disease. A Meta-Analysis. Apoe and Alzheimer Disease Meta Analysis Consortium**. *Journal of the American Medical Association*. [278:1349-1356].

71. Jiang Q., Lee C.Y., Mandrekar S., Wilkinson B., Cramer P., Zelcer N., Mann K., Lamb B., Willson T.M., Collins J.L., Richardson J.C., Smith J.D., Comery T.A., Riddell D., Holtzman D.M., Tontonoz P., and Landreth G.E. (2008). **Apolipoprotein E Promotes the Proteolytic Degradation of Abeta**. *Neuron*. [58:681-693].

72. McConnell L.M., Sanders G.D., and Owens D.K. (1999). **Evaluation of Genetic Tests: Apolipoprotein E Genotyping for the Diagnosis of Alzheimer Disease**. *Genetic Testing and Molecular Biomarkers*. [3:47-53].

73. Morgan C., Colombres M., Nunez M.T., and Inestrosa N.C. (2004). **Structure and Function of Amyloid in Alzheimer's Disease**. *Progress in Neurobiology*. [74:323-349].

74. Braak H., and Braak E. (1991). **Neuropathological Stageing of Alzheimer-Related Changes**. *Acta Neuropathologica*. [82:239-259].

75. Love S. (2004). **Contribution of Cerebral Amyloid Angiopathy to Alzheimer's Disease**. *Journal of Neurology, Neurosurgery & Psychiatry*. [75:1-4].

76. Jarrett J.T., Berger E.P., and Lansbury P.T., Jr. (1993). **The Carboxy Terminus of the Beta Amyloid Protein Is Critical for the Seeding of Amyloid Formation: Implications for the Pathogenesis of Alzheimer's Disease**. *Biochemistry*. [32:4693-4697].

77. Snyder S.W., Ladror U.S., Wade W.S., Wang G.T., Barrett L.W., Matayoshi E.D., Huffaker H.J., Krafft G.A., and Holzman T.F. (1994). **Amyloid-Beta Aggregation: Selective Inhibition of Aggregation in Mixtures of Amyloid with Different Chain Lengths**. *Biophysics Journal*. [67:1216-1228].

78. Rovelet-Lecrux A., Hannequin D., Raux G., Le Meur N., Laquerriere A., Vital A., Dumanchin C., Feuillette S., Brice A., Vercelletto M., Dubas F., Frebourg T., and Campion D. (2006). **App Locus Duplication Causes Autosomal Dominant Early-Onset Alzheimer Disease with Cerebral Amyloid Angiopathy**. *Nature Genetics*. [38:24-26].

79. Meyer-Luehmann M., Spires-Jones T.L., Prada C., Garcia-Alloza M., de Calignon A., Rozkalne A., Koenigsknecht-Talboo J., Holtzman D.M., Bacskai B.J., and Hyman B.T. (2008). **Rapid Appearance and Local Toxicity of Amyloid-Beta Plaques in a Mouse Model of Alzheimer's Disease**. *Nature*. [451:720-724].

80. Harkany T., Abraham I., Konya C., Nyakas C., Zarandi M., Penke B., and Luiten P.G. (2000). **Mechanisms of Beta-Amyloid Neurotoxicity: Perspectives of Pharmacotherapy**. *Reviews in the Neurosciences*. [11:329-382].

81. Takata M., Nakashima M., Takehara T., Baba H., Machida K., Akitake Y., Ono K., Hosokawa M., and Takahashi M. (2008). **Detection of Amyloid Beta Protein in the Urine of Alzheimer's Disease Patients and Healthy Individuals**. *Neuroscience Letters*. [435:126-130].

82. Mayeux R., Tang M.X., Jacobs D.M., Manly J., Bell K., Merchant C., Small S.A., Stern Y., Wisniewski H.M., and Mehta P.D. (1999). **Plasma Amyloid Beta-Peptide$_{1-42}$ and Incipient Alzheimer's Disease**. *Annals of Neurology*. [46:412-416].

83. Galasko D., Chang L., Motter R., Clark C.M., Kaye J., Knopman D., Thomas R., Kholodenko D., Schenk D., Lieberburg I., Miller B., Green R., Basherad R., Kertiles L., Boss M.A., and Seubert P. (1998). **High Cerebrospinal Fluid Tau and Low Amyloid Beta$_{42}$ Levels in the Clinical Diagnosis of Alzheimer Disease and Relation to Apolipoprotein E Genotype**. *Archives of Neurology*. [55:937-945].

84. Sjogren M., Davidsson P., Wallin A., Granerus A.K., Grundstrom E., Askmark H., Vanmechelen E., and Blennow K. (2002). **Decreased Cerebrospinal Fluid Beta-Amyloid$_{42}$ in Alzheimer's Disease and Amyotrophic Lateral Sclerosis May Reflect Mismetabolism of Beta-Amyloid Induced by Disparate Mechanisms**. *Dementia and Geriatric Cognitive Disorders*. [13:112-118].

85. Motter R., Vigo-Pelfrey C., Kholodenko D., Barbour R., Johnson-Wood K., Galasko D., Chang L., Miller B., Clark C., Green R., and et al. (1995). **Reduction of Beta-Amyloid Peptide$_{42}$ in the Cerebrospinal Fluid of Patients with Alzheimer's Disease**. *Annals of Neurology*. [38:643-648].

86. Kanemaru K., Kameda N., and Yamanouchi H. (2000). **Decreased Cerebrospinal Fluid Amyloid Beta$_{42}$ and Normal Tau Levels in Dementia with Lewy Bodies**. *Neurology*. [54:1875-1876].

87. Nagga K., Gottfries J., Blennow K., and Marcusson J. (2002). **Cerebrospinal Fluid Phospho-Tau, Total Tau and Beta-Amyloid$_{(1-42)}$ in the Differentiation between Alzheimer's Disease and Vascular Dementia**. *Dementia and Geriatric Cognitive Disorders*. [14:183-190].

88. Clark C.M., and Karlawish J.H. (2003). **Alzheimer Disease: Current Concepts and Emerging Diagnostic and Therapeutic Strategies**. *Annals of Internal Medicine*. [138:400-410].

89. Ballatore C., Lee V.M., and Trojanowski J.Q. (2007). **Tau-Mediated Neurodegeneration in Alzheimer's Disease and Related Disorders**. *Nature Reviews Neuroscience*. [8:663-672].

90. Sjogren M., Minthon L., Davidsson P., Granerus A.K., Clarberg A., Vanderstichele H., Vanmechelen E., Wallin A., and Blennow K. (2000). **Cerebrospinal Fluid Levels of Tau, Beta-Amyloid$_{(1-42)}$ and Growth Associated Protein 43 in Frontotemporal Dementia, Other Types of Dementia and Normal Aging**. *Journal of Neural Transmission*. [107:563-579].

91. Sjogren M., Davidsson P., Tullberg M., Minthon L., Wallin A., Wikkelso C., Granerus A.K., Vanderstichele H., Vanmechelen E., and Blennow K. (2001). **Both Total and Phosphorylated Tau Are Increased in Alzheimer's Disease**. *Journal of Neurology, Neurosurgery and Psychiatry*. [70:624-630].

92. Blennow K., Vanmechelen E., and Hampel H. (2001). **Cerebrospinal Fluid Total Tau, Abeta$_{42}$ and Phosphorylated Tau Protein as Biomarkers for Alzheimer's Disease**. *Molelcular Neurobiology*. [24:87-97].

93. Buerger K., Zinkowski R., Teipel S.J., Tapiola T., Arai H., Blennow K., Andreasen N., Hofmann-Kiefer K., DeBernardis J., Kerkman D., McCulloch C., Kohnken R., Padberg F., Pirttila T., Schapiro M.B., Rapoport S.I., Moller H.J., Davies P., and Hampel H. (2002). **Differential Diagnosis of Alzheimer Disease with Cerebrospinal Fluid Levels of Tau Protein Phosphorylated at Threonine 231**. *Archives of Neurology*. [59:1267-1272].

94. Lewczuk P., Esselmann H., Bibl M., Beck G., Maler J.M., Otto M., Kornhuber J., and Wiltfang J. (2004). **Tau Protein Phosphorylated at Threonine 181 in Cerebrospinal Fluid as a Neurochemical Biomarker in Alzheimer's Disease: Original Data and Review of the Literature**. *Journal of Molecular Neuroscience*. [23:115-122].

95. Hesse C., Rosengren L., Vanmechelen E., Vanderstichele H., Jensen C., Davidsson P., and Blennow K. (2000). **Cerebrospinal Fluid Markers for Alzheimer's Disease Evaluated after Acute Ischemic Stroke**. *Journal of Alzheimers Disease*. [2:199-206].

96. Brettschneider J., Maier M., Arda S., Claus A., Sussmuth S.D., Kassubek J., and Tumani H. (2005). **Tau Protein Level in Cerebrospinal Fluid Is Increased in Patients with Early Multiple Sclerosis**. *Multiple Sclerosis Journal*. [11:261-265].

97. de Bont J.M., Vanderstichele H., Reddingius R.E., Pieters R., and van Gool S.W. (2008). **Increased Total-Tau Levels in Cerebrospinal Fluid of Pediatric Hydrocephalus and Brain Tumor Patients**. *European Journal of Paediatric Neurology*. [12:334-341].

98. Sunderland T., Linker G., Mirza N., Putnam K.T., Friedman D.L., Kimmel L.H., Bergeson J., Manetti G.J., Zimmermann M., Tang B., Bartko J.J., and Cohen R.M. (2003). **Decreased Beta-Amyloid$_{1-42}$ and Increased Tau Levels in Cerebrospinal Fluid of Patients with Alzheimer Disease**. *Journal of the American Medical Association*. [289:2094-2103].

99. Sparks D.L., Kryscio R.J., Sabbagh M.N., Ziolkowski C., Lin Y., Sparks L.M., Liebsack C., and Johnson-Traver S. (2012). **Tau Is Reduced in Alzheimer's Disease Plasma and Validation of Employed Enzyme-Linked Immunosorbent Assay Methods**. *Americal Journal of Neurdegenerative Disease*. [1:99-106].

100. Weuve J., Press D.Z., Grodstein F., Wright R.O., Hu H., and Weisskopf M.G. (2013). **Cumulative Exposure to Lead and Cognition in Persons with Parkinson's Disease**. *Movement Disorders*. [28:176-182].

101. Tamaoka A., Fukushima T., Sawamura N., Ishikawa K., Oguni E., Komatsuzaki Y., and Shoji S. (1996). **Amyloid Beta Protein in Plasma from Patients with Sporadic Alzheimer's Disease**. *Journal of the Neurological Sciences*. [141:65-68].

102. Fukumoto H., Tennis M., Locascio J.J., Hyman B.T., Growdon J.H., and Irizarry M.C. (2003). **Age but Not Diagnosis Is the Main Predictor of Plasma Amyloid Beta-Protein Levels**. *Archives of Neurology*. [60:958-964].

103. Mehta P.D., Pirttila T., Mehta S.P., Sersen E.A., Aisen P.S., and Wisniewski H.M. (2000). **Plasma and Cerebrospinal Fluid Levels of Amyloid Beta Proteins$_{1-40}$ and $_{1-42}$ in Alzheimer Disease**. *Archives of Neurology*. [57:100-105].

104. Koyama A., O'Brien J., Weuve J., Blacker D., Metti A.L., and Yaffe K. (2013). **The Role of Peripheral Inflammatory Markers in Dementia and Alzheimer's Disease: A Meta-Analysis**. *Journals of Gerontology Series a-Biological Sciences and Medical Sciences*. [68:433-440].

105. Thambisetty M., and Lovestone S. (2010). **Blood-Based Biomarkers of Alzheimer's Disease: Challenging but Feasible**. *Biomarker Medicine*. [4:65-79].

106. Thambisetty M., Simmons A., Velayudhan L., Hye A., Campbell J., Zhang Y., Wahlund L.O., Westman E., Kinsey A., Guntert A., Proitsi P., Powell J., Causevic M., Killick R., Lunnon K., Lynham S., Broadstock M., Choudhry F., Howlett D.R., Williams R.J., Sharp S.I., Mitchelmore C., Tunnard C., Leung R., Foy C., O'Brien D., Breen G., Furney S.J., Ward M., Kloszewska I., Mecocci P., Soininen H., Tsolaki M., Vellas B., Hodges A., Murphy D.G.M., Parkins S., Richardson J.C., Resnick S.M., Ferrucci L., Wong D.F., Zhou Y., Muehlboeck S., Evans A., Francis P.T., Spenger C., and Lovestone S. (2010). **Association of Plasma Clusterin Concentration with Severity, Pathology, and Progression in Alzheimer Disease**. *Archives of General Psychiatry*. [67:739-748].

107. Hye A., Lynham S., Thambisetty M., Causevic M., Campbell J., Byers H.L., Hooper C., Rijsdijk F., Tabrizi S.J., Banner S., Shaw C.E., Foy C., Poppe M., Archer N., Hamilton G., Powell J., Brown R.G., Sham P., Ward M., and Lovestone S. (2006). **Proteome-Based Plasma Biomarkers for Alzheimer's Disease**. *Brain*. [129:3042-3050].

108. Silajdzic E., Minthon L., Bjorkqvist M., and Hansson O. (2012). **No Diagnostic Value of Plasma Clusterin in Alzheimer's Disease**. *PLoS One*. [7:e50237].

109. Kiddle S.J., Thambisetty M., Simmons A., Riddoch-Contreras J., Hye A., Westman E., Pike I., Ward M., Johnston C., Lupton M.K., Lunnon K., Soininen H., Kloszewska I., Tsolaki M., Vellas B., Mecocci P., Lovestone S., Newhouse S., and Dobson R. (2012). **Plasma Based Markers of [11c] Pib-Pet Brain Amyloid Burden**. *PLoS One*. [7:e44260].

110. Thambisetty M., An Y., Kinsey A., Koka D., Saleem M., Guntert A., Kraut M., Ferrucci L., Davatzikos C., Lovestone S., and Resnick S.M. (2012). **Plasma Clusterin Concentration Is Associated with Longitudinal Brain Atrophy in Mild Cognitive Impairment**. *Neuroimage*. [59:212-217].

111. Doecke J.D., Laws S.M., Faux N.G., Wilson W., Burnham S.C., Lam C.P., Mondal A., Bedo J., Bush A.I., Brown B., De Ruyck K., Ellis K.A., Fowler C., Gupta V.B., Head R., Macaulay S.L., Pertile K., Rowe C.C., Rembach A., Rodrigues M., Rumble R., Szoeke C., Taddei K., Taddei T., Trounson B., Ames D., Masters C.L., and Martins R.N. (2012). **Blood-Based Protein Biomarkers for Diagnosis of Alzheimer Disease**. *Archives of Neurology*1-8].

112. Laske C. (2013). **Blood-Based Biomarkers in Alzheimer Disease: Where Are We Now and Where Have We to Go?** *Journal of the American Medical Association Neurology*. [70:133-134].

113. Ray S., Britschgi M., Herbert C., Takeda-Uchimura Y., Boxer A., Blennow K., Friedman L.F., Galasko D.R., Jutel M., Karydas A., Kaye J.A., Leszek J., Miller B.L., Minthon L., Quinn J.F., Rabinovici G.D., Robinson W.H., Sabbagh M.N., So Y.T., Sparks D.L., Tabaton M., Tinklenberg J., Yesavage J.A., Tibshirani R., and Wyss-Coray T. (2007). **Classification and Prediction of Clinical Alzheimer's Diagnosis Based on Plasma Signaling Proteins**. *Nature Medicine*. [13:1359-1362].

114. Bjorkqvist M., Ohlsson M., Minthon L., and Hansson O. (2012). **Evaluation of a Previously Suggested Plasma Biomarker Panel to Identify Alzheimer's Disease**. *PLoS One*. [7:e29868].

115. Zipser B.D., Johanson C.E., Gonzalez L., Berzin T.M., Tavares R., Hulette C.M., Vitek M.P., Hovanesian V., and Stopa E.G. (2007). **Microvascular Injury and Blood-Brain Barrier Leakage in Alzheimer's Disease**. *Neurobiology of Aging*. [28:977-986].

116. Kalaria R.N. (1999). **The Blood-Brain Barrier and Cerebrovascular Pathology in Alzheimer's Disease**. *Annals of the New York Academy of Sciencesi*. [893:113-125].

117. Zarow C., Barron E., Chui H.C., and Perlmutter L.S. (1997). **Vascular Basement Membrane Pathology and Alzheimer's Disease**. *Annals of the New York Academy of Sciences*. [826:147-160].

118. Irizarry M.C. (2004). **Biomarkers of Alzheimer Disease in Plasma**. *NeuroRx*. [1:226-234].

119. Greenberg N., Grassano A., Thambisetty M., Lovestone S., and Legido-Quigley C. (2009). **A Proposed Metabolic Strategy for Monitoring Disease Progression in Alzheimer's Disease**. *Electrophoresis*. [30:1235-1239].

120. Madsen R., Lundstedt T., and Trygg J. (2010). **Chemometrics in Metabolomics - a Review in Human Disease Diagnosis**. *Analytica Chimica Acta*. [659:23-33].

121. Broadhurst D.I., and Kell D.B. (2006). **Statistical Strategies for Avoiding False Discoveries in Metabolomics and Related Experiments**. *Metabolomics*. [2:171-196].

122. Jackson J.E. 2004. *In* A User's Guide to Principal Components. John Wiley & Sons, Inc. i-3.

123. Wold S. (1976). **Pattern Recognition by Means of Disjoint Principal Components Models**. *Pattern recognition*. [8:127-139].

124. Fisher R.A. (1936). **The Use of Multiple Measurements in Taxonomic Problems**. *Annals of Eugenics*. [7:179-188].

125. Wold S., Sjöström M., and Eriksson L. (2001). **Partial Least Squares - Regression: A Basic Tool of Chemometrics**. *Chemometrics and Intelligent Laboratory Systems*. [58:109-130].

126. Ståhle L., and Wold S. (1987). **Partial Least Squares Analysis with Cross Validation for the Two Class Problem: A Monte Carlo Study**. *Journal of Chemometrics*. [1:185-196].

127. Bylesjö M., Rantalainen M., Cloarec O., Nicholson J.K., Holmes E., and Trygg J. (2006). **Orthagonal Partial Least Squares Discriminant Analysis: Combining the Strengths of Partial Least Squares-Discriminant Analysis and Simca Classification**. *Journal of Chemometrics*. [20:341-351].

128. Goodacre R., Vaidyanathan S., Dunn W.B., Harrigan G.G., and Kell D.B. (2004). **Metabolomics by Numbers: Acquiring and Understanding Global Metabolite Data**. *Trends in Biotechnology*. [22:245-252].

129. Kohonen T. 2000. *In* Self Organising Maps. Springer.

130. Sitter B., Bathen T.F., Tessem M.-B., and Gribbestad I.S. (2009). **High-Resolution Magic Angle Spinning Magnetic Resonance Spectroscopy in Metabolic Characterization of Human Cancer**. *Progress in Nuclear Magnetic Resonance Spectroscopy*. [54:239-254].

131. Jukarainen N., Korhonen S.-P., Laakso M., Korolainen M., Niemitz M., Soininen P., Tuppurainen K., Vepsäläinen J., Pirttilä T., and Laatikainen R. (2008). **Quantification of H^1 Nuclear Magnetic Resonance Spectra of Human Cerebrospinal Fluid: A Protocol Based on Constrained Total-Line-Shape Analysis**. *Metabolomics*. [4:150-160].

132. Gujar S.K., Maheshwari S., Bjorkman-Burtscher I., and Sundgren P.C. (2005). **Magnetic Resonance Spectroscopy**. *Journal of Neuro-Ophthalmology*. [25:217-226].

133. Whiley L., Godzien J., Ruperez F.J., Legido-Quigley C., and Barbas C. (2012). **In-Vial Dual Extraction for Direct Liquid Chromatography-Mass Spectrometry Analysis of Plasma for Comprehensive and Highly Reproducible Metabolic Fingerprinting**. *Analytical Chemistry*. [84:5992-5999].

134. Han X.L., and Gross R.W. (2003). **Global Analyses of Cellular Lipidomes Directly from Crude Extracts of Biological Samples by Electrospray Iionisation Mass Spectrometry: A Bridge to Lipidomics**. *Journal of Lipid Research*. [44:1071-1079].

135. Pratico D., Clark C.M., Lee V.M., Trojanowski J.Q., Rokach J., and FitzGerald G.A. (2000). **Increased 8,12-Iso-Ipf2alpha-Vi in Alzheimer's Disease: Correlation of a Noninvasive Index of Lipid Peroxidation with Disease Severity**. *Annals of Neurology*. [48:809-812].

136. Pratico D., Lee V.M.Y., Trojanowski J.Q., Rokach J., and Fitzgerald G.A. (1998). **Increased F_2-Isoprostanes in Alzheimer's Disease: Evidence for Enhanced Lipid Peroxidation in Vivo**. *Faseb Journal*. [12:1777-1783].

137. Kim S.B., Hill M., Kwak Y.T., Hampl R., Jo D.H., and Morfin R. (2003). **Neurosteroids: Cerebrospinal Fluid Levels for Alzheimer's Disease and Vascular Dementia Diagnostics**. *Journal of Clinical Endocrinology & Metabolism*. [88:5199-5206].

138. Volkel W., Sicilia T., Pahler A., Gsell W., Tatschner T., Jellinger K., Leblhuber F., Riederer P., Lutz W.K., and Gotz M.E. (2006). **Increased Brain Levels of 4-Hydroxy-2-Nonenal Glutathione Conjugates in Severe Alzheimer's Disease**. *Neurochemistry International*. [48:679-686].

139. Bohnstedt K.C., Karlberg B., Wahlund L.O., Jonhagen M.E., Basun H., and Schmidt S. (2003). **Determination of Isoprostanes in Urine Samples from Alzheimer Patients Using Porous Graphitic Carbon Liquid Chromatography-Tandem Mass Spectrometry**. *Journal of Chromatography B: Analytical Technologies in the Biomedical and Life Sciences*. [796:11-19].

140. **Enzyme-Linked Immunosorbant Assay**. *Cavitri*. (http://commons.wikimedia.org/wiki/File:ELISA_diagram.png used under an open license details at (http://creativecommons.org/licenses/by/3.0/)). [Last Accessed Online 17 June 2013].

141. Whiley L., and Legido-Quigley C. (2011). **Current Strategies in the Discovery of Small-Molecule Biomarkers for Alzheimer's Disease**. *Bioanalysis*. [3:1121-1142].

142. Pettegrew J.W., Panchalingam K., Hamilton R.L., and McClure R.J. (2001). **Brain Membrane Phospholipid Alterations in Alzheimer's Disease**. *Neurochemical Research*. [26:771-782].

143. Tsai G., and Coyle J.T. (1995). **N-Acetylaspartate in Neuropsychiatric Disorders**. *Progress in Neurobiology*. [46:531-540].

144. Mohanakrishnan P., Fowler A.H., Vonsattel J.P., Jolles P.R., Husain M.M., Liem P., Myers L., and Komoroski R.A. (1997). **Regional Metabolic Alterations in Alzheimer's Disease: An in Vitro H^1 Nuclear Magnetic Resonance Study of the Hippocampus and Cerebellum**. *Journals of Gerontology Series a-Biological Sciences and Medical Sciences*. [52:B111-B117].

145. Shonk T.K., Moats R.A., Gifford P., Michaelis T., Mandigo J.C., Izumi J., and Ross B.D. (1995). **Probable Alzheimer-Disease - Diagnosis with Proton Magnetic Resonance Spectroscopy**. *Radiology*. [195:65-72].

146. Huang W., Alexander G.E., Chang L., Shetty H.U., Krasuski J.S., Rapoport S.I., and Schapiro M.B. (2001). **Brain Metabolite Concentration and Dementia Severity in Alzheimer's Disease: A H^1 Magnetic Resonance Spectroscopy Study**. *Neurology*. [57:626-632].

147. Hancu I., Zimmerman E.A., Sailasuta N., and Hurd R.E. (2005). **H1-Magnetic Resonance Spectroscopy Using Te Averaged Press: A More Sensitive Technique to Detect Neuro Degeneration Associated with Alzheimer's Disease**. *Magnetic Resonance in Medicine*. [53:777-782].

148. Kantarci K., Jack C.R., Jr., Xu Y.C., Campeau N.G., O'Brien P.C., Smith G.E., Ivnik R.J., Boeve B.F., Kokmen E., Tangalos E.G., and Petersen R.C. (2000). **Regional Metabolic Patterns in Mild Cognitive Impairment and Alzheimer's Disease: A H1 Magnetic Resonance Spectroscopy Study**. *Neurology*. [55:210-217].

149. Block W., Jessen F., Traber F., Flacke S., Manka C., Lamerichs R., Keller E., Heun R., and Schild H. (2002). **Regional N-Acetylaspartate Reduction in the Hippocampus Detected with Fast Proton Magnetic Resonance Spectroscopic Imaging in Patients with Alzheimer Disease**. *Archives of Neurology*. [59:828-834].

150. Frederick B.D., Lyoo I.K., Satlin A., Ahn K.H., Kim M.J., Yurgelun-Todd D.A., Cohen B.M., and Renshaw P.F. (2004). **In Vivo Proton Magnetic Resonance Spectroscopy of the Temporal Lobe in Alzheimer's Disease**. *Progress in Neuro-Psychopharmacology and Biological Psychiatry*. [28:1313-1322].

151. Kantarci K., Knopman D.S., Dickson D.W., Parisi J.E., Whitwell J.L., Weigand S.D., Josephs K.A., Boeve B.F., Petersen R.C., and Jack C.R., Jr. (2008). **Alzheimer Disease: Postmortem Neuropathologic Correlates of Antemortem H1 Magnetic Resonance Spectroscopy Metabolite Measurements**. *Radiology*. [248:210-220].

152. Miller B.L., Moats R.A., Shonk T., Ernst T., Woolley S., and Ross B.D. (1993). **Alzheimer Disease: Depiction of Increased Cerebral Myo-Inositol with Proton Magnetic Resonance Spectroscopy**. *Radiology*. [187:433-437].

153. Martinez-Bisbal M.C., Arana E., Marti-Bonmati L., Molla E., and Celda B. (2004). **Cognitive Impairment: Classification by H1 Magnetic Resonance Spectroscopy**. *European Journal of Neurology*. [11:187-193].

154. Rupsingh R., Borrie M., Smith M., Wells J.L., and Bartha R. (2011). **Reduced Hippocampal Glutamate in Alzheimer Disease**. *Neurobiology of Aging*. [32:802-810].

155. Camps P., and Munoz-Torrero D. (2002). **Cholinergic Drugs in Pharmacotherapy of Alzheimer's Disease**. *Mini-Reviews in Medicinal Chemistry*. [2:11-25].

156. Modrego P.J., Pina M.A., Fayed N., and Diaz M. (2006). **Changes in Metabolite Ratios after Treatment with Rivastigmine in Alzheimer's Disease: A Nonrandomised Controlled Trial with Magnetic Resonance Spectroscopy**. *CNS Drugs*. [20:867-877].

157. Han X., Holtzman D.M., and McKeel D.W., Jr. (2001). **Plasmalogen Deficiency in Early Alzheimer's Disease Subjects and in Animal Models: Molecular**

Characterization Using Electrospray Ionization Mass Spectrometry. *Journal of Neurochemistry*. [77:1168-1180].

158. Sun G.Y. (1973). **Phospholipids and Acyl Groups in Subcellular-Fractions from Human Cerebral-Cortex**. *Journal of Lipid Research*. [14:656-663].

159. Vos J.P., Lopes-Cardozo M., and Gadella B.M. (1994). **Metabolic and Functional Aspects of Sulfogalactolipids**. *Biochimica et Biophysica Acta*. [1211:125-149].

160. Han X., D M.H., McKeel D.W., Jr., Kelley J., and Morris J.C. (2002). **Substantial Sulfatide Deficiency and Ceramide Elevation in Very Early Alzheimer's Disease: Potential Role in Disease Pathogenesis**. *Journal of Neurochemistry*. [82:809-818].

161. Hoyer S. (2004). **Glucose Metabolism and Insulin Receptor Signal Transduction in Alzheimer Disease**. *European Journal of Pharmacology*. [490:115-125].

162. Hoyer S. (2000). **Brain Glucose and Energy Metabolism Abnormalities in Sporadic Alzheimer Disease. Causes and Consequences: An Update**. *Experimental Gerontology*. [35:1363-1372].

163. Beal M.F. (1994). **Energy, Oxidative Damage, and Alzheimers-Disease - Clues to the Underlying Puzzle**. *Neurobiology of Aging*. [15:S171-S174].

164. Redjems-Bennani N., Jeandel C., Lefebvre E., Blain H., Vidailhet M., and Gueant J.L. (1998). **Abnormal Substrate Levels That Depend Upon Mitochondrial Function in Cerebrospinal Fluid from Alzheimer Patients**. *Gerontology*. [44:300-304].

165. Zhu X., Lee H.G., Casadesus G., Avila J., Drew K., Perry G., and Smith M.A. (2005). **Oxidative Imbalance in Alzheimer's Disease**. *Molecular Neurobiology*. [31:205-217].

166. Christen Y. (2000). **Oxidative Stress and Alzheimer Disease**. *American Journal of Clinical Nutrition*. [71:621S-629S].

167. Nourooz-Zadeh J., Liu E.H.C., Yhlen B., Anggard E.E., and Halliwell B. (1999). **F_4-Isoprostanes as Specific Marker of Docosahexaenoic Acid Peroxidation in Alzheimer's Disease**. *Journal of Neurochemistry*. [72:734-740].

168. Montine T.J., Beal M.F., Cudkowicz M.E., O'Donnell H., Margolin R.A., McFarland L., Bachrach A.F., Zackert W.E., Roberts L.J., and Morrow J.D. (1999). **Increased Cerebrospinal Fluid F_2-Isoprostane Concentration in Probable Alzheimer's Disease**. *Neurology*. [52:562-565].

169. Montine T.J., Kaye J.A., Montine K.S., McFarland L., Morrow J.D., and Quinn J.F. (2001). **Cerebrospinal Fluid a $Beta_{42}$, Tau, and F_2-Isoprostane Concentrations in Patients with Alzheimer Disease, Other Dementias, and in Age-Matched Controls**. *Archives of Pathology & Laboratory Medicine*. [125:510-512].

170. Montine T.J., Markesbery W.R., Morrow J.D., and Roberts L.J. (1998). **Cerebrospinal Fluid F_2-Isoprostane Levels Are Increased in Alzheimer's Disease**. *Annals of Neurology*. [44:410-413].

171. Montine T.J., Sidell K.R., Crews B.C., Markesbery W.R., Marnett L.J., Roberts L.J., and Morrow J.D. (1999). **Elevated Cerebrospinal Fluid Prostaglandin E_2 Levels in Patients with Probable Alzheimer's Disease**. *Neurology*. [53:1495-1498].

172. Kim K.M., Jung B.H., Paeng K.J., Kim I., and Chung B.C. (2004). **Increased Urinary F_2-Isoprostanes Levels in the Patients with Alzheimer's Disease**. *Brain Research Bulletin*. [64:47-51].

173. Quinn J.F., Montine K.S., Moore M., Morrow J.D., Kaye J.A., and Montine T.J. (2004). **Suppression of Longitudinal Increase in Cerebrospinal Fluid F_2-Isoprostanes in Alzheimer's Disease**. *Journal of Alzheimers Disease*. [6:93-97].

174. Yoshida Y., Yoshikawa A., Kinumi T., Ogawa Y., Saito Y., Ohara K., Yamamoto H., Imai Y., and Niki E. (2009). **Hydroxyoctadecadienoic Acid and Oxidatively Modified Peroxiredoxins in the Blood of Alzheimer's Disease Patients and Their Potential as Biomarkers**. *Neurobiology of Aging*. [30:174-185].

175. Brown R.C., Han Z.Q., Cascio C., and Papadopoulos V. (2003). **Oxidative Stress-Mediated Dhea Formation in Alzheimer's Disease Pathology**. *Neurobiology of Aging*. [24:57-65].

176. Attal-Khemis S., Dalmeyda V., Michot J.L., Roudier M., and Morfin R. (1998). **Increased Total 7-Alpha-Hydroxy-Dehydroepiandrosterone in Serum of Patients with Alzheimer's Disease**. *The Journals of Gerontology Series A: Biological Sciences and Medical Sciences*. [53:B125-132].

177. Wang J., Xiong S., Xie C., Markesbery W.R., and Lovell M.A. (2005). **Increased Oxidative Damage in Nuclear and Mitochondrial DNA in Alzheimer's Disease**. *Journal of Neurochemistry*. [93:953-962].

178. Ahmed N., Ahmed U., Thornalley P.J., Hager K., Fleischer G., and Munch G. (2005). **Protein Glycation, Oxidation and Nitration Adduct Residues and Free Adducts of Cerebrospinal Fluid in Alzheimer's Disease and Link to Cognitive Impairment**. *Journal of Neurochemistry*. [92:255-263].

179. Gackowski D., Rozalski R., Siomek A., Dziaman T., Nicpon K., Klimarczyk M., Araszkiewicz A., and Olinski R. (2008). **Oxidative Stress and Oxidative DNA Damage Is Characteristic for Mixed Alzheimer Disease/Vascular Dementia**. *Journal of the Neurological Sciences*. [266:57-62].

180. Siomek A., Gackowski D., Rozalski R., Dziaman T., Szpila A., Guz J., and Olinski R. (2007). **Higher Leukocyte 8-Oxo-7,8-Dihydro-2'-Deoxyguanosine and Lower Plasma Ascorbate in Aging Humans?** *Antioxidants and Redox Signaling*. [9:143-150].

181. Rinaldi P., Polidori M.C., Metastasio A., Mariani E., Mattioli R., Cherubini A., Catani M., Cecchetti R., Senin U., and Mecocci P. (2003). **Plasma Antioxidants Are Similarly Depleted in Mild Cognitive Impairment and in Alzheimer's Disease**. *Neurobiology of Aging*. [24:915-919].

182. Wang W., Shinto L., Connor W.E., and Quinn J.F. (2008). **Nutritional Biomarkers in Alzheimer's Disease: The Association between Carotenoids, N3 Fatty Acids, and Dementia Severity**. *Journal of Alzheimers Disease*. [13:31-38].

183. Sjögren M., Minthon L., Passant U., Blennow K., and Wallin A. (1998). **Decreased Monoamine Metabolites in Frontotemporal Dementia and Alzheimer's Disease**. *Neurobiology of Aging*. [19:379-384].

184. Walter A., Korth U., Hilgert M., Hartmann J., Weichel O., Hilgert M., Fassbender K., Schmitt A., and Klein J. (2004). **Glycerophosphocholine Is Elevated in Cerebrospinal Fluid of Alzheimer Patients**. *Neurobiology of Aging*. [25:1299-1303].

185. Feillet-Coudray C., Tourtauchaux R., Niculescu M., Rock E., Tauveron I., Alexandre-Gouabau M.-C., Rayssiguier Y., Jalenques I., and Mazur A. (1999). **Plasma Levels of 8-Epipgf2[Alpha], an in Vivo Marker of Oxidative Stress, Are Not Affected by Aging or Alzheimer's Disease**. *Free Radical Biology and Medicine*. [27:463-469].

186. Armanini D., Vecchio F., Basso A., Milone F.F., Simoncini M., Fiore C., Mattarello M.J., Sartorato P., and Karbowiak I. (2003). **Alzheimer's Disease**. *Endocrine*. [22:113-118].

187. Smith M.A., Richey Harris P.L., Sayre L.M., Beckman J.S., and Perry G. (1997). **Widespread Peroxynitrite-Mediated Damage in Alzheimer's Disease**. *Journal of Neuroscience*. [17:2653-2657].

188. Ghauri F.Y., Nicholson J.K., Sweatman B.C., Wood J., Beddell C.R., Lindon J.C., and Cairns N.J. (1993). **Nuclear Magnetic Resonance Spectroscopy of Human Post Mortem Cerebrospinal Fluid: Distinction of Alzheimer's Disease from Control Using Pattern Recognition and Statistics**. *NMR in Biomedicine*. [6:163-167].

189. Kork F., Holthues J., Hellweg R., Jankowski V., Tepel M., Ohring R., Heuser I., Bierbrauer J., Peters O., Schlattmann P., Zidek W., and Jankowski J. (2009). **A Possible New Diagnostic Biomarker in Early Diagnosis of Alzheimer's Disease**. *Current Alzheimer Research*. [6:519-524].

190. Kork F., Gentsch A., Holthues J., Hellweg R., Jankowski V., Tepel M., Zidek W., and Jankowski J. (2012). **A Biomarker for Severity of Alzheimer's Disease: H^1 Nuclear Magnetic Resonances in Cerebrospinal Fluid Correlate with Performance in Mini-Mental-State-Exam**. *Biomarkers*. [17:36-42].

191. Tukiainen T., Tynkkynen T., Makinen V.P., Jylanki P., Kangas A., Hokkanen J., Vehtari A., Grohn O., Hallikainen M., Soininen H., Kivipelto M., Groop P.H., Kaski K., Laatikainen R., Soininen P., Pirttila T., and Ala-Korpela M. (2008). **A**

Multi-Metabolite Analysis of Serum by H¹ Nuclear Magnetic Resonance Spectroscopy: Early Systemic Signs of Alzheimer's Disease. *Biochemical and Biophysical Research Communications*. [375:356-361].

192. Salek R.M., Xia J., Innes A., Sweatman B.C., Adalbert R., Randle S., McGowan E., Emson P.C., and Griffin J.L. (2010). **A Metabolomic Study of the Crnd8 Transgenic Mouse Model of Alzheimer's Disease**. *Neurochemistry International*. [56:937-947].

193. Han X., Rozen S., Boyle S.H., Hellegers C., Cheng H., Burke J.R., Welsh-Bohmer K.A., Doraiswamy P.M., and Kaddurah-Daouk R. (2011). **Metabolomics in Early Alzheimer's Disease: Identification of Altered Plasma Sphingolipidome Using Shotgun Lipidomics**. *PLoS One*. [6:e21643].

194. Wang D.-C., Sun C.-H., Liu L.-Y., Sun X.-H., Jin X.-W., Song W.-L., Liu X.-Q., and Wan X.-L. (2010). **Serum Fatty Acid Profiles Using Gas Chromatography-Mass Spectrometry and Multivariate Statistical Analysis: Potential Biomarkers of Alzheimer's Disease**. *Neurobiology of Aging*. [In Press, Corrected Proof.

195. Sato Y., Suzuki I., Nakamura T., Bernier F., Aoshima K., and Oda Y. (2012). **Identification of a New Plasma Biomarker of Alzheimer's Disease Using Metabolomics Technology**. *Journal of Lipid Research*. [53:567-576].

196. Oresic M., Hyotylainen T., Herukka S.K., Sysi-Aho M., Mattila I., Seppanan-Laakso T., Julkunen V., Gopalacharyulu P.V., Hallikainen M., Koikkalainen J., Kivipelto M., Helisalmi S., Lotjonen J., and Soininen H. (2011). **Metabolome in Progression to Alzheimer's Disease**. *Translational Psychiatry*. [1:e57].

197. Yehuda S., Rabinovitz S., and Mostofsky D.I. (1999). **Essential Fatty Acids Are Mediators of Brain Biochemistry and Cognitive Functions**. *Journal of Neuroscience Research*. [56:565-570].

198. Horrocks L.A., and Farooqui A.A. (2004). **Docosahexaenoic Acid in the Diet: Its Importance in Maintenance and Restoration of Neural Membrane Function**. *Prostaglandins, Leukotrienes and Essential Fatty Acids*. [70:361-372].

199. Piomelli D. (1993). **Arachidonic Acid in Cell Signaling**. *Current Opinion in Cell Biology* [5:274-280].

200. Barger P.M., and Kelly D.P. (1999). **Fatty Acid Utilization in the Hypertrophied and Failing Heart: Molecular Regulatory Mechanisms**. *The American Journal of the Medical Sciences*. [318:36-42].

201. Schaefer E.J., Bongard V., Beiser A.S., Lamon-Fava S., Robins S.J., Au R., Tucker K.L., Kyle D.J., Wilson P.W., and Wolf P.A. (2006). **Plasma Phosphatidylcholine Docosahexaenoic Acid Content and Risk of Dementia and Alzheimer Disease: The Framingham Heart Study**. *Archives of Neurology*. [63:1545-1550].

202. Sanchez-Mejia R.O., Newman J.W., Toh S., Yu G.Q., Zhou Y., Halabisky B., Cisse M., Scearce-Levie K., Cheng I.H., Gan L., Palop J.J., Bonventre J.V., and Mucke L. (2008). **Phospholipase A_2 Reduction Ameliorates Cognitive Deficits in a Mouse Model of Alzheimer's Disease**. *Nature Neuroscience*. [11:1311-1318].

203. Games D., Adams D., Alessandrini R., Barbour R., Berthelette P., Blackwell C., Carr T., Clemens J., Donaldson T., Gillespie F., and et al. (1995). **Alzheimer-Type Neuropathology in Transgenic Mice Overexpressing V717f Beta-Amyloid Precursor Protein**. *Nature*. [373:523-527].

204. Stephenson D.T., Lemere C.A., Selkoe D.J., and Clemens J.A. (1996). **Cytosolic Phospholipase A_2 Immunoreactivity Is Elevated in Alzheimer's Disease Brain**. *Neurobiology of Disease*. [3:51-63].

205. Stephenson D., Rash K., Smalstig B., Roberts E., Johnstone E., Sharp J., Panetta J., Little S., Kramer R., and Clemens J. (1999). **Cytosolic Phospholipase A_2 Is Induced in Reactive Glia Following Different Forms of Neurodegeneration**. *Glia*. [27:110-128].

206. Hicks J.B., Lai Y.Z., Sheng W.W., Yang X.G., Zhu D.H., Sun G.Y., and Lee J.C.M. (2008). **Amyloid-Beta Peptide Induces Temporal Membrane Biphasic Changes in Astrocytes through Cytosolic Phospholipase A_2**. *Biochimica et Biophysica Acta - Biomembranes*. [1778:2512-2519].

207. Prasad M.R., Lovell M.A., Yatin M., Dhillon H., and Markesbery W.R. (1998). **Regional Membrane Phospholipid Alterations in Alzheimer's Disease**. *Neurochemical Research*. [23:81-88].

208. Conquer J.A., Tierney M.C., Zecevic J., Bettger W.J., and Fisher R.H. (2000). **Fatty Acid Analysis of Blood Plasma of Patients with Alzheimer's Disease, Other Types of Dementia, and Cognitive Impairment**. *Lipids*. [35:1305-1312].

209. Cunnane S.C., Schneider J.A., Tangney C., Tremblay-Mercier J., Fortier M., Bennett D.A., and Morris M.C. (2012). **Plasma and Brain Fatty Acid Profiles in Mild Cognitive Impairment and Alzheimer's Disease**. *Journal of Alzheimers Disease*. [29:691-697].

210. Hamilton J.A., Hillard C.J., Spector A.A., and Watkins P.A. (2007). **Brain Uptake and Utilization of Fatty Acids, Lipids and Lipoproteins: Application to Neurological Disorders**. *Journal of Molecular Neuroscience*. [33:2-11].

211. Hamilton J.A., and Brunaldi K. (2007). **A Model for Fatty Acid Transport into the Brain**. *Journal of Molecular Neuroscience*. [33:12-17].

212. Rapoport S.I., Chang M.C., and Spector A.A. (2001). **Delivery and Turnover of Plasma-Derived Essential Poly-Unsaturated Fatty Acids in Mammalian Brain**. *Journal of Lipid Research*. [42:678-685].

213. Salm P., Taylor P.J., and Kostner K. (2011). **Simultaneous Quantification of Total Eicosapentaenoic Acid, Docosahexaenoic Acid and Arachidonic Acid in Plasma by High-Performance Liquid Chromatography-Tandem Mass Spectrometry**. *Biomedical Chromatography*. [25:652-659].

214. Howlett D.R., Richardson J.C., Austin A., Parsons A.A., Bate S.T., Davies D.C., and Gonzalez M.I. (2004). **Cognitive Correlates of Abeta Deposition in Male and Female Mice Bearing Amyloid Precursor Protein and Presenilin-1 Mutant Transgenes**. *Brain Research*. [1017:130-136].

215. Lovestone S., Francis P., Kloszewska I., Mecocci P., Simmons A., Soininen H., Spenger C., Tsolaki M., Vellas B., Wahlund L.O., Ward M., and Consortium A. (2009). **Addneuromed - the European Collaboration for the Discovery of Novel Biomarkers for Alzheimer's Disease**. *Biomarkers in Brain Disease*. [1180:36-46].

216. Simmons A., Westman E., Muehlboeck S., Mecocci P., Vellas B., Tsolaki M., Kloszewska I., Wahlund L.O., Soininen H., Lovestone S., Evans A., Spenger C., and Consortium A. (2009). **Magnetic Resonance Imaging Measures of Alzheimer's Disease and the Addneuromed Study**. *Biomarkers in Brain Disease*. [1180:47-55].

217. Matyash V., Liebisch G., Kurzchalia T.V., Shevchenko A., and Schwudke D. (2008). **Lipid Extraction by Methyl-Tert-Butyl Ether for High-Throughput Lipidomics**. *Journal of Lipid Research*. [49:1137-1146].

218. Hu Z.P., Browne E.R., Liu T., Angel T.E., Ho P.C., and Chan E.C. (2012). **Metabonomic Profiling of Tastpm Transgenic Alzheimer's Disease Mouse Model**. *Journal of Proteome Research*. [11:5903-5913].

219. Petursdottir A.L., Farr S.A., Morley J.E., Banks W.A., and Skuladottir G.V. (2007). **Lipid Peroxidation in Brain During Aging in the Senescence-Accelerated Mouse**. *Neurobiology of Aging*. [28:1170-1178].

220. Morley J.E. (2002). **The Samp8 Mouse: A Model of Alzheimer Disease?** *Biogerontology*. [3:57-60].

221. Samieri C., Feart C., Letenneur L., Dartigues J.F., Peres K., Auriacombe S., Peuchant E., Delcourt C., and Barberger-Gateau P. (2008). **Low Plasma Eicosapentaenoic Acid and Depressive Symptomatology Are Independent Predictors of Dementia Risk**. *American Journal of Clinical Nutrition*. [88:714-721].

222. Tully A.M., Roche H.M., Doyle R., Fallon C., Bruce I., Lawlor B., Coakley D., and Gibney M.J. (2003). **Low Serum Cholesteryl Ester-Docosahexaenoic Acid Levels in Alzheimer's Disease: A Case-Control Study**. *British Journal of Nutrition*. [89:483-489].

223. Laurin D., Verreault R., Lindsay J., Dewailly E., and Holub B.J. (2003). **Omega-3 Fatty Acids and Risk of Cognitive Impairment and Dementia**. *Journal of Alzheimers Disease*. [5:315-322].

224. Lopez L.B., Kritz-Silverstein D., and Barrett Connor E. (2011). **High Dietary and Plasma Levels of the Omega-3 Fatty Acid Docosahexaenoic Acid Are Associated with Decreased Dementia Risk: The Rancho Bernardo Study**. *The Journal of Nutrition Health and Aging*. [15:25-31].

225. Yamamura K., Hashimoto M., Arai Y., Shimizu K., Shido O., and Hirose N. (2007). **Relationship between Fatty Acid and Dementia in Japanese Centenarians**. *Experimental Gerontology*. [42:149].

226. Fraser T., Tayler H., and Love S. (2010). **Fatty Acid Composition of Frontal, Temporal and Parietal Neocortex in the Normal Human Brain and in Alzheimer's Disease**. *Neurochemical Research*. [35:503-513].

227. Morris M.C., Evans D.A., Bienias J.L., Tangney C.C., Bennett D.A., Wilson R.S., Aggarwal N., and Schneider J. (2003). **Consumption of Fish and N3 Fatty Acids and Risk of Incident Alzheimer Disease**. *Archives of Neurology*. [60:940-946].

228. Nicholson J.K., and Lindon J.C. (2008). **Systems Biology: Metabonomics**. *Nature*. [455:1054-1056].

229. Wang D.C., Sun C.H., Liu L.Y., Sun X.H., Jin X.W., Song W.L., Liu X.Q., and Wan X.L. (2012). **Serum Fatty Acid Profiles Using Gas Chromatography-Mass Spectrometry and Multivariate Statistical Analysis: Potential Biomarkers of Alzheimer's Disease**. *Neurobiology of Aging*. [33:1057-1066].

230. Rainville P.D., Stumpf C.L., Shockcor J.P., Plumb R.S., and Nicholson J.K. (2007). **Novel Application of Reversed-Phase Liquid Chromatography-T.O.F-Mass Spectrometry for Lipid Analysis in Complex Biological Mixtures: A New Tool for Lipidomics**. *Journal of Proteome Research*. [6:552-558].

231. Wishart D.S., Jewison T., Guo A.C., Wilson M., Knox C., Liu Y., Djoumbou Y., Mandal R., Aziat F., Dong E., Bouatra S., Sinelnikov I., Arndt D., Xia J., Liu P., Yallou F., Bjorndahl T., Perez-Pineiro R., Eisner R., Allen F., Neveu V., Greiner R., and Scalbert A. (2012). **H.M.D.B 3.0--the Human Metabolome Database in 2013**. *Nucleic Acids Research*.

232. Wishart D.S., Knox C., Guo A.C., Eisner R., Young N., Gautam B., Hau D.D., Psychogios N., Dong E., Bouatra S., Mandal R., Sinelnikov I., Xia J., Jia L., Cruz J.A., Lim E., Sobsey C.A., Shrivastava S., Huang P., Liu P., Fang L., Peng J., Fradette R., Cheng D., Tzur D., Clements M., Lewis A., De Souza A., Zuniga A., Dawe M., Xiong Y., Clive D., Greiner R., Nazyrova A., Shaykhutdinov R., Li L., Vogel H.J., and Forsythe I. (2009). **H.M.D.B: A Knowledgebase for the Human Metabolome**. *Nucleic Acids Research*. [37:D603-610].

233. Wishart D.S., Tzur D., Knox C., Eisner R., Guo A.C., Young N., Cheng D., Jewell K., Arndt D., Sawhney S., Fung C., Nikolai L., Lewis M., Coutouly M.A., Forsythe I., Tang P., Shrivastava S., Jeroncic K., Stothard P., Amegbey G., Block D., Hau D.D., Wagner J., Miniaci J., Clements M., Gebremedhin M., Guo N., Zhang Y., Duggan G.E., Macinnis G.D., Weljie A.M., Dowlatabadi R., Bamforth F., Clive D.,

Greiner R., Li L., Marrie T., Sykes B.D., Vogel H.J., and Querengesser L. (2007). **H.M.D.B: The Human Metabolome Database**. *Nucleic Acids Research*. [35:D521-526].

234. Smith C.A., O'Maille G., Want E.J., Qin C., Trauger S.A., Brandon T.R., Custodio D.E., Abagyan R., and Siuzdak G. (2005). **Metlin: A Metabolite Mass Spectral Database**. *Therapeutic Drug Monitoring*. [27:747-751].

235. **Simca-P+ and Multivariate Analysis - Frequently Asked Questions**. *Umetrics Umeå Sweden*. (www.umetrics.com/81:/downloads/KB/Multivariate%20FAQ.pdf). [Last Accessed Online 04 January 2013].

236. Zhao Y.Y., Xiong Y., and Curtis J.M. (2011). **Measurement of Phospholipids by Hydrophilic Interaction Liquid Chromatography Coupled to Tandem Mass Spectrometry: The Determination of Choline Containing Compounds in Foods**. *Journal of Chromatography A*. [1218:5470-5479].

237. Berdeaux O., Juaneda P., Martine L., Cabaret S., Bretillon L., and Acar N. (2010). **Identification and Quantification of Phosphatidylcholines Containing Very-Long-Chain Polyunsaturated Fatty Acid in Bovine and Human Retina Using Liquid Chromatography/Tandem Mass Spectrometry**. *Journal of Chromatography A*. [1217:7738-7748].

238. Frisardi V., Panza F., Seripa D., Farooqui T., and Farooqui A.A. (2011). **Glycerophospholipids and Glycerophospholipid-Derived Lipid Mediators: A Complex Meshwork in Alzheimer's Disease Pathology**. *Progress in Lipid Research*. [50:313-330].

239. Schaeffer E.L., da Silva E.R., Novaes Bde A., Skaf H.D., and Gattaz W.F. (2010). **Differential Roles of Phospholipases A_2 in Neuronal Death and Neurogenesis: Implications for Alzheimer Disease**. *Progress in Neuro-Psychopharmacology and Biological Psychiatry* [34:1381-1389].

240. Perttu E.K., Kohli A.G., and Szoka F.C., Jr. (2012). **Inverse-Phosphocholine Lipids: A Remix of a Common Phospholipid**. *Journal of the American Chemical Society*. [134:4485-4488].

241. Cramer P.E., Cirrito J.R., Wesson D.W., Lee C.Y., Karlo J.C., Zinn A.E., Casali B.T., Restivo J.L., Goebel W.D., James M.J., Brunden K.R., Wilson D.A., and Landreth G.E. (2012). **Apolipoprotein E-Directed Therapeutics Rapidly Clear Beta-Amyloid and Reverse Deficits in Ad Mouse Models**. *Science*. [335:1503-1506].

242. Pericak-Vance M.A., Bebout J.L., Gaskell P.C., Jr., Yamaoka L.H., Hung W.Y., Alberts M.J., Walker A.P., Bartlett R.J., Haynes C.A., Welsh K.A., and et al. (1991). **Linkage Studies in Familial Alzheimer Disease: Evidence for Chromosome 19 Linkage**. *The American Journal of Human Genetics*. [48:1034-1050].

243. Luft F.C. (1997). **Alzheimer's Disease, Blood Lipids, and Heart Disease: What Are the Interrelationships?** *Journal of Molecular Medicine*. [75:73-74].

244. Sando S.B., Melquist S., Cannon A., Hutton M.L., Sletvold O., Saltvedt I., White L.R., Lydersen S., and Aasly J.O. (2008). **Apolipoprotein Epsilon 4 Lowers Age at Onset and Is a High Risk Factor for Alzheimer's Disease; a Case Control Study from Central Norway**. *BioMedCentral Neurology*. [8:9].

245. Gaudin M., Panchal M., Auzeil N., Duyckaerts C., Brunelle A., Laprevote O., and Touboul D. (2012). **Choline-Containing Phospholipids in Microdissected Human Alzheimer's Disease Brain Senile Plaque Versus Neuropil**. *Bioanalysis*. [4:2153-5159].

246. Nitsch R.M., Blusztajn J.K., Pittas A.G., Slack B.E., Growdon J.H., and Wurtman R.J. (1992). **Evidence for a Membrane Defect in Alzheimer Disease Brain**. *Proceedings of the National Academy of Sciences*. [89:1671-1675].

247. Mulder C., Wahlund L.O., Teerlink T., Blomberg M., Veerhuis R., van Kamp G.J., Scheltens P., and Scheffer P.G. (2003). **Decreased Lysophosphatidylcholine/Phosphatidylcholine Ratio in Cerebrospinal Fluid in Alzheimer's Disease**. *Journal of Neural Transmission*. [110:949-955].

248. Sheikh A.M., and Nagai A. (2011). **Lysophosphatidylcholine Modulates Fibril Formation of Amyloid Beta Peptide**. *FEBS Journal*. [278:634-642].

249. Liebisch G., Lieser B., Rathenberg J., Drobnik W., and Schmitz G. (2004). **High-Throughput Quantification of Phosphatidylcholine and Sphingomyelin by Electrospray Ionization Tandem Mass Spectrometry Coupled with Isotope Correction Algorithm**. *Biochimica et Biophysica Acta*. [1686:108-117].

250. Kolesnick R.N. (1991). **Sphingomyelin and Derivatives as Cellular Signals**. *Progress in Lipid Research*. [30:1-38].

251. Fillet M., Van Heugen J.C., Servais A.C., De Graeve J., and Crommen J. (2002). **Separation, Identification and Quantitation of Ceramides in Human Cancer Cells by Liquid Chromatography-Electrospray Ionization Tandem Mass Spectrometry**. *Journal of Chromatography A*. [949:225-233].

252. Bandaru V.V., Troncoso J., Wheeler D., Pletnikova O., Wang J., Conant K., and Haughey N.J. (2009). **Apolipoprotein E4 Disrupts Sterol and Sphingolipid Metabolism in Alzheimer's but Not Normal Brain**. *Neurobiology of Aging*. [30:591-599].

253. Kosicek M., Zetterberg H., Andreasen N., Peter-Katalinic J., and Hecimovic S. (2012). **Elevated Cerebrospinal Fluid Sphingomyelin Levels in Prodromal Alzheimer's Disease**. *Neuroscience Letters*. [516:302-305].

254. Kosicek M., Kirsch S., Bene R., Trkanjec Z., Titlic M., Bindila L., Peter-Katalinic J., and Hecimovic S. (2010). **Nano-Liquid Chromatography-Mass Spectrometry Analysis of Phospholipids in Cerebrospinal Fluid of Alzheimer's Disease Patients - a Pilot Study**. *Analytical and Bioanalytical Chemistry*. [398:2929-2937].

255. Mielke M.M., Haughey N.J., Bandaru V.V., Weinberg D.D., Darby E., Zaidi N., Pavlik V., Doody R.S., and Lyketsos C.G. (2011). **Plasma Sphingomyelins Are Associated with Cognitive Progression in Alzheimer's Disease**. *Journal of Alzheimers Disease*. [27:259-269].

256. He X., Huang Y., Li B., Gong C.X., and Schuchman E.H. (2010). **Deregulation of Sphingolipid Metabolism in Alzheimer's Disease**. *Neurobiology of Aging*. [31:398-408].

257. Vance J.E., and Tasseva G. (2012). **Formation and Function of Phosphatidylserine and Phosphatidylethanolamine in Mammalian Cells**. *Biochimica et Biophysica Acta*.

258. Brugger B., Erben G., Sandhoff R., Wieland F.T., and Lehmann W.D. (1997). **Quantitative Analysis of Biological Membrane Lipids at the Low Picomole Level by Nano-Electrospray Ionization Tandem Mass Spectrometry**. *Proceedings of the National Academy of Sciences*. [94:2339-2344].

259. Yao J.K., Wengenack T.M., Curran G.L., and Poduslo J.F. (2009). **Reduced Membrane Lipids in the Cortex of Alzheimer's Disease Transgenic Mice**. *Neurochemical Research*. [34:102-108].

260. Wells K., Farooqui A.A., Liss L., and Horrocks L.A. (1995). **Neural Membrane Phospholipids in Alzheimer Disease**. *Neurochemical Research*. [20:1329-1333].

261. Guan Z.Z., Wang Y.N., Xiao K.Q., Hu P.S., and Liu J.L. (1999). **Activity of Phosphatidylethanolamine-N-Methyltransferase in Brain Affected by Alzheimer's Disease**. *Neurochemistry International*. [34:41-47].

262. Gómez-fernández J.C., Torrecillas A., and Corbalán-García S. (2004). **Diacylglycerols as Activators of Protein Kinase C (Review)**. *Molecular Membrane Biology*. [21:339-349].

263. Kalo P.J., Ollilainen V., Rocha J.M., and Malcata F.X. (2006). **Identification of Molecular Species of Simple Lipids by Normal Phase Liquid Chromatography–Positive Electrospray Tandem Mass Spectrometry, and Application of Developed Methods in Comprehensive Analysis of Low Erucic Acid Rapeseed Oil Lipids**. *International Journal of Mass Spectrometry*. [254:106-121].

264. Zambrzycka A., Strosznajder R.P., and Strosznajder J.B. (2000). **Aggregated Beta Amyloid Peptide$_{1\text{-}40}$ Decreases Ca^{2+} and Cholinergic Receptor-Mediated Phosphoinositide Degradation by Alteration of Membrane and Cytosolic Phospholipase C in Brain Cortex**. *Neurochemical Research*. [25:189-196].

265. Farooqui A., Liss L., and Horrocks L. (1990). **Elevated Activities of Lipases and Lysophospholipase in Alzheimer's Disease**. *Dementia and Geriatric Cognitive Disorders*. [1:208-214].

266. Ciborowski M., Teul J., Martin-Ventura J.L., Egido J., and Barbas C. (2012). **Metabolomics with Liquid Chromatography-Q.T.O.F-Mass Spectrometry Permits the Prediction of Disease Stage in Aortic Abdominal Aneurysm Based on Plasma Metabolic Fingerprint**. *PLoS One*. [7:e31982].

267. Ciborowski M., Lipska A., Godzien J., Ferrarini A., Korsak J., Radziwon P., Tomasiak M., and Barbas C. (2012). **Combination of Liquid Chromatography-Mass Spectrometry and Gas Chromatography-Mass Spectrometry Based Metabolomics to Study the Effect of Ozonated Autohemotherapy on Human Blood**. *Journal of Proteome Research*. [11:6231-6241].

268. Ang J.E., Revell V., Mann A., Mantele S., Otway D.T., Johnston J.D., Thumser A.E., Skene D.J., and Raynaud F. (2012). **Identification of Human Plasma Metabolites Exhibiting Time-of-Day Variation Using an Untargeted Liquid Chromatography-Mass Spectrometry Metabolomic Approach**. *Chronobiology International*. [29:868-881].

269. Choi B.K., Hercules D.M., and Gusev A.I. (2001). **Effect of Liquid Chromatography Separation of Complex Matrices on Liquid Chromatography-Tandem Mass Spectrometry Signal Suppression**. *Journal of Chromatography A*. [907:337-342].

270. Jessome L.L., and Volmer D.A. (2006). **Ion Supression: A Major Concern in Mass Spectrometry**. *LCGC North America*. [24:7-10].

271. Wilson I.D., Plumb R., Granger J., Major H., Williams R., and Lenz E.M. (2005). **High Performance Liquid Chromatography-Mass Spectrometry Based Methods for the Study of Metabonomics**. *Journal of Chromatography B: Analytical Technologies in the Biomedical and Life Sciences*. [817:67-76].

272. Chambers E., Wagrowski-Diehl D.M., Lu Z., and Mazzeo J.R. (2007). **Systematic and Comprehensive Strategy for Reducing Matrix Effects in Liquid Chromatography-Mass Spectrometry Analyses**. *Journal of Chromatography B: Analytical Technologies in the Biomedical and Life Sciences*. [852:22-34].

273. Ciborowski M., Martin-Ventura J.L., Meilhac O., Michel J.B., Ruperez F.J., Tunon J., Egido J., and Barbas C. (2011). **Metabolites Secreted by Human Atherothrombotic Aneurysms Revealed through a Metabolomic Approach**. *Journal of Proteome Research*. [10:1374-1382].

274. Ciborowski M., Javier Ruperez F., Martinez-Alcazar M.P., Angulo S., Radziwon P., Olszanski R., Kloczko J., and Barbas C. (2010). **Metabolomic Approach with Liquid Chromatography-Mass Spectrometry Reveals Significant Effect of Pressure on Diver's Plasma**. *Journal of Proteome Research*. [9:4131-4137].

275. Yanes O., Tautenhahn R., Patti G.J., and Siuzdak G. (2011). **Expanding Coverage of the Metabolome for Global Metabolite Profiling**. *Analytical Chemistry*. [83:2152-2161].

276. Masson P., Alves A.C., Ebbels T.M., Nicholson J.K., and Want E.J. (2010). **Optimization and Evaluation of Metabolite Extraction Protocols for Untargeted Metabolic Profiling of Liver Samples by Liquid Chromatography-Mass Spectromtery**. *Analytical Chemistry*. [82:7779-7786].

277. Fenton W.S., Hibbeln J., and Knable M. (2000). **Essential Fatty Acids, Lipid Membrane Abnormalities, and the Diagnosis and Treatment of Schizophrenia**. *Biological Psychiatry*. [47:8-21].

278. Cheng D., Jenner A.M., Shui G., Cheong W.F., Mitchell T.W., Nealon J.R., Kim W.S., McCann H., Wenk M.R., Halliday G.M., and Garner B. (2011). **Lipid Pathway Alterations in Parkinson's Disease Primary Visual Cortex**. *PLoS One*. [6:e17299].

279. Kreisberg R.A., and Oberman A. (2002). **Clinical Review 141: Lipids and Atherosclerosis: Lessons Learned from Randomized Controlled Trials of Lipid Lowering and Other Relevant Studies**. *The Journal of Clinical Endocrinology & Metabolism*. [87:423-437].

280. Negro F. (2010). **Abnormalities of Lipid Metabolism in Hepatitis C Virus Infection**. *Gut*. [59:1279-1287].

281. Zaas D.W., Duncan M., Rae Wright J., and Abraham S.N. (2005). **The Role of Lipid Rafts in the Pathogenesis of Bacterial Infections**. *Biochimica et Biophysica Acta*. [1746:305-313].

282. Nicholas S.B. (1999). **Lipid Disorders in Obesity**. *Current Hypertension Reports*. [1:131-136].

283. Dullaart R.P. (1995). **Plasma Lipoprotein Abnormalities in Type 1 (Insulin-Dependent) Diabetes Mellitus**. *Netherlands Journal of Medicine*. [46:44-54].

284. Savage D.B., Petersen K.F., and Shulman G.I. (2007). **Disordered Lipid Metabolism and the Pathogenesis of Insulin Resistance**. *Physiological Reviews*. [87:507-520].

285. van Meer G., Voelker D.R., and Feigenson G.W. (2008). **Membrane Lipids: Where They Are and How They Behave**. *Nature Reviews Molecular Cell Biology*. [9:112-124].

286. Zweytick D., Athenstaedt K., and Daum G. (2000). **Intracellular Lipid Particles of Eukaryotic Cells**. *Biochimica et Biophysica Acta*. [1469:101-120].

287. Pawson T., and Nash P. (2003). **Assembly of Cell Regulatory Systems through Protein Interaction Domains**. *Science*. [300:445-452].

288. Girotti A.W. (2001). **Photosensitized Oxidation of Membrane Lipids: Reaction Pathways, Cytotoxic Effects, and Cytoprotective Mechanisms**. *Journal of Photochemistry and Photobiology B*. [63:103-113].

289. Godzien J., Ciborowski M., Angulo S., Ruperez F.J., Martinez M.P., Senorans F.J., Cifuentes A., Ibanez E., and Barbas C. (2011). **Metabolomic Approach with Liquid Chromatography-Q.T.O.F to Study the Effect of a Nutraceutical Treatment on Urine of Diabetic Rats**. *Journal of Proteome Research*. [10:837-844].

290. Suhre K., and Schmitt-Kopplin P. (2008). **Masstrix: Mass Translator into Pathways**. *Nucleic Acids Research*. [36:W481-484].

291. Folch J., Ascoli I., Lees M., Meath J.A., and Le B.N. (1951). **Preparation of Lipide Extracts from Brain Tissue**. *The Journal of Biological Chemistry*. [191:833-841].

292. Sandra K., Pereira Ados S., Vanhoenacker G., David F., and Sandra P. (2010). **Comprehensive Blood Plasma Lipidomics by Liquid Chromatography/Quadrupole Time-of-Flight Mass Spectrometry**. *Journal of Chromatography A*. [1217:4087-4099].

293. Ganda O.P., Rossini A.A., and Like A.A. (1976). **Studies on Streptozotocin Diabetes**. *Diabetes*. [25:595-603].

294. Lester-Coll N., Rivera E.J., Soscia S.J., Doiron K., Wands J.R., and de la Monte S.M. (2006). **Intracerebral Streptozotocin Model of Type 3 Diabetes: Relevance to Sporadic Alzheimer's Disease**. *Journal of Alzheimers Disease*. [9:13-33].

295. Salkovic-Petrisic M., Osmanovic-Barilar J., Bruckner M.K., Hoyer S., Arendt T., and Riederer P. (2011). **Cerebral Amyloid Angiopathy in Streptozotocin Rat Model of Sporadic Alzheimer's Disease: A Long-Term Follow up Study**. *Journal of Neural Transmission*. [118:765-772].

296. Lovestone S., Anderton B.H., Hartley C., Jensen T.G., and Jorgensen A.L. (1996). **The Intracellular Fate of Apolipoprotein E Is Tau Dependent and Apolipoprotein E Allele-Specific**. *Neuroreport*. [7:1005-1008].

297. Di Paolo G., and Kim T.W. (2011). **Linking Lipids to Alzheimer's Disease: Cholesterol and Beyond**. *Nature Reviews Neuroscience*. [12:284-296].

298. Want E.J., Wilson I.D., Gika H., Theodoridis G., Plumb R.S., Shockcor J., Holmes E., and Nicholson J.K. (2010). **Global Metabolic Profiling Procedures for Urine Using Ultra Performance Liquid Chromatography-Mass Spectrometry**. *Nature Protocols*. [5:1005-1018].

299. Burton L., Ivosev G., Tate S., Impey G., Wingate J., and Bonner R. (2008). **Instrumental and Experimental Effects in Liquid Chromatography-Mass Spectrometry Based Metabolomics**. *Journal of Chromatography B: Analytical Technologies in the Biomedical and Life Sciences*. [871:227-235].

300. Illig T., Gieger C., Zhai G., Romisch-Margl W., Wang-Sattler R., Prehn C., Altmaier E., Kastenmuller G., Kato B.S., Mewes H.W., Meitinger T., de Angelis M.H., Kronenberg F., Soranzo N., Wichmann H.E., Spector T.D., Adamski J., and

Suhre K. (2010). **A Genome-Wide Perspective of Genetic Variation in Human Metabolism**. *Nature Genetics*. [42:137-141].

301. Li Z., and Vance D.E. (2008). **Phosphatidylcholine and Choline Homeostasis**. *Journal of Lipid Research*. [49:1187-1194].

302. Selvy P.E., Lavieri R.R., Lindsley C.W., and Brown H.A. (2011). **Phospholipase D: Enzymology, Functionality, and Chemical Modulation**. *Chemical Reviews*. [111:6064-6119].

303. Dennis E.A., Cao J., Hsu Y.H., Magrioti V., and Kokotos G. (2011). **Phospholipase A_2 Enzymes: Physical Structure, Biological Function, Disease Implication, Chemical Inhibition, and Therapeutic Intervention**. *Chemical Reviews*. [111:6130-6185].

304. Gattaz W.F., Maras A., Cairns N.J., Levy R., and Forstl H. (1995). **Decreased Phospholipase A_2 Activity in Alzheimer Brains**. *Biological Psychiatry*. [37:13-17].

305. Gattaz W.F., Cairns N.J., Levy R., Forstl H., Braus D.F., and Maras A. (1996). **Decreased Phospholipase A_2 Activity in the Brain and in Platelets of Patients with Alzheimer's Disease**. *European Archives of Psychiatry and Clinical Neuroscience*. [246:129-131].

306. Ross B.M., Moszczynska A., Erlich J., and Kish S.J. (1998). **Phospholipid-Metabolizing Enzymes in Alzheimer's Disease: Increased Lysophospholipid Acyltransferase Activity and Decreased Phospholipase A_2 Activity**. *Journal of Neurochemistry*. [70:786-793].

307. Talbot K., Young R.A., Jolly-Tornetta C., Lee V.M., Trojanowski J.Q., and Wolf B.A. (2000). **A Frontal Variant of Alzheimer's Disease Exhibits Decreased Calcium-Independent Phospholipase A_2 Activity in the Prefrontal Cortex**. *Neurochemistry International*. [37:17-31].

308. Colangelo V., Schurr J., Ball M.J., Pelaez R.P., Bazan N.G., and Lukiw W.J. (2002). **Gene Expression Profiling of 12633 Genes in Alzheimer Hippocampal Ca1: Transcription and Neurotrophic Factor Down-Regulation and up-Regulation of Apoptotic and Pro-Inflammatory Signaling**. *Journal of Neuroscience Research*. [70:462-473].

309. Chan R.B., Oliveira T.G., Cortes E.P., Honig L.S., Duff K.E., Small S.A., Wenk M.R., Shui G., and Di Paolo G. (2012). **Comparative Lipidomic Analysis of Mouse and Human Brain with Alzheimer Disease**. *The Journal of Biological Chemistry*. [287:2678-2688].

310. Mielke M.M., Bandaru V.V., Haughey N.J., Rabins P.V., Lyketsos C.G., and Carlson M.C. (2010). **Serum Sphingomyelins and Ceramides Are Early Predictors of Memory Impairment**. *Neurobiology of Aging*. [31:17-24].

311. Satoi H., Tomimoto H., Ohtani R., Kitano T., Kondo T., Watanabe M., Oka N., Akiguchi I., Furuya S., Hirabayashi Y., and Okazaki T. (2005). **Astroglial**

Expression of Ceramide in Alzheimer's Disease Brains: A Role During Neuronal Apoptosis. *Neuroscience*. [130:657-666].

312. Ryan S.D., Whitehead S.N., Swayne L.A., Moffat T.C., Hou W., Ethier M., Bourgeois A.J., Rashidian J., Blanchard A.P., Fraser P.E., Park D.S., Figeys D., and Bennett S.A. (2009). **Amyloid-Beta$_{42}$ Signals Tau Hyperphosphorylation and Compromises Neuronal Viability by Disrupting Alkylacylglycerophosphocholine Metabolism**. *Proceedings of the National Academy of Sciences*. [106:20936-20941].

313. Dyrks T., Weidemann A., Multhaup G., Salbaum J.M., Lemaire H.G., Kang J., Muller-Hill B., Masters C.L., and Beyreuther K. (1988). **Identification, Transmembrane Orientation and Biogenesis of the Amyloid A4 Precursor of Alzheimer's Disease**. *EMBO Journal*. [7:949-957].

314. Pettegrew J.W., Panchalingam K., Moossy J., Martinez J., Rao G., and Boller F. (1988). **Correlation of P^{31} Magnetic Resonance Spectroscopy and Morphologic Findings in Alzheimer's Disease**. *Archives of Neurology*. [45:1093-1096].

315. Kantarci K., Weigand S.D., Petersen R.C., Boeve B.F., Knopman D.S., Gunter J., Reyes D., Shiung M., O'Brien P.C., Smith G.E., Ivnik R.J., Tangalos E.G., and Jack C.R., Jr. (2007). **Longitudinal H^{1} Magnetic Resonance Spectroscopy Changes in Mild Cognitive Impairment and Alzheimer's Disease**. *Neurobiology of Aging*. [28:1330-1339].

316. Small D.H., Maksel D., Kerr M.L., Ng J., Hou X., Chu C., Mehrani H., Unabia S., Azari M.F., Loiacono R., Aguilar M.I., and Chebib M. (2007). **The Beta-Amyloid Protein of Alzheimer's Disease Binds to Membrane Lipids but Does Not Bind to the Alpha7 Nicotinic Acetylcholine Receptor**. *Journal of Neurochemistry*. [101:1527-1538].

317. Fawcett T. (2006). **An Introduction to R.O.C Analysis**. *Pattern Recognition Letters*. [27:861-874].

318. Biagioni M.C., and Galvin J.E. (2011). **Using Biomarkers to Improve Detection of Alzheimer's Disease**. *Neurodegenerative Disease Management*. [1:127-139].

319. NIA-AA. (1998). **Consensus Report of the Working Group On: "Molecular and Biochemical Markers of Alzheimer's Disease". The Ronald and Nancy Reagan Research Institute of the Alzheimer's Association and the National Institute on Aging Working Group**. *Neurobiology of Aging*. [19:109-116].

320. Rau G.A., Dombrowsky H., Gebert A., Thole H.H., von der Hardt H., Freihorst J., and Bernhard W. (2003). **Phosphatidylcholine Metabolism of Rat Trachea in Relation to Lung Parenchyma and Surfactant**. *Journal of Applied Physiology*. [95:1145-1152].